FAT AND PROTEIN METABOLISM: INTERACTIONS IN HUMAN SKELETAL MUSCLE

Robert Jones, BSc, MSc

A thesis submitted for the degree of Doctor of Philosophy from

the University of Nottingham

September 2019

Abstract

Obesity is associated with insulin resistance, which may be underpinned by spill over of excess lipids into ectopic tissue(s) including skeletal muscle. Insulin resistance has been associated with dysregulated protein metabolism and anabolic resistance. The aim of this thesis was to further explore the interactions between insulin and anabolic resistance in human skeletal muscle. This was achieved by using nutritional approaches to alter the availability of substrates proposed to play an important role in mediating this association.

In Chapters 3 and 4, the effects of exogenous provision of saturated fatty acids were examined *in vivo* and in primary human myotubes. Restricting the length of the daily energy intake window, which alters the pattern of exogenous substrate availability, enhances insulin sensitivity in rodents. Preliminary evidence in humans shows beneficial effects of extending the overnight fast and shifting energy intake to earlier in the day. In Chapter 5 and 6, this approach was combined to test the hypothesis that early time-restricted feeding (eTRF) will enhance skeletal muscle insulin and anabolic sensitivity independently of energy balance.

In Chapter 3, prior oral ingestion of a saturated fatty acid drink did not impair any index of insulin sensitivity and increased the incorporation of dietary [1-^{13}C] phenylalanine into the myofibrillar pool of middle-aged, overweight/obese males. This was contrary to our hypotheses and suggested a potential role for improved amino acid transport. However, in Chapter 4, pre-treatment of myotubes with 0.25 mM palmitate induced insulin resistance, decreased system A transport of amino acids and tended to downregulate rates of muscle protein synthesis.

In Chapter 5, two weeks of restricting daily energy intake to between 08:00 and 16:00 improved skeletal muscle and whole-body insulin sensitivity in healthy males. This was associated with an increased net uptake of branched chain amino acids (an index of anabolic sensitivity) in response to oral protein ingestion. However, eTRF was associated with an involuntary reduction in free-living energy intake and a modest (-1.04 ± 0.71 kg) but significant reduction in body mass. To assess what extent this magnitude of weight loss may have played in our findings, the response of an additional group (matched for age, body mass index and physical activity) to a ~400 kCal daily energy deficit was examined in Chapter 6. Despite comparable weight loss, none of the metabolic improvements associated with eTRF were found. This suggests that the benefits of eTRF are, at least in part, independent of its effects on energy balance.

In conclusion, changes in insulin sensitivity may be associated with improvements in anabolic sensitivity under certain conditions. However, in the absence of insulin resistance, elevated lipid availability *per se* has no detrimental effects on the anabolic response to amino acid ingestion.

Publications

Manuscripts

Tsintzas, K., **Jones, R.**, Pabla, P., Barrett, D., Kim, D., Cooper, S., Taylor, T., Chee, C., Gaffney, C., Doherty, C., Mallinson, J., van Loon, L., Stephens, F.B. Effect of acute and chronic dietary fat ingestion on postprandial skeletal muscle protein synthesis rates in middle-aged, overweight and obese men. Currently under review in *The American Journal of Physiology-Endocrinology and Metabolism.*

Jones, R., Pabla, P., Mallinson, J., Taylor, T., Bennett, A., Tsintzas, K. Two weeks of early time restricted feeding (eTRF) improves whole-body and skeletal muscle insulin sensitivity in healthy men. Currently under review in *The American Journal of Clinical Nutrition.*

Conference abstracts

Jones, R., Pabla, P., Mallinson, J., Taylor, T., Tsintzas, K. Effects of two-weeks of time restricted feeding on basal and postprandial metabolism in healthy men. Presented at *Physiology 2019*, Aberdeen.

Jones, R., Pabla, P., Mallinson, J., Taylor, T., Tsintzas, K. Effects of two-weeks of time restricted feeding on basal and postprandial metabolism in healthy men. Poster and 3-min 'data blitz' talk at *Physiology of Obesity and Diabetes Satellite Meeting, Physiology 2019,* Aberdeen.

Declarations

- Sally Cordon performed all insulin, free-fatty acid and triglyceride analysis in Chapters 3, 5 and 6. In addition, to the ghrelin measurements in Chapter 5.
- Professor Luc van Loon's group at Maastricht university analysed [1-^{13}C] phenylalanine incorporation and plasma amino acids in Chapter 3.
- Dr Joanne Mallinson measured forearm blood flow in Chapters 5 and 6.
- Pardeep Pabla assisted with all *in vivo* data collection in Chapters 5 and 6.
- Dr Tariq Taylor and Dr Natalie Shur obtained muscle biopsies (all experimental chapters) and cannulations in Chapters 3, 5 and 6.
- Aline Nixon assisted with cannulations and DEXA analysis to obtain lean forearm mass in Chapter 5.

I declare that the thesis is the result of my own work which has been undertaken during my period of registration for this degree at The University of Nottingham.

Signed: _____

Date: _____

Acknowledgements

I would like to express my gratitude to Dr Kostas Tsintzas for encouraging me to apply for a PhD. Your advice and mentorship throughout my project proved invaluable. Thank you to Dr Andrew Bennett for your expert insight into the primary muscle cell culture work and to Monika Owen for her assistance. I am grateful to the Biotechnology and Biological Sciences Research Council for offering me the opportunity to pursue a PhD.

Like all human physiology research, none of this work would be possible without the commitment and enthusiasm of study volunteers. I also appreciate the assistance of staff at the David Greenfield Human Physiology Unit; particularly Jo, Sara and Aline. Pardeep, you were a massive help on study days and your company made them far more enjoyable (and successful) than they would have been otherwise. Scott, thank you for training me in many of the analytical techniques used in this thesis.

Shout out to all the other PhD students in the office for your camaraderie and friendship. It was great to always have somebody around to discuss science with or to bounce ideas off and I wish you all the best of luck with your upcoming submissions. To the football lads, your company (both on the pitch and in the pub) provided much needed stress relief and enjoyment.

I am enormously grateful to Sophia for her support and love over the last four years. Finally, I owe a special thank you to my family and especially my parents. This would not have been possible without the countless sacrifices that you have made to provide me with opportunities throughout my life and education.

Table of Contents

Abstract i
Publications iii
Declarations iv
Acknowledgements v
Table of Contents vi
List of Abbreviations xi
Table of Tables xiv
Table of Figures xv
Chapter 1. Review of Literature 1
1.1 General Background 1
1.2 Energy Metabolism 2
1.2.1 Energy Balance 2
1.2.2 Metabolic States 4
1.2.3 Integration of Fat and Carbohydrate Metabolism 7
1.3 Role of Insulin 9
1.3.1 Insulin Resistance 9
1.3.2 Aetiology of Type II Diabetes 11
1.3.3 Techniques to Assess Insulin Sensitivity 12
1.3.4 Mechanistic Role of Insulin 14
1.4 Lipid Metabolism 17
1.4.1 Association between Dietary Fat Intake and Insulin Resistance 17
1.4.2 Lipid Transport in Skeletal Muscle 19
1.4.3 Associations between Intramyocellular Lipid and Insulin Resistance 22
1.4.4 Accumulation of Lipid Intermediates and Insulin Resistance 23
1.4.5 Different Types of Fatty Acids 29
1.5 Protein Metabolism 31
1.5.1 Muscle Protein Balance 31
1.5.2 Mammalian Target of Rapamycin Pathway 32
1.5.3 Amino Acid Transporters 36
1.5.4 Regulation of Amino Acid Transporters 37
1.5.5 Physiological Importance of Amino Acid Transporters 39
1.6 Proposed Interactions between Insulin Resistance and Anabolic Resistance 40
1.7 Intermittent Fasting and Chrononutrition 42
1.7.1 Adaptive Responses to Fasting 42
1.7.2 Influence of Meal Timing on Health 44
1.7.3 Association between Meal Patterns and Health Outcomes 45
1.7.4 Diurnal Variations in Metabolism 47
1.7.5 Intermittent Fasting 48
1.7.6 Time-Restricted Feeding: Animal Models 49
1.7.7 Time-Restricted Feeding: Human Studies 51
1.8 Aims and Objectives 56

Chapter 2. General Methods 59

2.1 Participant Enrolment 59

2.1.1 Recruitment 59
2.1.2 Consent and Health Screening 59
2.1.3 General Exclusion Criteria 60
2.1.4 Standardisation Prior to Laboratory Visits 61

2.2 Laboratory Methods: Blood 61

2.2.1 Blood Sampling 61
2.2.2 Arterialisation of Venous Blood 62
2.2.3 Blood Flow Measurement 63
2.2.4 Arteriovenous Forearm Balance Model 64
2.2.5 Blood Glucose 65
2.2.6 Isolation of Plasma 66
2.2.7 Isolation of Serum 66
2.2.8 Serum Insulin 67
2.2.9 Indexes of Insulin Sensitivity 67
2.2.10 Plasma Free Fatty Acids 68
2.2.11 Serum Triglycerides 69
2.2.12 Branched Chain Amino Acids 69
2.2.13 Plasma Total Ghrelin 70
2.2.14 Serum Testosterone 70
2.2.15 Reliability of Serum and Plasma Assays 71

2.3 Laboratory Methods: Skeletal Muscle 71

2.3.1 Muscle Biopsy Sampling 71
2.3.2 Incorporation of [1-^{13}C] Phenylalanine 72
2.3.3 Muscle Glycogen 73
2.3.4 Pyruvate Dehydrogenase Complex Activation 74
2.3.5 Messenger RNA Expression 76
2.3.6 Protein Extraction 78
2.3.7 Protein Quantification 79
2.3.8 Electrophoresis/SDS-PAGE 80

2.4 Energy Expenditure and Body Composition 81

2.4.1 Calculation of Energy Expenditure 81
2.4.2 Indirect Calorimetry 82
2.4.3 Urinary Nitrogen Excretion 83
2.4.4 Dual Energy X-ray Absorptiometry 84

2.5 Free-Living Measurements 85

2.5.1 Physical Activity Monitoring 85
2.5.2 Combined Heart Rate and Accelerometery 86
2.5.3 Continuous Glucose Monitoring 88
2.5.4 Dietary Analysis 89
2.5.5 Data Analysis 90

2.6 Primary Skeletal Muscle Cell Culture 91

2.6.1 Isolation of Satellite Cells 91
2.6.2 Proliferation into Myoblasts and Differentiation into Myotubes 92
2.6.3 Fatty Acid Treatment 93
2.6.4 Glucose Uptake 93
2.6.5 System A Amino Acid Transport 94
2.6.6 Protein Synthesis 95

Chapter 3. Effect of Dietary Fat Ingestion on Muscle Protein Metabolism and Insulin Sensitivity in Overweight Men 97

3.1 Introduction 97

3.2 Methods 98

3.2.1 Participants 98
3.2.2 Statistical Power 99
3.2.3 Experimental Design 99
3.2.4 Metabolic Testing 100
3.2.5 Statistical Analysis 102

3.3 Results 102

3.3.1 Blood Glucose and Serum Insulin 102
3.3.2 Serum Triacylglycerol and Plasma Free-Fatty Acids 104
3.3.3 Respiratory Exchange Ratio and Substrate Oxidation 105
3.3.4 Plasma Amino Acids 106
3.3.5 [1-^{13}C]-Phenylalanine Appearance and Incorporation into Muscle 108
3.3.6 Muscle Protein Content 109
3.3.7 Muscle Glycogen and Pyruvate Dehydrogenase Complex Activity 111
3.3.8 Intramyocellular Lipid Content 112

3.4 Discussion 113

Chapter 4. Effect of Palmitate on Protein Metabolism in Primary Human Skeletal Myotubes 120

4.1 Introduction 120

4.2 Methods 122

4.2.1 Primary Skeletal Myotubes 122
4.2.2 Statistical Analysis 122

4.3 Results 123

4.3.1 Effects of Leucine and Insulin on System A Amino Acid Transport 123
4.3.2 Effect of Insulin on Glucose Uptake 125
4.3.3 Effect of Palmitate on Basal and Insulin-Stimulated Glucose Uptake 126
4.3.4 Effect of Palmitate on System A Transport of Amino Acids 129
4.3.5 Effect of Palmitate on Rates of Protein Synthesis 131
4.3.6 Effect of Palmitate on PP2A and 4E-BP1 Content 132

4.4 Discussion 134

Chapter 5. Effects of Two Weeks of Time-Restricted Feeding on Basal and Postprandial Metabolism in Healthy Men 140

5.1 Introduction 140

5.2 Methods 142

5.2.1 Participants 142
5.2.2 Experimental Design 143
5.2.3 Metabolic Testing 144
5.2.4 Statistical Power 146
5.2.5 Statistical Analysis 147

5.3 Results 149

5.3.1 Energy Intake 149

5.3.2 Free-Living Energy Expenditure 152
5.3.3 Body Weight and Composition 153
5.3.4 Fasting Plasma Ghrelin and Testosterone 154
5.3.5 Continuous Glucose Monitoring 155
5.3.6 Glycaemic Response(s) 157
5.3.7 Forearm (Muscle) Blood Flow and Glucose Uptake 159
5.3.8 Serum Insulin and Indexes of Whole-Body Insulin Sensitivity 160
5.3.9 Plasma Free-Fatty Acids 162
5.3.10 Serum Triglycerides (TAG) 163
5.3.11 Branched Chain Amino Acids (BCAA) 165
5.3.12 Correlation Analysis 167
5.3.13 Resting Metabolic Rate and Substrate Oxidation 167
5.3.14 Muscle Glycogen Content and Pyruvate Dehydrogenase Complex (PDC) Activity 168
5.3.15 Muscle Protein Content 169
5.3.16 Muscle Messenger RNA Expression 170
5.4 Discussion 176

Chapter 6. Effects of Two Weeks of Daily Caloric Restriction on Basal and Postprandial Metabolism in Healthy Men 192
6.1 Introduction 192
6.2 Methods 194
6.2.1 Participants 194
6.2.2 Experimental Design 194
6.2.3 Dietary Prescription 195
6.2.4 Statistical Analysis 196
6.3 Results 197
6.3.1 Free-Living Energy Expenditure 197
6.3.2 Body Composition 198
6.3.3 Continuous Glucose Monitoring 199
6.3.4 Glycaemic, Haemodynamic and Muscle Insulin Sensitivity Response(s) 200
6.3.5 Serum Insulin and Indexes of Whole-Body Insulin Sensitivity 204
6.3.6 Plasma Free-Fatty Acids 205
6.3.7 Serum Triglycerides (TAG) 207
6.3.8 Plasma Branched Chain Amino Acids 207
6.3.9 Resting Metabolic Rate and Substrate Oxidation 210
6.4 Discussion 211

Chapter 7. General Discussion 215
7.1 Overview of Findings 215
7.2 Interactions between Insulin and Anabolic Resistance 216
7.3 Applications of Time-Restricted Feeding 218
7.4 Strengths and Limitations 220
7.5 Future Research Directions 222
7.6 Conclusion 223

References 225

Appendix 267
Appendix A. [^{14}C] Oxaloacetate Preparation 267
Appendix B. Actiheart Calibration 267
Appendix C. Full List of Genes Measured 268
Appendix D. Glycaemic Profiles 269
Appendix E. PIPS Reflective Statement 270

List of Abbreviations

∅	Diameter
2-DOG	2-Deoxy-D-Glucose
4E-BP1	Eukaryotic Initiation Factor 4E-Binding Protein 1
AA	Amino Acid
ADF	Alternate Day Fasting
Akt	Protein Kinase B
AMP	Adenosine Monophosphate
AMPK	Adenosine Monophosphate-Activated Protein Kinase
ANOVA	Analysis of Variance
AS160	Akt Substrate for 160 kDa
ATP	Adenosine Triphosphate
A-V	Arteriovenous
BCAA	Branched Chain Amino Acid
BMI	Body Mass Index
cDNA	Complimentary DNA
CGM	Continuous Glucose Monitor
CHO	Carbohydrate
CoA	Coenzyme A
CPT-1	Carnitine Palmitoyl Transferase 1
CR	Caloric Restriction
C_T	Cycle Threshold
DAG	Diacylglycerol
DEXA	Dual Energy X-Ray Absorptiometry
DIT	Diet Induced Thermogenesis
DNA	Deoxyribonucleic Acid
DPM	Disintegrations Per Min
EDTA	Ethylenediaminetetraacetic Acid
EE	Energy Expenditure
EI	Energy Intake
eTRF	Early Time-Restricted Feeding
FFA	Free-Fatty Acid
FoxO	Forkhead Box O
FSR	Fractional Synthetic Rate
GCMS	Gas Chromatography Mass Spectrometry
GLUT4	Glucose Transporter 4
GSK3	Glycogen Synthase Kinase 3
HFD	High Fat Diet

HK	Hexokinase
HOMA-IR	Homeostatic Model Assessment of Insulin Resistance
HR	Heart Rate
IF	Intermittent Fasting
IMCL	Intramyocellular Lipid
IR	Insulin Resistance
IRS-1	Insulin Receptor Substrate 1
kCal	Kilocalorie
L-LDH	L-Leucine Dehydrogenase
MAFbx	Muscle Atrophy F-Box
Me-AIB	Methylaminoisobutyric Acid
METs	Metabolic Equivalent of Task
M-ISI	Matsuda Insulin Sensitivity Index
MPE	Molar Percent Excess
MPS	Muscle Protein Synthesis
mRNA	Messenger Ribonucleic Acid
mTOR	Mammalian Target of Rapamycin
mTORC1	mTOR Complex 1
mTORC2	mTOR Complex 2
MUFA	Monounsaturated Fatty Acid
MuRF1	Muscle RING Finger 1
NAD^+	Nicotinamide Adenine Dinucleotide (Oxidised)
NADH	Nicotinamide Adenine Dinucleotide (Reduced)
OGTT	Oral Glucose Tolerance Test
PA	Physical Activity
PAEE	Physical Activity Energy Expenditure
PDC	Pyruvate Dehydrogenase Complex
PDK	Pyruvate Dehydrogenase Kinase
PIP2	Phosphatidylinositol 4,5-Diphosphate
PIP3	Phosphatidylinositol 3,4,5-Triphosphate
PKC	Protein Kinase C
PP2A	Protein Phosphatase 2A
PP2Ac	Catalytic Subunit of Protein Phosphatase 2A
PPAR	Peroxisome Proliferator-Activated Receptor
PUFA	Polyunsaturated Fatty Acid
RAPTOR	Regulatory Associated Protein of mTOR
RCT	Randomised Control Trial
RER	Respiratory Exchange Ratio
RICTOR	Rapamycin Insensitive Companion of mTOR

RMR	Resting Metabolic Rate
S6K1	Ribosomal Protein S6 Kinase 1
SD	Standard Deviation
SEM	Standard Error of the Mean
SFA	Saturated Fatty Acid
SNAT2	Sodium-Coupled Neutral Amino Acid Transporter 2
SUnSET	SUrface SEnsing of Translation
TAG	Triacylglycerol/Triglyceride
TBS-T	Tris-Buffered Saline with 0.1% Tween 20
TRF	Time-Restricted Feeding
TZD	Thiazolidinediones
UNE	Urinary Nitrogen Excretion
$\dot{V}CO_2$	Carbon Dioxide Production
$\dot{V}O_2$	Oxygen Consumption
w/v	Weight:Volume

Table of Tables

Table 2.1. Coefficient of variations.....71

Table 3.1. Descriptive characteristics of study participants.....99
Table 3.2. Respiratory exchange ratio and substrate oxidation. 106
Table 3.3. Intramyocellular lipid content.....113

Table 5.1. Descriptive characteristics of study participants.....142
Table 5.2. Pearson's correlation coefficients 151
Table 5.3. Intensity and distribution of physical activity.....153
Table 5.4. Continuous glucose monitoring. 156
Table 5.5. Measures of fasting whole-body insulin sensitivity.....161
Table 5.6. Correlation analysis of metabolic outcomes. 167
Table 5.7. Indirect calorimetry measurements.....168
Table 5.8. Genes that changed in expression between the Habitual and TRF trial in the fasted state.....173
Table 5.9. Summary of genes that changed in expression between the Habitual and TRF trial.....175

Table 6.1. Descriptive characteristics of study participants.....194
Table 6.2. Intensity of physical activity.....197
Table 6.3. Body composition. 199
Table 6.4. Continuous glucose monitoring. 200
Table 6.5. Measures of fasting and postprandial whole-body insulin sensitivity.....204
Table 6.6. Indirect calorimetry measurements.....210

Table of Figures

Figure 1.1. Glucose sources during fasting. 5
Figure 1.2. Plasma metabolite and hormone concentrations in response to prolonged fasting. 6
Figure 1.3 Insulin signalling pathway. 16
Figure 1.4. Fat and CHO metabolism in skeletal muscle. 27
Figure 1.5. PI3K/Akt/mTOR signalling pathway. 34
Figure 1.6 System A and L amino acid transport. 38
Figure 2.1. Ultrasound of brachial artery. 64
Figure 3.1. Schematic of metabolic testing protocol. 100
Figure 3.2. Blood glucose. 103
Figure 3.3. Serum insulin. 103
Figure 3.4. Serum triacylglycerol 104
Figure 3.5. Plasma free-fatty acids. 105
Figure 3.6. Plasma amino acids 107
Figure 3.7. Plasma [1-^{13}C] phenylalanine enrichment. 108
Figure 3.8. [1-^{13}C] Phenylalanine incorporation. 109
Figure 3.9. Phosphorylation of 4E-BP1, mTOR and Akt. 110
Figure 3.10. Muscle glycogen content. 111
Figure 3.11. Muscle PDC activity. 112
Figure 4.1. Effect of leucine and insulin on system A transport of amino acids. 124
Figure 4.2. Effect of insulin on glucose uptake. 126
Figure 4.3. Effect of palmitate on glucose uptake and phosphorylation of Akt. 128
Figure 4.4. Effect of palmitate on system A of amino acid transport. 130
Figure 4.5. Effect of different fatty acids on system A of amino acid transport. 130
Figure 4.6. Example of images used for SUnSET quantification. 131
Figure 4.7. Effect of palmitate on protein synthesis. 132
Figure 4.8. Effect of palmitate on PP2A and p-4E-BP1 content. 133
Figure 5.1. Schematic of experimental design. 144
Figure 5.2. Schematic of main visit/metabolic testing protocol. 146

Figure 5.3. Individual change in macronutrient intake. 150
Figure 5.4. Energy and macronutrient intake. 151
Figure 5.5. Physical activity energy expenditure. 153
Figure 5.6. Changes in body composition. 154
Figure 5.7. Diurnal glycaemic profiles. 156
Figure 5.8. Arterialised, venous and A-V differences in glucose. 158
Figure 5.9. Blood flow and glucose uptake 160
Figure 5.10. Arterialised serum insulin. 161
Figure 5.11. Matsuda insulin sensitivity index. 162
Figure 5.12. Plasma free-fatty acids. 164
Figure 5.13. Arterialised serum triglycerides. 165
Figure 5.14. Plasma branched chain amino acids. 166
Figure 5.15. Pyruvate dehydrogenase complex activity. 169
Figure 5.16. Phosphorylation of Akt and 4E-BP1. 170
Figure 5.17. Change in mRNA expression in the fasted state. 172
Figure 5.18. Change in mRNA expression after feeding. 174

Figure 6.1. Schematic of experimental design. 196
Figure 6.2. Physical activity energy expenditure. 198
Figure 6.3. Diurnal glycaemic profiles. 200
Figure 6.4. Arterialised and venous glucose. 202
Figure 6.5. Glucose uptake and influencing factors. 203
Figure 6.6. Arterialised serum insulin. 205
Figure 6.7. Plasma free-fatty acids. 206
Figure 6.8. Arterialised serum triglycerides. 207
Figure 6.9. Plasma branched chain amino acids. 209

Chapter 1. Review of Literature

1.1 General Background

Modern Western lifestyles have had a deleterious impact on the prevalence of obesity and associated metabolic disorders. Technological advancements and a growth in sedentary, desk-bound jobs have contributed to the diminished levels of physical activity (PA) required to sustain daily routines (Brownson et al., 2005; Church et al., 2011). Exacerbating this is the wide availability of cheap, processed and energy-dense food which tends to promote overconsumption (Hall et al., 2019).

This starkly contrasts to the hunter-gatherer lifestyle adopted by early *Homo sapiens* during the late Palaeolithic era, which would have involved cyclical alterations between feast and famine, due to the necessary PA requirements to source food and its more sporadic availability. The selection pressures of this era are postulated to have played a key role in shaping the modern human genome. 'Thrifty' genes, that promote efficient storage and utilisation of energy, would confer a survival advantage and may have been favourably retained (Chakravarthy and Booth, 2004). Unsurprisingly, these adaptations are likely to be disadvantageous in a sedentary environment with overabundant food availability. Unlike in the past, the increased prevalence of chronic disease(s) associated with excessive food intake and physical inactivity will not exert a comparative negative selection pressure.

Indigenous populations adopting a more Western lifestyle illustrate its detrimental impact. Pima Indians of Arizona have an extremely high prevalence (38%) of obesity and type II diabetes (T2D). In contrast, those living a more traditional lifestyle in rural Mexico have T2D rates closer to non-Pima Mexicans (6.9 vs 2.6%) (Schulz et al.,

2006). Australian aborigines also experienced a sharp rise in obesity and T2D prevalence after transitioning from a traditional hunter-gatherer lifestyle (O'Dea, 1991). Whilst these observational studies do not exclude an influence of genetic factors, they clearly implicate much risk can be abrogated through lifestyle behaviours and choices (Esparza et al., 2000).

1.2 Energy Metabolism

1.2.1 Energy Balance

Energy balance describes the dynamic relationship between energy expenditure (EE) and energy intake (EI). The first law of thermodynamics states that energy cannot be created or destroyed, only modified in form. EI is determined from nutritional intake, principally the three major macronutrients; carbohydrates (CHO), fat and protein. The former two serve as predominant energy sources and their relative contribution to energy metabolism varies across different metabolic states. CHO may be synthesised into glycogen, with around 80% of this stored in skeletal muscles and most of the rest in the liver (1996; Taylor et al., 1993). Smaller amounts are also stored in other tissues including the kidneys and brain. Overall storage capacity is relatively finite, with an average fed 70 kg male having ~500 g providing around 2000 kilocalories (kCal) in total. Dietary fat is predominantly stored in the form of triacylglycerol (TAG) within adipose tissue which can expand in capacity, but also to a lesser extent in the liver and skeletal muscle. Adipose tissue provides a much larger energy reservoir than glycogen stores even within lean individuals. Although around a third of the body's total energy is stored as protein in muscles, the contribution of amino acid (AA) oxidation to energy metabolism is limited in healthy individuals without undergoing prolonged fasting.

Total EE is the sum of resting metabolic rate (RMR), diet induced thermogenesis (DIT) and physical activity energy expenditure (PAEE). RMR typically comprises 50 to 70% total EE and is the energy cost of basic metabolic processes required to sustain life, such as the functioning of vital organs. Skeletal muscle, which comprises 30 to 40% of total body mass (Janssen et al., 2000), is a major determinant of resting EE (Zurlo et al., 1990) and accounts for much of the interindividual variation between similar sized individuals (Cunningham, 1991). DIT is the energy cost associated with processing and storing nutrients. Its contribution to EE varies according to dietary composition (Raben et al., 2003) but is generally considered 10% in individuals consuming a mixed diet (Westerterp, 2004). PAEE is the energy cost associated with the daily living activities and, as such, is the most malleable component of EE. Importantly, regular PA provides a plethora of health benefits independently from its effects on adiposity (Paffenbarger et al., 1993; Sui et al., 2007)

A positive energy balance arises when EI exceeds EE. Most weight gain arises from storage of dietary fat into adipose tissue as extreme overfeeding protocols are necessary to stimulate de novo lipogenesis from CHO (Acheson et al., 1988). However, an individual's capacity to expand adipose tissue is limited and once exceeded, can lead to spill over of lipid deposition into ectopic tissues including the liver, skeletal muscle and pancreas. This is posited to play a causative role in the development of insulin resistance (IR) (Pan et al., 1997; Shulman, 2000).

Today in the United Kingdom over 2 in 3 male adults and 1 in 3 primary school aged children are classified as overweight (Body Mass Index $25 < BMI < 30$ kg·m^{-2}) or obese ($BMI \geq 30$ kg·m^{-2}) (National Health Service, 2018). This is associated with an increased risk of all-cause mortality and a major risk factor for the development of

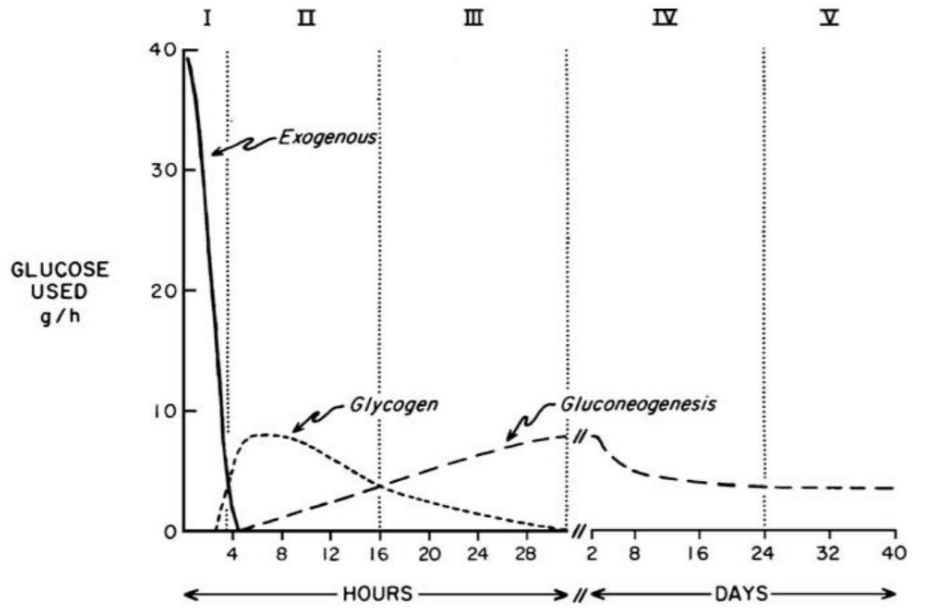
various metabolic diseases including T2D and cardiovascular disease (Calle et al., 1999). Currently, around 20% of the annual healthcare budget is attributable to the management of obesity and its related conditions (McKinsey Global Institute, 2014).

1.2.2 Metabolic States

The human body has evolved to cope with prolonged periods of low food availability by adapting fuel metabolism. The postabsorptive (fasted) state is when food from the previous meal has been absorbed and processed. Typically, this occurs several hours post-meal ingestion, but its onset is dependent on the quantity and type of food consumed. Euglycaemia is maintained through endogenous glucose sources, principally from the liver and to a lesser extent the kidneys. Figure 1.1 shows how this can be derived from the breakdown of stored glycogen (glycogenolysis) and conversion of non-CHO substrates such as lactate and AA (gluconeogenesis). This homeostatic mechanism precisely matches the rate of glucose disposal to endogenous glucose production, maintaining blood glucose concentrations between 4 and 5.4 $mmol \cdot L^{-1}$ in healthy adults. It is considered essential since the brain is reliant on glucose as a primary energy source, together with the splanchnic area accounting for ~75% of glucose utilisation at rest.

Hormonal changes during fasting include increased secretion of glucagon, growth hormone and catecholamines, whilst insulin release is supressed. The latter is predominantly responsible for the increase in lipolysis (Jensen et al., 1989) by activating lipolytic enzymes including hormone sensitive lipase and adipose triglyceride lipase. The subsequent elevation of plasma free-fatty acids (FFA) promotes their increased uptake and oxidation in the liver and skeletal muscle (discussed further in Section 1.2.3). Glycerol concentrations will also increase, which

is an important gluconeogenic precursor during fasting (Baba et al., 1995). As hepatic glycogen stores deplete during prolonged fasting the liver also synthesises ketone bodies from acetyl-CoA (formed from β-oxidation of FFA). Ketone bodies can cross the blood-brain barrier and are essential to meet the energy demands of the brain during starvation. Outside of this and when not adhering to a very low CHO diet, their contribution to energy metabolism is considered minimal and will not be discussed at length here. The change in plasma metabolite and hormonal concentrations is summarised below in **Error! Reference source not found.**.



		(I)	(II)	(III)	(IV)	(V)
ORIGIN OF BLOOD GLUCOSE	:	Exogenous	Glycogen Hepatic gluco-neogenesis	Hepatic gluconeo-genesis Glycogen	Gluconeogenesis, hepatic and renal	Gluconeogenesis, hepatic and renal
TISSUES USING GLUCOSE	:	All	All except liver. Muscle and adipose tissue at diminished rates	All except liver. Muscle and adipose tissue at rates intermediate between II and IV	Brain, rbcs, renal medulla. Small amount by muscle	Brain at a diminished rate, rbcs, renal medulla
MAJOR FUEL OF BRAIN	:	Glucose	Glucose	Glucose	Glucose, ketone bodies	Ketone bodies, glucose

Figure 1.1. Glucose sources during fasting.
A summary of how glucose utilisation and sources of glucose varies with increasing duration of fasting; rbc = red blood cells. Taken from (Cahill, 2006).

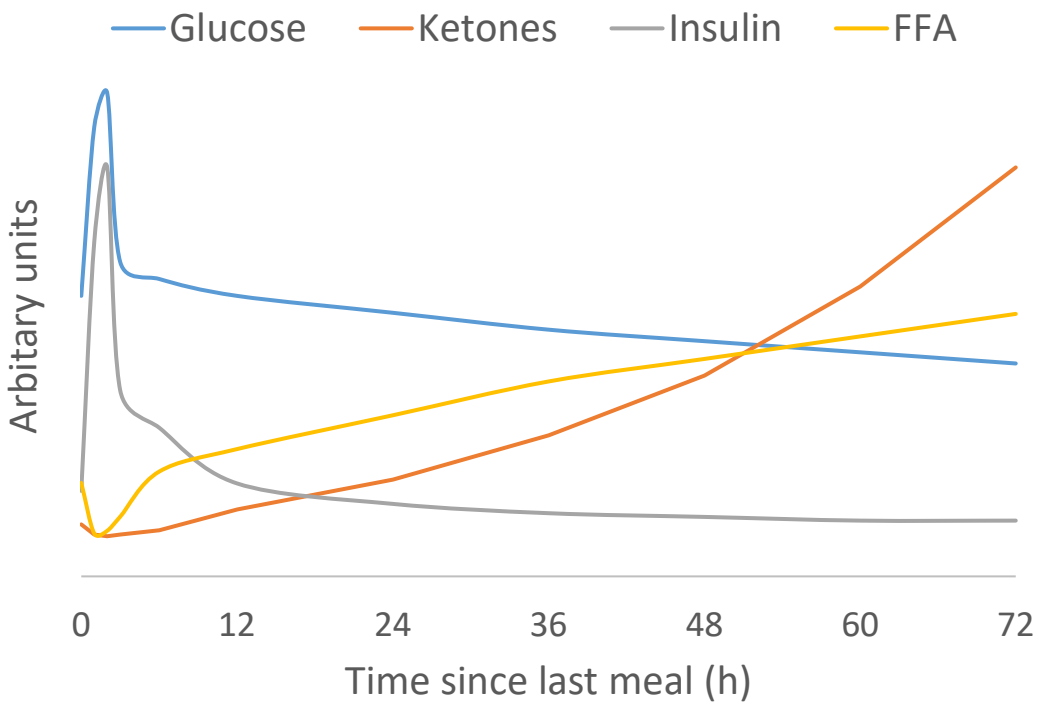


Figure 1.2. Plasma metabolite and hormone concentrations in response to prolonged fasting.

Upon ingestion of a mixed meal, the predominant fuel selection for energy metabolism shifts from fat to CHO. The β-cells of the pancreatic islets of Langerhans are highly sensitive to elevations in blood glucose and secrete insulin into the bloodstream in a dose-response fashion (Byrne et al., 1995). The rise in glucose and insulin also have inhibitory actions on the secretion of the counterregulatory hormone glucagon (Cooperberg and Cryer, 2010). These hormones are major drivers of the metabolic adaptations during the transition from a postabsorptive to postprandial (fed) state.

Glucose transporter 4 (GLUT4) translocates to the cell membrane in response to insulin stimulation and facilitates increased glucose uptake into adipose tissue and skeletal muscle (Goodyear et al., 1996). The latter is the predominant site for glucose

disposal during a euglycaemic hyperinsulinaemic clamp (DeFronzo et al., 1985; Thiebaud et al., 1982) and accounts for ~25% in response to an oral glucose load (Kelley et al., 1988). Glucose uptake into the liver also increases, principally in an insulin-independent manner, as the liver is exposed to very high glucose concentrations (Moore et al., 2012). Under postprandial conditions, glycogen synthesis in the liver and skeletal muscle are also upregulated. Fatty acid uptake increases in the insulin-stimulated condition and the metabolism of glucose (glycolysis) provides the glycerol-3-phosphate necessary to esterify FFA into TAG.

1.2.3 Integration of Fat and Carbohydrate Metabolism

The reciprocal relationship between glucose and fat metabolism is well established although the precise regulatory mechanisms are less clear. Over 50 years ago the glucose-fatty cycle was proposed by Randle et al. (Randle et al., 1963) and is based on the concept that glucose and fatty acids compete for oxidation in the mitochondria. High plasma concentrations of FFAs will favour their increased uptake and β-oxidation, the resulting products acetyl coenzyme A (acetyl-CoA) and nicotinamide adenine dinucleotide (NADH) will increase the ratio of acetyl-CoA:CoA and NADH:NAD^+, respectively. This activates pyruvates dehydrogenase kinases (PDK), principally PDK4 in skeletal muscle, which inhibit pyruvate dehydrogenase complex (PDC) (Bowker-Kinley et al., 1998; Pettit et al., 1975). PDC catalyses the irreversible formation of acetyl-CoA from pyruvate (produced from glycolysis) and hence is a key regulator in the rate of CHO oxidation. When PDC is activated, the acetyl-CoA groups formed in excess of oxidative capacity are converted to malonyl-CoA. This in turn, inhibits carnitine palmitoyl transferase 1 (CPT-1), which is the rate-limiting step for

the entry of fatty acids into the mitochondria (Ruderman et al., 1999). Conversely, a fall in malonyl CoA concentrations, when acetyl-CoA concentrations are low, promotes increased fatty acid oxidation (Foster, 2012). Other key regulatory steps proposed in the Randle cycle include the inhibition of the glycolytic enzyme phosphofructokinase via increased citrate formation (from fatty acid oxidation). This would lead to an accumulation of phosphofructokinases substrate: glucose-6-phosphate and reduce its formation by inhibiting hexokinase (HK), i.e. the initial step of glycolysis.

There is some contention as to whether all components of the Randle cycle are operational in skeletal muscle. For instance, elevating fatty acid concentrations under hyperinsulinaemic conditions attenuates glucose uptake (lipid-induced IR) but does not reduce the proportion that is oxidised (Thiébaud et al., 1982), suggesting that fatty acids may limit glucose transport rather than impair their intracellular oxidation. This was supported by (Dresner et al., 1999) who observed reductions in intracellular glucose and glucose-6-phosphate during a lipid infusion. Indeed, several studies suggest that, rather than fatty acids controlling the rate of glucose oxidation, glucose regulates the rate of fatty acid oxidation i.e. a reverse of the original Randle cycle. For instance, increasing glucose availability during a hyperinsulinaemic hyperglycemic clamp whilst maintaining constant fatty acid concentrations inhibits the rate of fat oxidation (Sidossis et al., 1998).

Regardless of the overriding mechanism, the integration of fat and CHO metabolism is highly regulated and involves a complex interplay between nutrients, hormones and transcription factors. After ingesting a CHO containing meal, healthy individuals can switch their principal energy supply from fat to CHO which is reflected

by an increased respiratory exchange ratio (RER). The RER is the ratio of carbon dioxide production to oxygen consumption and provides an index of fuel metabolism due to the increased oxygen costs associated with metabolising fat compared to glucose. Insulin is a major driver of this shift in substrate utilisation, facilitating energy storage and transition from catabolism to anabolism. Individuals with IR or obesity have an impaired ability to adapt fuel oxidation to fuel availability (Kelley and Mandarino, 2000). Considering that skeletal muscle an important site of insulin-mediated glucose uptake (Thiebaud et al., 1982), skeletal muscle IR likely plays a role in this impaired metabolic flexibility.

1.3 Role of Insulin

1.3.1 Insulin Resistance

Insulin resistance is where a normal or elevated concentration of insulin produces a diminished biological response. This is typically characterised as an impaired ability of insulin to stimulate glucose uptake primarily into skeletal muscle, but also adipose tissue and the liver (Olefsky and Nolan, 1995). Individuals with IR are less responsive to the antilipolytic actions of insulin (Groop et al., 1989) and display impaired translocation of GLUT4 in skeletal muscle, which attenuates glucose uptake and glycogen synthesis (Petersen and Shulman, 2006; Roden and Shulman, 1999). Indeed, reduced glucose disposal rates and hyperinsulinaemia are strong predictors for the development of T2D (Warram et al., 1990) and skeletal muscle IR precedes β-cell dysfunction (DeFronzo and Tripathy, 2009).

As well as reduced glucose uptake, individuals with IR are characterised by an impaired insulin-mediated suppression of hepatic glucose production (Abdul-Ghani et

al., 2006). Together these effects manifest in poorer glycaemic control, which is particularly evident in response to a meal challenge. Initially, insulin secretion is upregulated through β-cell expansion to deal with the persistent hyperglycaemia arising from IR. Over time, the excessive demand is proposed to cause dysfunctional changes as the rate of β-cell apoptosis exceeds the rate of replication. This leads to an impaired insulin response to a glucose challenge and results in a persistent hyperglycaemia that ultimately characterises T2D.

The notion that once onset, T2D is a progressive and irreversible health condition has been challenged recently. The twin cycle hypothesis (Taylor, 2008) proposes that peripheral IR will exacerbate the deposition of fat in the liver when individuals are in a chronically positive energy balance due to hyperinsulinaemia. This accumulation will lead to a reduction in hepatic insulin sensitivity, including reduced insulin-mediated suppression of hepatic glucose production and an increase in insulin concentrations necessary to maintain euglycaemia. Elevated levels of hepatic fat will increase its secretion into the bloodstream and, over time, promote increased fat infiltration into pancreatic cells and further impair the insulin response.

This theory was examined by studying the response of obese individuals with T2D to a very low-calorie diet comprising of 600 kCal per day for eight weeks (Lim et al., 2011). Remarkably, fasting plasma glucose declined from 9.2 to 5.9 $mmol \cdot L^{-1}$ within just one week. This was accompanied by a 30% reduction in hepatic fat which reached 70% by eight weeks. Alongside this, pancreatic fat was lowered by around 25% and normal insulin secretion was restored. Insulin sensitivity also increased, which was primarily attributed to an increased capability to supress hepatic glucose production. This study essentially demonstrated that T2D is a reversible condition (at least in the

short-term) but only early diagnosed (< 4 years) T2D patients were studied. An additional study replicated this design whilst including both early diagnosed (< 4 years) and longer diagnosed (> 8 years) individuals with T2D (Steven et al., 2016). They also incorporated a six-month follow-up of a stepped return to normal eating with a goal of body weight maintenance. Twelve of 30 participants responded, defined as a fasting plasma glucose < 7 $mmol \cdot L^{-1}$ after follow-up. Responders had a significantly shorter duration of T2D (3.8 ± 1.0 vs. 9.8 ± 1.6 years) and lower fasting glucose at baseline (8.9 ± 0.7 vs. 13.2 ± 0.6 $mmol \cdot L^{-1}$) than non-responders.

1.3.2 Aetiology of Type II Diabetes

The aetiology of T2D is complex and multifactorial. Its progressive nature makes it difficult to study rigorously, hence many risk factors have been derived from cross-sectional and epidemiological studies. Familial studies support a genetic role in the susceptibility for T2D, as individuals with first-degree relatives with T2D are around three times more likely to develop it themselves (Meigs et al., 2000). However, it remains difficult to differentiate and quantify the relative contribution of genetics, lifestyle and their interaction to this. This is compounded by the sheer number of genes that are likely involved, with 36 T2D-associated genes only able to account for ~10% of heritability risk (Herder and Roden, 2011). A recent genome-wide association study on around 900,000 people of European-descent uncovered around 400 genetic loci leading to an increased susceptibility to T2D (Mahajan et al., 2018). Nevertheless, the growing incidence of T2D in the modern era exceeds the levels attributable to genetic factors, implicating lifestyle-related behaviours including smoking, physical inactivity and inadequate/overnutrition.

Interestingly, the rise in T2D is currently prominent in developing countries (Ramachandran et al., 2012). This is postulated as due to rapid urbanisation and adoption of an increasingly Western lifestyle characterised by sedentary behaviour and excessive intake of highly palatable, energy-dense food (Hu, 2011). Indeed, the risk of T2D increases exponentially as a function of BMI (Chan et al., 1994) and around 85% of individuals with T2D are classified as overweight or obese (Daousi et al., 2006). It is estimated that for each 500-kCal reduction in weekly EE from leisure-time PA, age-adjusted T2D risk increases by 6% (Helmrich et al., 1991). On the other hand, adherence to a moderate energy deficit leads to improvement in cardio-metabolic risk factors including insulin sensitivity in obese (Bradley et al., 2009) and non-obese individuals alike (Kraus et al., 2019).

1.3.3 Techniques to Assess Insulin Sensitivity

Longitudinal studies demonstrate that insulin sensitivity is a good indicator of metabolic health and independent predictor of future cardiovascular disease risk and all-cause mortality in T2D patients and non-diabetics alike (Ausk et al., 2010; Facchini et al., 2001; The Emerging Risk Factors Collaboration, 2010; Yip et al., 1998). Insulin sensitivity can be directly assessed using a hyperinsulinaemic euglycaemic clamp, which is widely considered as the gold standard technique (DeFronzo et al., 1979). This technique quantifies the exogenous glucose infusion rate necessary to maintain euglycaemia in response to a primed-continuous infusion of insulin elevating concentrations to a fixed increment (steady state). When insulin concentrations are raised sufficiently (> 40 $mU \cdot L^{-1}$ in healthy subjects and > 100 $mU \cdot L^{-1}$ in IR subjects), hepatic glucose production is considered suppressed, thus blood glucose concentrations reflect the balance between glucose infusion rate and disposal. Since

under hyperinsulinaemic conditions ~80% of infused glucose is transported into skeletal muscle (Ferrannini, 1998), this primarily reflects skeletal muscle insulin sensitivity. Using this technique in combination with stable isotopic tracers permits the quantification of tissue-specific rates of glucose uptake. Whilst the clamp is a highly sensitive technique, it is time-consuming, expensive and requires skilled professionals to administer. Therefore, more simplistic approaches that provide indexes of insulin sensitivity are often used.

The glucose tolerance test is a widely used alternative; which can be administered intravenously or orally (OGTT). Route of glucose delivery is an important consideration since hepatic glucose uptake is much higher after an oral load (Cherrington, 1999). Moreover, the insulinaemic response to an oral (versus intravenous) glucose load is markedly elevated at matched concentrations of blood glucose (Nauck et al., 1986). This is likely mediated by the release of incretin hormones from the gut, such as glucagon like peptide 1, augmenting the insulin response. An advantage of the OGTT is that it accounts for inter-individual variations in gastric emptying time and incretin release, which arguably makes it a more physiologically relevant test than intravenous administration. To perform an OGTT, a fasted blood sample is obtained before the participant ingests a glucose bolus (typically either 75 g or 1 g per kg of body weight) and blood samples are obtained at regular intervals for at least 120 min. Blood samples are analysed for glucose concentrations and can be used to measure insulin.

Despite an incomplete suppression of hepatic glucose production in response to an oral load, OGTT-derived indexes correlate reasonably ($r = 0.73$) with whole-body glucose disposal rates from a clamp (DeFronzo and Matsuda, 2010; Matsuda and

DeFronzo, 1999). The Matsuda Insulin Sensitivity Index (M-ISI) is commonly used to provide an estimation of whole-body insulin sensitivity. It utilises the product of glucose (G_0) and insulin (I_0) in the fasted state which primarily reflects hepatic insulin sensitivity, as well as their postprandial responses (G_{mean} and I_{mean}) during an OGTT, which primarily reflects peripheral insulin sensitivity:

$$\text{M-ISI} = \frac{10000}{\sqrt{(G_0 \times I_0 \times G_{mean} \times I_{mean})}}$$

Both dynamic measurements are relatively time consuming to administer and can have limited practical applications within a clinical setting. More simplistic approaches include the homeostatic model assessment of IR (HOMA-IR), which is underpinned by the assumption that an increase in fasting blood glucose will result in a corresponding increase in insulin. The HOMA-IR is calculated as follows:

$$\text{HOMA-IR} = \frac{(I_0 \times G_0)}{22.5}$$

However, this static approach primarily reflects hepatic glucose production and minimises the important contribution of the periphery to glycaemic control.

1.3.4 Mechanistic Role of Insulin

As discussed, the primary action of insulin is to augment glucose uptake through increased translocation of GLUT4 stored in intracellular vesicles to the plasma membrane (Shepherd and Kahn, 1999). The insulin receptor is embedded within the cell membrane, it comprises of an extracellular membrane (two α units) connected to an intracellular domain (two β units) via disulphide bonds. The binding of insulin to the α receptor causes a conformational change resulting in the activation of tyrosine protein kinases on the β units. This leads to phosphorylation of tyrosine residues,

which facilitates the binding and subsequent activation of docking proteins, including insulin-receptor substrate 1 (IRS-1), which plays an integral role in GLUT4 translocation (Huang et al., 2005).

IRS-1 is referred to as an adapter protein, as rather than activating proteins itself, it acts as a binding site for the lipid kinase phosphoinositide 3-kinase (PI3K). Inhibiting PI3K using wortmannin abolishes the augmentation of glucose uptake in response to insulin (Yeh et al., 1995), demonstrating its fundamental role in insulin signalling. The role of PI3K is to catalyse the phosphorylation of phosphatidylinositol 4,5-diphosphate (PIP2) into phosphatidylinositol 3,4,5-triphosphate (PIP3). The latter acts as a secondary messenger by travelling along the cell membrane to activate PDK1, which is crucial to phosphorylate protein kinase B (Akt). These signalling events are summarised below in Figure 1.3.

Phosphorylated Akt can freely diffuse within the cell and phosphorylates Akt substrate for 160 kDa (AS160), which ultimately increases GLUT4 translocation (Cong et al., 1997; Mîinea et al., 2005). It also activates glycolytic enzymes including HK and phosphorylates glycogen synthase kinase 3 (GSK3) (Cross et al., 1995). The latter action prevents this enzyme from deactivating glycogen synthase and hence promotes increased glycogen synthesis. Akt also plays a key role in the regulation of cell growth, via its stimulatory effects on the mammalian target of rapamycin (mTOR) pathway (Vander Haar et al., 2007), which is discussed further in Section 1.5.2.

The secondary effects of insulin also facilitate increased glucose uptake. For instance, phosphorylation of Akt by insulin stimulates the release of nitric oxide synthase from the endothelium (Montagnani et al., 2001) causing vasodilation of blood vessels (Scherrer et al., 1994). It is also proposed to exert actions on the

microvasculature that increase capillary surface area for substrate exchange (Gudbjörnsdóttir et al., 2003). Inhibiting these actions has been shown to blunt glucose uptake by ~40% in rodents (Vincent et al., 2003). Interestingly, the decreased insulin sensitivity of obese individuals is associated with an impaired ability of insulin to augment blood flow to skeletal muscle (Laakso et al., 1990).



Figure 1.3 Insulin signalling pathway.
A summary of the insulin signalling pathway and its involvement in the regulation of glucose transport and glycogen synthesis. Taken from Yu and Chai (2015).

Insulin also exerts strong antilipolytic effects by reducing the activity of hormone sensitive lipase (Duncan et al., 2007) and adipose triglyceride lipase (Kershaw et al., 2006). The function of insulin appears to be tissue-specific; since it increases the expression of lipoprotein lipase in adipocytes (Sadur and Eckel, 1982) but has opposing effects in muscle (Kiens et al., 1989). This facilitates the uptake of FFA into adipose tissue and these combined actions lower plasma concentrations of FFA. This will limit the competitive inhibition of glucose metabolism, as elevated FFA can

disrupt insulin signalling (Dresner et al., 1999) and inhibit glycolysis (Jucker et al., 1997). Finally, increased glucose and insulin concentrations result in increased formation of malonyl-CoA which inhibits CPT-1 (Ruderman et al., 1999), the rate-limiting step of fatty acid transport into the mitochondria. Together these actions underpin the pivotal role of insulin in the regulation of energy metabolism.

1.4 Lipid Metabolism

1.4.1 Association between Dietary Fat Intake and Insulin Resistance

High fat diets (HFD) have been implicated in the development of IR, which may be partially mediated by their effect on adiposity (Bray and Popkin, 1998). An elegant 90-day feeding across five rodent species utilising 29 diets varying in macronutrient composition found that only increasing dietary fat intake (up to 60% total EI) was associated with increased EI and adiposity (Hu et al., 2018). Fat is the most energy dense macronutrient and may promote overconsumption due to its high palatability, influence on hypothalamic reward centres in the brain and relatively weak actions on satiety (Blundell et al., 1993). Rodents fed *ad libitum* tend to gain more weight and have increased fasting glucose concentrations than those consuming an isocaloric low-fat diet (Petro et al., 2004). As a result, HFD fed rodents are commonly used as a model to study the development of impaired glucose tolerance and pathophysiology of T2D (Winzell and Ahrén, 2004).

A four-year randomised control trial (RCT) of orlistat, which limits the absorption of dietary fat, found reduced incidence of T2D in individuals with obesity (Torgerson et al., 2004). However, these effects may be mediated by the greater weight loss

observed in the treatment group, as this independently reduces risk of T2D (Hamman et al., 2006) and can even lead to T2D remission (Lean et al., 2018). Typically, individuals with obesity have elevated plasma FFA which may be underpinned by a reduced responsiveness to the antilipolytic actions of insulin (Jensen et al., 1989). Indeed, even lean and nondiabetic offspring of T2D patients have elevated FFA concentrations, which are inversely related to insulin sensitivity (Perseghin et al., 1997).

Acutely elevating plasma FFA concentrations via infusion of a lipid emulsion combined with heparin (to activate lipoprotein lipase) under hyperinsulinaemic conditions causes a dose-dependent inhibition of insulin-stimulated glucose uptake in healthy volunteers (Boden et al., 1994). Similar findings have been demonstrated in individuals with obesity (Petersen et al., 1998) and T2D (Rothman et al., 1992). In these groups, glucose tolerance is further impaired from the attenuated insulin-mediated suppression of hepatic glucose production (Roden et al., 2000) and lipolysis (Kelley et al., 1993). On the other hand, short-term (7 days) treatment with the lipolysis inhibitor acipimox significantly lowers plasma FFA in T2D patients and promotes increased insulin sensitivity via an increase in insulin-stimulated nonoxidative glucose disposal (Bajaj et al., 2005). The authors also noted strong correlations between the reduction in intramyocellular long-chain fatty acyl CoAs and improvements in insulin sensitivity.

Thiazolidinediones (TZD) are a class of insulin sensitising drugs that are used for the treatment of T2D by lowering plasma FFAs. After two months of treatment with TZD, individuals with T2D had a 20% reduction in fasting plasma FFA, a 13% increase in basal fatty acid oxidation and a 46% increase in insulin-stimulated glucose

uptake (Boden et al., 2005). After TZD treatment, the expression of various genes involved in the uptake, binding and β-oxidation of fatty acids were increased in subcutaneous adipose tissue but largely unchanged in skeletal muscle. This may be attributed to the action of TZD as peroxisome proliferator-activated receptor (PPAR) agonists. More specifically on PPAR-γ, which is more abundantly expressed in adipose tissue than skeletal muscle (Kruszynska et al., 1998). In support of this, mice that are PPAR-gamma deficient in adipose tissue do not respond to the insulin sensitising effects of TZD treatment (He et al., 2003). This suggests that the insulin sensitising effects of TZD on skeletal muscle are likely secondary to the lowering of plasma FFA via PPAR-γ activation.

These findings indicate that manipulating FFA levels (both acutely and chronically) can have important effects on IR. Lipid oversupply is postulated to lead to an influx of lipids into ectopic tissue(s) such as skeletal muscle. When transportation exceeds the capacity of the tissue to store or oxidise the lipids, a build-up of lipid-derived intermediates is likely to occur. An accumulation of these are postulated to disrupt insulin signalling and lead to skeletal muscle lipotoxicity (discussed further in Section 1.4.3/1.4.4), which is strongly implicated in the pathophysiology of IR.

1.4.2 Lipid Transport in Skeletal Muscle

The adipose tissue expandability hypothesis infers that an individual's capacity to expand adipose tissue mass is limited and once exceeded, leads to ectopic lipid deposition. Excessive lipid infiltration into non-adipose tissue(s) are widely implicated as causative factors in the development of IR (Pan et al., 1997; Shulman, 2000). Obese individuals have impaired postprandial clearance of dietary fat into adipose tissue (McQuaid et al., 2011; Potts et al., 1995). Thus, levels in the blood remain elevated

which can contribute to the ‘spill over’ into ectopic tissue(s), including the liver and skeletal muscle.

Dietary fat is mainly stored as TAG, which comprises a glycerol backbone attached to three side chains of esterified fatty acids. TAG is packaged into lipoprotein carriers known as chylomicrons, for transportation in the bloodstream, with the majority deposited in subcutaneous or visceral adipose tissue. TAGs are an important fuel source for peripheral tissues, including muscle, but are first hydrolysed to fatty acids and glycerol by lipoprotein lipase before entering the cell. Plasma FFAs can freely diffuse into skeletal muscle cells but are also shuttled in by transporters, including cluster of differentiation 36 and fatty acid transporting protein. These translocate to the cell membrane during muscular contraction (Bonen et al., 2000) and in response to insulin stimulation (Luiken et al., 2002). The effects of insulin and contraction are additive and there appears to be distinct intracellular pools more sensitive to translocation via contraction or insulin (Jain et al., 2009). Cluster of differentiation 36 plays a prominent role in the adaptive regulation of fatty acid transport into muscle as knockout mice have an impaired ability to respond to insulin stimulation (Bonen et al., 2007). Translocation of all these carrier proteins to the cell membrane will contribute to determining the rates of fatty acid uptake, along with their delivery (local blood flow) and concentration.

Upon entering the cell, FFA are converted to fatty acyl CoA before re-esterification into TAG for storage, synthesis into phospholipids or to undergo β-oxidation in the mitochondria (Boden, 2001). Long-chain acyl CoA groups must initially be converted to acylcarnitines via CPT-1, in order to enter the inner mitochondrial membrane (carnitine shuttle). Generally, the fate of lipids is determined by the intramyocellular

flux; the balance between FFA entry and oxidative capacity of the muscle. When the rate of entry exceeds oxidative capacity, FFAs may be stored as TAG but are also synthesised into lipid intermediates such as ceramides and diacylglycerol (DAG) (Itani et al., 2002). The accumulation of these intermediates is thought to be limited in healthy individuals as the majority of FFAs are oxidised or stored as TAG (Dyck et al., 1997).

Chronically elevated insulin levels, as well as the accumulation of intramuscular TAG, are proposed to result in the permanent translocation of cluster of differentiation 36 transporters, leading to an excess influx of FFA (Bonen et al., 2004). Moreover, muscle from individuals with obesity and T2D has elevated malonyl CoA content (Bandyopadhyay et al., 2006) and displays mitochondrial dysfunction (Heilbronn et al., 2007; Kelley et al., 2002). This would be proposed to result in excessive accumulation of lipids and their intermediates within skeletal muscle.

However, the latter findings were derived by measuring mitochondrial enzyme activities as indexes of mitochondrial function. When directly measuring mitochondrial respiration in muscle samples, the lower oxygen flux capacity in T2D patients is normalised to that of age-matched non-diabetic controls, when expressed relative to mitochondrial deoxyribonucleic acid (DNA) levels (Boushel et al., 2007). Thus, whilst it appears that mitochondrial content is lower, perhaps due to increased inactivity/sedentary lifestyle, mitochondrial function remains largely uncompromised. Indeed, IR still develops in response to an HFD in rodents despite an adaptive increase in mitochondrial content (Hancock et al., 2008). However, it is possible that the increase in oxidative capacity was unable to fully compensate for the increased uptake of fatty acids.

1.4.3 Associations between Intramyocellular Lipid and Insulin Resistance

It was previously believed that the accumulation of intramyocellular lipids (IMCL) *per se* was key in the pathophysiology of skeletal muscle IR. For instance, a strong inverse relationship was demonstrated between IMCL content and insulin sensitivity, independently of total adiposity (Pan et al., 1997). Furthermore, accumulation of IMCL after acutely elevating FFA availability to supraphysiological concentrations, leads to a decline in insulin sensitivity (Bachmann et al., 2001). Similar findings were also observed in a more physiologically relevant model of a short-term HFD.

This was challenged when Goodpaster et al. (2001) found elevated IMCL levels in highly trained endurance athletes. These athletes exhibit mitochondrial adaptations that increase capacity for fat oxidation. They also likely have much higher turnover rates, since IMCLs are a key fuel source during light to moderate intensity PA (van Loon et al., 2003). There is a need to distinguish between subcellular fractions of lipid, with obese T2D individuals having three times higher subsarcolemmal lipid content but similar levels of intermyofibrillar lipids of normoglycaemic obese controls (Nielsen et al., 2010).

Exercise training studies have reported increased IMCL content, including the number of droplets residing close to mitochondria (Tarnopolsky et al., 2007), which likely function as a local energy store. Interestingly, the training-induced improvements of insulin sensitivity in overweight/obese IR individuals have been associated with increased IMCL content but reduced lipid intermediates (Dubé et al., 2008). When considered together, these findings suggest that the accumulation of IMCL *per se* does not cause IR and may simply act as a biomarker of dysfunctional

glucose metabolism in individuals with obesity and T2D. Instead, the focus has largely shifted to the accumulation of lipid intermediates including long-chain fatty acyl-CoAs, acylcarnitines, ceramides and DAG. The proposed effects of these are summarised in the next Section and Figure 1.4.

1.4.4 Accumulation of Lipid Intermediates and Insulin Resistance

Diacylglycerol

Diacylglycerol can be formed from the hydrolysis of TAG or synthesised from glycerol combining with long-chain fatty acyl CoA. Lipid infusion induces a transient increase in muscle DAG content that precedes the activation of protein kinase C (PKC) theta. This was associated with impaired insulin-stimulated activation of IRS-1 and supressed downstream activity of PI3K/Akt (Szendroedi et al., 2014). Accumulation of DAGs and subsequent activation of PKCθ were augmented in individuals with obesity or T2D. This could reflect differential lipid partitioning caused by an increased ratio of TAG hydrolase to DAG hydrolase (Moro et al., 2009) or reduced levels of hormone sensitive lipase (Blaak, 2004). The proposed role of PKCθ is supported in rodent knockout models which are protected from lipid-induced IR (Kim et al., 2004).

However, in other studies the peripheral IR induced by acutely elevating FFA availability has not been associated with impaired PI3K/Akt signalling (Høeg et al., 2011; Tsintzas et al., 2007). Indeed, short-term consumption of a HFD induces IR independently of changes in the proximal insulin signalling pathway (Lundsgaard et al., 2017). This study did find an increase in 1,3-DAG (position where fatty acids are

bound to glycerol) but only 1,2-DAGs accumulate in the cell membrane and activate PKCs (Wakelam, 1998).

Rodents overexpressing DAG acetyl transferase, which increases the conversion of DAG into TAG, are protected from lipid-induced IR (Liu et al., 2007). A similar overexpression model observed a paradoxical increase in DAG content, accompanied by an improvement in insulin sensitivity (Timmers et al., 2011). This suggests a more complex role for DAGs and the importance of considering the turnover rate (balance between supply and oxidation). This may explain the increased DAG content in highly trained and obese individuals (Amati et al., 2011). Exercise has been shown to increase DAG acetyl transferase (Liu et al., 2007), which suggests the increased DAG content in highly trained individuals may be from increased supply, whereas it may reflect incomplete oxidation of fatty acids in the obese population. This could explain why the DAG composition varies considerably between these groups.

Ceramides

Ceramides are sphingolipids that can be derived from palmitate and are strongly associated with IR. Previous research has shown inverse correlations between ceramide content and insulin sensitivity (Adams et al., 2004; Straczkowski et al., 2004). Elevated levels of ceramides (both saturated and unsaturated) are found in obese, but not well-trained individuals (Amati et al., 2011). This suggests ceramide synthesis is linked to lipid oversupply, but it has also been shown that inflammatory agonists augment ceramide production (Holland et al., 2011). This is important to consider as obesity and IR are widely considered as pro-inflammatory states. Although in a group of females with obesity, elevated ceramide levels were only found in those with IR (Coen et al., 2010), which could suggest a more specific role for ceramides

mediating insulin signalling. Interestingly, exercise-induced improvements in insulin sensitivity of obese adults were correlated with the reduction in ceramide but not DAG content (Dubé et al., 2008).

Supplying long-chain saturated fatty acids such as palmitate (C16:0) or stearate (C18:0) increases ceramide synthesis both *in vitro* (Chavez et al., 2003) and *in vivo* (Blachnio-Zabielska et al., 2010). Both chemically inhibiting (Holland et al., 2007) and reducing the expression of serine palmitoyl transferase (Watson et al., 2009), a key enzyme in the synthesis of ceramide from palmitate, ameliorates lipid-induced IR. The relatively low abundance of saturated fatty acids (SFA) in intralipid infusions may therefore explain why some studies do not see an acute increase in ceramide content despite inducing IR (Itani et al., 2002). Recent findings using genetic ablation to block the synthesis of specific chain lengths of ceramides, implicate C18:0 as most abundant in skeletal muscle and disruptive to glucose homeostasis (Turpin-Nolan et al., 2019).

Mechanistically, ceramides are thought to exert their effect by impaired insulin-stimulated activation of Akt through activation of PKC (Fox et al., 2007) and hyperactivation of protein phosphatase 2A (PP2A) (Dobrowsky et al., 1993). Interestingly, the modulation of PP2A activity may partly explain the variable effects of different types of fatty acids on insulin sensitivity. In support of this, only provision of palmitate was shown to activate PP2A and included IR in C2C12 cells, whereas oleic and linoleic acid were associated with enhanced Akt signalling but no effect on IRS-1/PI3K (Nardi et al., 2014). Furthermore, PP2A activation has been implicated in the dephosphorylation of eukaryotic initiation factor 4e-binding protein 1 (4E-BP1) (Gingras et al., 1999), a key translation regulator of muscle protein synthesis. This

provides a potential mechanism for the associations between IR and anabolic resistance which will be discussed in further detail in Section 1.6.

Long-Chain Acyl CoAs and Acylcarnitines

An oversupply of lipid has been implicated in the increased formation of long-chain acyl CoAs and acylcarnitines. Long-chain acyl CoAs accumulate when the rate of fatty acid uptake exceeds the capacity for fatty acid partitioning towards TAG synthesis or β-oxidation. If the acetyl-CoA formed from the latter is in excess of the capacity of the tricarboxylic acid cycle, then it is coupled to carnitine to form acetylcarnitine which can be transported out of the mitochondria to form acyl CoA and carnitine. These in turn can be converted to form malonyl-CoA or combined to form long chain acylcarnitines by CPT-1. Malonyl-CoA inhibits CPT-1 so acts to reduce fatty acid oxidation by limiting influx into the mitochondria. Acylcarnitines can enter the mitochondria where CPT2 splits them to their constituents, so that long-chain acyl CoAs can undergo β-oxidation, whilst carnitine can be recycled to buffer excess acetyl CoA groups out of the mitochondria (carnitine shuttle). Shorter chain acylcarnitines may also be formed from oxidation of AA.

The study of Tsintzas et al. (2007) observed increased accumulation of both intramuscular long-chain fatty acyl CoAs and its precursor acetylcarnitine after a 6 h lipid infusion. This likely reflects the imbalance of excessive fatty acid entry into the cell and capacity for oxidation, as well as the capacity to use the lipid-derived acetyl CoA formed in the tricarboxylic acid cycle. Coupled with a reduction in muscle glucose oxidation, they observed an increased expression of PDK4 leading to impaired insulin-stimulated activation of PDC. Both lipid intermediates have been positively associated with IR (Ellis et al., 2000; Mihalik et al., 2010) and IR is associated with

reduced expression of CPT-1, although it is currently unclear whether this is a cause or consequence of IR.

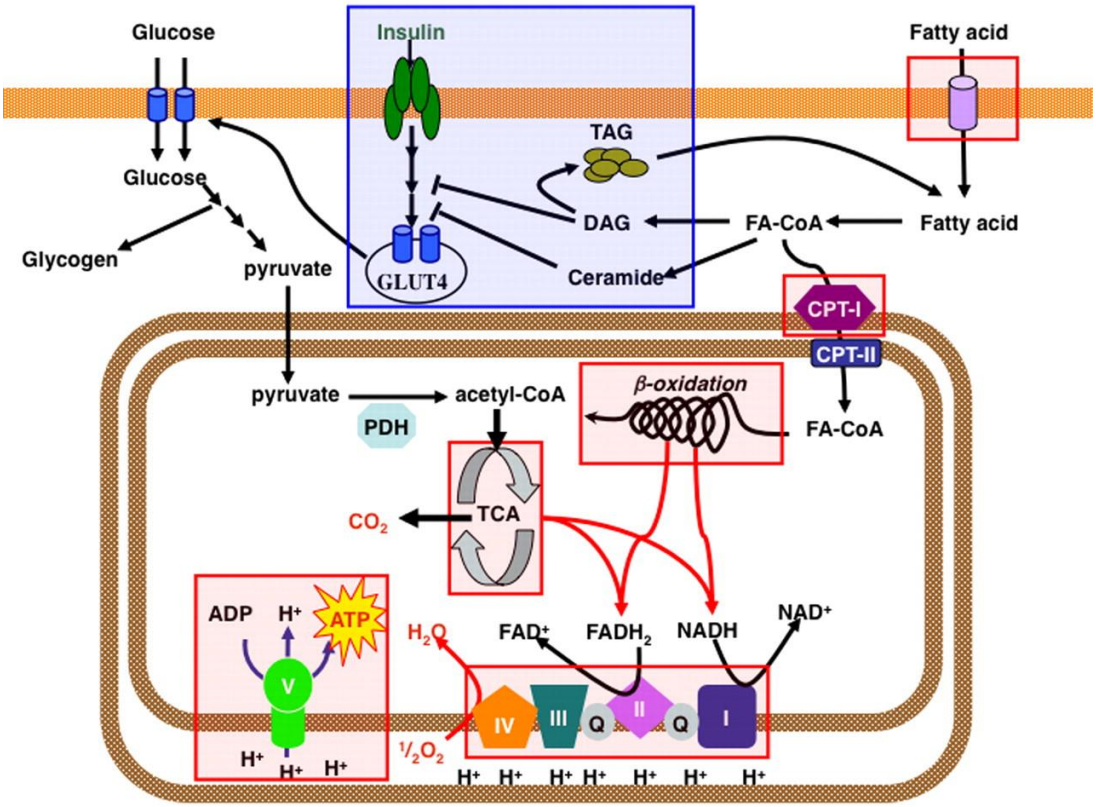


Figure 1.4. Fat and CHO metabolism in skeletal muscle.
When fatty acid uptake is in excess of utilisation lipid intermediates i.e. DAGs and ceramides accumulate. These are proposed to disrupt insulin signalling and impair the translocation of GLUT4 (blue shaded box). Fatty acid metabolism is regulated by uptake into the cell, entry into the mitochondrion (CPT-1) and β-oxidation capacity. Taken from Kraegen et al. (2008).

Role of Peroxisome Proliferator-Activated Receptors

Peroxisome proliferator-activated receptors (PPARs) are transcription factors activated by ligands that play a key role in lipid and glucose homeostasis. The ligands that activate PPARs include fatty acids and their derivatives, hence they are referred to as lipid sensors. There are three subtypes of PPAR; PPAR-α, PPAR-δ and PPAR-γ, which differ in their distribution across tissues. Of these, PPAR-α and -δ are most

strongly implicated in lipid metabolism and insulin sensitivity. Generally, the activation of PPARs increase the expression of genes involved in lipid uptake, metabolism and oxidation.

PPAR-α is highly expressed in the liver and plays a key role in regulating fatty acid oxidation, including in the adaptive response to fasting. PPAR-α knockout rodents display increased hepatic lipid accumulation in response to prolonged fasting (Leone et al., 1999), whereas wildtype mice can better upregulate fatty acid oxidation in response (Kersten et al., 1999). PPAR-α is also expressed in skeletal muscle, where its activation has been shown to upregulate the expression of PDK4 (Wu et al., 1999). This may explain the association between the lipid infusion derived accumulation of long-chain acyl CoAs with the activation of PDK4 (Tsintzas et al., 2007). However, the upregulated expression of PDK4 associated with short-term starvation, another scenario leading to a shift in substrate utilisation from CHO to fat, is paradoxically associated with downregulated PPARα expression (Tsintzas et al., 2006).

PPAR-γ is predominantly expressed in adipose tissue and involved in the storage of lipids. TZD exert their insulin sensitising effects on individuals with T2D via activation of PPAR-γ (Section 1.4.1). The targets of PPAR-γ include various genes involved in the uptake of lipids including lipoprotein lipase and fatty acid transport protein (Lehrke and Lazar, 2005). PPAR-γ activation also increases the secretion of adiponectin from adipocytes (Maeda et al., 2001) and increased circulating adiponectin promotes insulin sensitivity (Tschritter et al., 2003). This provides an additional mechanistic explanation on how PPAR-γ agonists/TZD can have an insulin sensitising effect in skeletal muscle (where PPAR-γ expression is low).

1.4.5 Different Types of Fatty Acids

Fatty acids are classified according to the chemical structure of their hydrocarbon chain. SFA are fully saturated with hydrogen (e.g. palmitic acid: $CH_3(CH_2)_{14}COOH$), whereas unsaturated fatty acids contain ≥ 1 double bond between carbon atoms (e.g. oleic acid: $CH_3(CH_2)_7CH=CH(CH_2)_7COOH$). The latter may be further grouped into mono- (MUFA) or poly-unsaturated fatty acids (PUFA) based on the number of double bonds in their structure. Length and saturation of fatty acids appear to play an important role in mediating their physiological effect. Dietary lipid profiles of rodents are a major determinant of phospholipid membrane composition (Pan and Storlien, 1993) and similar findings have been reported in humans (Andersson et al., 2002). Phospholipid membrane composition alters its fluidity and is proposed as an important factor modulating the actions of insulin (Borkman et al., 1993).

In rodents most forms of HFD (45 to 60% EI) induce IR, although generally more deleterious outcomes are associated with an increased SFA content (Buettner et al., 2006; Storlien et al., 1991). Indeed, rodents that were fed an oleate-enriched (MUFA) compared to a palmitate-enriched (SFA) diet display improved insulin and anabolic sensitivity (Tardif et al., 2011). Even different individual fatty acids within the same subclass can have variable effects. For instance, PUFA are classified as omega-3 or omega-6 according to the position of the double bond, substituting 6% of omega-6 present in an HFD with omega-3 has been shown to ameliorate IR (Storlien et al., 1987). PUFA must be obtained by dietary sources and are metabolised in a series of desaturation and elongation reactions. It is proposed that high intake of omega-6 may disrupt the processing of omega-3 fatty acids due to competition for the same enzymes, which in turn leads to an accumulation of pro-inflammatory compounds. Interestingly,

incorporation of omega-6 fatty acids into phospholipid membranes increases its permeability (Hennig and Watkins, 1989), which may lead to an increased influx of fatty acids. The increased ratio of omega-6 to omega-3 in the modern diet is proposed to be a causative factor in the rising obesity prevalence (Simopoulos, 2016).

Dietary studies in rodents should be interpreted with caution before translating findings to humans. The control group for most HFD studies is grain-based chow, which is highly variable in nutritional quality. Housing inbred mouse strains (e.g. C57BL/6J) that are genetically predisposed to gain weight in sedentary environments with continual food access is clearly not an ideal model to translate to human health (Lai et al., 2014). Indeed, emerging evidence shows that restricting food access to the active phase of the day (night-time) without caloric restriction can be protective against the deleterious effects of an HFD (Chaix et al., 2014).

It is postulated that the effects of different types of fatty acids may be from the variable partitioning into different metabolic pathways. For instance, co-incubation of palmitate with oleate ameliorates palmitate-induced IR by channelling increased TAG formation and upregulating fat oxidation (Coll et al., 2008). The palmitate-induced elevation in certain DAG species is also repressed by coincubation with palmitoleate, which limits mitochondrial dysfunction and promotes a shift towards increased neutral lipid storage (Macrae et al., 2013).

PUFA can upregulate the expression of genes encoding proteins involved in fatty acid oxidation (Clarke, 2000), which may limit the accumulation of lipotoxic intermediates. Jans et al. (2012) studied the acute effects of consuming a high fat meal varying in fatty acid composition in obese men with IR. They used the arteriovenous forearm balance model to assess flux into the muscle in combination with a dual

stable-isotope tracer (infusion of [^{2}H] palmitate and addition of [^{13}C] palmitate to the meal) so that the metabolic fate of dietary and endogenous fatty acids could be distinguished. The insulin and glucose responses were higher after the SFA meal than the PUFA meal, whereas concentrations were intermediate of these after the MUFA meal. Interestingly, the improved insulin sensitivity in the PUFA trial was associated with reduced muscle uptake of TAG-derived fatty acids which could be related to the lower postprandial insulin concentrations.

On a more chronic level, substituting dietary SFA with MUFA over three months is associated with an improvement in insulin sensitivity (Vessby et al., 2001). However, no differences could be shown when fatty acid intake was > 37% of EI and there were no protective effects of 3.6 g daily omega-3 supplementation. This contrasts with an acute study where addition of omega-3 to a lipid infusion (providing either 60 g omega-6 soybean oil or 40 g soybean oil with 20 g omega-3) partially prevented the resulting IR (Stephens et al., 2014). Moreover, eight weeks of daily supplementation with 4 g of omega-3 significantly augmented the anabolic response to hyperinsulinaemia-hyperaminoacidaemia amongst healthy individuals (Smith et al., 2011b). This likely involved the increased activation of the mammalian target of rapamycin (mTOR) pathway, discussed in more detail in Section 1.5.2.

1.5 Protein Metabolism

1.5.1 Muscle Protein Balance

Approximately 1 to 2% of skeletal muscle proteins turnover daily. This involves the opposing anabolic process of muscle protein synthesis (MPS) and catabolic process of muscle protein breakdown. The dynamic equilibrium between these

ultimately determines net muscle protein balance. Skeletal muscle displays high levels of plasticity in response to environmental stimuli. For instance, it is well known that regular resistance training with adequate nutritional intake will stimulate muscular hypertrophy (Phillips et al., 1997). On the other hand, prolonged periods of disuse (Drummond et al., 2012) or even decreased levels of PA (Breen et al., 2013) result in muscular atrophy.

Some research has suggested that insulin promotes MPS (Fujita et al., 2006), but most evidence suggests that insulin facilitates a net positive muscle protein balance by supressing proteolysis/muscle protein breakdown (Wilkes et al., 2009). Dietary protein ingestion increases the concentration of AA in the plasma and insulin has a key role in stimulating uptake into the muscle (Bonadonna et al., 1993). Most AA are used to maintain the intracellular AA pool as increasing amounts are incorporated into myofibrillar protein, which helps to sustain the stimulation of MPS (Wolfe, 2002).

1.5.2 Mammalian Target of Rapamycin Pathway

The mTOR pathway is a key regulator of cell growth and postulated to play a central role in MPS (Dickinson et al., 2011). This protein kinase is comprised of two distinct complexes: mTOR complex 1 (mTORC1) and 2 (mTORC2). Specifically inhibiting regulatory-associated protein (RAPTOR), which is an adaptor protein of mTORC1, but not rapamycin-insensitive companion of mTOR (RICTOR) which is a subunit of mTORC2, causes dysfunctional changes that result in muscular dystrophy (Bentzinger et al., 2008). Furthermore, pharmacological inhibition of mTORC1 by administering rapamycin blocks the contraction-induced augmentation of MPS in humans (Drummond et al., 2009). Importantly, mTORC1 is sensitive to the

availability of AAs which appears to be regulated through its interaction with Rag guanidine triphosphates (Sancak et al., 2008).

Provision of AAs, particularly the branched chain AA (BCAA) leucine, is a potent activator of mTORC1 (Anthony et al., 2001). Numerous growth factors, including insulin and insulin-like growth factor, also phosphorylate this complex via the PI3K/Akt signalling pathway (Rommel et al., 2001). Interestingly, mTORC2 plays an indirect role as it is required to fully activate Akt which is an important upstream regulator of mTORC1. As mentioned briefly in Section 1.3.4, Akt phosphorylates (inactivates) GSK3 and Forkhead box O (FoxO) transcription factors. The latter are key signalling molecules involved in stimulating the transcription of two E3 ligases, muscle atrophy F-box (MAFbx) and muscle RING finger 1 (MuRF1), which are involved in the ubiquitin-proteasome pathway of muscle breakdown. This helps to augment the anabolic effect of the mTOR signalling pathway by further promoting a positive protein balance. A detailed description of the complexity of this signalling pathway is provided by Bond (2016) and summarised in Figure 1.5.

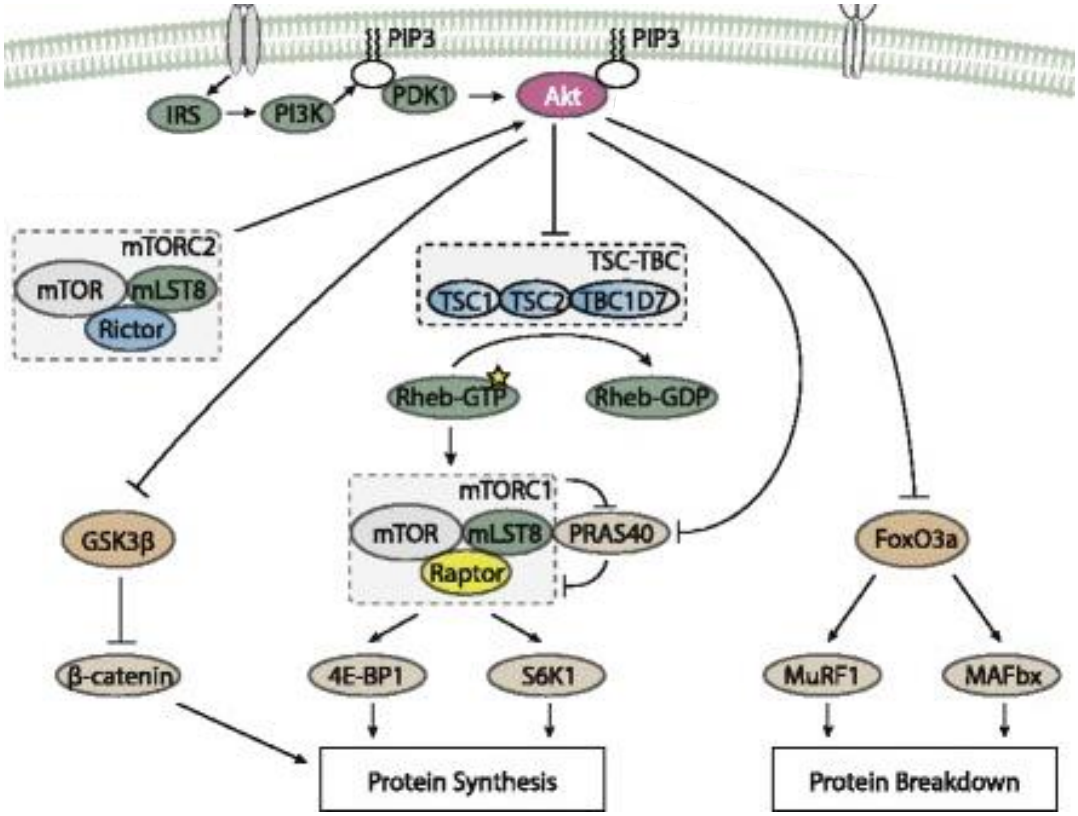


Figure 1.5. PI3K/Akt/mTOR signalling pathway.
The regulation of PI3K/Akt/mTOR signalling pathway by growth factors. Phosphorylation of Akt inhibits the TSC-TBC complex removing the inhibitory effect of Rheb-GDP on mTORC1 activation. This leads to increased phosphorylation of its downstream effectors: 4E-BP1 and S6K1 which are key regulators of MPS. Activation of Akt also promotes a positive muscle protein balance through its inhibitory effects on GSK3 and FOXO signalling. Adapted from Bond (2016).

On the other hand, AMP (adenosine monophosphate)-activated protein kinase (AMPK) which becomes activated by an increased ratio of AMP:ATP (adenosine triphosphate) (Kahn et al., 2005) is a negative regulator of mTORC1. Indeed, pharmacological activation of AMPK using 5-aminoimidazole-4-carboxamide-1-b-D-ribofuranoside reduces MPS by around 50% in rodents and blunts the phosphorylation of mTOR (Bolster et al., 2002). Thus, the activation status of mTOR is governed by its integrated response to several intracellular and extracellular signals including growth factors and nutrient availability.

Activation of mTORC1 results in phosphorylation of two downstream targets: Ribosomal protein S6 kinase 1 (S6K1) and 4E-BP1. The former results in phosphorylation of ribosomal protein 6, whereas the latter prevents the inhibitory action of 4E-BP1 on eukaryotic translation initiation factor 4E (Saxton and Sabatini, 2017). Both actions are implicated in exerting the anabolic actions of mTORC1 signalling through messenger ribonucleic acid (mRNA) translation initiation and increased ribosomal biogenesis. The complexity of this signalling pathway was demonstrated by Dreyer et al. (2006), who observed that contraction-induced activation of AMPK impairs MPS during exercise and blunts the phosphorylation of 4E-BP1 independent of mTORC1. This may suggest that 4E-BP1 is partially regulated independent of mTOR (Thoreen et al., 2009) or due to measuring phosphorylation of mTOR at serine 2448, which is an incomplete marker of mTORC1 activation (Figueiredo et al., 2017). Interestingly, a recent study found that 4E-BP1 and 4E-BP2 double knockout rodents exhibit increased MPS and are protected from the age-related loss of muscle mass (Le Bacquer et al., 2019).

Not all studies have correlated the activation of anabolic signalling with changes in MPS. This was demonstrated by Greenhaff et al. (2008) by intravenously infusing AAs at a fixed rate whilst experimentally manipulating serum insulin concentrations. Whilst elevating insulin concentrations above 30 $mU \cdot L^{-1}$ increased the activation of Akt and S6K1, it had no additive effect on MPS. This suggests a more permissive role for the effect of insulin on MPS when AA concentrations are elevated. Furthermore, provision of an isonitrogenous essential AA mixture with variable leucine concentrations found that leucine content was positively associated with mTORC1 signalling but had no synergistic effect on MPS (Glynn et al., 2010). Indeed, the

increased availability of extracellular leucine did not increase transport rate into the muscle, potentially implicating AA transporters as a rate-limiting factor regulating intracellular AA concentrations and governing the rate of MPS.

1.5.3 Amino Acid Transporters

Generally, AAs are unable to diffuse across lipid membranes. Despite this, the intracellular concentration of most AAs is appreciably higher than extracellular. Thus, active transporters are usually required to shuttle AAs into the cell against a concentration gradient. These transporters reside in pools within the cytoplasm and translocate to the cell membrane in a similar fashion to GLUT4. Several systems of AA transporters have been identified, which differ in substrate specificity, transport mechanism and regulatory characteristics (Hyde et al., 2003). More recently, they have been classified into 'families' according to their gene sequences. For instance, system A transporters (SLC38 gene family) are involved in the sodium-coupled influx of small neutral AAs such as alanine. The sodium-coupled neutral AA transporter 2 (SNAT2) (SLC38A2 gene) is ubiquitous across different tissues and most abundant isoform of this system in skeletal muscle. It utilises the trans-membrane sodium gradient to deliver AAs into the cell and is highly responsive to stimuli including insulin (McDowell et al., 1998; Walker et al., 2014), AAs (McDowell et al., 1995) and glucocorticoids (Adams, 2007).

System L transporters (gene family SLC3 and SLC7) are involved in the uptake of large neutral AAs, including BCAA, and hence play a key role in the regulation of cell growth. In this system AAs are passively transported across the cell membrane into the cell coupled with efflux of AAs out of the cell. An important AA in this exchange is glutamine, which is maintained at intracellular concentrations around 20 times

higher than extracellular (Mittendorfer et al., 2001). Glutamine can be transported via several transport systems or synthesised from BCAAs. Competitively inhibiting system A transport, by suppling a saturating dose of a non-metabolisable SNAT2 analog methylaminoisobutyric acid (Me-AIB), leads to significant depletion of intracellular glutamine and leucine (Evans et al., 2007). Since the latter is a system L substrate, this supports coupling between systems A and L.

In support of this, intracellular glutamine depletion abolishes the inward transport of leucine (Nicklin et al., 2009) and extracellular glutamine depletion causes a dose-dependent effect on intracellular leucine levels (Evans et al., 2007). Indeed, dual overexpression of these transport systems results in appreciably higher intracellular leucine accumulation than either system independently (Baird et al., 2009). Importantly, the depletion of intracellular leucine via SNAT2 inhibition or glutamine depletion blunts activation of the mTOR pathway and impairs rates of MPS (Evans et al., 2007; Nicklin et al., 2009). The involvement of SNAT2 as a determinant of intracellular system L substrates is summarised below in Figure 1.6.

1.5.4 Regulation of Amino Acid Transporters

The mRNA expression of SNAT2 is responsive to dietary and hormonal stimuli including AAs (Luo et al., 2013) and insulin (Walker et al., 2014). Administering rapamycin to inhibit mTORC1 or the PI3K inhibitor wortmannin suppresses this adaptation and the activation of anabolic signalling pathways in response to these stimuli (Peyrollier et al., 2000). These mechanisms help to augment transport activity and enhance the stimulation of anabolic pathways when the availability of AAs is elevated. Paradoxically, AA deprivation also increases the expression and surface localisation of SNAT2, known as adaptive regulation (Hundal and Taylor, 2009). This

was demonstrated by showing increased uptake of Me-AIB after AA deprivation (Nardi et al., 2015).

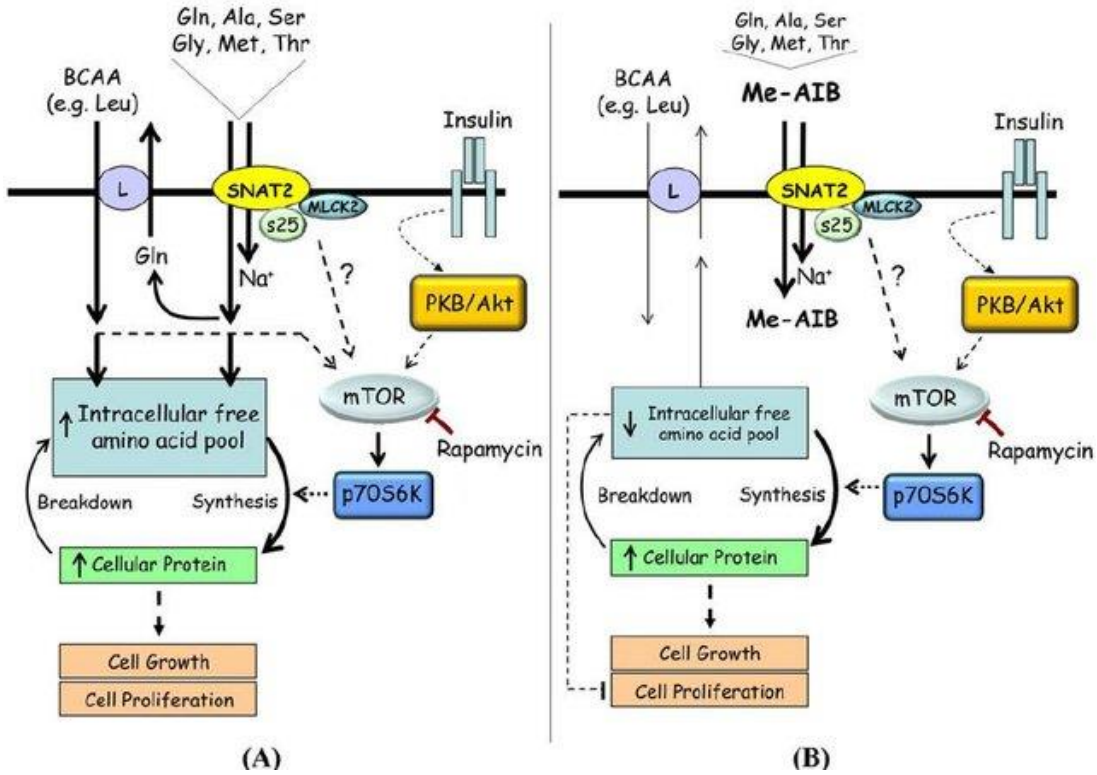


Figure 1.6 System A and L amino acid transport.
(A) How the sodium-coupled inward transport of SNAT2 substrates is involved in the regulation of System L substrates which are known to exert anabolic effects on muscle. (B) How supplying a saturating dose of Me-AIB limits this heteroexchange and diminishes the intracellular free AA pool. Taken from Pinilla et al. (2011).

Deprivation of AAs is sensed by the general control nonderepressible 2 pathway which has antagonistic actions on mTORC1, i.e. reduced translation. This induces upregulation of stress-induced activating factor 4, which directly upregulates the SLC38A2 gene encoding SNAT2 (Palii et al., 2006). Remarkably, this starvation induced response is absent when either Me-AIB or any single SNAT2 substrate is supplied (Hyde et al., 2007). Indeed, incubating AA deprived cells with a single SNAT2 substrate including Me-AIB enhances the subsequent phosphorylation of

S6K1 despite a reduction in total intracellular AAs (Pinilla et al., 2011). This implicates the transporter-substrate complex as playing a role in the initiation of anabolic signalling independently of its effects on intracellular AA concentrations and is in support of the view of SNAT2 as a transceptor; for its dual functions as transporter and receptor.

1.5.5 Physiological Importance of Amino Acid Transporters

In vitro cell culture models have provided substantial mechanistic insight into the regulation and function of AA transporters. Although some of the experimental conditions used to elucidate these, such as AA starving the cells and studying transport function upon refeeding, are extreme scenarios unlikely to occur *in vivo*. Even during prolonged starvation, plasma concentrations of most AAs do not dramatically decline, although a notable exception is alanine which is a key gluconeogenic precursor (Felig et al., 1969). An additional consideration is that the concentrations of AA and insulin used in these experimental models far exceed what would be encountered in the postprandial state *in vivo*.

Nevertheless, AA transporters have been shown to be responsive to both anabolic and catabolic stimuli *in vivo*. Ingestion of 10 g of essential AAs increases the AA concentration in the plasma and transiently upregulates the mRNA expression of several AA transporters (Drummond et al., 2010). This coincided with increased intracellular leucine accumulation and augmented phosphorylation of S6K1. A subsequent study from the same group revealed opposing responses after seven days of bedrest in healthy elderly adults (Drummond et al., 2012). Together these findings

suggest AA transporters are sensitive to both environmental stimuli *in vivo*, which implicates them as having a central role in the regulation of MPS.

1.6 Proposed Interactions between Insulin Resistance and Anabolic Resistance

Anabolic resistance is defined as the diminished capability for anabolic stimuli, such as AAs and growth factors, to stimulate MPS. This is proposed to be a primary causative factor in the age-related decline in skeletal muscle mass known as sarcopenia (Katsanos et al., 2005; Volpi et al., 2001). Young adults who are overweight or obese also have a blunted MPS response to a protein dense meal than their healthy-weight counterparts (Beals et al., 2016). However, the HOMA-IR score and insulinaemic response to the meal were comparable between the overweight and lean group, suggesting that the degree of anabolic insensitivity may be independent or earlier onset than that of IR. Interestingly, these differences were elicited despite similar rates of AA appearance in the plasma and feeding-induced upregulation of key AA transporters including SNAT2. This could suggest that a deterioration of the intrinsic quality of the muscle with increasing adiposity, such as increased intracellular accumulation of lipids, may be primarily culpable. In line with this, Murton et al. (2015) found that obese older male subjects with increased leg fat mass had reduced insulin-stimulated leg glucose disposal and are resistant in the anabolic response to AA ingestion under hyperinsulinaemia in comparison to those with lower leg fat mass.

Anabolic resistance is compounded by an increased catabolic sensitivity in the elderly, reflected by an impairment in the insulin-mediated suppression of proteolysis (Wilkes et al., 2009). Interestingly, this can be overcome upon raising insulin to

supraphysiological concentrations (Fujita et al., 2009), implicating a loss of insulin sensitivity in this population. Moreover, overweight and obese men with T2D have impaired net protein anabolism from hyperinsulianaemia when AAs were clamped at postabsorptive levels, which arises primarily from blunted stimulation of MPS, in comparison to weight matched nondiabetic controls (Pereira et al., 2008).

It is plausible that dietary fat consumption may underpin the association between IR and anabolic resistance. Acutely inducing IR through elevating FFA availability under hyperinsulinaemia has also been shown to impair the subsequent anabolic response to a bolus of protein in healthy young men (Stephens et al., 2015). The impaired phosphorylation of 4E-BP1 suggests this could be due to a disrupted anabolic signalling. Feeding rodents a HFD leads to the accumulation of intramyocellular TAG, which is exacerbated in older rats, likely reflecting their lower oxidative capacity (Tardif et al., 2014). This increase in lipid infiltration into the muscle manifests in the reduced incorporation of AAs into the muscle and lowered MPS response (Masgrau et al., 2012). As previously discussed, chronically excessive fatty acid availability may exert deleterious effects via the build-up of lipid metabolism intermediates that are proposed to impair insulin signalling (Erion and Shulman, 2010).

It appears likely that the type of fatty acid plays a key role in mediating their effect on protein metabolism. Indeed, dietary omega-3 supplementation has been shown to improve the anabolic response to AA ingestion in elderly individuals (Smith et al., 2011a). Furthermore, rats fed an oleate-enriched diet (MUFA) have improved anabolic sensitivity in comparison to those fed a palmitate-enriched diet (SFA) (Tardif et al., 2011). As mentioned in Section 1.4.5, this is likely attributed to the partitioning towards different metabolic pathways.

One plausible link between IR and anabolic resistance is via SFA-induced hyperactivation of PP2A which causes dephosphorylation of 4E-BP1 (Gingras et al., 1999) and S6K1 (Peterson et al., 1999). Moreover, the inhibitory effects of rapamycin treatment on mTORC1 activity is associated with activated PP2A and these effects are attenuated when inhibiting PP2A using okadaic acid (Liu et al., 2010).

Another possibility is that fatty acid availability directly modulates AA transport. In support of this pre-incubation of L6 muscle cells with ceramide leads to a time and dose-dependent inhibition of Me-AIB uptake (Hyde et al., 2005). This was attributed to a depletion of plasma membrane SNAT2 abundance and associated with blunted anabolic signalling and an impairment in MPS. Furthermore, pre-incubation of L6 muscle cells with linoleic acid abolishes the adaptive response to AA deprivation by promoting degradation of the SNAT2 transporter (Nardi et al., 2015). Finally, increasing the ratio of omega-3 to omega-6 in the feed of pigs across 60 days upregulates AA transporter expression in muscle including SNAT2 (Li et al., 2015). When taken together, these findings support an association between IR and anabolic resistance both at the level of AA transport into skeletal muscle and their incorporation into muscle protein, that are warranting of further investigation.

1.7 Intermittent Fasting and Chrononutrition

1.7.1 Adaptive Responses to Fasting

Fasting can be defined as the abstention of all food and drink of any caloric value. Stricter definitions also prohibit the consumption of non-caloric, caffeine containing beverages such as black coffee, which can influence metabolic rate and substrate utilisation (Acheson et al., 1980). Fasting has been used to promote health and

spirituality throughout human history and is still a prominent characteristic of some religious belief systems to this day (Trepanowski and Bloomer, 2010). Over the last century, researchers have examined the effect of prolonged fasting on body composition, typically of overweight and obese adults. A 382-day medically supervised fast demonstrates the remarkable capabilities of the human body to adapt to periods of starvation by altering fuel metabolism (Stewart and Fleming, 1973). However, such prolonged fasts are not advisable due to the associated health risks and reductions in lean body mass.

Shorter-term fasts (1 to 3 days) are also associated with several adaptive responses which drive a progressive shift in energy metabolism from glucose towards fatty acids and their derivatives. Most of the decline (~70%) in circulating insulin concentrations occurs within the first 24 h (Klein et al., 1993), which, along with the increased levels of catecholamines and growth hormone, are postulated as responsible for the increased mobilisation of TAG from adipose tissue. This increase in circulating FFA during short-term fasting (Wolfe et al., 1987) likely contributes to the impairment in whole-body insulin sensitivity, which is almost solely attributed to decreased oxidative glucose disposal (Mansell and Macdonald, 1990).

The liberation of AAs from skeletal muscle (proteolysis) and leucine oxidation rates also increase from 12 to 60 h of fasting (Fryburg et al., 1990). This was likely mediated by the increasing hypoinsulinemia as modest local hyperinsulinaemia ameliorated these differences. This suggests that insulin sensitivity with respect to muscle protein metabolism, unlike glucose metabolism, is largely conserved after short-term fasting. It is likely that the increased release of AAs, along with glycerol and lactate, serve as important gluconeogenic precursors for the liver (Garber et al.,

1974). Indeed, gluconeogenesis accounts for nearly all glucose production after just 48 h of fasting (Rothman et al., 1991). Thus, repeated fasts of this duration would lead to an inevitable decline in skeletal muscle mass and regularly fasting for ≥ 24 h is generally not recommended.

1.7.2 Influence of Meal Timing on Health

Most nutritional interventions have examined the effect of altering dietary composition and/or quantity of food intake. Recently, there has been a growing awareness of the influence of meal timing *per se*, a concept referred to as chrononutrition. The notion of three meals per day has become entrenched in society and the modern era has an unprecedented availability of cheap, energy dense food. Indeed, snacking in between meals accounts for ~25% of daily EI of adults living in the US (Kant and Graubard, 2015).

Accurately capturing eating patterns of free-living individuals is notoriously difficult. Two recent studies using camera phones to remotely track caloric events have extended our insight into temporal feeding patterns. Remarkably, around half of each cohort were found to spread their daily EI window across ≥ 15 h (Gill and Panda, 2015; Gupta et al., 2017). Consuming food with such regularity is likely to result in near continuous elevations of exogenous substrates (i.e. glucose, TAGs) across the extended postprandial periods of the day (Ruge et al., 2009). This would result in limited metabolic demand to mobilise endogenous fat stores and be further exacerbated by two prevalent lifestyle conditions prevalent in modern society; overconsumption of food and physical inactivity. This sits in stark contrast to the cyclical alterations between feast and famine throughout our evolutionary background (Chakravarthy and Booth, 2004).

1.7.3 Association between Meal Patterns and Health Outcomes

Most research looking into the association of meal patterns with health outcomes is cross-sectional and primarily focused on body composition. A systematic analysis involving 135,000 participants concluded there to be insufficient evidence to make an association between eating frequency and body composition (Canuto et al., 2017). The authors identified multiple confounding factors potentially influencing health outcomes, the vast majority were cross-sectional and only four of 31 studies were deemed high quality. RCTs that prescribe eating patterns for participants to follow are more powerful sources of evidence. One meta-analysis encompassing 15 RCTs associated increased eating frequency with reduced fat and increased fat-free mass (Schoenfeld et al., 2015). However, these effects were almost wholly mediated by a single study (Arciero et al., 2013) and predominantly undertaken on overweight/obese study populations. This demonstrates the lack of consensus on this topic within the literature.

The Adventist Health Study involved over 50,000 adults with an average follow-up time of seven years (Kahleova et al., 2017). In addition to assessing the impact of eating frequency on BMI, they included the length of overnight fast, timing of largest meal and whether individuals regularly consumed breakfast as exposure variables. Results showed that ≤ 2 meals per day was associated with lower BMI than 3 meals per day and that consuming ≥ 3 meals per day was positively associated with BMI. Interestingly, undergoing a longer overnight fast (≥ 18 h), regular breakfast consumption and consuming the largest meal at breakfast vs dinner were all independently associated with lower adiposity.

The latter finding has been replicated in a twelve-week RCT on overweight or obese individuals with metabolic syndrome (Jakubowicz et al., 2013). The group allocated a higher calorie breakfast also had greater improvements in glucose tolerance, TAG and an index of insulin sensitivity. However, these were potentially confounded by the greater weight loss in this group, despite prescribing an isocaloric diet and reporting similar degrees of dietary compliance. Another weight loss study in 420 overweight and obese individuals over 20-weeks found that those consuming a later lunch (after 3pm) lost less weight and an increased HOMA-IR score (Garaulet et al., 2013). Lunch was the predominant contributor to daily EI (~40%) in this Mediterranean study cohort and these effects were observed despite similar reported levels of EI and EE. Late lunch eaters were more likely to shift dinner to later, skip breakfast and consume a lower proportion of daily EI earlier in the day.

Koopman et al. (2014) extended some of these benefits to lean and healthy men. They prescribed a 40% hypercaloric diet for 36 men to follow over six weeks. Excess calories were from fat and/or sugar which were consumed with or between meals (as snacks). Despite similar increases in BMI, snacking was associated with increased intrahepatic TAG content and abdominal fat (visceral and subcutaneous) assessed using gold standard magnetic resonance imaging techniques. The hyperinsulinaemic-euglycaemic clamp showed no differences in peripheral insulin sensitivity but a small impairment in hepatic insulin sensitivity in the high fat-high sugar snacking group. When considered together, there appears to be preliminary evidence that meal timing *per se* can exert an influence on health outcomes. Generally, more favourable outcomes are observed when an increased proportion of EI is shifted towards earlier in the day and/or the length of overnight fast is extended at the start of it.

1.7.4 Diurnal Variations in Metabolism

On an acute level, it has been established for several decades that oral glucose tolerance and insulin sensitivity are higher in the morning than evening (Aparicio et al., 1974; Bowen and Reeves, 1967). This was initially thought to be due to earlier release of incretin hormones but persists when glucose is administered intravenously (Van Cauter et al., 1989). Reduced peripheral glucose uptake is primarily responsible for the impaired glucose tolerance in the evening (Verrillo et al., 1989). It has been theorised that the increased availability of circulating FFA (from earlier meals) may partly mediate this response (Yoshino et al., 2014). However, this is unable to explain the lower insulin, FFA and elevations in DIT in response to a meal consumed in the morning vs the evening (Bo et al., 2015). Importantly, these responses were compared within the same individual after standardisation of diet, PA level, length of fasting and duration of rest.

Interestingly, humans exhibit robust day-night rhythms in oxidative capacity, a key determinant of mitochondrial function (van Moorsel et al., 2016). Prior to waking and in the early active phase transcriptional programs promoting lipid storage, insulin sensitivity and glucose metabolism are activated (Hodge et al., 2015). Whilst simultaneously, expression of genes that are involved in lipid oxidation and protein catabolism are repressed (Dyar et al., 2018; Yoshino et al., 2014). Furthermore, an RCT found that delaying the timing of an identical lunch for one week (16:30 vs 13:30; comprising 47% total daily EI) impaired glucose tolerance in a group of young and healthy women (Bandín et al., 2015). Overall, these findings suggest there may be an acute benefit of consuming a greater proportion of EI earlier in the day, although whether these would persist on a chronic basis remains poorly understood.

1.7.5 Intermittent Fasting

Intermittent fasting (IF) has captured considerable public interest in recent years. Different IF protocols include the 5:2 diet and alternate day fasting (ADF). Most of these prescribe caloric restriction, for instance the 5:2 diet involves consuming 500 kCal on each of the two fasting days per week. This has led to some researchers questioning whether the purported benefits of IF are simply attributed to the diet-induced weight loss. To address this issue, higher quality studies include a caloric restriction control arm that seeks to match the weight loss of the IF group without altering the distribution of EI.

Generally, there is a lack of consensus on the effects of IF in the literature. Comparability is hindered by the diverse range of approaches used to study IF. These include but are not limited to; type of IF (e.g. ADF vs 5:2), participant characteristics (e.g. lean vs obese), EI (*ad libitum* vs controlled), length of intervention and even the chronological time window used for fasting/feeding. Indeed, differential effects have been observed within the same IF protocol. For instance, more favourable effects of the 5:2 diet (vs daily caloric restriction) are observed when the two fasting days were consecutive (Antoni et al., 2018a; Harvie et al., 2011) vs. non-consecutive days of the week (Carter et al., 2016). This may reflect the longer fasting duration associated with the former, although deciphering its contribution is problematic as EI is typically not confined to specific time windows in this protocol (Templeman et al., 2019).

Most IF research has been undertaken on overweight and obese individuals; longer-term interventions can elicit pronounced weight loss in these populations. Shorter-term interventions on lean participants are a viable approach to limit the confounding effect of weight loss and permit insight into the metabolic effects of IF independent of

energy balance. Both Halberg et al. (2005) and Soeters et al. (2009) utilised a 15-day ADF protocol (20 h fasts from 22:00 to 18:00 the next day). Participants total body and fat mass did not change significantly, suggesting they adequately compensated for the extended durations of fasting by increasing EI across non-fasting periods. Both studies used hyperinsulinaemic euglycaemic clamps to assess the metabolic effects of ADF, but the increase in insulin-mediated glucose uptake and suppression of lipolysis by Halberg et al. (2005) were not replicated by Soeters et al. (2009). The latter study observed increased phosphorylation of GSK3 in the basal and insulin-stimulated skeletal muscle biopsies, this would typically promote increased glycogen synthesis but was not reflected in increased whole-body non-oxidative glucose disposal. On the other hand, Halberg et al. (2005) found no significant changes in muscle glycogen content before and after ADF despite increased whole-body glucose uptake. The reasons for the discrepancy of the metabolic effects of ADF are unclear but could potentially be related to the differences in adiposity of the participants at inclusion [Halberg et al. (2005) vs. Soeters et al. (2009); body fat 20.1 vs. 14.8%; BMI 25.7 vs 21.3 $kg \cdot m^{-2}$]. Although near identical fasting plasma glucose and insulin concentrations were obtained, suggesting similar levels of hepatic insulin sensitivity.

1.7.6 Time-Restricted Feeding: Animal Models

An alternative approach to those outlined above is to allow *ad libitum* food intake within a defined daily time window (typically between 4 and 10 h). Initial evidence supporting this stems from rodent models. Arble et al. (2009) found that mice fed a HFD over six weeks in the light (nocturnal) phase gained more fat and body mass than those fed in the dark (active) phase. Diets were isocaloric suggesting that chronically altering the timing of food intake can have effects on weight gain and body

composition. However, a more sceptical viewpoint would attribute this to small, undetectable increases in EE and/or reductions in EI.

Nevertheless, these findings were extended by Hatori et al. (2012) who fed mice an isocaloric HFD or standard chow for four weeks, allowing continual food access or restricting it to the dark phase. A subsequent study from the same group replicated this finding and observed similar protective effects in response to a high sucrose diet (Chaix et al., 2014). They termed this pattern of eating time-restricted feeding (TRF). Its proposed benefits were strengthened by uncovering a dose-response relationship between length of the permitted feeding window and resulting changes in body mass. Furthermore, the beneficial effects persisted in the TRF group when allowing 24-hour food access over the weekends. Notable metabolic benefits included reduced serum TAG, lower fasting insulin and improved glucose tolerance. It has been proposed that TRF may offset some of the disruptive effects of HFDs on circadian rhythms (Sherman et al., 2012). Interestingly, it was recently demonstrated the benefits of TRF are more pronounced when feeding is restricted to the early compared to the latter half of the active phase (Delahaye et al., 2018).

Whilst rodent and humans share similar organ systems, there are several key differences that are often neglected when extrapolating findings from these studies. For instance, the relative metabolic rate of mice is seven times greater than humans (Demetrius, 2005). Of principal relevance to this discussion is the different time course of hepatic glycogen depletion during fasting, which is a primary signal to switch from glycogenolysis to metabolising fatty acids and their derivatives (Izumida et al., 2013). This ‘flipping of the metabolic switch’ has been postulated to underlie some of the benefits of IF (Anton et al., 2018). Rodents progress far more rapidly into a fasted state

with near maximal hepatic glycogen depletion within twelve hours (Chen et al., 1992). In humans, whilst most hepatic glycogen depletion occurs within 24 h (Nilsson and Hultman, 1973), it has been shown to still be declining albeit at a slower rate after 40 h of fasting (Rothman et al., 1991). Finally, an acute prolonged fast is associated with IR in humans (Hoeks et al., 2010) whereas fasted mice display improved insulin-stimulated glucose uptake (Heijboer et al., 2005). Thus, whilst TRF appears to be a promising approach in rodents, it may not exert similar effects in humans. This emphasises the need to replicate similar protocols in rigorously controlled studies using human volunteers.

1.7.7 Time-Restricted Feeding: Human Studies

The effects of distributing daily EI spread across one or three meals on 15 normal weight middle-aged participants was examined in an eight-week RCT by Stote et al. (2007) and Carlson et al. (2007). All food was provided, which allowed the macronutrient composition of each diet to be matched and EI adjusted throughout to maintain body weight. Dinner consumption was supervised and participants in the one meal a day group were required to consume all allocated food between 17:00 and 21:00 (minimum 20 h fast between days). Although study completers maintained their body weight within 2 kg across the six-month study period, there was an increased loss of body and fat mass in the one vs three meal per day group. Despite this, they found impaired glucose homeostasis including; increased fasting glucose concentration, lower postprandial insulin sensitivity and an elevated glycaemic response to an OGTT. However, the authors acknowledged these findings may be confounded by the increased amount of food consumed the evening before the OGTT. Alternatively, they could represent a maladaptive circadian response to becoming

unaccustomed to EI in the morning as participants were all habitual breakfast consumers prior to entering the study.

Moro et al. (2016) utilised an alternative approach by assessing the effect of changing the timing of 3 meals within the day. Both groups consumed their evening meals at 20:00 with the first meal of the day consumed at 08:00 in the control or 13:00 in the TRF group. Thus, the TRF group had a minimum daily fasting duration of 16 h. Diets were matched for macronutrient composition and aimed to meet the daily energy requirements of the resistance-trained males in full. These meal patterns were applied across eight weeks in combination with a standardised resistance training program performed on 3 non-consecutive days of the week (between 16:00 and 18:00). Fat-free mass was maintained after both diets despite a reduction in testosterone and insulin-growth factor 1 after TRF. Reductions in fat mass were only found in the TRF group, which corresponded with a lower fasted RER post-TRF, suggesting a shift towards increased fat metabolism. Other notable metabolic changes after TRF were reductions in fasting insulin, glucose and TAG. Unfortunately, no postprandial measurements were undertaken in this study.

Perhaps the most extensive body of research on TRF has been undertaken during the Islamic calendar month of Ramadan. This entails the complete abstention from food (fasting) and drink from dawn to sunset, although the actual length of daily fasting time can vary substantially across different calendar years and according to geographical location. Most Ramadan studies undertaken are observational and do not include a control group with matched weight loss. Consequently, the cardio-metabolic effects of Ramadan fasting can often not be directly attributed to IF.

This pattern of eating has also been associated with disrupted sleep patterns and lower PA levels (BaHammam et al., 2010; 2013; Lessan et al., 2018). These lifestyle changes associated with Ramadan can lead to a delay in circadian rhythms and altered release pattern of important regulatory hormones such as cortisol (Bahijri et al., 2013). Moreover, the timing of the feeding window during Ramadan is in direct chronological opposition of when genes involved in insulin sensitivity and glucose metabolism are most activated (Hodge et al., 2015), thus it appears unlikely that this pattern of eating is an optimal approach for TRF to promote metabolic health.

Studies have also examined the impact of prolonging the overnight fast by skipping breakfast. The Bath Breakfast Project was a series of six-week RCTs that allocated groups of lean and obese individuals to either daily breakfast consumption or fasting (water only) until noon. Groups were comprised of both habitual breakfast consumers and skippers. Participants allocated to the breakfast group were free to choose what food and drink they consumed but were instructed to consume ≥ 700 kCal before 11:00 and ≥ 350 kCal within 2 h of waking up. Thus, whilst strict daily feeding/fasting regimens were not prescribed, there were likely to be pronounced differences in daily fasting time between groups.

The project was predominantly focused on energy balance and used a combined heart rate / accelerometer to objectively measure free-living PA levels in combination with weighed food diaries. Interestingly, the PA levels of lean individuals in the breakfast group were elevated, primarily due to increased light-intensity PA in the morning (Betts et al., 2014). Although habitual PA levels of participants before the intervention were not reported, these are unlikely to fully account for this difference. Moreover, the breakfast group also had an improvement in glycaemic variability

during the afternoon/evening. Obese individuals in the breakfast group also had increased PA levels in the morning but this was not significant when assessed across the full day (Chowdhury et al., 2016). More interestingly, the insulinaemic response to an OGTT was lower after six weeks of regular breakfast consumption despite numerically higher weight gain in this group (1.0 kg; 95% CI: 0.2, 1.7 kg vs 0.2 kg; 95% CI: -0.5, 1.0 kg).

Overall, the results of this RCT suggest that extended morning fasting across six weeks does not have favourable metabolic effects. Instead, the increased postprandial insulin response of the obese fasting group could suggest deleterious effects of skipping breakfast on insulin sensitivity. Similar findings were reported in a shorter-term (two-week) RCT on breakfast omission from our group on healthy lean women (Farshchi et al., 2005). In line with this, longitudinal studies have shown detrimental effects of breakfast skipping on cardiometabolic health including increased fasting insulin concentrations (Smith et al., 2010). However, untangling the independent contribution of breakfast from associated lifestyle related behaviours of regular breakfast consumers is notoriously difficult.

Hutchison et al. (2019) undertook an RCT to compare the effects of different time windows of TRF (08:00 to 17:00 vs 12:00 to 21:00) on 15 middle-aged men with obesity. Metabolic responses to a mixed liquid-nutrient meal test were assessed pre and post each 7-day intervention after undergoing a matched duration of fast. Both schedules of TRF elicited improvements in the glycaemic response with a tendency for a reduced insulinaemic response. These differences could not be attributed to changes in gastric emptying time. At the start of the study, participants lifestyle

behaviours were monitored across a habitual (baseline) week. This showed no differences in PA or mean 24 h glucose levels between conditions.

The most promising study to date on the metabolic effects of time-restricted feeding was undertaken by Sutton et al. (2018). This RCT allocated eight overweight men with pre-diabetes to a five-week isocaloric diet using a daily EI window of 6 or 12 h. The researchers hypothesised that shifting EI to earlier in the day (in closer alignment with the diurnal variation in insulin sensitivity) may confer additional benefits over traditional TRF approaches that extend the overnight fast by skipping breakfast. As a result, participants in the TRF group consumed dinner before 15:00 which was classified as early TRF (eTRF). Four participants completed the eTRF intervention first to minimise any treatment order effect. All meals were consumed under supervision which permitted food intake to be precisely matched between study arms and body weight to be closely monitored throughout. Despite this, they did observe a small amount of weight loss in both groups (1.4 ± 1.3 kg in eTRF group and 1.0 ± 0.5 kg in the other). The primary outcomes of the study were the glycaemic and insulinaemic response to an OGTT. The eTRF group had reductions in fasting and postprandial insulin concentrations, as well as improvements in the insulinogenic index and a lowering of IR (incremental AUC ratio) in this population. The mechanisms behind these improvements are warranting of further investigation. They also found an increase in fasting TAGs but this likely reflected the longer fasting duration (18 versus 12 h) prior to metabolic testing. Considering a single bout of prolonged fasting can acutely decrease insulin sensitivity, the authors speculate this study may have even underestimated the extent of insulinaemic benefits of eTRF. Although it is unclear whether 18 h is enough to elicit a tangible difference as most

studies used acute fasting lengths ≥ 24 h. Overall, these preliminary findings suggest that the metabolic benefits of eTRF cannot be directly attributed to weight loss *per se*.

1.8 Aims and Objectives

The general aim of the studies presented in this thesis were to further explore the interactions between insulin and anabolic resistance in human skeletal muscle using nutritional approaches to alter substrate availability. In Chapters 3 and 4, the effects of an acute lipid overload were examined *in vivo* and in a relevant *in vitro* cell model. In Chapters 5 and 6, the metabolic effects of eTRF, an intervention purported to improve insulin sensitivity through repeated prolonged daily fasting periods, were investigated. This was undertaken to assess the effects of a change in insulin sensitivity, in the absence of elevating dietary lipid availability, on skeletal muscle metabolism.

Chapters Three and Four

Excess consumption of dietary SFAs is postulated to play a key role in the development of IR, which has been associated with an impaired ability of AAs to stimulate MPS. This may underpin the muscle mass loss associated with ageing (sarcopenia) and T2D. Our laboratory recently demonstrated that elevating FFA availability through a lipid infusion under hyperinsulinaemia can induce IR of CHO metabolism and impair the subsequent MPS response in healthy, young males. In study one (Chapter 3), we aimed to extend upon this by investigating whether the incorporation of dietary [1-^{13}C] phenylalanine into the myofibrillar pool is impaired after a high fat meal in overweight/obese middle-aged individuals. Ingestion of a high fat liquid meal induces a comparable degree of muscle IR to a lipid infusion and may

provide a more physiologically relevant model to study the proposed interactions between insulin and anabolic resistance.

Surprisingly, ingestion of the lipid drink did not lead to an impairment in insulin sensitivity and was associated with a two-fold greater incorporation of dietary [1-^{13}C] phenylalanine into the myofibrillar pool. The mechanism behind this was unclear, but lower postprandial AA concentrations in the lipid trial may indicate enhanced AA transport into the muscle. To further investigate this, in Chapter 4, the effect of fatty acid incubations on a primary human skeletal muscle cell culture model was explored. Pre-incubation of myotubes with 0.25 mM palmitate was shown to induce IR of CHO metabolism (i.e. attenuated insulin-stimulated glucose transport), inhibited system A transport of AA and tended to downregulate MPS. Potential mechanisms behind these responses were also explored.

Chapters Five and Six

TRF is a form of IF that permits *ad libitum* EI within a defined daily time window, typically between 4 to 10 h. This would be a significant intervention considering many adults spread their daily EI across ≥ 14 h. The benefits of IF are postulated to be underpinned by the switch in substrate metabolism from glucose to fatty acids during fasting. In rodents, TRF elicits metabolic benefits that include enhanced insulin sensitivity, independently of energy balance. Most IF studies undertaken in humans to date have involved prolonging the overnight fast (i.e. by skipping breakfast) or eating throughout the night (i.e. during Ramadan). Considering that the acute metabolic response to a meal is improved in the morning, we hypothesised that there may be a benefit of chronically restricting EI to earlier in the day (eTRF).

To address this in study three (Chapter 5) we instructed a group of healthy young males to restrict their daily EI window to between 08:00 and 16:00 for two weeks. By permitting *ad libitum* food intake and objectively monitoring PA levels, we were able to assess the impact of eTRF on both components of energy balance in a free-living setting. Extensive metabolic testing was undertaken before and after eTRF to assess their metabolic response to a CHO and protein drink using the arterio-venous forearm balance model. This permitted an estimation of the flux of metabolic substrates (i.e. glucose and BCAA) across the forearm to provide an index of skeletal muscle insulin and anabolic sensitivity. Muscle biopsies were obtained to investigate metabolic function and DEXA scans were used to assess changes in body composition.

We identified several favourable metabolic adaptations after following this temporal eating pattern including enhanced whole-body and skeletal muscle insulin sensitivity. However, eTRF led to an involuntary reduction in EI and a small, but significant weight loss of around 1 kg. Therefore, to address this potentially confounding factor, in study four (Chapter 6) an additional group (matched for age, BMI and physical activity) were recruited. We prescribed diets (matched in macronutrient composition) with the aim of replicating the energy deficit and associated weight loss observed during eTRF, without altering the temporal distribution of EI.

Chapter 2. General Methods

2.1 Participant Enrolment

2.1.1 Recruitment

Participants were recruited via posters, briefly outlining details of each study and key inclusion criteria. These were placed around the university campus and posted on online social media platforms (e.g. www.facebook.com). Individuals that expressed an interest were provided with an information sheet providing more details of the study and the commitments entailed. Those who maintained an interest were invited to attend a health screening to assess their eligibility to participate. The health screening and all other *in vivo* experimentation were undertaken at the David Greenfield Human Physiology Unit at the Medical School, Queens Medical Centre, University of Nottingham. All studies were approved by the Faculty of Medicine & Health Sciences Research Ethics Committee.

2.1.2 Consent and Health Screening

Initially, a detailed verbal explanation of the study was provided and participants were encouraged to ask any questions that arose. If happy to proceed, they were asked to sign two copies of a witnessed consent form. They kept one copy for reference and were reminded that consent was ongoing, so they were free to withdraw at any time without being obligated to provide a reason. All consenting individuals were then given a health screening prior to any study enrolment. This was to determine the suitability of the individual to participate, including whether they met the inclusion criteria for the respective study.

All individuals completed an information sheet asking basic questions on their general health and lifestyle behaviours, including the presence of any chronic medical condition(s). After checking this, they were asked to remove shoes and any item(s) in pockets prior to the measurement of body mass (to the nearest 0.1 kg) on an electronic scale. Next, height was measured (to the nearest 0.1 cm) using a stadiometer. From this BMI could be calculated to provide an index of adiposity:

$$\text{BMI } (\text{kg}\cdot\text{m}^{-2}) = \frac{\text{Body mass (kg)}}{\text{Height (m)}}$$

Next, a 12-lead electrocardiogram was recorded with participants lying in a supine position. After identification of the sternal angle, six leads were attached to electrode pads across the chest and four on the periphery (both wrists and ankles). The trace of the chart was subsequently examined for the presence of any heart abnormalities by a qualified medical doctor. Two supine blood pressure measurements were obtained with an automated inflatable cuff placed around the upper arm. A further two measurements were recorded after standing for one minute to assess orthostatic hypotension. Finally, a small blood sample was obtained from a superficial forearm vein via venepuncture for routine testing at Clinical Pathology (Queens Medical Centre, Nottingham, UK); this included a full blood count, urea + electrolyte count and a test of clotting factors.

2.1.3 General Exclusion Criteria

General exclusion criteria applicable to all studies presented in this thesis are stated below. Specific criteria for each study are mentioned in the relevant experimental chapter. This exclusion criteria included:

- Smoking

- Any metabolic (e.g. diabetes), endocrine (e.g. hyperthyroidism) or cardiovascular (heart or blood) abnormalities including hypertension.
- Clinically significant abnormalities on screening.
- Routine medication that may alter cardiovascular function and blood flow (e.g. blood pressure-lowering drugs or drugs that cause hypertension).
- High alcohol consumption (routinely > 4 units per day).

2.1.4 Standardisation Prior to Laboratory Visits

All participants were instructed to refrain from any intense exercise and alcohol consumption for at least 24 h prior to each main visit (Brouns et al., 2005). Where metabolic measurements were undertaken, a standardised ready-meal was provided for consumption the evening before. This was to control for its effects on fasting and postprandial substrate metabolism the next day (Robertson et al., 2002). Participants were asked to undergo an overnight fast (water only permitted), before arriving at the laboratory at ~08:00 using either public transport or a taxi that was provided for them. Muscle biopsy donors for the generation of primary muscle cultures arrived in the morning after an overnight fast or in the early afternoon after consuming a light breakfast ≥ 5 h prior to the visit.

2.2 Laboratory Methods: Blood

2.2.1 Blood Sampling

In Chapters 3, 5 and 6 all blood samples were obtained via intravenous cannulas using a three-way tap. An alcohol wipe was used to clean the injection site prior to provision of local anaesthetic (1% lidocaine) and insertion of a sterile 12G cannula. In Chapters 5 and 6, the first cannula was placed into a deep lying branch of an antecubital vein identified using ultrasound, this was assumed to be principally

draining skeletal muscles of the forearm (Coles et al., 1958). The hand of the contralateral arm was immersed in warm water to promote vasodilatation, before inserting a cannula retrograde in a superficial dorsal hand vein. This hand was placed in a heated plexiglass box maintained at 55℃ to arterialise the venous blood (see 2.2.2). Arterialised-venous and deep venous blood samples were drawn simultaneously at all sampling times. The first 2 ml of blood drawn was discarded and lines were kept patent by flushing with a sterile saline solution (0.9% NaCl) after sampling.

2.2.2 Arterialisation of Venous Blood

Due to the inherent risks associated with direct cannulation of an artery, the heated hand technique was used. As the skin temperature of the hand is warmed to above 37℃ there is an increased blood flow from vasodilation of the forearm muscle and opening of the arteriovenous anastomoses (McGuire et al., 1976). Capillary beds open to increase blood flow to the skin and disperse heat, the heat-induced vasodilatation reduces blood transit time and results in arterialised-venous blood that is similar in concentrations of metabolites to arterial blood (McGuire et al., 1976).

Liu et al. (1992) showed that glucose concentrations of arterialised-venous were around 0.1 $mmol \cdot L^{-1}$ lower than arterial blood (95% CI of differences; −0.19 to 0.41 $mmol \cdot L^{-1}$) under euglycaemic hyperinsulinaemic conditions. The elevation in skin temperature was achieved by placing the hand in a heated box with almost static warm air at 55℃. Unlike other methods used, such as a warm blanket, this technique has minimal effects on core temperature and blood flow distribution to the contralateral forearm (Gallen and Macdonald, 1990). A ten min incubation is necessary to sufficiently arterialise the blood with oxygen saturations of 96% and a skin

temperature of ~45℃ (Kurpad et al., 1994). Therefore, each participants hand was maintained in the heated box for a ≥ 10 min prior to obtaining any samples.

2.2.3 Blood Flow Measurement

In Chapters 5 and 6 blood flow of the brachial artery was estimated by a trained technician using Doppler ultrasound (Toshiba Aplio XV SSA-770A, Toshiba Medical Systems Corporation, Tokyo, JP) immediately after all blood sample collections. This technique correlates well (r^2 = 0.87 to 0.98) with strain-gauge venous occlusion plethysmography over a wide range of blood flows (Tschakovsky et al., 1995). The probe was placed 2 to 5 cm proximal to the antecubital fossa to visualise the brachial artery longitudinally, which was marked to ensure comparable accurate placement for repeated measurements. Three brachial artery diameter (∅) measurements; the distance from the anterior to posterior 'm' line (the interface between the media and adventitia), were recorded in both the diastolic and systolic phases of the cardiac cycle (Figure 2.1). Velocity of the flowing blood was measured using a pulsed doppler signal at 60° to the artery. The emitted high frequency soundwaves reflect off circulating red blood cells and the resulting change in frequency is detected. All measurements were performed by the same investigator and in order to account for any contralateral differences in the vasculature, the same arm was used for deep vein cannulation and blood flow assessment in both visits where possible. Blood flow could then be estimated using the following equations:

$$\text{Brachial artery } \emptyset \text{ (BAD)} = \left(\frac{2 \times \text{diastolic } \emptyset}{3}\right) + \left(\frac{\text{systolic } \emptyset}{3}\right)$$

$$\text{Brachial artery CSA} = \pi \times (0.5 \times BAD)^2$$

$$\text{Blood flow } (cm^3 \cdot min^{-1} \text{ or } ml \cdot min^{-1}) = \text{BACSA } (cm^2) \times \text{velocity } (cm \cdot min^{-1})$$

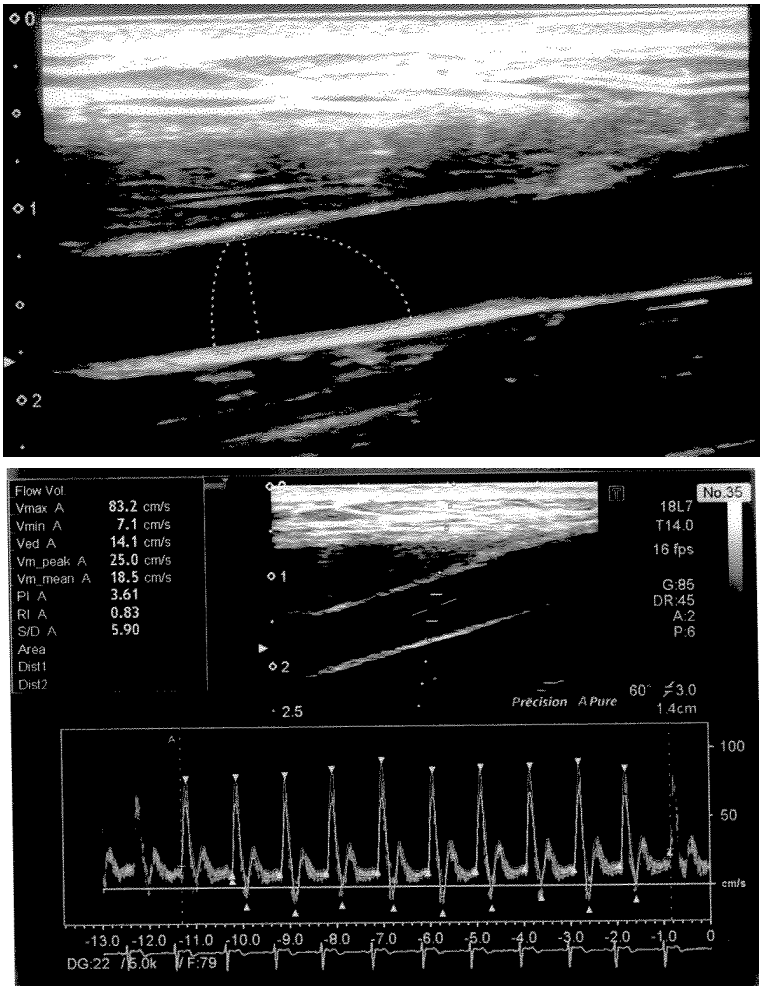


Figure 2.1. Ultrasound of brachial artery.
An example of how brachial artery diameter and velocity of the flowing blood was estimated.

2.2.4 Arteriovenous Forearm Balance Model

The arteriovenous (A-V) balance method has been widely adopted to study flux of metabolites across peripheral tissues such as the arm or leg. The technique relies on the Fick principle, which states that the rate of uptake ($\dot{Q}$) of a substrate by a given tissue is proportional to the product of the A-V difference in concentration and local (brachial artery) blood flow (F). In Chapters 5 and 6, this was standardised relative to the lean mass of the forearm (M) determined by DEXA. Forearm substrate uptake:

$$\dot{Q} = \frac{F\ (A - V)}{M}$$

Skeletal muscle accounts for ~70% of the volume of the forearm (Maughan et al., 1984) and receives ~80% of its blood flow under resting conditions (Cooper et al., 1955). It also plays a key role in glucose disposal in the postprandial state and hence is considered the dominant contributor to the observed metabolic balance in this model. As stated above, many studies observe small to no differences between arterial and arterialised concentrations of various metabolic substrates (Abumrad et al., 1981; Jensen and Heiling, 1991). As a result, the A-V model had been widely adopted as a practical research tool that avoids the use of expensive tracers.

However, like all models it has limitations and appropriate caution must be taken when interpreting results obtained from this approach. Any small divergence from 'true' arterial concentrations of metabolites can become rapidly magnified as flux values when multiplied by estimates of blood flow. Moreover, it cannot be assumed that metabolism of the forearm is representative of all peripheral tissues. Indeed, substrate balance across the leg and forearm were different in the fasted state, despite obtaining identical arterial concentrations (Möller-Loswick et al., 1991). Ultimately, this is likely accounted for by the large differences in tissue/volume mass, as well as variation in fibre type composition between these regions.

2.2.5 Blood Glucose

Immediately after collection, 0.5 ml of whole blood was added to micro tubes (Sarstedt, Nümbrecht, DE) containing sodium fluoride (to inhibit glycolysis) and heparin (to prevent clotting). These were inverted to mix and placed on a roller for a ≥ 3 min prior to determining glucose concentrations using the glucose oxidase method

(YSI 2300 STAT PLUS Glucose & Lactate Analyser, Yellow Springs Instruments, Ohio, USA). Glucose oxidase catalyses the conversion of glucose to hydrogen peroxide (H_2O_2), which is subsequently oxidised and releases electrons. When the reaction is in dynamic equilibrium, the electron flow is linearly proportional to H_2O_2 concentration, which is determined by the initial blood glucose concentration. The YSI analyser was calibrated on the morning of each study visit using an internal glucose standard of 10 mM.

2.2.6 Isolation of Plasma

Blood was dispensed into two vacutainers; one coated with ethylenediaminetetraacetic acid (EDTA) and the other with sodium heparin. Aprotinin (500 KIU·ml^{-1}of whole blood) was added to EDTA vacutainers and egtazic acid-glutathione (7.5 µl·ml^{-1} of whole blood) was added to sodium heparin vacutainers for the preservation of 'appetite' hormones and catecholamines, respectively. Vacutainers were gently mixed prior to being spun at 4400 x g for 10 min at 4℃ in a centrifuge. The resultant supernatant was quickly transferred into a −20℃ freezer. Plasma from the sodium heparin tube was transferred to tubes containing tetrahydralipostatin to inhibit lipolytic activity for the subsequent determination of FFA.

2.2.7 Isolation of Serum

Blood was dispensed into a vacutainer containing clotting activation factors and left to clot at room temperature for ≥ 20 min. Vacutainers were spun at 4400 x g for 10 min at 4℃, before the supernatant was transferred into a freezer at −20℃. At the end of each study day, all samples were moved to freezers maintained at −80℃.

2.2.8 Serum Insulin

In Chapters 3, 5 and 6 serum insulin concentrations were determined using a solid phase ^{125}I radioimmunoassay kit (Human Insulin Assay HI-14K, Merck Millipore, Burlington, MI, USA). This assay utilises ^{125}I-labelled human insulin, diluted with human insulin antiserum, to determine insulin concentrations using the double antibody technique (Morgan and Lazarow, 1962). The unlabelled (endogenous) insulin in the sample competes with the ^{125}I-labelled insulin antigen for the limited and fixed number of binding sites on the antibody lining the test tubes. After 20 to 24 h, the test tubes were decanted, blotted and left inverted for 30 min to dry, prior to measuring gamma radiation in a scintillation counter (COBRA II auto gamma, Canberra Packard, Melbourne, AU). Serum insulin values were determined using a standard curve of known insulin concentrations (0 to 200 $\mu U \cdot ml^{-1}$) normalised to the blank. All participants samples were measured on the same assay and two quality control samples were included in each assay, to ensure they fit within the concentration range provided by the supplier. The reported average intra and inter-assay coefficient of variations were 3.2 and 3.9%, respectively.

2.2.9 Indexes of Insulin Sensitivity

Concentrations of blood glucose and insulin were used to calculate indexes of insulin sensitivity. The HOMA-IR (Matthews et al., 1985) was calculated using fasting values of glucose (G_0 in $mmol \cdot L^{-1}$) and insulin (I_0 in $\mu IU \cdot ml^{-1}$), as a proxy of insulin sensitivity:

$$\text{HOMA-IR} = \frac{(I_0 \times G_0)}{22.5}$$

The Matsuda Insulin Sensitivity Index (M-ISI) was also calculated. Unlike the HOMA-IR, this incorporates postprandial responses and as such, is considered more reflective of peripheral insulin sensitivity. Indeed, it correlates well with whole-body glucose disposal during a hyperinsulinaemic euglycaemic clamp (Matsuda and DeFronzo, 1999). The M-ISI is typically assessed across 120 min of an OGTT. In Chapters 5 and 6, we used a dextrose drink with added protein, which will delay gastric emptying (Karamanlis et al., 2007), possibly due to the increased caloric density (Calbet and MacLean, 1997). This is likely to prolong the return to the basal (fasted) state; therefore, we calculated the M-ISI over both 120 and 180 min.

$$\text{M-ISI} = \frac{10000}{\sqrt{[G_0(\text{mg}\cdot\text{dL}^{-1}) \times I_0(\mu\text{IU}\cdot\text{mL}^{-1}) \times G_{\text{mean}}(\text{mg}\cdot\text{dL}^{-1}) \times I_{\text{mean}}(\mu\text{IU}\cdot\text{mL}^{-1})]}}$$

2.2.10 Plasma Free-Fatty Acids

In chapters 3, 5 and 6 FFA were quantified using an enzymatic colorimetric assay (NEFA-HR(2), Wako, Osaka, JP) on a benchtop clinical chemistry analyser (ABX Pentra 400, Horiba Ltd., Kyoto, JP). In brief, FFA present in the samples was converted to acyl-CoA which was subsequently oxidised to form hydrogen peroxide. The latter undergoes an oxidation condensation reaction catalysed by peroxidase to form a blue-purple pigment, which was quantified for absorbance at 546/660 nm. An internal standard of oleic acid was used to obtain a calibration curve, from which FFA concentrations could be derived from.

2.2.11 Serum Triglycerides

In Chapters 3, 5 and 6 concentrations of serum triglycerides (TAG) were determined using an enzymatic colorimetric assay on a clinical chemistry analyser (ABX Pentra 400, Horiba Ltd., Kyoto, JP). In this assay, TAG was hydrolysed to their constituent fatty acids and glycerol. A phosphate group was then added to glycerol to form glycerol-3-phosphate, which was subsequently oxidised to form hydrogen peroxide. This was converted to a blue-purple pigment and quantified for absorbance as detailed above in 2.2.10.

2.2.12 Branched Chain Amino Acids

The three BCAAs are leucine, iso-leucine and valine. In chapters 5 and 6, total plasma BCAA concentrations were determined using a rapid spectrophotometric assay developed by Beckett et al. (1996). This is based on the principle that BCAA are oxidatively deaminated by L-Leucine Dehydrogenase (L-LDH) with a stoichiometric reduction of NAD^+ (to NADH). L-LDH (Cat #L5135, Sigma-Aldrich, St. Louis, MO, USA) was suspended into a 25 mM sodium phosphate buffer and 20 $U \cdot ml^{-1}$was prepared, aliquoted and frozen. On the day of the assay, a glycine-KCl-KOH buffer (0.2 M glycine; 0.2 KOH, 2 mM EDTA, pH to 10.5 with KOH) was prepared and NAD^+ added at a concentration of 120 mM to plasma samples in a 96-well plate. Absorbance at 340 nm on a spectrophotometer (Spectra Max 190, Molecular Devices Ltd., Wokingham, UK) was determined before and 60 min after, the addition of 0.04 units of L-LDH. The change in absorbance corresponds to NADH formation, which is proportional to concentration of BCAA. Samples and six leucine standards (range 0 to 1 mM) were measured in duplicate, with all participants samples assayed on the same plate.

2.2.13 Plasma Total Ghrelin

In Chapters 5, total ghrelin levels of fasting arterialised plasma samples were determined using a ^{125}I radioimmunoassay kit (Total Ghrelin Assay GHRT89HK, Merck Millipore, Burlington, MA, USA). This utilises the double antibody technique and followed a similar protocol to the insulin assay described in Section 2.2.8. Samples were assayed in single as variability between duplicates was shown to be ≤ 5%. Activated ghrelin was unable to be measured, as it is recommended to immediately acidify samples with HCl and add phenylmethylsulfonyl fluoride to prevent its degradation.

2.2.14 Serum Testosterone

Fasting serum samples were analysed for testosterone concentrations using an enzyme-linked immunosorbent assay (KGE010; R & D Systems, Minneapolis, MN, USA). The assay uses the competitive binding technique. The primary monoclonal antibody (anti-testosterone) was added to all wells except the non-specific binding wells and incubated for 60 min. The wells were washed before adding samples and standards in duplicate, together with testosterone conjugated to horseradish peroxidase. This was incubated for a further 3 h prior to adding a substrate solution (hydrogen peroxide and stabilised chromogen) and incubating for a further 30 min in the dark. A stop solution of sulfuric acid was then added prior determining the optical density using a spectrophotometer (Spectra Max 190, Molecular Devices) at 540 nm with a wavelength correction of 450 nm.

2.2.15 Reliability of Serum and Plasma Assays

Reported intra-assay coefficient of variations for the serum and plasma assays detailed in this Section are shown below in Table 2.1.

Table 2.1. Coefficient of variations.
Manufacturer reported intra-assay coefficient of variations for plasma and serum assays.

	Intra-assay coefficient of variation
Serum Insulin	3.2%
Plasma FFA	< 1.5%
Serum TAG	< 2.9%
Plasma Ghrelin	6.4%
Serum Testosterone	3.5%

2.3 Laboratory Methods: Skeletal Muscle

2.3.1 Muscle Biopsy Sampling

The percutaneous needle biopsy (Bergstrom, 1975; Bergström and Hultman, 1966) was used to obtain muscle from the vastus lateralis in Chapters 3, 4, 5 and 6. Initially the area was cleaned with an antiseptic iodine solution prior to administering local anaesthetic (2% lidocaine) to the skin and surrounding fascia. After a short time, a small incision (< 1 cm) was made with a sterile scalpel prior to insertion of a five-millimetre Bergström needle (Bignell Surgical Instruments Ltd, Sussex, UK). Suction assistance was used to improve sample yield (Hennessey et al., 1997) and upon removal, the needle was immersed in either chilled phosphate buffered saline (for generation of primary culture) or isopentane cooled with liquid nitrogen to preserve

optimal muscle morphology (Meng et al., 2014). In the former case, any visible fat, blood or connective tissue was removed before isolating satellite cells (Section 2.6). In Chapters 3, 5 and 6 two biopsies were taken from the same leg on the first main visit and from a different leg in the subsequent trial. In all instances, a randomised leg was used for the first visit and the second biopsy was obtained from a separate incision ~3 cm proximal to the first. An identical procedure was followed for the contralateral leg on the follow-up visit.

2.3.2 Incorporation of [1-^{13}C] Phenylalanine

In Chapter 3, participants consumed a milk protein and dextrose drink that had been intrinsically labelled with [1-^{13}C] phenylalanine. This was obtained by infusing a lactating cow with [1-^{13}C] phenylalanine, collecting the milk and fractionating it into whey/casein protein concentrate (Pennings et al., 2011). Unlike the ingestion of freely labelled AAs, this is incorporated into the protein matrix and hence better accounts for digestion and absorption kinetics. The incorporation of [1-^{13}C] phenylalanine into myofibrillar protein was quantified as a marker of fractional synthetic rate (FSR).

Briefly, freeze-dried powdered muscle was homogenised in ice-cold 2% perchloric acid, the resulting protein pellet from centrifugation was dried under nitrogen and hydrolysed with 6 M HCl at 120℃ for 15 to 18 h. The free AAs were then dried under nitrogen at 120℃, resuspended in 50% acetic acid and passed over a DOWEX ion exchange resin. AAs were eluted with 2 M NH_4OH, dried and derivatised with tetr-butyl dimethylsilyl. This was analysed for ^{13}C:^{12}C (tracer:tracee) ratio using gas chromatography mass spectrometry (GCMS; Agilent 7890A GC/5975C; MSD, Little Falls, DE).

2.3.3 Muscle Glycogen

The glycogen content of muscle samples was determined using a modified version of the protocol established by Harris et al. (1974). In Chapter 5, freeze-dried, powdered muscle was solubilised in 0.1 M sodium hydroxide and heated at 80℃ for 10 min. A neutralisation buffer (150 mM citric acid, 150 mM disodium phosphate and 25 mM HCl) was then added, before hydrolysing the glycogen using amyloglucosidase for 1 h at room temperature. The samples were then spun at 14,000 rpm for 2 min and supernatants transferred.

Glucose concentrations were measured on a spectrophotometer (Spectra Max 190, Molecular Devices). Twenty microliters of muscle extract were added to a 96-well plate in duplicate and mixed with 200 µl of 120 mM triethanolamine buffer (pH 8.2) containing 0.90 mM ATP, 0.60 mM NAD and 0.12 mM dithiothreitol. A baseline absorbance at 340 nm was obtained, prior to the rapid addition of equal parts (2 units) of glucose-6-phosphate dehydrogenase (G6DPH) and HK (Both from Roche, Basel, CH). The plate was mixed prior to a 20 min incubation at room temperature, before reading the final absorbance. The change in absorbance was adjusted for a 'blank' sample of distilled water and samples were corrected to a 1.5 $mmol \cdot L^{-1}$ glucose standard.

Reactions involved:

$$\text{Glucose} + \text{ATP} \xrightarrow{\textbf{G6DPH}} \text{Glucose-6-phosphate} + \text{ADP}$$

$$\text{Glucose-6-phosphate} + \text{NAD}^{+} \xrightarrow{\textbf{HK}} \text{6-P-gluconolactone} + \text{NADH} + \text{H}^{+}$$

Concentrations of glycogen in glycosyl units per kg of dry muscle were calculated using the following equation:

$$[\text{Glycogen}] = \frac{[(A2 \times V2) - (A1 \times V1)] - [(AB2 \times V2) - (AB1 \times V1)]}{\text{Standard vol. (µl)} \times 6.22 \text{ (extinction coefficient)}}$$

Where V1 and V2 are the pre and post-enzyme well volumes, respectively. A1 and A2 are the pre and post-enzyme absorbance values at 340 nm whilst AB is the same for the absorbance of the blank. The extraction factor (EF) was calculated using the following equation:

$$EF = \frac{\text{NaOH (µl)} + \text{HCl: Citric acid (µl)} + \text{AGDase (µl)} + \text{powder weight (mg)}}{\text{powder weight (mg)}}$$

2.3.4 Pyruvate Dehydrogenase Complex Activation

The activity of PDC provides an index of the phosphorylation status and activity of the enzyme (Constantin-Teodosiu et al., 1991). In Chapters 3 and 5, wet muscle was homogenised at 400 rpm for 50 sec in 30 volumes (ratio of µl to mg) of ice-cold buffer (200 mM sucrose, 50 mM KCl, 50 mM Tris, 50 mM NaF, 5 mM MgCl2.6H_2O, 5 mM egtazic acid, 5 mM dichloroacetate, 0.1% triton X-100, pH 7.8). Thirty microliters of homogenate were added to 720 µl buffer (100 mM Tris, 0.5 mM disodium EDTA, 1 mM $MgCl_2$.6H_2O, pH 7.8). NAD, thiamine pyrophosphate and coenzyme A (CoA) were prepared fresh and added to the buffer at final concentrations of 1, 1 and 0.5 mM, respectively. The buffer was prewarmed for 10 min at 37℃ prior to initiating the decarboxylation reaction by adding 30 µl of 26 mM sodium pyruvate.

$$\text{Pyruvate} + \text{CoA} + \text{NAD}^+ \xrightarrow{\textbf{PDC}} \text{Acetyl-CoA} + \text{NADH} + \text{H}^+$$

Subsequently, 210 µl aliquots of this mixture were transferred to tubes containing 40 µl of 0.5 M perchloric acid at 1, 2 and 3 min after adding the pyruvate. The aliquots were immediately vortexed and after a five min incubation a room temperature, 10 µl of 2.2 M potassium bicarbonate was added to neutralise the solution. Afterwards,

samples were spun at 20,000 x g for 3 min and supernatants frozen at −20℃ for the subsequent determination of acetyl-CoA formation in a radioenzymatic assay.

The acetyl-CoA extracts were defrosted and spun at 10,000 x g for 3 min. Samples were diluted 1:10 in distilled water, prior to adding 20 µl of copper sulphate/potassium acetate/water (3:2:2) and incubating for 30 min, in order to remove any excess endogenous oxaloacetate. Twenty microliters of 60 mM EDTA was then added to complex the copper. The assay was initiated with the addition of 30 µl of 30 mM N-ethylmaleimide (NEM) before adding 20 µl of [^{14}C] oxaloacetate [prepared from [^{14}C] aspartate (PerkinElmer, Waltham, MA, USA); see Appendix] and 10 µl of citrate synthase [0.22 units; Sigma-Aldrich, St. Louis, MO, USA) at timed intervals. The NEM was added to bind CoA and hence drive the reaction towards the consumption of [^{14}C] oxaloacetate:

$$[^{14}\mathrm{C}]\mathrm{Oxaloacetate} + \mathrm{Acetyl\text{-}CoA} \xrightarrow{\textbf{Citrate Synthase}} [^{14}\mathrm{C}]\mathrm{Citrate} + \mathrm{CoA}$$

After a 20 min incubation, 30 µl of transamination mix (133 mM glutamate and 18 U·ml^{-1}of glutamate-oxaloacetate transaminase) was added for a further 20 min. This was to convert the excess [^{14}C] oxaloacetate back to [^{14}C] citrate. One millilitre of DOWEX hydrogen counter-ion exchange resin was then added to separate [^{14}C] citrate (negatively charged) from [^{14}C] oxaloacetate (positively charged). The solution was vortexed and left to sediment, before 500 µl of the clear supernatant was added to 5 ml of scintillation fluid. Total counts of [^{14}C] radiation was determined using a scintillation counter (TriCarb, 2100TR, Canberra-Packard, Melbourne, AU). Radiation counts were converted to acetyl-CoA concentrations through interpolation of a six-point standard curve (0 to 125 ρmol·L^{-1}). All samples and standards were

assayed in duplicate, with all a participant's samples assayed on one run. Acetyl-CoA production rates were corrected for total protein concentrations of the muscle homogenates using the pierce bicinchoninic acid assay (see Section 2.3.6).

2.3.5 Messenger RNA Expression

RNA Extraction

In Chapter 5, approximately 20 mg of wet muscle was transferred from liquid nitrogen into 800 µl of TRI reagent (Thermo Fisher Scientific, Waltham, MA, USA) containing 200 µg of glycogen, to extract ribonucleic acid (RNA). Samples were then homogenised for approximately 30 sec using a polytron. The homogenate was incubated at room temperature for a minimum of 5 min, prior to the addition of 160 µl chloroform:isoamyl alcohol (49:1). Samples were mixed by repeated inversions for 30 sec before being spun at 12,000 x g for 15 min at 4℃. Subsequently, 400 µl of the aqueous phase was transferred to an Eppendorf containing an equal volume of ice-cold isopropanol. These samples were incubated at −20℃ overnight.

The mixture was then spun at 12,000 x g 4℃ for 15 mins and resulting pellet washed in 75% ethanol. This was spun at 10,000 x g for 10 mins, prior to removing the supernatant and drying the pellet using a water aspirator. The pellet was then resuspended in 20 µl for RNase-free H_2O, prior to estimating RNA concentrations using the NanoDrop One UV-Vis spectrophotometer (Thermo Fisher Scientific). The software uses mathematical algorithms to identify and quantify the absorbance contribution of contaminants, such as phenol or guanidine, in the sample and corrects RNA concentrations accordingly. The a260/280 ratio of pure RNA is ~2.0, we determined acceptable ratios for downstream applications as between 1.75 and 2.05.

First Strand cDNA Synthesis

First stand complimentary DNA (cDNA) was synthesised from RNA via reverse transcription using superscript III reverse transcriptase (Thermo Fisher Scientific). A total of 500 ng of RNA was combined with 25 ng of random primers and a final concentration of 0.77 mM deoxynucleotide triphosphates. This mixture was incubated at 65℃ to denature the secondary structure of RNA and then placed on ice to allow the primers to anneal to the RNA. Next, 4 µl of 5x first strand buffer, 1 µl of 0.1 M DTT, 1 µl of RNaseOUT inhibitor (40 $U \cdot ml^{-1}$) and 1 µl of superscript reverse transcriptase was added. The solution was initially incubated at 25℃ for 5 min and then 50℃ for 60 min to facilitate transcription. Finally, the enzyme was inactivated by heating the mixture to 70℃ for 15 min.

TaqMan Custom Array Cards

A total of 200 ng of cDNA was added to Taqman Universal PCR master mix and loaded on Custom Array Micro Fluidic Gene Cards (ABI Applied Biosystems, Thermo Fisher Scientific). The card was then spun at 1200 rpm for 2 x 1 min in a centrifuge (Multifuge 3, Heraeus, Hanau, DE) and then sealed prior to removing the fill reservoir. Gene cards were run on a 7900HT Fast Real-Time Polymerase Chain Reaction System (Thermo Fisher Scientific) for approximately 2 h and saved for analysis. The cycle threshold (C_T), defined as the number of cycles required to amplify the fluorescent signal above background levels, was determined by the software.

Analysis of mRNA expression

The NormFinder software program (https://moma.dk/normfinder-software) was used to analyse which single or combination of the three housekeeping genes; Actin-

Alpha 1, Hydroxymethylbilane Synthase and Glyceraldehyde 3-phosphate dehydrogenase provided the most stable level of expression between samples. A Grubb's test ($\alpha < 0.01$) was performed on ΔC_T values to identify potential outlier values. Outliers were replaced with the mean ΔC_T value for the gene in that condition in order to minimise bias. The change in gene expression between two conditions, for instance from fasted to fed, was then computed using the comparative C_T method (Schmittgen and Livak, 2008). For example:

$$\Delta C_T = C_{T(\text{GENE OF INTEREST})} - C_{T(\text{HOUSEKEEPING GENE})}$$

$$\Delta\Delta C_T = \Delta C_{T(\text{FED})} - \Delta C_{T(\text{FASTED})}$$

The obtained value could then be used to calculate relative fold-change as $2^{-\Delta\Delta Ct}$. Values were logarithmically transformed prior to plotting heatmaps to summarise the array of genes measured.

2.3.6 Protein Extraction

In Chapter 3 wet muscle (~30 mg) was extracted in HEPES buffer (50 mM HEPES, 10% glycerol, 1 mM EDTA, 10 mM NaF, 1 mM Na_3VO_4, 150 mM NaCl, 1% Triton x-100, pH 7.5). Sodium orthovanadate and sodium fluoride were added as phosphatase inhibitors and a protease inhibitor cocktail (Cat# P8340, Sigma-Aldrich, St. Louis, MO, USA) was added on the day. Each sample was homogenised on ice for 30 sec and left on ice for 20 min prior to centrifugation at 12,000 x g for 15 min at 4℃. The supernatant was then transferred to a fresh tube, prior to quantifying total protein concentrations with the Pierce bicinchoninic acid assay (see 2.3.7).

In Chapter 5, proteins were isolated from the Trizol RNA extraction described above. As a result, mRNA expression and protein content were determined from the

same part of each tissue sample. Proteins were precipitated from the phenol-ethanol supernatant by adding 1.2 ml isopropanol and incubating for 10 min. Samples were then spun at 12,000 x g at 4℃ for 10 min to pellet the proteins, before washing 3 times with 0.3 M guanidine HCl in 95% ethanol. A final wash of 100% ethanol was performed, prior to spinning samples at 7500 x g for 5 min. The supernatant was discarded and pellet air dried, before resuspending in 400 µl of 8 M urea (deionised with amberlite ion exchange resin), 50 mM Tris and 4% SDS buffer. To aid with resuspension, samples were heated to 35℃ and pipetted up and down. Next, samples were sonicated on ice for 3 x 10 sec at 20 kHz, before a final spin at 10,000 x g for 10 min to isolate soluble proteins. This was transferred to a fresh tube prior to quantifying total protein concentrations with the Pierce bicinchoninic acid assay (see 2.3.7).

2.3.7 Protein Quantification

In Chapters 3, 4 and 5, the Pierce bicinchoninic acid assay (Thermo Fisher Scientific) was used to quantify total protein concentrations against a range (0 to 2000 $\mu g \cdot ml^{-1}$) of albumin concentrations. Typically, samples were diluted 1 in 10 with water before loading and the standards were diluted in the same buffer used for the respsective extraction. All samples were measured in duplicate and the plate was incubated for 30 min at 37℃ before quantifying absorbance on a spectrophotometer (Spectra Max 190, Molecular Devices) at 562 nm. From this a standard curve was derived and the diluted concentrations of the samples were calculated. To assess protein content, all samples were diluted to a uniform concentration with the appropriate extraction before and then mixed with 4 x SDS loading buffer (containing

bromophenol blue). This mixture was heated for 5 min at 95℃ to fully denature proteins, before being left to cool at room temperature and frozen at −20℃.

2.3.8 Electrophoresis/SDS-PAGE

Gels were hand cast on the day at either a fixed % of acrylamide or a gradient (5 to 20%) depending on the molecular weight(s) of the proteins being probed for. A standard 4% stacking buffer was used, and plates were inserted into an electrophoresis cell (Atto, Tokyo, JP) filled with 1x Tris-Glycine-SDS running buffer. Ten µl of protein ladder (Precision Plus Protein, Bio-Rad, Hercules, CA, USA) was loaded on each gel. The gels were run at a constant amplitude of either 40 (one gel) or 80 (two gels) mA for approximately 2 h to separate proteins via electrophoresis. Proteins were then transferred onto a polyvinylidene difluoride membrane in an electrophoresis transfer cell (Bio-Rad, Hercules, CA, USA) filled with Tris-Glycine-Methanol transfer buffer. This was done overnight (≥ 16h) at a constant amplitude of 40 mA.

The next day, adequate transfer of proteins was visually inspected using a ponceau-S stain, this was extensively washed out in distilled water in tris-buffered saline containing 0.1% (w/v) tween 20 (TBS-T). Membranes were then blocked, typically in 5% (w/v) skimmed milk power or bovine serum albumin (BSA) diluted in TBS-T for 1 h at room temperature. After blocking, membranes were washed 3 x 10 min in TBS-T, before incubation with the appropriate primary antibody on a rocking table overnight at 4℃.

The next day, membranes were again washed 3 x 10 min in TBS-T prior to incubation with an anti-host (of animal primary antibody was raised in) horseradish peroxidase-linked secondary antibody (Dako, Glostrup, DK) for 1 h at room

temperature. A final wash step was performed prior to the addition of enhanced chemiluminescence (Amersham ECL Prime, GE Healthcare Life Sciences, Buckinghamshire, UK) solution for 5 min. Protein expression was then visualised in a dark room using X-ray film (Hyperfilm, Amersham Biosciences, Buckinghamshire, UK) for a variety of different exposure times. Films were then digitally scanned and intensity of band(s) quantified using 2D densitometry software (AIDA Image Analyser). Proteins of interest were normalised against an endogenous loading control of α-actin expression. The only exceptions were using Ponceau and Coomassie stains to assess total protein content after measuring puromycin incorporation in Chapter 4.

2.4 Energy Expenditure and Body Composition

2.4.1 Calculation of Energy Expenditure

Traditionally EE was assessed in direct calorimeters that measure heat production by recording pressure changes in an enclosed chamber. Weir (1949) observed that total heat energy output was proportional to the amount of oxygen consumed ($\dot{V}O_2$) and carbon dioxide produced ($\dot{V}CO_2$). The accuracy of the estimate can be further improved by measuring urinary nitrogen excretion (UNE) (see Section 2.4.3) which provides an index of protein oxidation rate. Although the contribution of protein oxidation to metabolism in non-pathological conditions is small and often ignored.

$$\begin{aligned}\text{EE}\left(\text{kCal}\cdot\text{min}^{-1}\right) &= \left[3.941 \times \dot{V}O_2\left(\text{L}\cdot\text{min}^{-1}\right)\right] + \left[1.1106 \times \dot{V}CO_2\left(\text{L}\cdot\text{min}^{-1}\right)\right] \\ &\quad - \left[2.17 \times \text{UNE}\left(\text{g}\cdot\text{min}^{-1}\right)\right]\end{aligned}$$

Substrate utilisation can be estimated due to the different oxygen costs and carbon dioxide production associated with fat and CHO metabolism. A relative index of this is the ratio between $\dot{V}O_2$: $\dot{V}CO_2$, referred to as the respiratory exchange ratio (RER). An RER value of 0.70 indicates pure fat oxidation, whereas a value of 1.0 represents pure carbohydrate oxidation (Frayn, 1983). However, care must be taken when using the RER as prolonged periods of fasting can induce a state of ketosis and the RER oxidation values of the two most common ketone bodies are 1.0 and 0.89. In this thesis, the following stoichiometric equations were used to calculate rates of fuel oxidation (Frayn, 1983).

$$\text{CHO}\left(\text{g}\cdot\text{min}^{-1}\right) = \left[4.55 \times \dot{V}CO_2\left(\text{ml}\cdot\text{min}^{-1}\right)\right] - \left[3.21 \times \dot{V}O_2\left(\text{ml}\cdot\text{min}^{-1}\right)\right] - \left[2.87 \times \text{UNE}\left(\text{g}\cdot\text{min}^{-1}\right)\right]$$

$$\text{Fat}\left(\text{g}\cdot\text{min}^{-1}\right) = \left[1.67 \times \dot{V}O_2\left(\text{ml}\cdot\text{min}^{-1}\right)\right] - \left[1.67 \times \dot{V}CO_2\left(\text{ml}\cdot\text{min}^{-1}\right)\right] - \left[1.97 \times \text{UNE}\left(\text{g}\cdot\text{min}^{-1}\right)\right]$$

2.4.2 Indirect Calorimetry

In Chapters 5 and 6 the volume and composition of participants expired gas were analysed on a portable open-circuit metabolic cart (Cosmed Quark RMR, Rome, IT). Before commencing any measurements, this was calibrated using a 3 L syringe attached to a turbine flowmeter (18 mm for resting, 25 mm for exercise). The syringe piston was slowly pumped whilst maintaining a flow rate between ± 1 $L\cdot sec^{-1}$. Afterwards, the concentration of room air was determined, prior to a reference gas calibration with known concentrations of oxygen (16%) and carbon dioxide (5%). The latter calibration was re-performed immediately prior to any successive measurements

made within the same day. No measurements were undertaken until all calibration errors were within acceptable ranges.

Resting Measurements

Participants rested quietly in a semi-supine position on a hospital bed for ≥ 15 min prior to recording any measurements. A vacuum pump was used to draw atmospheric air into a canopy hood placed over the participants face, the flow rate was adjusted to maintain $FeCO_2$ concentrations between 0.5 and 0.6%. The expired gas was sampled in 10 sec bins for 20 min and data saved for subsequent analyses. Typically, the first 5 and last 1 min of data was excluded, before calculating average rates of $\dot{V}O_2$ and $\dot{V}CO_2$ in order to determine EE and substrate utilisation rates.

Exercise Measurements

Participants were fitted with a continuous heart rate (HR) monitor (Cosmed, Rome, IT) and face mask to collect expired air breath-by-breath during exercise. This was used to obtain an individualised relationship between HR and EE in order to calibrate the Actiheart (see Section 2.5.2).

2.4.3 Urinary Nitrogen Excretion

In Chapters 5 and 6, participants urine was collected into a vessel upon arrival to the laboratory and prior to recording body mass. An additional vessel was used to collect urine passed after consumption of the test meal. The vessels were mixed to homogenise the urine and total volumes recorded, before freezing a small aliquot at −80℃. Urinary nitrogen excretion rates were determined with an enzymatic ultraviolet test (Cat# UR220, Randox, County Atrim, UK), catalysed by urease and glutamate dehydrogenase on a clinical chemistry analyser (ABX Pentra 400, Horiba

Ltd., Kyoto, JP). Briefly, urea was hydrolysed by urease to form ammonium, which reacts with 2-oxoglutarate and NADH using glutamate dehydrogenase to form NAD^+. The oxidation rate of NADH is proportional to the urea concentration of the sample.

2.4.4 Dual Energy X-ray Absorptiometry

In Chapters 5 and 6 Dual Energy X-Ray Absorptiometry (DEXA) scans (Lunar Prodigy DEXA; GE Medical Systems, Bedford, UK) were used to determine whole-body and regional changes in body composition. All participants filled out a questionnaire prior to each scan to assess suitability and wore light clothing free from any metallic items. Scans were undertaken with the participant motionless in a supine position with arms placed by their side and hands pronated. The same technician undertook each participants pre/post measurements and all regional analysis were performed using specialised software (enCORE; GE Medical Systems, Chicago, IL, USA).

The scanner passes two low-dose X-ray beams through the body (40 and 70 keV). Due to the different elemental composition of fat, muscle tissue and bones, the X-rays pass through regions of the body at different rates. Regional determination of fat, lean mass and bone mineral density can then be calculated by linear decomposition of the measured X-ray beam attenuation (Pietrobelli et al., 1996). DEXA offers an accurate and convenient, non-invasive estimation of body composition. Limitations stem from the assumptions that there is a constant fractional composition of lean tissue (water, protein and mineral content), which can vary with hydration states. To limit the influence of nutrition and hydration status, all scans were undertaken in the morning at approximately 08:00 after an overnight fast and voiding of the bladder.

Alternative techniques to assess body composition include computed tomography and magnetic resonance imaging. These offer increased image resolution and accuracy, including the ability to differentiate between subcutaneous and visceral adipose tissue depots (Jensen et al., 1995). Nevertheless, reasonable correlations (r = 0.78) between DEXA-derived android fat and visceral fat assessed by a computed tomography scan have been obtained (Hill et al., 2007). Furthermore, magnetic resonance imaging scans are very expensive and computed tomography scans expose participants to higher levels of radiation.

2.5 Free-Living Measurements

2.5.1 Physical Activity Monitoring

Physical activity (PA) is a complex and multidimensional behaviour that does not sit in isolation from related constructs including sedentary behaviour or EE (Pettee Gabriel et al., 2012). Large-scale epidemiological studies typically use self-report measures to assess and monitor PA at a population level. Whilst a simple and cost-effective model, this lacks both precision and accuracy in estimating EE (Neilson et al., 2008), particularly at low intensities (Besson et al., 2010). For instance, only 9% of a population self-reporting to meet national PA recommendations met these based on objective data from a validated accelerometer (Health and Social Care Information Centre, 2009).

Technological advancements, reductions in cost and the limitations of previous devices have led to activity monitors becoming a key element of PA research (Troiano, 2005). Accelerometers directly record movement with time-stamped data that allows

researchers to analyse PA patterns including frequency, intensity and duration. Accelerometers can be calibrated against indirect calorimetry to convert activity counts into EE units with linear regression (Bassett, 2012).

2.5.2 Combined Heart Rate and Accelerometery

The Actiheart (CamNtech inc., Cambridge, UK) simultaneously measures HR and movement via an accelerometer to estimate EE via branched equation modelling (Brage et al., 2005). Monitors incorporating combined HR and movement measurements improve the precision of EE estimates by around 20% compared to using either independently (Strath et al., 2005). Sound technical reliability and validity has been demonstrated during walking and running-based activities compared to indirect calorimetry and an electrocardiogram (Brage et al., 2005).

The Actiheart has been extensively validated in a laboratory setting against indirect calorimetry. Two studies that included a range of low-to-moderate intensity activities aimed at replicating daily living, demonstrated a small mean negative EE prediction bias between 6 to 8% (Crouter et al., 2008; Thompson et al., 2006). It has also been validated in free-living settings against the criterion measurement of doubly labelled water (Berntsen et al., 2010). Free-living PAEE was assessed over seven days in 33 rural and urban dwellers of Cameroon and over ten days in 35 lean and overweight men of varying fitness levels (Assah et al., 2011; Villars et al., 2012). Using individual calibration of the HR and PAEE relationship, both studies reported small mean bias values between -1.3 to -1.8 $kCal \cdot kg^{-1} \cdot day^{-1}$. This emphasises the importance of using individual calibration protocols to minimise EE prediction bias.

Free-Living Energy Expenditure

In Chapters 5 and 6, the Actiheart was used to estimate free-living EE. It was worn across the chest attached to a HR monitor strap or electrode pads. Participants were instructed to wear the Actiheart at all times, other than during water-based activities. Individual user profiles were personalised by replacing the estimated RMR from the Schofield equation (Schofield, 1985) to that directly measured in the laboratory using indirect calorimetry. Predicted EE at a range of HR, determined from the calibration protocol (see below), were also included. All measurements were recorded with 1-minute epochs using the 'group calibration: individual HR + stress' model. The stress compensation adjusts EE in instances where the device detects an elevation in HR but little or no accompanying movement from the accelerometer.

Calibration Protocol

Participants completed a modified treadmill protocol (Brage et al., 2007) to account for inter-individual differences in the relationship between HR and EE, which can be influenced by body composition and level of aerobic fitness. This comprised of six 3 min stages of gradually increasing intensity beginning at a slow walk (3.2 $km \cdot h^{-1}$) and finishing at a moderate running speed (9 to 12 $km \cdot h^{-1}$). During the test they wore a HR monitor (Polar, Kempele, FI) and expired into a facemask connected to a portable metabolic cart (Cosmed Quark RMR, Rome, IT). Mean HR and EE over the last min (steady state) of each stage were plotted to obtain a regression equation. This data was input into the user profile of each participant on the Actiheart software and used to calibrate the algorithm model (group calibration: individual HR + stress) used by the Actiheart software to estimate EE.

2.5.3 Continuous Glucose Monitoring

Continuous glucose monitors (CGM) typically estimate glucose concentrations in the interstitial fluid, where glucose freely diffuses between the capillaries and interstitial space. CGMs provide a convenient means of capturing individual daily glycaemic profiles at an increased resolution than traditional approaches that directly measure capillary blood glucose obtained via finger prick. Indeed, individuals with type I diabetes that use CGM display improved glycaemic control (Pickup et al., 2011). The use of CGMs is forecast to rise as the accuracy and affordability continues to improve, particularly as healthcare and insurance providers become more aware of the benefits of improved glycaemic control and reduced episodes of severe hypoglycaemia.

In Chapters 5 and 6, the FreeStyle Libre (Abbott Diabetes Care, Maidenhead, Berkshire, UK) was used to measure interstitial glucose levels. This is a commercially available flash glucose monitoring system that arrives pre-calibrated. This avoids the expense and inconvenience of performing regular finger prick calibrations. A small glucose-sensing filament is inserted 5 mm subcutaneously on the back of the upper arm, this is attached to a larger sensor residing above the skin. Each sensor can measure interstitial fluid glucose concentrations for up to 14 days and users can obtain real-time glucose readings every minute. Scanning the sensor captures the previous 8 h of data which is recorded in 15 min epochs.

Bailey et al. (2015) compared the accuracy of the FreeStyle Libre against capillary and venous blood glucose concentrations. Seventy-two diabetic individuals wore sensors on both arms and visited the laboratory on three separate occasions across the sensor lifespan. In total, over 25,000 scans were paired for comparison with venous

blood analysed by the YSI and capillary blood from the built-in blood glucose monitor when the participants were away from the laboratory. Overall, the mean absolute relative difference was 11.4% with capillary and 12% with venous glucose concentrations. One contributory factor was the physiological differences between interstitial and capillary blood during times of rapidly changing glucose concentrations such as after a meal. Specifically, there was a mean lag time of around 5 min with the sensor. Similar mean absolute relative differences between 10 and 11% were observed in a population of diabetics in China (Ji et al., 2017), although the mean lag time reported was slightly lower than 5 min. Importantly, both studies found the accuracy of the sensor to be stable across its lifespan. Although it seems to be reduced on the day of insertion, which could be related to localised tissue inflammation after insertion of the sensor.

2.5.4 Dietary Analysis

In Chapters 5 and 6 participants dietary intake was recorded using 7-day food diaries to fully capture habitual dietary intake across the week (Black et al., 1991). Participants were provided with digital weighing scales and encouraged to be as detailed in their descriptions of portion sizes as possible. Attempts were made to clarify any unclear entries with the participants on study visits. Where no food intake or portion sizes were indicated, a medium portion size was assumed. All data were manually input into Nutritics (Dublin, IE), which performed a comprehensive dietary analysis. The main outcomes from this were total energy intake (EI) and distribution between carbohydrate, fat and protein. The total duration of daily EI was also calculated for comparison between the baseline and intervention period. Although it is well established that individuals tend to underreport their EI, the degree of

underreporting is likely to be similar between the baseline and intervention periods. Thus, whilst lacking in precision, meaningful comparisons can still be inferred.

2.5.5 Data Analysis

Free-Living Energy Expenditure

Data from the Actiheart is 'lost' when the device is removed by the participant. Any days with more than 10% (> 144 min per day) of lost data were excluded from analyses. The 'auto fill' function was used to interpolate these missing data points with the average of that day's activity energy expenditure (excluding the missing data). In addition, the device can temporarily lose HR signal at times, in these instances the software uses a 'recovered' HR and subsequently gives a stronger weighting for the accelerometer data in the proprietary algorithm used to estimate activity EE. If greater than 22.5% (> 325 min per day) of data was 'recovered', this day was also excluded from subsequent analyses. It should also be noted that the Actiheart assumes diet-induced thermogenesis to be 10% of total EE.

The recorded data was analysed for total and PAEE, as well as PA level (PAL) calculated by diving total daily energy expenditure by resting metabolic rate. The intensity of activity was classified using metabolic equivalent of task (METs), which expresses the energy cost of an activity as a ratio to RMR. These were categorised into daily time spent at light ($1.5 < METs \leq 2.99$), moderate ($3 \leq METs < 5.99$) and vigorous (≥ 6 METs) intensities. In addition, in the TRF study (Chapter 5) a sub analysis of EE was performed by splitting the day into two 8-hour sections to see if the restricted eating pattern influenced the temporal distribution of EE; from 08:00 to 16:00 and from 16:00 to 00:00.

Continuous Glucose Monitoring

The device must be scanned at least every eight hours or gaps in the dataset arise. To maximise data integrity, only days where ≥ 80% of the day was measured were included in the subsequent analyses. The timing outputs are unique to when each sensor was inserted, thus in order to obtain more comparable results all data points were shifted back to the nearest 15 min increment. For instance, if a glucose concentration of 4.8 $mmol \cdot L^{-1}$ was recorded at 13:53, this would be switched to 13:45 for the purpose of analyses.

In Chapters 5 and 6, the baseline period consisted of six full days commencing from midnight on the day of the first visit. The first day was not included as participants arrived fasted which likely altered their typical daily routine. The sensor was replaced after the first main study visit and the 14-day intervention period commenced the next day at 08:00. Averages were then computed for each 15 min time point for all valid days included.

In Vitro Methods

2.6 Primary Skeletal Muscle Cell Culture

2.6.1 Isolation of Satellite Cells

Satellite cells were isolated from vastus lateralis muscle biopsies (see Section 2.3.1) obtained from healthy young volunteers, as described by O'Leary et al. (2017). This technique has been shown to consistently produces desmin positive, multinucleated myotubes. All work was undertaken in a sterile class II safety cabinet. Initially the sample was washed with ice-cold phosphate-buffered saline, before removing any

visible fat or connective tissue. It was then minced into small pieces using a scalpel and enzymatically digested using trypsin-EDTA for 20 min with a magnetic stirrer at 37℃. In the meantime, six-well plates were pre-coated with 1 ml of 0.2% gelatin and placed in a tissue culture incubator (37℃, 95% CO_2 and 5% O_2). The supernatant from the trypsin digest was mixed with an equal volume of pre-warmed growth media [Ham's F10 with 2 mM L-glutamine supplemented with 20% HyClone foetal bovine serum and 1% penicillin/streptomycin (all from Sigma-Aldrich)]. This was then spun in a centrifuge at 1700 rpm, before discarding the supernatant and resuspending the pellet in a larger volume (~30 ml) of growth media. This mixture was dispensed into an uncoated T75 tissue culture flask and placed in an incubator for 40 min. Total number of viable cells in the suspension were quantified on an automated cell counter (Cedex, Roche, Basel, CH) by mixing the cells with an equal volume of trypan blue stain. The gelatin was aspirated prior to seeding the satellite cells at an approximate density of 100,000 cells per well in a volume of 2 ml.

2.6.2 Proliferation into Myoblasts and Differentiation into Myotubes

Satellite cells were allowed to adhere and proliferate in an incubator for 72 h before replacing the media with fresh pre-warmed growth media. Subsequent media changes were undertaken approximately every 48 h and proliferation of the cells regularly observed under a microscope. Myoblasts were not sub cultured/passaged, as this can result in developmental and metabolic impairments (Nehlin et al., 2011) as well as a gradual loss of resemblance to the donor phenotype (Covington et al., 2015), as the fastest proliferating cells are selectively retained. Myoblasts were grown to approximately 90% confluence before lowering the foetal bovine serum concentration

in the growth medium to 10% for 48 h. After, cells were fed with media containing 6% horse serum (Sigma-Aldrich) to promote the differentiation and fusion of myoblasts into myotubes. All experiments were commenced 7 to 10 days post-induction of differentiation.

2.6.3 Fatty Acid Treatment

Fatty acids must be coupled to carriers such as BSA to prevent them forming toxic micelles. Initially, a 24% (w/v) solution of fatty acid-free BSA (Sigma-Aldrich) was prepared by slowly adding it to a 150 mM NaCl solution and adjusting the pH to 7.4. This solution was passed through a 0.45 μM filter before freezing at −20℃ or coupling with fatty acids. Fatty acids were dissolved at a concentration of 20 mM, in 3.5 ml of a 150 mM NaCl and 35 mM NaOH solution on a hot plate with a magnetic stirrer. The beaker was removed from the heat and mixed with an equal volume of ice-cold 24% fatty acid-free BSA, then stirred for a further 10 min. Fatty acid-free BSA has between 4 and 7 binding sites for fatty acid moieties; the ratio used for this complexing was approximately 1:5. The final 10 mM solution was stored at −20℃. Conjugated fatty acids or vehicle (12% fatty acid-free BSA) were mixed into differentiation media for the times and concentrations stated in the figure legends. Following this, cells were washed twice with pre-warmed PBS and serum deprived in Ham's F10 media for a further 2 h.

2.6.4 Glucose Uptake

After serum starvation, cells were incubated in 2 ml of reaction buffer (138 mM NaCl, 1.85 mM $CaCl_2$, 1.3 mM $MgSO_4$, 4.8 mM KCl, 50 mM HEPES pH 7.4 and 0.2% (w/v) BSA) for 3 h. Insulin (Actrapid, Novo Nordisk, DK) treatment was also

induced at this stage. Glucose uptake was determined by the addition of [^{3}H] 2-Deoxy-D-Glucose (2-DOG; PerkinElmer, Waltham, MA, USA) at 28 kBq per well mixed with 10 µM of non-radioactive 2-DOG. This was added to each well at timed intervals on a plate warmer at 37℃, after a 15 min incubation each well was aspirated with a vacuum pump. Next, three washes with ice-cold PBS supplemented with 10 mM D-Glucose were undertaken to outcompete any remaining 2-DOG. Cells were subsequently lysed in 0.05 M NaOH and 0.1% SDS with scraping. Initially, aliquots were taken at this stage to quantify protein concentration. After observing no effect of fatty acid treatment on protein content this was not done in future experiments. Radioactivity was quantified as disintegrations per min (DPM) using liquid scintillation counting (TriCarb, 2100TR, Canberra-Packard, Melbourne, AU).

2.6.5 System A Amino Acid Transport

After serum starvation, cells were incubated in 2 ml of transport buffer (140 mM NaCl, 1.8 mM $CaCl_2$, 0.08 mM $MgSO_4$, 5.4 mM KCl, 25 mM HEPES pH 7.4 and 5 mM of D-Glucose) supplemented with 2 mM L-leucine for 3 h unless otherwise stated. Insulin (Actrapid, Novo Nordisk, DK) treatment was also induced at this stage. Amino acid transport was determined from the uptake of the non-metabolisable transport analog α-[^{14}C] methylaminoisobutyric acid (Me-AIB; PerkinElmer, Waltham, MA, USA) at 37℃. A total of 9.25 kBq of Me-AIB was added to each well at timed intervals for 15 min, before aspirating with a vacuum pump. Cells were washed three times with ice-cold saline solution (0.9% NaCl) before quantifying radioactivity as stated above.

2.6.6 Protein Synthesis

Global rates of muscle protein synthesis were estimated using the SUrface SEnsing of Translation (SUnSET) technique (Goodman and Hornberger, 2013). This was developed as an alternative to using radiolabelled AAs. Puromycin is an antibiotic that is a structural analogue of tyrosyl-RNA, whilst toxic at high concentrations it has no effect on protein synthesis at low concentrations (Schmidt et al., 2009). When puromycin is incorporated into translating polypeptide chains, it terminates peptide elongation and is released from the ribosome as a puromycin-conjugated peptide. These can subsequently be detected using an anti-puromycin antibody.

After serum starvation and incubation with leucine-containing transport buffer (see above), cells were treated at a final concentration of 1 µM puromycin dihydrochloride (Sigma-Aldrich) for 30 min. After aspirating the media, the plates were placed on ice and washed 2 x with ice-cold PBS. Cells were then harvested in 100 µl of RIPA lysis buffer (150 mM NaCl, 25 mM Tris-HCl pH 7.6, 1% Triton x-100. 1% Na-deoxycholate and 0.1% SDS) with added protease inhibitor (Cat# P8340, Sigma-Aldrich). Samples were left on ice for 15 min before repeatedly passing them through narrow gel loading tips and centrifugation at 13,000 x g for 15 min at 4℃. Supernatants were transferred, protein concentrations quantified using a Pierce bicinchoninic acid assay and samples mixed with SDS loading buffer. Twenty micrograms of protein were loaded onto a 12% gel which was subsequently probed with Anti-Puromycin (clone 12D10; EMD Millipore, Burlington, MA, USA) at a concentration of 1:10,000. After immunodetection, the membranes were stained for 10 min with 0.1% Coomassie R-250 in methanol:water 1:1 and destained for 10 min

in acetic acid:ethanol:water (1:5:4), before washing with distilled water and air drying. The membrane was then imaged for use as a loading control.

Chapter 3. Effect of Dietary Fat Ingestion on Muscle Protein Metabolism and Insulin Sensitivity in Overweight Men

3.1 Introduction

There is controversy over whether the relationship between insulin resistance (IR) and anabolic resistance is causal. The association could be mediated by the increased levels of adiposity commonly found in individuals with IR. For instance, older (55 to 75 years old) obese males with increased leg fat mass had reduced insulin-stimulated leg glucose disposal and were more anabolic resistant to amino acid (AA) ingestion under hyperinsulinaemia than those with lower leg fat mass (Murton et al., 2015). In line with this, overweight or obese young adults had a blunted muscle protein synthesis (MPS) response to a protein-dense meal in comparison to healthy weight adults (Beals et al., 2016). This was shown despite similar circulating AA concentrations and upregulation of AA transporter expression after feeding. However, only the obese, but not the overweight group were insulin resistant. This implicates other factors that tend to worsen with increasing adiposity, such as the deterioration in the metabolic quality of skeletal muscle (i.e. increased intramyocellular lipid (IMCL) and lipid-derived intermediates). This deterioration is likely exacerbated by a sedentary lifestyle (Smeuninx et al., 2017; St-Jean-Pelletier et al., 2017). Indeed, physically active obese middle-aged (30 to 55 years old) men had comparable rates of MPS to lean control subjects, despite increased IR in the obese group (Kouw et al., 2019).

On an acute basis, elevating fatty acid availability via an intravenous lipid and heparin infusion induces skeletal muscle IR and blunts the anabolic response to AA ingestion under hyperinsulinemia in healthy young males (Stephens et al., 2015). This was associated with complete suppression of 4E-BP1 phosphorylation i.e. impaired anabolic signalling. Oral ingestion of 100 ml of soy-bean oil (61% PUFA, 23% MUFA and 16% SFA) induces similar impairments to a lipid infusion in skeletal muscle insulin sensitivity of healthy participants (Nowotny et al., 2013). The degree of IR may even be exacerbated by providing a meal richer in SFA content and/or in overweight participants. However, the effects of oral fat ingestion on the subsequent anabolic response to ingestion of AAs is not well understood, particularly under more 'real life' conditions of an oral fat load (vs. infusion).

Aims

This study was undertaken to examine the hypothesis that; increasing circulating fatty acids in overweight/obese individuals via ingestion of a high-SFA oral liquid meal will induce IR of CHO metabolism and anabolic resistance i.e. an impaired skeletal muscle protein synthetic response to dietary AA ingestion. Unlike most previous research, we aimed to replicate a more 'real life' situation by not using lipid infusions or clamping insulin levels at hyperinsulinaemic concentrations.

3.2 Methods

3.2.1 Participants

This study recruited eight middle-aged (40 to 60 years old) males who were all overweight/obese (BMI > 27 $kg \cdot m^{-2}$). All subjects were physically inactive and not

diagnosed with T2D. Exclusion criteria outlined in the general methods chapter were also applied. Participant characteristics and an index of fasting insulin sensitivity (HOMA-IR) is summarised below in Table 3.1.

Table 3.1. Descriptive characteristics of study participants.

Age (years)	Body mass (kg)	BMI ($kg \cdot m^{-2}$)	HOMA-IR
46 (4)	96.7 (5.3)	32.3 (5.4)	4.7 (4.0)

Data presented as mean (SD); n=8.

3.2.2 Statistical Power

The repeated measures coefficient of variation for measuring [1-^{13}C] phenylalanine incorporation into the myofibrillar protein pool in muscle (FSR; fractional synthetic rate) is 10%. Our group has previously demonstrated that lipid infusion (vs. saline) halved the FSR response to ingestion of AAs (Stephens et al., 2015). Oral ingestion of lipid rich liquid meals and intravenous infusions of lipid emulsion induce comparable levels of skeletal muscle IR (Nowotny et al., 2013). Therefore, if similar differences in FSR were found in the present study, these should be detectable using 8 subjects with a power of 80%.

3.2.3 Experimental Design

This was a randomised crossover study with each experimental trial separated by a minimum of two weeks. On each occasion, subjects arrived at the laboratory at 08:00 after an overnight fast, having abstained from heavy exercise and alcohol consumption in the previous 48 h. Participants consumed an oral test meal 4 h before (0 h time point) ingestion of a bolus of milk protein (0.35 $g \cdot kgBW^{-1}$), which was intrinsically labelled with [1-^{13}C] phenylalanine, along with 0.8 $g \cdot kgBW^{-1}$ dextrose and mixed into 4 $ml \cdot kgBW^{-1}$ of water. The oral test meal was consumed at the 4 h time point and

comprised of a warm, chocolate-flavoured drink containing either 0.7 g·kgBW^{-1} palm stearin (~65% SFA) with 1 g of monoglyceride (emulsifier) or water (control). Both test meals contained 5 g of chocolate powder (1.15 g protein, 0.5 g CHO, 1.0 g fat) with 1 g of aspartame-based sweetener and was dissolved into 6 ml·kgBW^{-1} of water.

3.2.4 Metabolic Testing

Upon arrival, participants voided their bladder and rested in a semi-supine position on a hospital bed. An intravenous cannula was inserted retrograde into a superficial dorsal hand vein, this was placed in a heated box maintained at 55℃ for the sampling of arterialised-venous blood (Section 2.2.2). This was kept patent using a saline drip. Blood samples were collected at the times indicated below in Figure 3.1. All blood samples were analysed for concentrations of glucose (Section 2.2.5), insulin (Section 2.2.8), FFAs (Section 2.2.10), and TAG (Section 2.2.11). In addition, samples collected after consumption of the protein drink were analysed for the appearance of phenylalanine, tyrosine and leucine, as well as [1-^{13}C]-phenylalanine enrichment (see below).

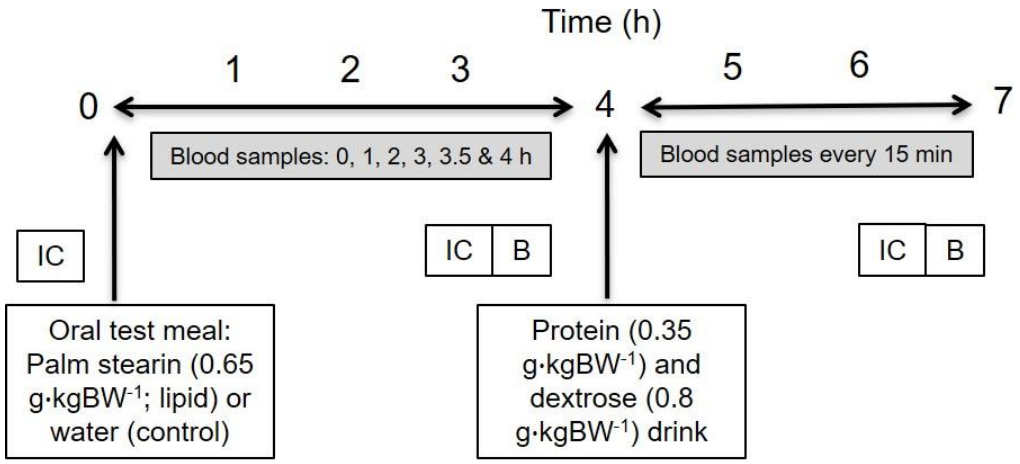


Figure 3.1. Schematic of metabolic testing protocol.
IC = Indirect calorimetry, B = Vastus lateralis muscle biopsy.

Indirect calorimetry measurements (Section 2.4.2) were undertaken; prior to ingestion of the oral test meal, before and 2.5 h after ingestion of the protein drink. Additional urine samples were collected at the 4 and 7 h timepoints and analysed for urea nitrogen to correct calculations of RER/substrate oxidation rates for protein oxidation (Section 2.4.3). Vastus lateralis muscle biopsies were obtained at 4 and 7 h using the percutaneous needle biopsy technique (Section 2.3.1) from the same leg on each visit. The needle was rapidly frozen in liquid nitrogen cooled isopentane, before long-term storage in liquid nitrogen. Biopsies were subsequently analysed for [1-^{13}C] phenylalanine incorporation as an index of FSR (Pennings et al., 2011), as described in Section 2.3.2.

Muscle protein content of phosphorylated Akt^{Ser473}, mTOR^{Ser2448} and 4E-BP1$^{Thr37/46}$ (all from Cell Signalling Technology, Danvers, MA, USA) were determined using SDS-PAGE (Section 2.3.8) and normalised to the content of α-actin. Glycogen concentrations were determined from freeze-dried, powdered muscle as described in Section 2.3.3. Muscle pyruvate dehydrogenase complex (PDC) activity was assessed as described in Section 2.3.4. In addition, 5 μm thickness muscle cross-sections were stained with LipidTOX (Thermo Fisher Scientific, Waltham, MA, USA) and anti-fade gold, then imaged with confocal microscopy as previously described (Tsintzas et al., 2017). Images were subsequently quantified for IMCL content using Volocity image analysis software (PerkinElmer, Waltham, MA, USA).

Blood collected for AA analysis was deproteinised with dry 5-sulfosalicyclic acid for 10 min and centrifuged to collect plasma. These were purified using an ion exchange column and free AAs were converted to tert-butly dimethylsilyl derivatives before analysing with GC-MS. Enrichment of plasma with [1-^{13}C] phenylalanine was

determined in a similar fashion to muscle enrichment and expressed as molar percent excess (MPE) using the following equation:

$$\text{MPE} = 100 \times \frac{(^{13}C)}{(^{12}C + {}^{13}C)}$$

3.2.5 Statistical Analysis

Data analysis was undertaken using GraphPad Prism 7.0 (GraphPad Software Inc., San Diego, CA, USA). Differences in [1-^{13}C] phenylalanine incorporation were assessed using a Student's paired t-test. All other data was analysed using a two-way (treatment x time) repeated measures analysis of variance (ANOVA). Post-hoc tests were conducted on significant findings using the Bonferroni correction for multiple comparisons. Data in text and tables is presented as mean ± standard deviation (SD) and error bars in the figures represent standard error of the mean (SEM). Significance was accepted at $p \leq 0.05$.

3.3 Results

3.3.1 Blood Glucose and Serum Insulin

Blood glucose (Figure 3.2) and serum insulin (Figure 3.3) were similar between trials at baseline (fasted) and did not change in the first 4 h after consumption of the oral test meal. After consumption of the CHO and protein drink, blood glucose concentrations increased from just under 5 mmol·L^{-1} to 8.5 mmol·L^{-1} but declined to fasting levels by 180 min and were similar between trials. Serum insulin followed a similar pattern of response with no differences found between trials. However, unlike glucose concentrations, insulin levels remained around four times higher than fasting values at 180 min post-consumption of the CHO and protein drink.

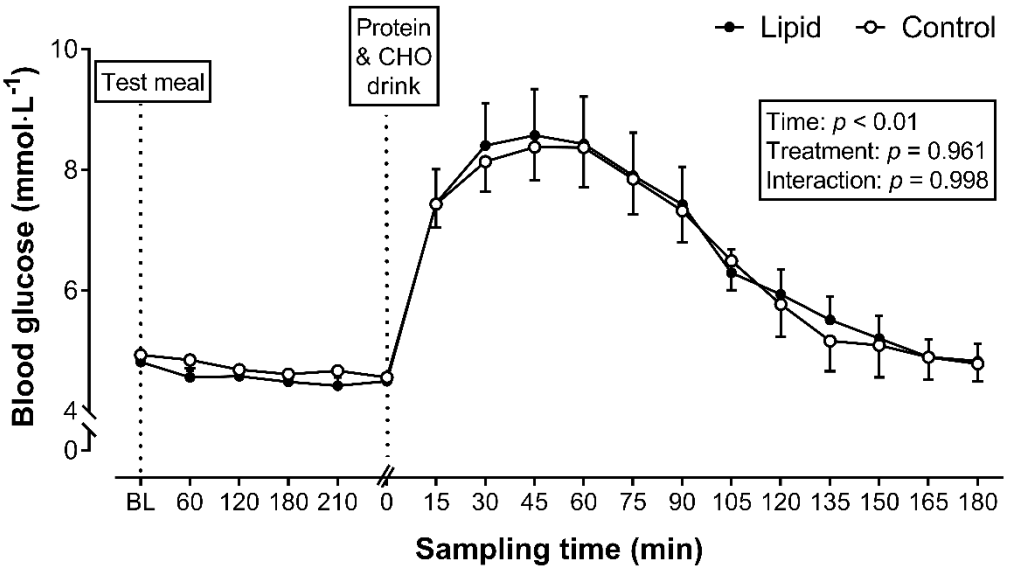


Figure 3.2. Blood glucose.
Arterialised whole blood glucose after consumption of the test meal (lipid or water) followed by a protein and dextrose drink 4 h later. Data is presented as mean ± SEM; n=8.

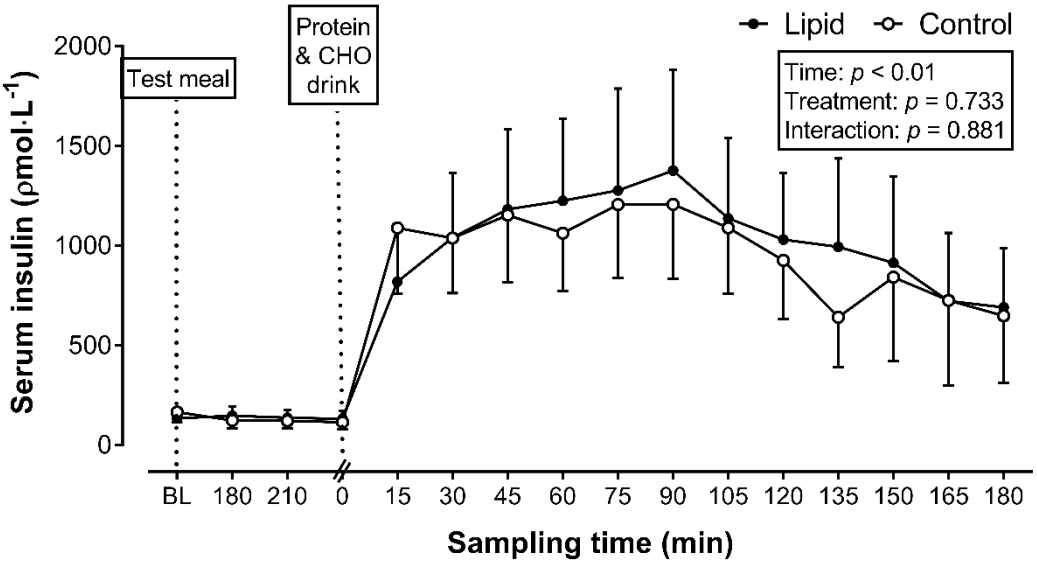


Figure 3.3. Serum insulin.
Serum insulin concentrations after consumption of the test meal (lipid or water) followed by a protein and dextrose drink 4 h later. Data is presented as mean ± SEM; n=8.

3.3.2 Serum Triacylglycerol and Plasma Free-Fatty Acids

Serum TAG and plasma FFA concentrations were similar at baseline. There was a significant interaction (time x treatment) effect (F=7.558; $p < 0.001$) for TAG responses. As shown in Figure 3.4, ingestion of the lipid drink increased TAG concentrations by around two-fold, whereas the control drink had minimal effect. In the Lipid trial, TAG concentrations began to decrease 30 min after consumption of the CHO and protein drink but remained significantly elevated above the Control trial up until 105 min postprandial.

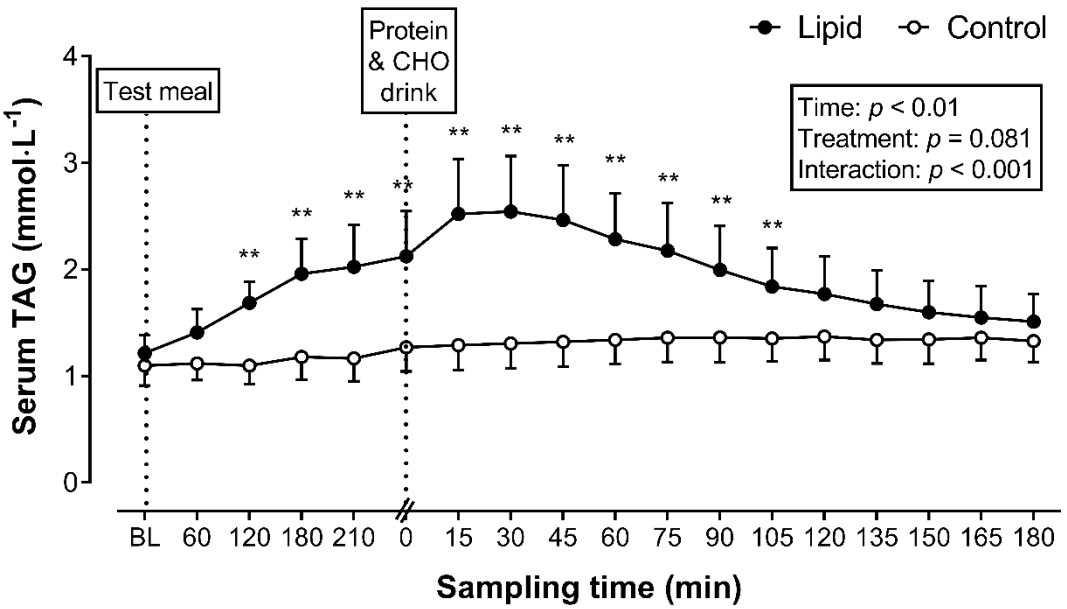


Figure 3.4. Serum triacylglycerol.
Serum triacylglycerol (TAG) concentrations after consumption of the test meal (lipid or water) followed by a protein and dextrose drink 4 h later. Data is presented as mean ± SEM; n=8. $^{**}p < 0.01$ from Control.

There was a significant interaction effect for FFAs (F=4.346; $p < 0.001$). Plasma FFA concentrations increased to a greater extent after consumption of the lipid drink, reaching a peak of 0.68 vs 0.52 mmol·L^{-1} at 4 h. Following ingestion of the CHO and protein drink, FFAs were suppressed at a similar rate and as a result, concentrations in

the Lipid trial remained elevated in the initial 90 min when compared with the Control (Figure 3.5). There was also a significant treatment effect (F=6.768; p = 0.035).

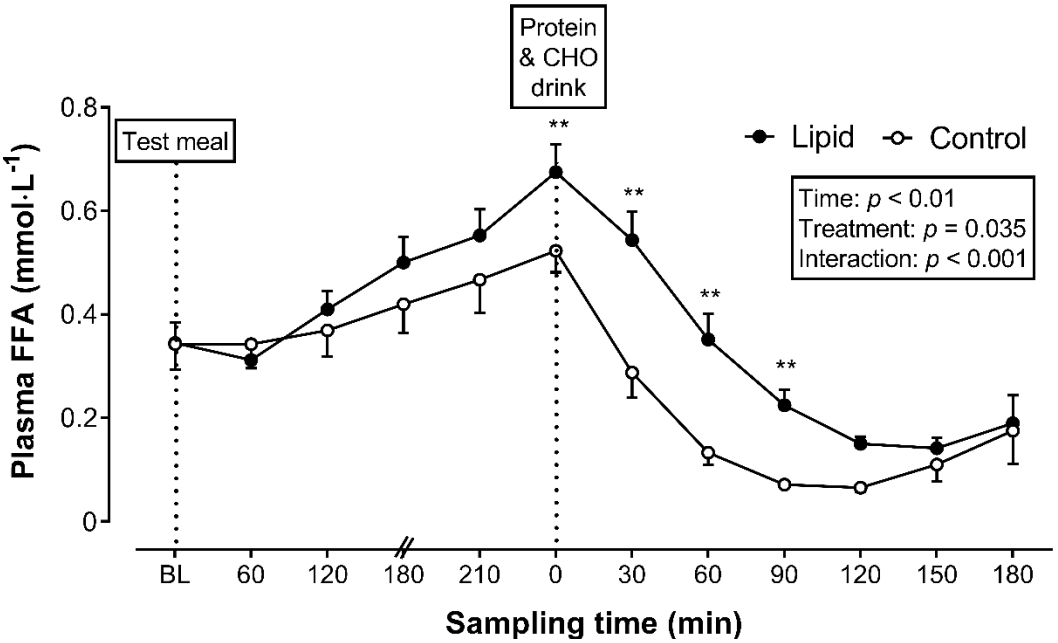


Figure 3.5. Plasma free-fatty acids.
Plasma free-fatty acids (FFA) concentrations after consumption of the test meal (lipid or water) followed by a protein and dextrose drink 4 h later. Data is presented as mean ± SEM; n=8. ** p < 0.01 from Control.

3.3.3 Respiratory Exchange Ratio and Substrate Oxidation

Non-protein RER tended to be lower (F=4.95; p = 0.061) throughout the lipid trial but increased to a similar extent after consumption of the CHO and protein drink (Table 3.2). In accordance with this, fat oxidation was also greater in the lipid trial at both timepoints (F=7.443; p = 0.029). CHO oxidation increased in both trials after consumption of the CHO plus protein drink and tended to be higher at 180 min in the control trial (p = 0.054).

Table 3.2. Respiratory exchange ratio and substrate oxidation.
Non-protein respiratory exchange ratio (RER) and rates of CHO/fat oxidation in the Control (water) and Lipid trial at 0 and 180 min (relative to consumption of CHO and protein drink).

	Control		Lipid	
	0 min	180 min	0 min	180 min
RER	0.80	0.83	0.75*	0.78**
	(0.05)	(0.05)	(0.04)	(0.04)
CHO oxidation (g·min^{-1})	0.05	0.13	0.01	0.07
	(0.09)	(0.10)	(0.10)	(0.05)
Fat oxidation (g·min^{-1})	0.06	0.06	0.11**	0.11*
	(0.09)	(0.06)	(0.03)	(0.04)

Data are displayed as mean ± SD; n=8. Lipid vs Control: *$p \leq 0.05$, **$p < 0.01$.

3.3.4 Plasma Amino Acids

Fasted concentrations of leucine, phenylalanine and tyrosine were similar between trials, but all changed significantly over time ($p < 0.01$). Slight non-significant reductions were evident in the first 4 h after consumption of the lipid drink, whereas AA concentrations were more stable in the control trial. In both trials, AA concentrations increased in response to consumption of the CHO and protein drink. There was a tendency for higher leucine (F=3.9; $p = 0.089$; Figure 3.6a) and phenylalanine (F=5.373; $p = 0.054$; Figure 3.6c) concentrations throughout the Control trial. The interaction effect for tyrosine concentrations approached significance (F=2.035; $p = 0.058$; Figure 3.6b). This indicated a greater reduction after the test drink and lower increase after consumption of the CHO and protein drink in the Lipid trial.

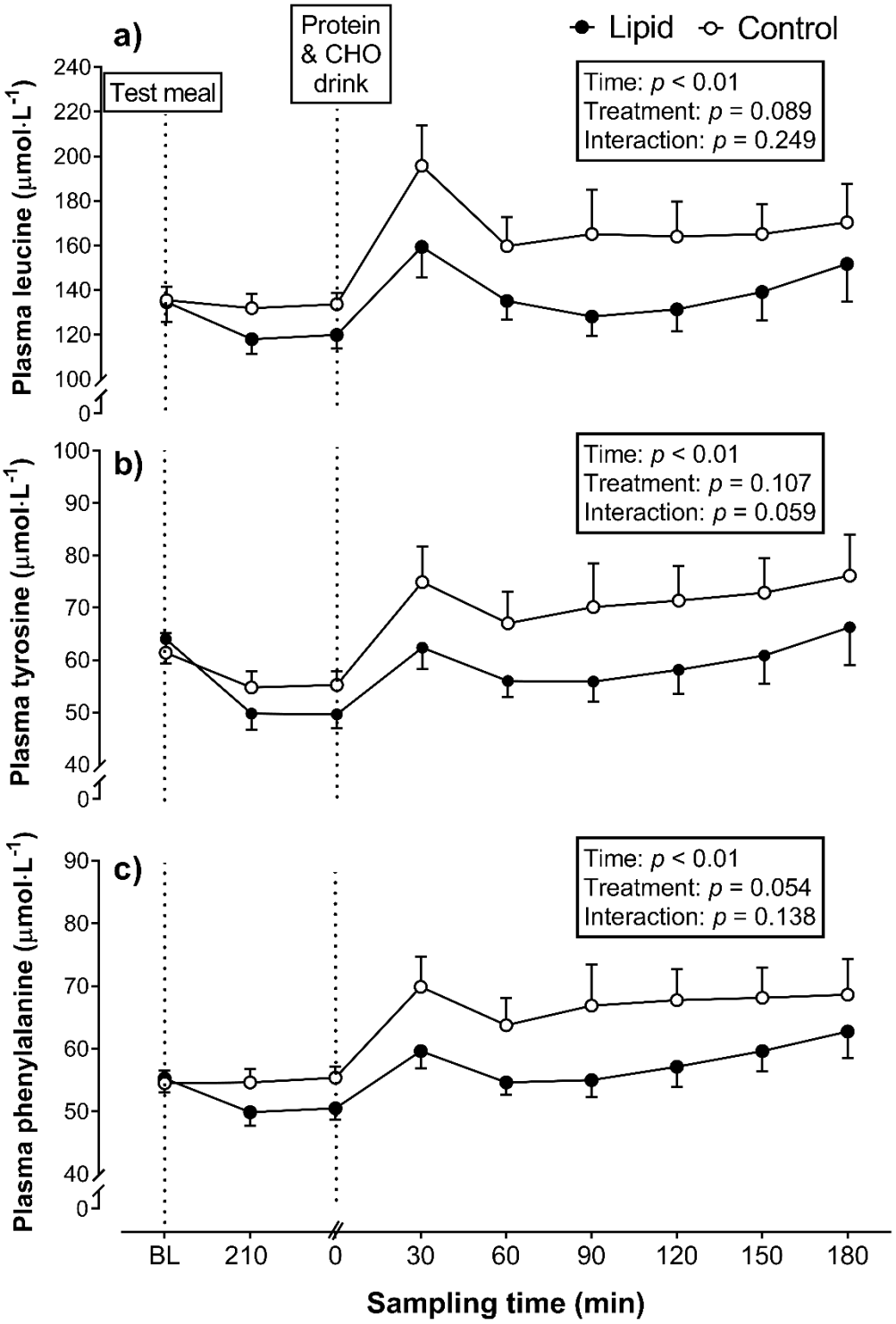


Figure 3.6. Plasma amino acids.
Plasma concentrations of (a) leucine, (b) tyrosine and (c) phenylalanine after consumption of the test meal (lipid or water) followed by a protein and dextrose drink 4 h later. Data are presented as mean ± SEM; n=8.

3.3.5 [1-^{13}C]-Phenylalanine Appearance and Incorporation into Muscle

Plasma [1-^{13}C] phenylalanine enrichment (MPE) was negligible before and 4 h after consumption of the test meal (Figure 3.7). This increased significantly after consumption of the CHO and protein drink in both trials ($p < 0.01$), reaching a plateau between 150 to 180 min. There were no differences between trials. However, incorporation of [1-^{13}C] phenylalanine into the myofibrillar protein pool in the Lipid trial was two-fold higher ($p = 0.026$) than the Control trial (Figure 3.8).

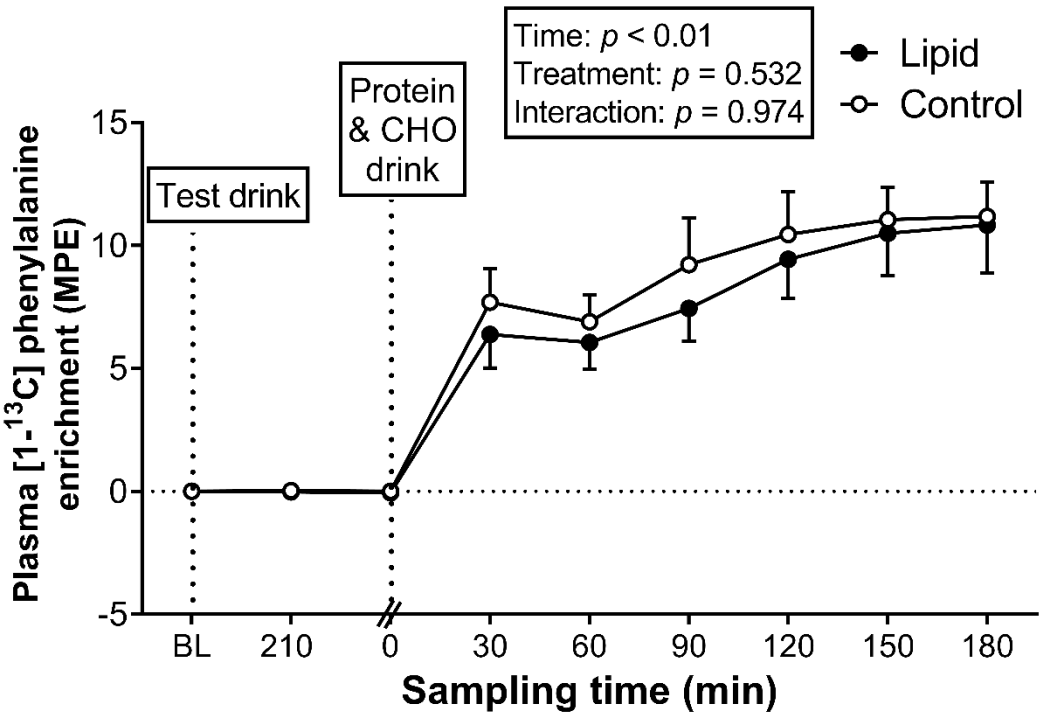


Figure 3.7. Plasma [1-^{13}C] phenylalanine enrichment.
Plasma enrichment of [1-^{13}C] phenylalanine after consumption of the test meal (lipid or water) followed by a protein and dextrose drink 4 h later, expressed in molar percent excess (MPE). Data is presented as mean ± SEM; n=8.

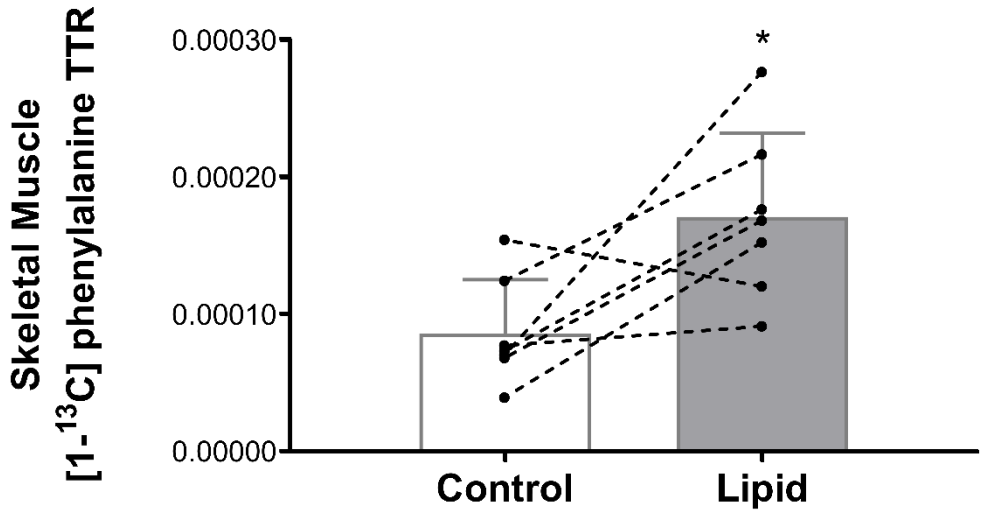


Figure 3.8. [1-^{13}C] Phenylalanine incorporation.
Incorporation of [1-^{13}C] phenylalanine into the muscle myofibrillar pool (TTR; tracer to tracee ratio) as an index of fractional synthetic rate after consumption of the dextrose and intrinsically labelled milk protein drink. Data are displayed as mean ± SEM; n=7. *$p \leq 0.05$.

3.3.6 Muscle Protein Content

There were no changes in 4E-BP1$^{Thr37/46}$ content between trials or after consuming the CHO and protein drink (Figure 3.9a). The content of mTOR^{Ser2448} increased (F=5.846; $p = 0.046$) in both trials after consumption of the drink and there was a slight tendency for increased content throughout the lipid trial (F=3.51; $p = 0.103$; Figure 3.9b). The content of Akt^{Ser473} was similar at baseline and significantly increased (F=26.79; $p < 0.001$) in both trials after consumption of the CHO and protein drink (Figure 3.9c). There were no differences between trials.

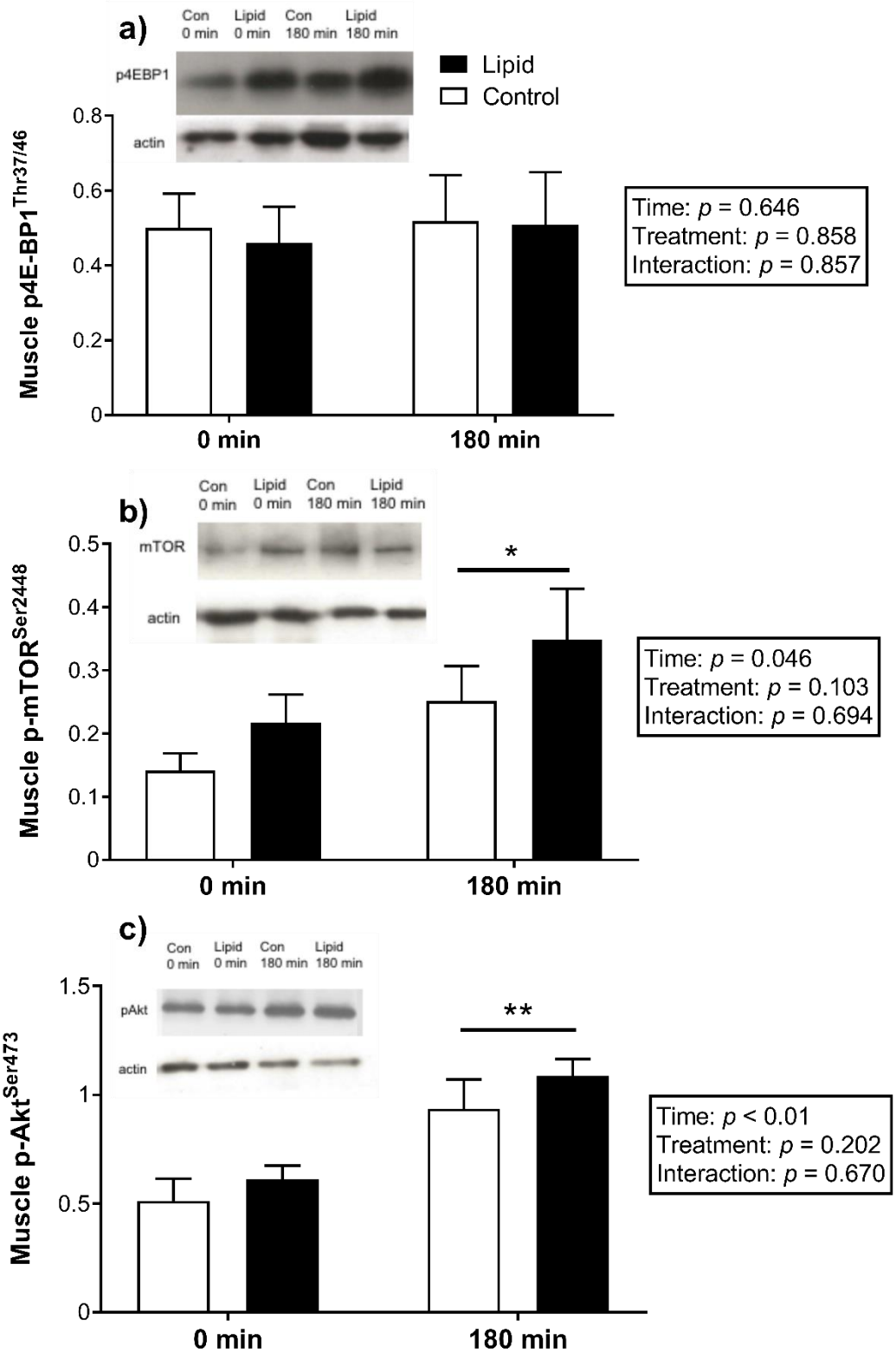


Figure 3.9. Phosphorylation of 4E-BP1, mTOR and Akt.
Skeletal muscle protein content of (a) 4E-BP1$^{Thr37/46}$, (b) mTOR^{Ser2448} and (c) Akt^{Ser473} normalised to α-actin. Data are displayed as mean ± SEM; n=8. *$p \leq 0.05$. **$p < 0.01$ from 0 min.

3.3.7 Muscle Glycogen and Pyruvate Dehydrogenase Complex Activity

Due to an insufficient amount of muscle tissue remaining, one sample was missing from PDC analysis and three samples were missing from glycogen analysis. These were replaced using missing value analysis. Both muscle glycogen (Figure 3.10) and PDC activity (Figure 3.11) were similar prior to, and unchanged in response to, consumption of the CHO and protein drink. There were no differences between the Control and Lipid trial.

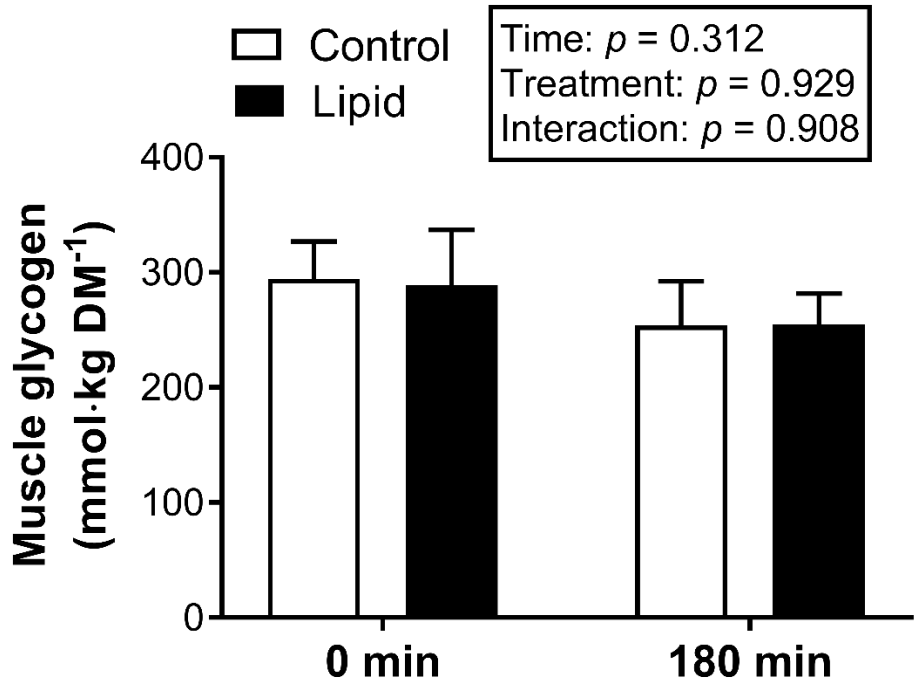


Figure 3.10. Muscle glycogen content.
Muscle glycogen content before (0 min) and after (180 min) consumption of a CHO and protein drink. Data is displayed as mean ± SEM of glycosyl units; n=8.

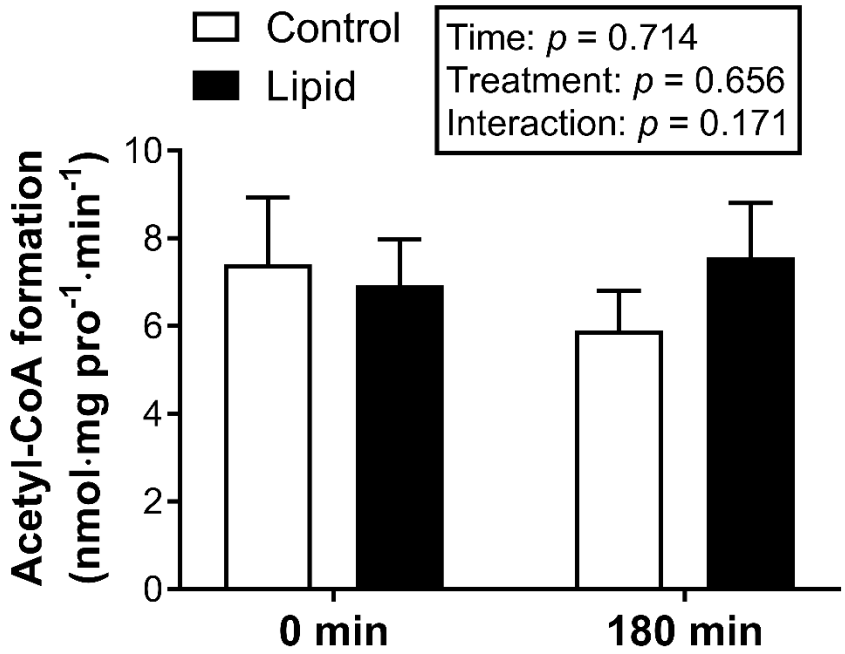


Figure 3.11. Muscle PDC activity.
Muscle pyruvate dehydrogenase complex activity before (0 min) and after (180 min) consumption of a CHO and protein drink. Data is displayed as mean ± SEM; n=8.

3.3.8 Intramyocellular Lipid Content

Only four subjects were included in the IMCL analysis shown in Table 3.3, due to an insufficient amount of muscle tissue remaining for the other participants. There was a main effect for time (F=11.73; p = 0.042) in the number of lipid droplets per fibre, which decreased after consumption of the CHO and protein drink. However, no differences were shown between trials. The interaction effect (time x treatment) for IMCL as a % of fibre area approached but did not reach statistical significance (F=9.624; p = 0.053). The proportion of IMCL coverage was higher at 0 min and tended to decrease after consumption of the drink in the Control trial, whereas IMCL % remained similar in the Lipid trial.

Table 3.3. Intramyocellular lipid content.
Number/area of lipid droplets per fibre and proportion of lipid coverage per fibre in the Control or Lipid trial at 0 and 180 min (relative to consumption of CHO and protein drink).

	Control		Lipid	
	0 min	180 min	0 min	180 min
Lipid droplet area (μm^2)	0.49 (0.06)	0.45 (0.05)	0.46 (0.05)	0.46 (0.06)
Lipid droplets per fibre	842 (81)	614 (21)	728 (141)	740 (70)
IMCL (% area of fibre)	7.5 (1.6)	6.1 (0.9)	6.6 (1.3)	6.6 (1.3)

Data are displayed as mean ± SD; n=4.

3.4 Discussion

The primary finding from this study was that oral fat ingestion doubled the incorporation of dietary [1-^{13}C]-phenylalanine into the myofibrillar pool in response to a subsequent CHO and protein drink in middle-aged, overweight participants. This finding, along with the absence of any lipid-induced impairments in CHO metabolism in response to the intrinsically labelled protein and dextrose drink, is contrary to our hypotheses that the lipid drink would induce both IR of CHO metabolism and an impaired anabolic response to the subsequent ingestion of AAs.

The enhanced incorporation of dietary [1-^{13}C]-phenylalanine into the myofibrillar pool in the Lipid trial was independent of changes in 4E-BP1 signalling. Previous research from our group (Stephens et al., 2015) and others (Smiles et al., 2019), has implicated attenuated 4E-BP1 phosphorylation in the blunted MPS response from acutely elevating lipid availability. The former study used a 10% intralipid infusion, providing a similar total dose of lipid to the current study, to elevate FFA levels to comparable levels of ~0.7 mM in healthy young males. This resulted in marked IR in the lipid group, whilst the present study did not see any impairments in indexes of insulin sensitivity. This could relate to differences in participant characteristics as the current study was undertaken on overweight/obese middle-aged males. Whilst this

group is likely more susceptible to (chronic) IR, Manco et al. (2004) found that unlike in healthy controls, obese participants display no marked impairment of insulin sensitivity in response to ingestion of SFA. This is consistent with the findings of the present study and is presumably due to this population already showing a degree of resistance to the effects of insulin, which is supported by participants' HOMA-IR.

An additional factor to consider are the difference(s) in experimental design. This study used a more physiological model of oral lipid ingestion 4 h prior to ingestion of a CHO and protein drink. Whereas in the study by Stephens et al. (2015), the lipid infusion persisted after AA ingestion and throughout the hyperinsulinaemic eugylcaemic clamp. In both instances, the increase in insulin (either endogenous or exogenous) suppressed FFA levels, in the Lipid and Control conditions. However, the differences in FFA between the conditions, particularly between 90-180 min postprandial, were greater during the clamp than in the present study. More specifically, FFA concentrations were maintained at postabsorptive concentrations throughout the clamp in the Lipid trial but approached zero in the Control trial.

Elevating FFA levels during hyperinsulinaemic conditions has been shown to increase IMCL content (Brechtel et al., 2001) and the intramuscular accumulation of lipid-derived intermediates; long-chain acyl-CoA and acetylcarnitine (Stephens et al., 2015; Tsintzas et al., 2007). However, under unclamped insulin concentrations in the present study, we found no changes in IMCL content despite the increased rates of whole-body fat oxidation in the Lipid trial.

Interestingly, another lipid-derived intermediate ceramide, has been shown to disrupt anabolic signalling and downregulate MPS *in vitro* (Hyde et al., 2005). This suggests a possible link between the accumulation of lipid-derived intermediates and

anabolic resistance. Whilst similar muscle ceramide content has been shown after oral or intravenous administration of lipid (Nowotny et al., 2013), this was not assessed after the insulin clamp, thus differences at this stage cannot be discounted. Moreover, both routes of lipid delivery induced IR in this young, lean and insulin-sensitive cohort. Nevertheless, increases in membrane C18:2 DAG were only shown after intravenous lipid administration. The precise role of specific DAGs are emerging, but they likely have distinctive effects on signalling when present in the membrane fraction.

Both Smiles et al. (2019) and Katsanos et al. (2009) utilised 20% intralipid infusions to elevate plasma FFA levels to concentrations approaching supraphysiological levels (> 2 mM). The former study investigated the subsequent anabolic response of middle-aged, overweight individuals to the ingestion of 30 g of whey protein. In contrast to this study, but in accordance with Stephens et al. (2015), they showed reductions in MPS in the Lipid trial. Unfortunately, insulin sensitivity was not quantified, thus it is unclear whether this finding supports our assertion that IR may be a prerequisite to observe anabolic resistance.

Katsanos et al. (2009) examined the subsequent anabolic response of young and healthy participants to the ingestion of 7 g of essential AA, after receiving a lipid or saline infusion, by measuring phenylalanine balance across the leg. Like Stephens et al. (2015), these infusions persisted throughout the postprandial period, but insulin levels were left unclamped. This led to appreciably higher insulin concentrations in the Lipid group prior to and in the 3 h postprandial. Nevertheless, AA ingestion elicited comparable improvements in net phenylalanine balance and in mixed-muscle FSR between the Lipid and Control groups. Interestingly, absolute values of net

phenylalanine balance before and in the 3 h postprandial period were more positive in the Lipid trial compared with Control. This was primarily attributed to lower rates of phenylalanine appearance into the vein (an index of muscle protein breakdown), perhaps due to the elevated insulin concentrations in the Lipid trial. This is unlikely to have played a role in our findings, since insulin concentrations in the Lipid and Control trials were similar.

An additional distinction between the current study with previous lipid infusion studies is fatty acid composition. Lipid infusions primarily consist of soybean oil (~60% PUFA), whereas we used a palm stearin drink (~65% SFA) to elevate FFA concentrations. SFAs are postulated as most deleterious to insulin sensitivity (Vessby et al., 2001). Although insulin sensitivity of glucose uptake was not directly measured in the present study; similar glycaemic responses, muscle PDC activation levels and muscle glycogen levels were shown. Furthermore, no differences in muscle Akt phosphorylation were found, which increased in response to ingestion of the CHO and dextrose drink in both trials. Considering that the insulinaemic responses were also comparable, this suggests that prior ingestion of an oral fat load does not impair CHO metabolism. These findings were surprising, given that oral administration of soy bean oil had been shown to induce comparable reductions in insulin sensitivity to a lipid infusion in healthy young individuals (Nowotny et al., 2013). It remains possible that overweight/obese participants are less susceptible to lipid-induced IR (Manco et al., 2014).

The enhanced incorporation of dietary [1-^{13}C]-phenylalanine into the myofibrillar pool in the lipid trial is difficult to reconcile. Interestingly, there was a slight tendency (p = 0.103) for increased phosphorylation of mTOR in the lipid trial. Although this

increased to a similar extent after consuming the protein and CHO drink, presumably due to the resulting increase in insulin and AA, basal levels were numerically ~50% greater in the Lipid trial. This could reflect the increased energy availability after provision of the lipid vs water (control) and may be mediated through increased inhibition of AMPK (Kwon and Querfurth, 2015; Rivas et al., 2009). However, no differences in basal mTOR phosphorylation were shown in response to an intralipid vs saline infusion previously (Stephens et al., 2015). Water was chosen as a control drink to examine the independent effects of acutely elevating FFA. However, we cannot exclude the possibility that being in a more acute positive energy balance played a role in the increased incorporation of dietary [1-^{13}C]-phenylalanine into the myofibrillar pool. Although it is difficult to conceive of an alternative / energy-matched drink that will not perturb metabolism and potentially influence subsequent responses.

The milk protein (~80% casein) and dextrose drink was consumed 4 h after the lipid or water drink. Despite this, there was a tendency for lower plasma AA (leucine, tyrosine and phenylalanine) in the Lipid trial after consumption of the protein and CHO drink. It is possible that this reflects a delayed appearance of AA into the circulation from lower rates of gastric emptying. However, this appears unlikely since co-ingestion of milk fat with micellar casein does not blunt or delay the appearance of dietary protein-derived phenylalanine, or attenuate subsequent rates of MPS when assessed over a 5 h postprandial period (Gorissen et al., 2017).

AA concentrations remained elevated at 180 min in both trials, which could suggest that we did not capture the full stimulatory effects of the CHO and protein drink on MPS. Previous research has shown that ingestion of milk protein primarily exerts its

anabolic effects within the initial 90 min in middle-aged men (Mitchell et al., 2015). However, co-ingestion with dextrose is likely to further slow protein digestion and absorption (Gorissen et al., 2014). Although intuitively, differences between the Lipid and Control trial would be more likely to be seen closer to the consumption of the respective drinks.

The comparable plasma enrichment of [1-^{13}C] phenylalanine between both trials, combined with the lower plasma AA concentrations in the lipid trial, could potentially implicate enhanced transport of AA into the skeletal muscle. This would increase the intracellular availability of AA and provide a greater anabolic stimulus. It is also possible that being in a more acute positive energy balance i.e. in the Lipid trial, promotes an increased partitioning of these AAs towards protein synthesis rather than oxidation.

This study used a crossover design to examine the hypothesis that ingestion of a high-SFA oral liquid meal will induce IR of CHO metabolism and anabolic resistance. As each participant acts as their own control this approach limits confounding variables between different individuals. An equal number of participants undertook the control/lipid trial first and the subsequent trial was separated by a minimum washout period of two weeks. However, a limitation was that the analysis was not stratified by treatment order, thus we cannot definitively rule out the presence of carryover effects (Wellek and Blettner, 2012).

In summary, acute oral ingestion of a high SFA drink positively impacts the subsequent skeletal muscle protein synthetic response to CHO and protein ingestion of middle-aged, overweight/obese individuals. The mechanism(s) behind these findings are elusive but could relate to differences in anabolic signalling and/or AA

transporter function, which are both warranting of further investigation. Since ingestion of the SFA drink did not induce IR of CHO metabolism, this study supports the notion that in the absence of IR, oral ingestion of lipids may exert a positive anabolic response to dietary protein.

Chapter 4. Effect of Palmitate on Protein Metabolism in Primary Human Skeletal Myotubes

4.1 Introduction

Examining the response of cultured muscle to fatty acid treatment is pertinent since elevated levels of circulating fatty acids are widely implicated in the pathogenesis of insulin resistance (IR) and type 2 diabetes (T2D). Saturated fatty acids (SFA) are postulated to be most deleterious to insulin sensitivity (Vessby et al., 2001). Palmitate is the most abundant SFA, with postabsorptive plasma concentrations of ~0.1 mM (Koutsari et al., 2011), comprising around 25% of the fatty acids in plasma and subcutaneous abdominal fat (Mittendorfer et al., 2003).

In Chapter 3, prior ingestion of a palm stearin drink (~60% SFA) was associated with a two-fold increase in the incorporation of dietary derived [1-^{13}C] phenylalanine into the myofibrillar pool of middle-aged overweight/obese men. The mechanism behind this response was unclear. The lower postprandial amino acid (AA) concentrations in the Lipid trial could implicate enhanced AA transport into the muscle. Increasing the intracellular availability of AA will likely increase the proportion of AAs incorporated into the myofibrillar protein (Wolfe, 2002). This in turn, potentially implicates AA transporter function.

It is well established that palmitate treatment induces IR (i.e. attenuated insulin-stimulated glucose uptake) *in vitro* (Coll et al., 2008; Dimopoulos et al., 2006; Perdomo et al., 2004; Powell et al., 2004). However, much of this work has been

undertaken on immortalised cell lines and using supraphysiological concentrations of palmitate. Most fatty acids transported into cultured muscle are channelled into phospholipids and triacylglycerol (TAG). However, palmitate is a poor substrate for TAG synthesis and tends to promote the synthesis of ceramides and diacylglycerol (DAG) (Pickersgill et al., 2007; Powell et al., 2004), which are widely implicated in IR (Section 1.4.4).

Interestingly, treatment of L6 muscle cells with ceramide leads to a dose-dependent inhibition of system A transport of AA by depleting sodium-coupled neutral AA transporter 2 (SNAT2) abundance in the plasma membrane and blunting anabolic signalling (Hyde et al., 2005). SNAT2 is established to play a role in the intracellular accumulation of system L substrates e.g. leucine and in regulating the activity of key nutrient signalling pathways, including mTOR (Section 1.5.3/1.5.4). Thus, SNAT2/AA transporters may play a role in anabolic resistance in both the basal (Hyde et al., 2005) and insulin-stimulated (Tardif et al., 2014) state after palmitate treatment.

Palmitate is also associated with hyperactivation of protein phosphatase 2A (PP2A), whereas provision of MUFA (e.g. oleate) antagonises these changes (Nardi et al., 2014). The key downstream effectors of mTOR: 4E-BP1 and S6K1 are proposed targets of PP2A (Gingras et al., 1999; Peterson et al., 1999). More specifically, activation of PP2A would lead to dephosphorylation (inactivation) of these key anabolic signals. This pathway could therefore underpin some of the associations between IR and AR observed *in vivo* and warrants further investigation.

The aims of this chapter were to investigate the effect of fatty acid treatment (with particular emphasis on palmitate) on glucose uptake, AA transport and MPS in

primary human skeletal myotubes. The response of relevant signalling pathways involved in these e.g. PI3K/Akt and mTOR, were also examined.

4.2 Methods

4.2.1 Primary Skeletal Myotubes

Satellite cells were isolated from vastus lateralis muscle biopsies obtained from healthy physically active donors [6 males, 1 female, age 23 (1) years, BMI 22.6 (3.1) $kg \cdot m^{-2}$; mean (SD)] and grown into confluent myotubes as described in Section 2.6. All experiments were conducted 7 to 10 days post induction of differentiation. Glucose uptake (2.6.4), AA transport (2.6.5), rates of protein synthesis (2.6.6) and protein content (2.3.8) were assessed as described. The duration and concentration of fatty acid treatment, in addition to the number of treatment and biological replicate(s) for each experiment are stated in the legend below each figure. All treatments were added to Ham's F10 medium, which has a glucose concentration of ~6 $mmol \cdot L^{-1}$. This was to maintain normal glucose delivery to the cells, as glucose starvation during fatty acid treatment will augment rates of fatty acid oxidation (Gaster, 2010). This will impact on subsequent metabolic function and measurements, including abolishing the effects of palmitate on IR (Lipina et al., 2013).

4.2.2 Statistical Analysis

All statistical analysis was undertaken in GraphPad Prism 7.0 (GraphPad Software Inc., San Diego, CA, USA) on the raw disintegrations per min (DPM) values for radioactive experiments i.e. [^{3}H] 2-DOG or [^{14}C] Me-AIB uptake. In most instances, data are presented as mean ± SEM, with individual biological replicates represented

as shapes in the Figure. The number of treatment and biological replicate(s) for each experiment is noted in the legend below each Figure.

Paired t-tests were used to compare differences between two means. A two-way repeated measures ANOVA was used to compare the responses of the same biological replicate(s) to multiple treatments i.e. palmitate/vehicle ± insulin. A mixed design two-way ANOVA was used to compare treatment responses from different biological replicates. Significance was accepted at $p \leq 0.05$.

4.3 Results

4.3.1 Effects of Leucine and Insulin on System A Amino Acid Transport

Initial experiments were undertaken to determine the uptake of [1-^{14}C] methylaminoisobutyric acid (Me-AIB), as an index of system A transport of AA, at varying concentrations of leucine and insulin. This was done to establish whether primary skeletal myotubes were responsive to stimuli known to increase the uptake of AA *in vivo*. As shown below in Figure 4.1a, increasing the leucine concentration from 0 to 0.5 mM resulted in a strong, linear increase in Me-AIB uptake which tended to plateau as concentrations were further elevated to 2 mM. Previous work on L6 skeletal muscle cells suggested 2 mM leucine as a maximally effective concentration (McDowell et al., 1995), although in accordance with the present results they did not appear to show a significant increase beyond 0.5 mM. However, we chose to use 2 mM leucine in all further experiments due to the reduced variability in the responses compared to 0.5 and 1 mM.

The effect of insulin on system A transport of AA (Figure 4.1b) was examined in the same biological replicate prior to analysing the above results, hence a leucine concentration of 1 mM was used. Elevating insulin concentrations to supraphysiological levels (≥ 10 nM) elicited a small increased in AA transport, which continued to rise from 25 to 100 nM insulin. We chose to use 100 nM in further experiments to maximise the stimulatory effect of insulin. Although we did not assess SNAT2 content or expression, increasing the availability of both leucine and insulin upregulates SNAT2 expression and is associated with increased mTOR signalling in L6 (Luo et al., 2013) and C2C12 (Walker et al., 2014) myotubes.

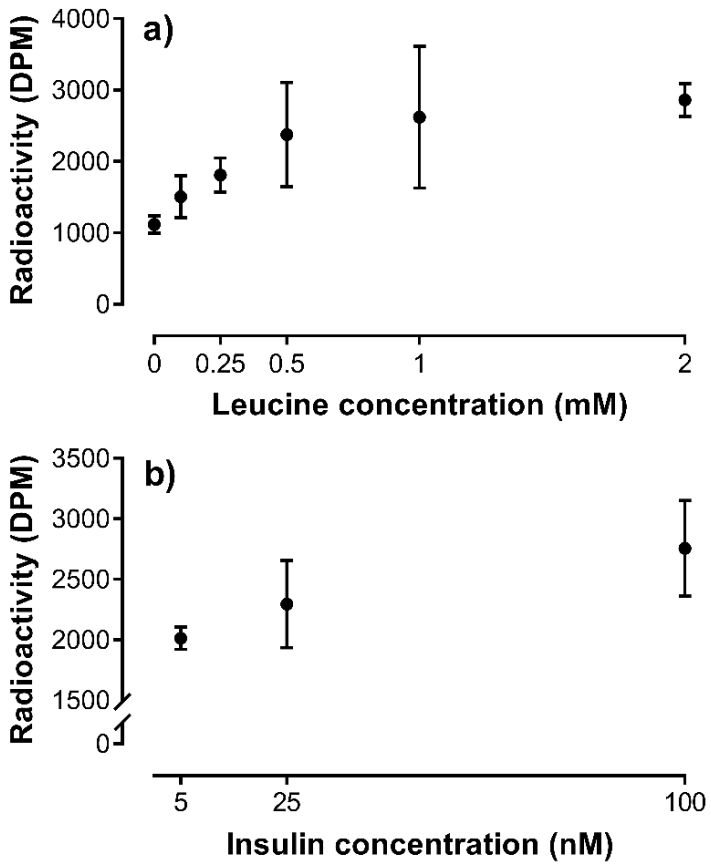


Figure 4.1. Effect of leucine and insulin on system A transport of amino acids.

Effect of increasing (a) leucine concentrations in the absence of insulin and (b) insulin concentrations in the presence of 1 mM leucine on system A amino acid transport ([^{14}C] Me-AIB uptake). Data displayed is from the mean (SD); n =3 treatment replicates of one biological sample.

4.3.2 Effect of Insulin on Glucose Uptake

One of the primary functions of insulin *in vivo* is to stimulate glucose transport, principally via augmented translocation of GLUT4. Cultured human muscle expresses relatively higher levels of GLUT1:GLUT4 content (molar ratio ~7:1 in membrane fraction) than *in vivo* (Sarabia et al., 1992). Thus, supraphysiological concentrations of insulin are typically used to overcome the reduced sensitivity to insulin stimulation *in vitro*.

As shown in Figure 4.2, treatment of human myotubes with 100 nM insulin elicited a ~35% increase in glucose uptake ($p = 0.008$). This is comparable to previous research (Al-Khalili et al., 2003; Krützfeldt et al., 2000). As it does *in vivo*, insulin stimulation promotes increased cell membrane GLUT4 content and glycogen synthesis (Al-Khalili et al., 2003). Biological variability in sensitivity to insulin stimulation was also evident (range 1.2 to 1.48-fold). There is contention whether *in vivo* insulin sensitivity is accurately reflected *in vitro* (Krützfeldt et al., 2000). Although there appears to be reasonable evidence that defects in insulin signalling are retained in myotubes established from T2D donors (Gaster et al., 2002). We obtained all biopsies from young and healthy donors to limit the effect(s) of any intrinsic metabolic defects in the response to treatments.

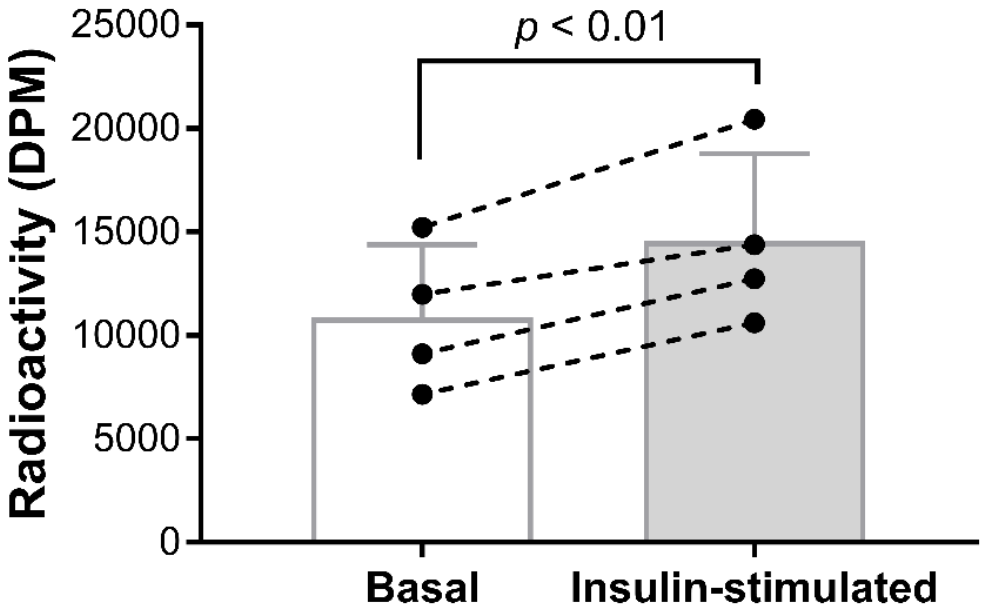


Figure 4.2. Effect of insulin on glucose uptake.
Radioactivity from [^{3}H]-2-DOG uptake ± 100 nM insulin for 3 h. The bar is mean ± SEM (n=4) with each dot representing a different biological sample (all derived from n=3 treatment replicates). The *p*-value is from a paired t-test.

4.3.3 Effect of Palmitate on Basal and Insulin-Stimulated Glucose Uptake

As previously mentioned, much of the work on palmitate-induced IR has been undertaken on immortalised cell lines with considerable variations on the duration and concentration of treatment. Indeed, numerous studies utilise palmitate concentrations ≥ 0.75 mM, which is likely to be in excess of what would be encountered *in vivo* and moreover, may have cytotoxic effects that impair cell viability (Yang et al., 2013; Yuzefovych et al., 2010). Therefore, we decided to treat human myotubes with a lower concentration of 0.25 mM palmitate to mitigate any cytotoxic effects. This will also more closely resemble the chronically elevated FFA levels in obesity and T2D (Arner

and Rydén, 2015) and acute enrichment of the plasma FFA pool with more SFA post-ingestion of a high fat meal (Griffiths et al., 1994).

We identified a significant interaction (insulin x treatment) effect ($F=53.28$; $p = 0.018$) after overnight (16 h) treatment with 0.25 mM palmitate. As shown in Figure 4.3, palmitate attenuated the insulin-stimulated increase in glucose uptake. In cultured muscle, palmitate-induced IR is typically associated with impaired insulin-stimulated phosphorylation of Akt via PI3K. This is established to play a key role in the translocation of GLUT4 and thus implicated in palmitate-induced IR. Surprisingly, we detected no differences in the phosphorylation of Akt between palmitate and control.

This discrepancy could reflect the lower concentration of palmitate used in the present study. For instance, Feng et al. (2012) examined the response of C2C12 myotubes to a range (0 to 0.5 mM) of palmitate concentrations and despite observing IR at 0.25 mM, only presented blunted Akt phosphorylation after 0.5 mM treatment. However, another study found that palmitate dose-dependently inhibits Akt^{Ser473} from 0.25 mM but not at 0.1 mM in L6 muscle cells (Yuzefovych et al., 2010).

The absence of any inhibitory effect of palmitate on Akt phosphorylation could also relate to differences in experimental design. After palmitate treatment, myotubes were incubated for 2 h in serum-free media in order to remove effects of exogenous growth factors and potentiate subsequent responsiveness to insulin (Ching et al., 2010; Klip et al., 1984). Following this, myotubes were incubated for 3 h in reaction buffer (± 100 nM insulin) prior to assessing glucose uptake or lysing the cells for western blot analysis. This was chosen to more closely mimic the design of *in vivo* experiments such as during a hyperinsulinaemic clamp that typically lasts between 3 to 4 hours. Since most research utilises shorter insulin stimulations (10 to 60 min), it is possible

we did not detect transient differences in Akt phosphorylation due to the extended interval after palmitate treatment and/or the prolonged insulin stimulation.

Both lipid-induced IR (Kruszynska et al., 2002; Stephens et al., 2015; Tsintzas et al., 2007) and chronic IR in T2D (Kim et al., 1999), is not always associated with impaired Akt phosphorylation under hyperinsulinemia *in vivo*. This suggests glucose transport can be impaired independently of Akt signalling and implicates alternative pathways, or pathways downstream of Akt, in the regulation of GLUT4 translocation (Gonzalez and McGraw, 2006), such as activation of protein kinase theta (PKCθ).

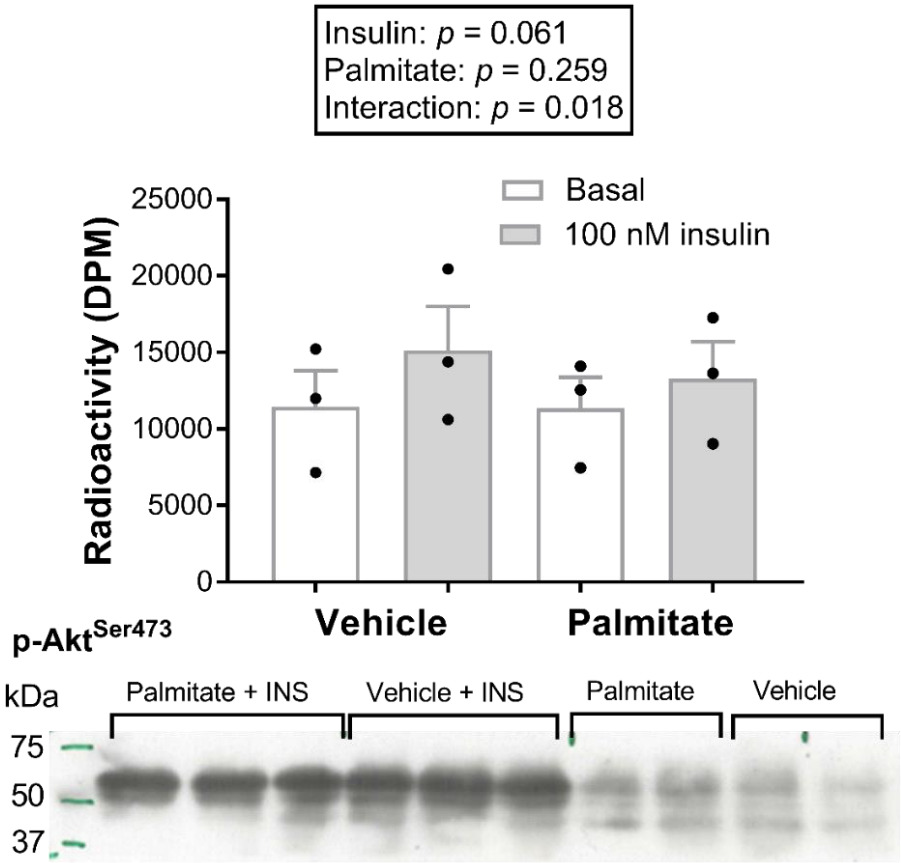


Figure 4.3. Effect of palmitate on glucose uptake and phosphorylation of Akt.

Radioactivity from [^{3}H] 2-DOG uptake after 16 h of treatment with 0.25 mM palmitate or vehicle ± 100 nM insulin for 3 h. Data is displayed as mean ± SEM (n=3) all derived from n=3 treatment replicates. *P*-values were determined from a two-way repeated measures ANOVA. Phosphorylation of Akt at serine 473 (~60 kDa) was determined from 20 µg of cell lysate obtained immediately after insulin stimulation.

4.3.4 Effect of Palmitate on System A Transport of Amino Acids

Previous research has shown that 0.75 mM palmitoleate treatment for up to 16 h has no effect on Me-AIB uptake in L6 cells (Dimopoulos et al., 2006). However, under these same conditions palmitate inhibited system A transport of AA by almost 50% (Hyde et al., 2005). This discrepancy likely relates to the increased palmitate-derived ceramide accumulation, since treatment with ceramide alone also blunts system A transport of AA (Hyde et al., 2005).

This study found reductions in system A transport of AA in cultured human muscle, despite using three-fold lower palmitate concentrations ($F=14.07$; $p = 0.020$). Surprisingly, the deleterious effects of palmitate were most evident under basal conditions ($p = 0.060$). To assess whether the effects of fatty acid on AA transport are specific to palmitate, incubations with 0.25 mM linoleate or oleate were also examined in a subset of experiments in Figure 4.4.

Oleate (MUFA) induced comparable results with palmitate treatment (Figure 4.5). This contrasts with work in primary trophoblast cells, which found that oleate increased, whilst palmitate had no effect on, system A AA transport (Lager et al., 2014). The observation that linoleate (PUFA) is most detrimental to AA transport is less surprising, given findings that it promotes SNAT2 degradation via the ubiquitin proteasome pathway in L6 muscle cells (Nardi et al., 2015).

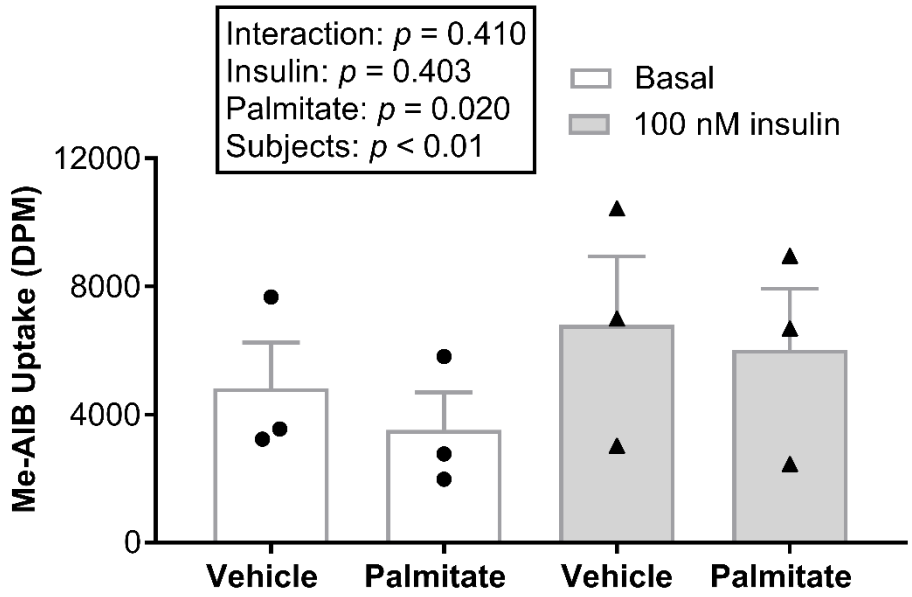


Figure 4.4. Effect of palmitate on system A of amino acid transport.
Effect of 16 h treatment with 0.25 mM palmitate or vehicle ± 100 nM insulin on the uptake of [^{14}C] Me-AIB uptake, as an index of system A transport of AA. Data is mean ± SEM (n=3 treatment replicates for each condition) and each shape represents a biological replicate. *P*-values are derived from a mixed design two-way ANOVA.

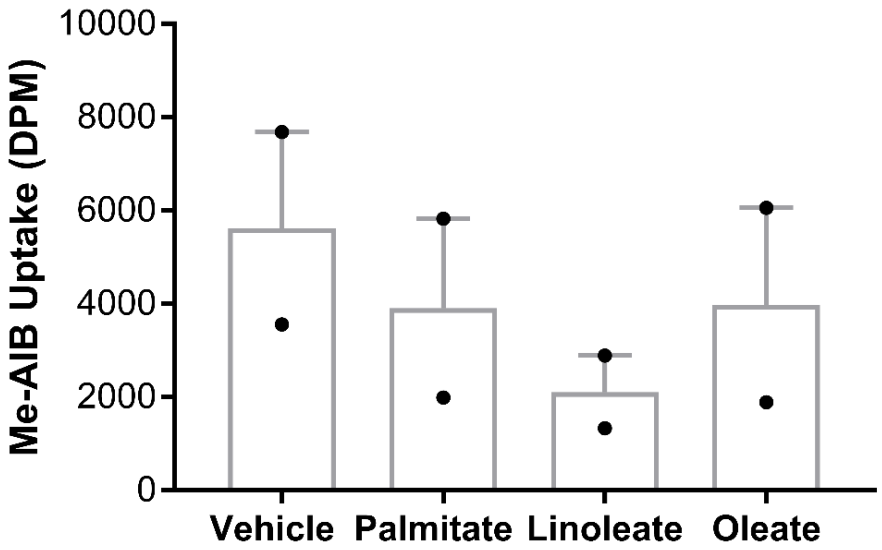


Figure 4.5. Effect of different fatty acids on system A of amino acid transport.
Effect of 16 h treatment with 0.25 mM of palmitate, linoleate, oleate or vehicle on the uptake of [^{14}C] Me-AIB uptake, as an index of system A transport of AA. Data is mean ± SEM from two biological samples with 4 treatment replicates for each condition.

4.3.5 Effect of Palmitate on Rates of Protein Synthesis

Next, we determined whether the tendency for palmitate to reduce AA transport will translate to reduced MPS. We utilised the SUrface SEnsing of Translation (SUnSET) technique to estimate global rates of protein synthesis (Figure 4.6). The increase in puromycin-labelled peptides from this technique correlates well with the incorporation of [^{3}H] phenylalanine into nascent peptides (Goodman et al., 2011). Overnight (16 h) incubation with 0.25 mM palmitate tended (p = 0.086) to downregulate global rates of protein synthesis (Figure 4.7). The average reduction was around 15% and slightly lower than the ~25% impairment of system A transport of AA under basal conditions.

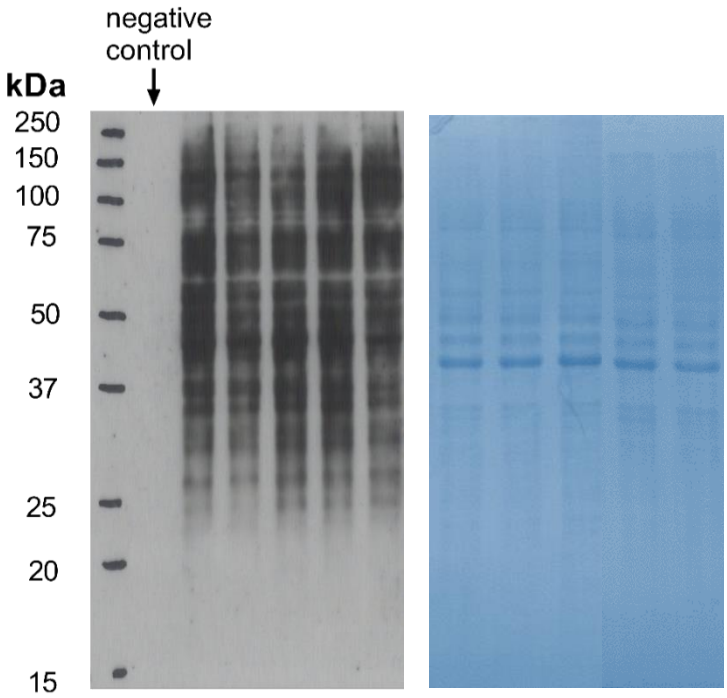


Figure 4.6. Example of images used for SUnSET quantification.
The image on the left shows the detection of puromycin-labelled peptides using SDS-PAGE. Lane 1 is a negative control (no puromycin) used to assess non-specific antibody binding. After obtaining images, the membrane was Coomassie stained (image on the right) to control for total protein content.

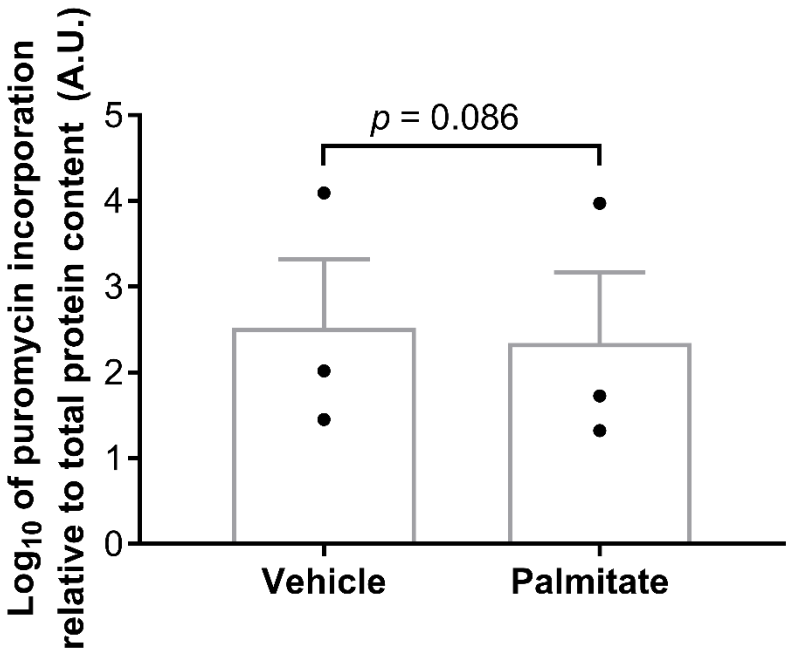


Figure 4.7. Effect of palmitate on protein synthesis.
Puromycin-labelled peptides (expressed relative to total protein content) after 16 h treatment with 0.25 mM palmitate or vehicle. Data is displayed as mean ± SEM (n=3) and the dots represent biological replicates (initial sample with 5 treatment replicates and further experiments with 2 treatment replicates). *P*-value is from a paired t-test after log transforming the protein expression values.

4.3.6 Effect of Palmitate on PP2A and 4E-BP1 Content

Palmitate caused a reduction in AA transport ($p = 0.020$) and a trend to reduce MPS in the basal state ($p = 0.086$). We next sought to examine if these effects were mediated by changes in anabolic signalling. *In vivo* work has attributed the lipid-induced attenuation of MPS to a suppression in 4E-BP1 signalling (Stephens et al., 2015; Smiles et al., 2019). One potential cross-link between IR and anabolic resistance is PP2A, which is proposed to exert its effects, at least in part, through regulating the phosphorylation of 4E-BP1 (Gingras et al., 1999).

However, this study detected no changes in content of the catalytic subunit of PP2A (PP2Ac) or in the phosphorylation of 4E-BP1, following palmitate treatment (Figure

4.8). The regulation of PP2Ac is highly complex, it is activated by methylation and dephosphorylation. Treatment of C2C12 myotubes with 0.75 mM palmitate for 16 h increased basal PP2A-like activity and antagonised the inhibitory effect of insulin (Cazzolli et al., 2001). The latter finding was replicated by Nardi et al. (2014) who observed reduced demethylation and phosphorylation (events associated with activation) of PP2A after exposing L6 muscle cells to palmitate for 16 h.

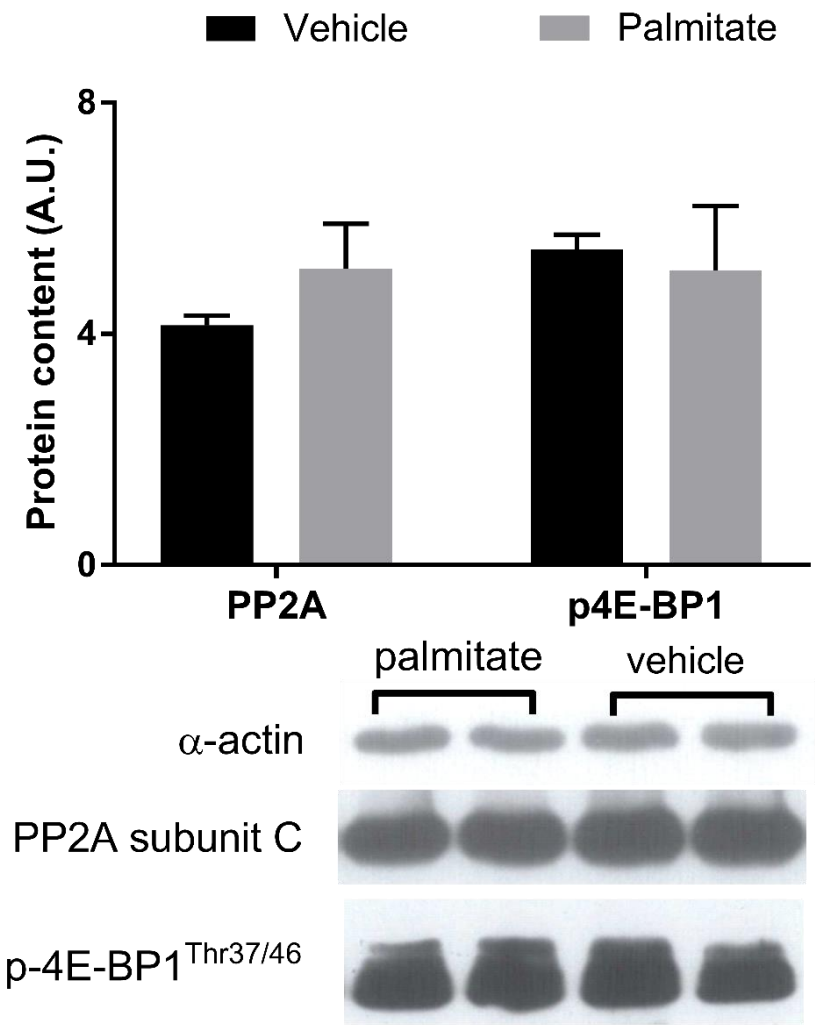


Figure 4.8. Effect of palmitate on PP2A and p-4E-BP1 content. Protein content of PP2A subunit C and phosphorylation of 4E-BP1$^{Thr37/46}$ after 16 h treatment with 0.25 mM palmitate or vehicle. Data is mean ± SEM from three biological replicates (both n=2 treatment replicates).

4.4 Discussion

The data presented here demonstrate that treatment of primary human myotubes for 16 h with 0.25 mM palmitate induces IR, which was associated with impaired system A of AA transport, and a tendency for lower rates of protein synthesis. These effects occurred independent of changes in PP2Ac, p-4E-BP1 or insulin-stimulated p-Akt protein content. Together these findings implicate reduced AA transporter activity, as opposed to impairments in anabolic signalling through the mTOR pathway, as culpable in the association between fatty acids and anabolic resistance in this primary cell model.

Precisely what causes the reduction in system A transport of AA is unknown. Palmitate-derived ceramide accumulation is a primary candidate, since treatment of L6 myotubes with ceramide or 0.75 mM palmitate downregulates system A and reduces plasma membrane SNAT2 content (Hyde et al., 2005). Ceramide-treated cells have reductions in basal S6K1 phosphorylation but retained their sensitivity to insulin stimulation. This may explain why Tardif et al. (2014) showed no impairments in 4E-BP1 or S6K1 content, despite blunted insulin-stimulated MPS after treatment of C2C12 myotubes with 0.375 mM palmitate. Although S6K1 phosphorylation was not measured in this study, we detected no changes in basal p-4E-BP1 content, suggesting that unlike conditions with ceramide treatment (Hyde et al., 2005), mTOR signalling was unaffected by palmitate treatment.

Palmitate-induced hyperactivation of PP2A is proposed to blunt the phosphorylation of Akt. In support of this, inhibition of PP2A using okadaic acid, antagonises the blunted phosphorylation of Akt (Cazzolli et al., 2001). However, inhibition of PP2A does not ameliorate the effects of palmitate or ceramide on system

A transport in L6 myotubes (Hyde et al., 2005). Moreover, L6 myotubes expressing a constitutively active membrane targeted Akt construct retain insulin responsiveness to glucose uptake (Hajduch et al., 2001), but not system A transport of AA (Hyde et al., 2005), after ceramide treatment. This implicates divergent signalling pathways in the regulation of glucose and AA transport after fatty acid treatment in cultured muscle.

Previous work showing palmitate-induced activation of PP2A has used concentrations ≥ 0.7 mM (Cazzolli et al., 2001; Nardi et al., 2014), thus it is plausible that 0.25 mM was insufficient to elicit a response. However, this concentration was sufficient to attenuate AA transport and MPS. It is possible we did not detect any changes in PP2Ac due to measuring total protein content, which has been shown to have a strong autoregulatory mechanism (Baharians and Schönthal, 1998), rather than PP2Ac activity *per se*. Although a previous study has reported reduced insulin-mediated PP2Ac expression in T2D patients compared to healthy controls (Højlund et al., 2002).

Another consideration is that previous experiments were undertaken using immortalised cell lines. Treatment of human myoblasts, derived from a group of overweight/obese males, with a more physiological concentration of palmitate (0.24 mM) in the absence of insulin, found that the degree of PP2A activation was related to glucose tolerance *in vivo* (Mott et al., 2008). More specifically, that as oral glucose tolerance worsens the effects of palmitate on PP2A changed from inhibition to activation. This may relate to the impaired oxidation of palmitate in myotubes derived from donors with T2D (Cha et al., 2005). All donors in this study were lean, healthy and presumed to be insulin sensitive. This group may be less susceptible to palmitate-induced activation of PP2A.

A proinflammatory response to palmitate may also have played a role in our findings. Inhibiting ceramide synthesis after treating L6 myotubes with tumour necrosis factor-α attenuates the reductions in MPS and increase in proteolysis (De Larichaudy et al., 2012). Moreover, incubation of C2C12 myotubes with 0.2 to 0.6 mM palmitate led to a dose-dependent loss of myotubes and associated upregulation of Atrogin1/MuRF1 (Yang et al., 2013). These effects appear to be independent of mTOR/PI3K signalling, since inhibiting these pathways did not ameliorate the effect of palmitate. Using similar approaches, treatment of C2C12 myotubes with 0.5 mM palmitate caused 25% atrophy within 48 h (Bryner et al., 2012) and increased proteolysis within 28 h (Woodworth-Hobbs et al., 2014).

Interestingly, these effects were ameliorated when palmitate was co-incubated with an omega-3 fatty acid: docosahexaenoic acid. A similar strategy has been shown to partially prevent lipid induced IR *in vivo* (Stephens et al., 2014) and it is tempting to speculate, may help to improve the impairment in AA transport shown here. Although the present study and its findings were obtained from acute models, there is evidence that high dietary intake of SFA raises muscle ceramide content (Blachnio-Zabielska et al., 2010), and therefore may be a contributory factor to more chronic, pathophysiological models such as T2D.

To maximise the physiological relevance of our findings, all experiments were undertaken on primary human skeletal myotubes that had not been passaged. Moreover, all palmitate treatments were at lower concentration than typically applied in the literature and for lower durations than have been reported to increase atrophy/proteolysis (Bryner et al., 2012; Woodworth-Hobbs et al., 2014). Nevertheless, it is important to recognise the limitations of the model and examine the

translatability of findings from this *in vitro* model to *in vivo*. The expression of AA transporters is known to respond to both anabolic (Drummond et al., 2010) and catabolic (Drummond et al., 2012) stimuli *in vivo*. This suggests they do play a role in regulating anabolic responses, although there is a paucity of studies directly measuring AA transport rates into human muscle.

After entering the bloodstream, AAs must first cross the endothelial wall of the blood vessel to the interstitial space. From here, they can be transported into the muscle cells via AA transporters. Miller et al. (2004) used a four-compartment model (samples from artery, vein, interstitial fluid and muscle) to examine AA transport kinetics between these compartments in young and healthy volunteers. Four isotopically labelled AAs; leucine, phenylalanine, lysine and alanine were infused to steady state, before transport rates were quantified from micro dialysis probes along with blood and muscle biopsy samples. They determined that AA exchange between the blood and interstitial fluid was significantly slower than between the interstitial and intracellular fluid. Thus, concluding that the rate-limiting step in the accumulation of intracellular AA is the transport rate between the blood and interstitial fluid.

This process is not represented in the primary cell culture model and the results of Miller et al. (2004) appear to downplay the importance of AA transporters *in vivo.* However, it is possible that AA transport kinetics and therefore, the contribution of AA transporters may differ across populations. For instance, elderly individuals have a blunted capacity to upregulate SNAT2 expression after ingestion of essential AAs post-exercise (Dickinson et al., 2013). Tentatively suggesting that AA transporters may play a role in the age-related loss of skeletal muscle. Moreover, a negative correlation between leg fat mass and the stimulation of MPS in response to AAs and

insulin has also been shown in this population (Murton et al., 2015). The latter study found no impairments in Akt/mTOR signalling in the obese group, potentially implicating impairments in AA transporter function.

In future studies, it would be interesting to use a larger pool of biological replicates with a more diverse range of metabolic health and age. The major strength of the primary cell culture model is the retention of elements of the donor's metabolic phenotype (Gaster et al., 2002). This would permit insight into whether the effects of palmitate on AA transporter function are mediated by the health of the donor and if these impairments are associated with physiologically meaningful reductions in MPS. In addition, whether AA transporter function *in vivo* is modulated by fatty acid availability remains an unexplored area.

Strategies to alleviate the IR effects of palmitate include co-incubation with oleate (Pickersgill et al., 2007; Coll et al., 2008) and/or pharmacological activation of CPT-1 (Henique et al., 2010; Perdomo et al., 2004). These promote increased oxidation of palmitate and/or influence the intracellular partitioning of lipids. Our results do not support a beneficial effect of oleate on AA transport function *per se*. As previously mentioned, a more promising avenue of research would likely be co-incubation of palmitate with docosahexaenoic acid.

In summary, palmitate treatment is associated with attenuated insulin-stimulated glucose uptake, system A transport of AA and rates of MPS in primary human myotubes derived from young and healthy donors. These effects appear to be independent of 4E-BP1 and PP2A in this cell model. This suggests that the increased incorporation of dietary [1-^{13}C] phenylalanine into the myofibrillar pool after prior

ingestion of a lipid drink (Chapter 3), is unlikely to be attributed to an enhancement in AA transporter function.

Chapter 5. Effects of Two Weeks of Time-Restricted Feeding on Basal and Postprandial Metabolism in Healthy Men

5.1 Introduction

Restricting the length of the daily energy intake (EI) window to between 4 to 8 h has been shown to elicit favourable metabolic effects in rodents including enhanced insulin sensitivity, independently of energy balance (Chaix et al., 2014; Hatori et al., 2012; Mitchell et al., 2019; Sherman et al., 2012). This would be a significant intervention in humans, considering that many adult's habitual daily EI lengths are ≥ 14 h (Gill and Panda, 2015; Gupta et al., 2017). However, it is currently unclear whether these benefits will translate since there are key metabolic differences between rodents and humans. For instance, the basal metabolic rate of rodents is ~7 times higher per g of body weight (Demetrius, 2005). This is associated with an increased reliance on CHO metabolism and results in accelerated hepatic glycogen depletion in rodents (Nilsson and Hultman, 1973; Rothman et al., 1991; Chen et al., 1991), which is a key adaptive response to fasting (Anton et al., 2018).

Concomitantly, there is a growing appreciation that when you eat matters. Diurnal variations in metabolic function, including insulin sensitivity, were first shown several decades ago (Bowen and Reeves, 1967; Aparicio et al., 1974). Generally, there are more favourable acute metabolic responses to a meal consumed earlier in the day (Bandín et al., 2015; Bo et al., 2015). Preliminary evidence suggests that shifting a greater proportion of daily EI to earlier in the day may also confer health benefits

(Jakubowicz et al., 2013; Garaulet et al., 2013). Indeed, restricting daily EI to the early vs latter half of the active phase in rodents augments the benefits of time-restricted feeding (TRF) (Delahaye et al., 2018).

A dietary strategy that utilises both approaches is early TRF (eTRF), where EI is chronically shifted to earlier in the day and the length of daily fasting duration is also extended. The most promising study to date on eTRF in humans was an RCT that showed improved whole-body insulin sensitivity in prediabetic individuals independently of energy balance (Sutton et al., 2018). Thus, eTRF appears to be a promising intervention that warrants further investigation.

Gaps in the Literature

This study seeks to extend upon the recent findings of Sutton et al. (2018) to examine whether eTRF confers beneficial metabolic effects in a healthier study population. Importantly, pre and post-intervention assessments will be directly compared after participants underwent a matched duration of fasting following consumption of a standardised evening meal. To our knowledge, this will be the first study of its kind to measure the effect of TRF on skeletal muscle substrate uptake using the arteriovenous (A-V) forearm balance method. Continuous glucose monitors (CGM) will be used throughout to monitor adherence and permit insight into the effect of TRF on diurnal glycaemic profiles. Finally, permitting *ad libitum* food intake and objectively monitoring PA levels, will allow the assessment of how TRF impacts on all components of energy balance in a free-living setting.

Aims

The primary aim of this study was to assess the effects of two weeks of eTRF on markers of whole-body and skeletal muscle insulin and anabolic sensitivity in healthy young men. Secondary aim(s) were to assess the changes in body composition and energy balance during two weeks of TRF.

5.2 Methods

5.2.1 Participants

This study recruited eight healthy young males with a BMI between 18 to 27.5 $kg \cdot m^{-2}$. Exclusion criteria stipulated in Section 2.1.3 were applied. In addition, individuals that did not regularly consume breakfast (< 5 days per week), had significant weight changes in the previous three months (> 5%), were currently on an energy-restricted diet, were very active (PAL ≥ 2) or had an Eating Attitudes Test-26 score > 20 (marker of symptoms and concerns characteristic of eating disorders) were also excluded. Eligible participants were provided with a 3-day food diary including a worked example for reference. They were asked to record their dietary intake across two week- and one weekend day(s) to obtain an index of their habitual temporal distribution of EI across the week. This also provided an ideal opportunity to provide feedback on the quality of their completion prior to commencing the study. Characteristics of the participants at the time of study inclusion are displayed below in Table 5.1.

Table 5.1. Descriptive characteristics of study participants.

Age (years)	Body mass (kg)	Height (m)	BMI ($kg \cdot m^{-2}$)
22 (2)	73.8 (8.6)	1.75 (0.06)	24.1 (2.0)

Data presented as mean (SD); n=8.

5.2.2 Experimental Design

This study consisted of a one-week baseline period followed by a two-week intervention and the experimental design is summarised below in Figure 5.1. Each participant visited the laboratory to undergo an incremental treadmill protocol to obtain an individual HR-EE relationship (Brage et al., 2007). This was used to individually calibrate the Actiheart (Section 2.5.2; example shown in Appendix). Following this, they were fitted with an Actiheart and CGM (Section 2.5.3), as well as requested to record all EI in food diaries (Section 2.5.4) during a typical week to establish habitual dietary and PA patterns (baseline period). They then visited the laboratory to assess their metabolic response to a CHO and protein liquid test meal (see below). From the next day, they were asked to restrict their daily EI window to between 08:00 and 16:00 (TRF period) whilst not consciously altering the type/quantity of dietary intake for two weeks. No beverages other than water were permitted during the 16 h fasts as non-caloric drinks can still influence circadian rhythms (Burke et al., 2015). Participants were encouraged to maintain their usual PA patterns throughout. One week into the intervention they visited the laboratory at 08:00 after a ≥ 16 h fast to undergo a resting indirect calorimetry measurement. After a further week of TRF, they returned to the laboratory to after a ~12 h fast to undergo identical metabolic testing.

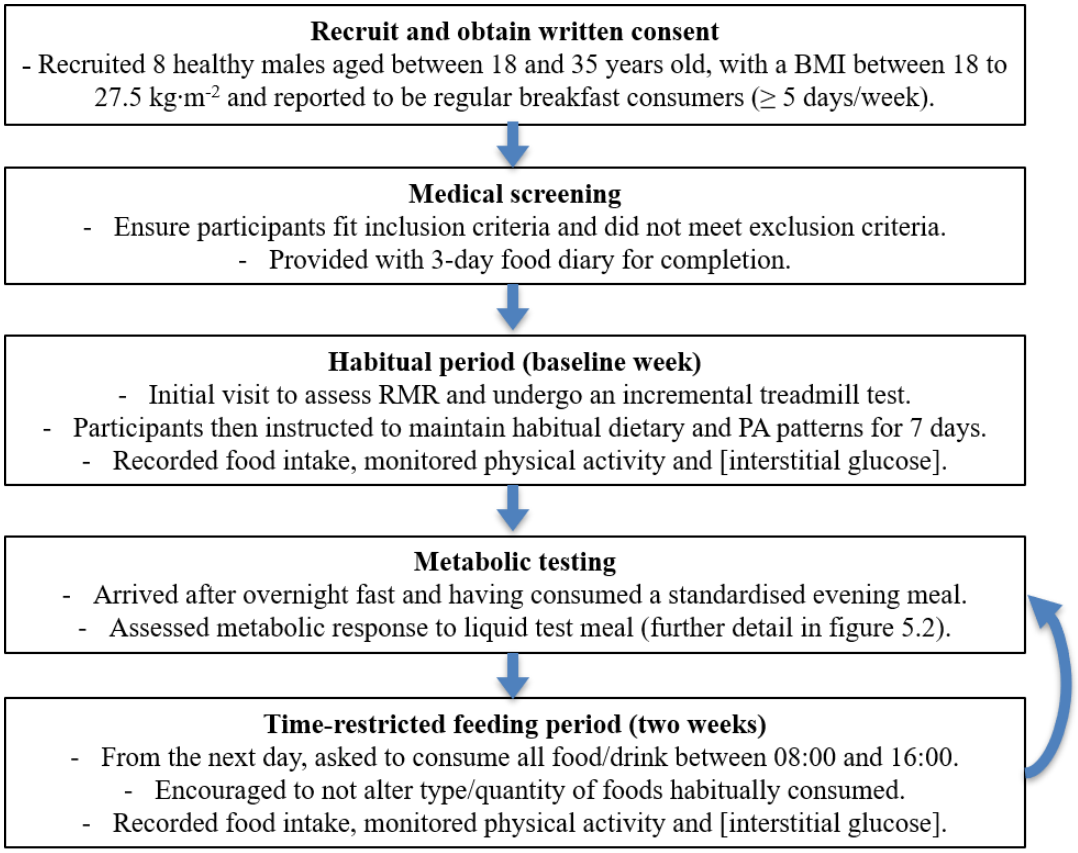


Figure 5.1. Schematic of experimental design.

5.2.3 Metabolic Testing

Main visits were undertaken prior to and immediately after the two-week TRF intervention. Participants were asked to refrain from any strenuous exercise or alcohol consumption during the 24 h preceding each visit. They were provided with a standardised evening meal (~50% CHO, 30% fat, 20% protein) to consume 12 h before arriving to the lab at 08:00 having undergone an overnight fast. Upon arrival, participants voided their bladder into a vessel container and their body mass was recorded in light clothing. Body composition was then determined using a DEXA scan (Section 2.4.4). Next, they rested in a semi-supine position on a hospital bed for 20 min prior to measuring respiratory gas exchange under a canopy hood (Section 2.4.2).

Participants were then fitted with two intravenous cannulas; one inserted retrograde into a superficial hand vein and one contralateral into a deep vein draining the forearm muscle. The former was placed into a heated plexiglass box maintained at 55℃ to arterialise the venous blood (Gallen and Macdonald, 1990; Section 2.2.2). Where possible, the same arm was used for deep venous sampling in the pre and post-intervention visit. A suction-modified percutaneous needle biopsy was then obtained from the vastus lateralis of one randomly assigned leg (Bergström, 1975; Hennessey et al., 1997; Section 2.3.1). Upon removal, the needle was rapidly immersed in isopentane cooled with liquid nitrogen to preserve optimal muscle morphology (Meng et al., 2014), before being snap frozen in liquid nitrogen for long-term storage. Muscle samples were used to determine glycogen concentrations (Section 2.3.3), pyruvate dehydrogenase complex activity (Section 2.3.4), messenger RNA expression of selected genes (Section 2.3.5; see Appendix for full list of genes) and protein phosphorlyation of Akt^{Ser473} and $4E\text{-}BP1^{Thr37/46}$ (Both from Cell Signalling Technology, Danvers, MA, USA; Section 2.3.8).

Approximately 15 min after obtaining the biopsy, baseline blood samples were drawn simultaneously from each cannula. Blood flow of the brachial artery was estimated using Doppler ultrasound (Section 2.2.3) immediately after all blood sample collections. After this, participants were provided with an oral liquid test meal comprising of 1 $g \cdot kgBW^{-1}$ of dextrose (Bulk Powders, Colchester, Essex, UK), 0.4 $g \cdot kgBW^{-1}$ unflavoured micellar casein protein (Bulk Powders, Colchester, Essex, UK) and 2 g of cocoa powder (Cadbury Bournville, Birmingham, UK) blended into 4 $ml \cdot kgBW^{-1}$ of water. Separately, 2 $ml \cdot kgBW^{-1}$ of water was provided for consumption immediately to wash down the test meal. Participants were informed they had 10 min

to finish both drinks and the study timer was set immediately after (t=0). A summary of the experimental protocol followed is outlined in Figure 5.2.

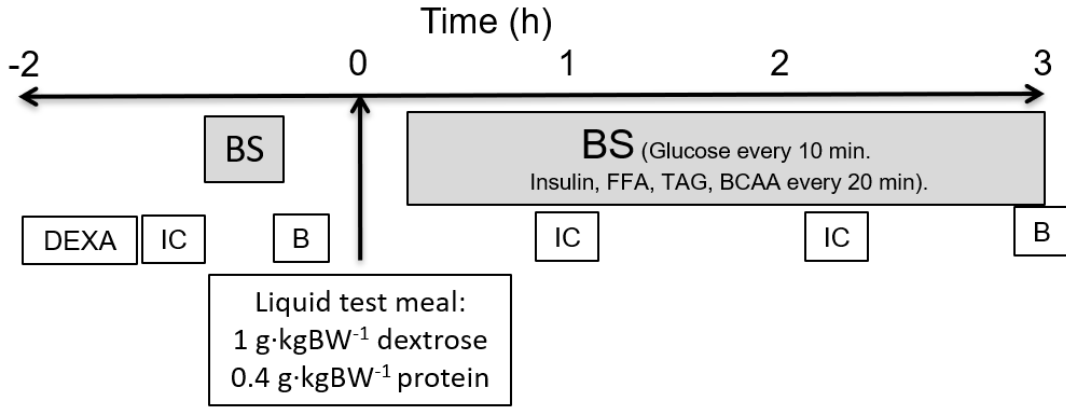


Figure 5.2. Schematic of main visit/metabolic testing protocol.
BS = Blood sampling, IC = Indirect calorimetry, B = Vastus lateralis muscle biopsy, DEXA = Dual Energy X-ray Absorptiometry.

Blood samples for the determination of glucose concentrations (Section 2.2.5) were obtained every 10 min. Larger samples were collected every 20 min to isolate plasma and serum for subsequent analyses. These included; serum insulin (Section 2.2.8), plasma FFA (Section 2.2.10), serum TAG (Section 2.2.11), plasma BCAA (Section 2.2.12), plasma ghrelin (Section 2.2.13) and serum testosterone (Section 2.2.14). Two further 20-min indirect calorimetry measurements were undertaken 1 h and 2 h 15 min post-drink consumption. Finally, a second muscle biopsy was obtained from the same leg at 3 h post drink-consumption. A different leg was used for the biopsy procedures in the TRF visit. Cannulas were then removed before asking the participant to provide a further urine sample. They were then provided with refreshments before leaving the laboratory.

5.2.4 Statistical Power

At the time of planning there was a paucity of studies investigating the metabolic effects of TRF in humans. Moro et al. (2016) observed reductions in fasted blood

glucose, insulin and TAG over 8-weeks in 32 resistance-trained men. A comparable two-week free-living intervention using alternate day fasting (ADF; 20 h fast every 2 days) uncovered a significant increase in insulin-mediated glucose uptake during the final 30 min of a hyperinsulinaemic clamp (pre 6.3 ± 0.6 vs. post 7.3 ± 0.3 $mg \cdot min^{-1} \cdot kg^{-1}$) using eight healthy young males (Halberg et al., 2005). Thus, dynamic measurements of insulin sensitivity are likely more sensitive to capture these improvements than a single fasted timepoint. If a similar magnitude of difference is expected in the present study, it should be detectable using eight subjects (within-group contrasts) with a power of 80% at a significance level of $\alpha < 0.05$.

5.2.5 Statistical Analysis

All statistical analysis was undertaken using GraphPad Prism 7.0 (GraphPad Software Inc., San Diego, CA, USA) and significance was accepted at $p \leq 0.05$. Data in text and tables is presented as mean ± SD. Error bars in figures represent SEM unless otherwise stated. Where appropriate, missing data were manually replaced with the average values. For instance, if a blood sample could not be collected at 90 min, this would be replaced with the average of the 80- and 100-min values. Data cleaning and assessment of data validity for the CGM and Actiheart are described in section 2.5.5. The flux of metabolic substrates into skeletal muscle was calculated using the product of the concentration differences of A-V blood samples and the estimate of forearm blood flow (standardised to lean forearm mass). EE was estimated using the equation of Weir (1949) and rates of substrate metabolism were estimated using the equations of Frayn (1983).

Comparisons between two means were made using Student's paired t-test (two-tailed), e.g. body mass. A one-way ANOVA was used to compare pre, mid and post-

TRF indirect calorimetry values. Most variables were assessed using a two-way repeated measures ANOVA (time x trial). When significant treatment or treatment x time effects were identified, post-hoc multiple comparisons were undertaken using Bonferroni corrections to reduce the chance of type I error. Pearson's correlation coefficients were used to investigate the strength of the relationship between two variables. When time-dependent variables were used (e.g. insulin response), incremental area under the curves were calculated using the trapezoid rule. All area(s) below the curve and above the fasting value were included, with any area(s) beneath the fasting value ignored.

For the mRNA expression data all statistical analysis was performed on the raw ΔC_T values (Yuan et al., 2006), as this study was interested in change in expression within the same biological donor. Fasted expression ΔC_T values in the habitual and TRF trial were compared using a paired t-test. A two-way repeated measures ANOVA (feeding x trial) was undertaken to assess the change in expression of genes in response to feeding. Note that *p*-values for the interaction effect in this model are equivalent to *p*-values obtained from a paired t-test on the $\Delta\Delta C_T$ for each visit.

5.3 Results

5.3.1 Energy Intake

All participants completed food diaries for each day enrolled in the study. There was one reported food intake event outside of the stipulated time period during TRF, this was included in the analysis as they missed the window by 20 min. TRF shortened the reported average daily EI window by around 5 h 30 min (~12 h 20 min during habitual period vs ~6 h 50 min during TRF, $p < 0.001$). Self-reported daily EI was around 15% lower during TRF in comparison to habitual [2315 (397) vs. 2722 (601) kCal·day^{-1}, $p < 0.001$)]. Although the absolute reported consumption of all macronutrients declined during TRF, only the change in fat consumption was significant ($p = 0.017$). Whilst the absolute reduction in CHO ($p = 0.081$) and protein ($p = 0.087$) intake both approached significance (Figure 5.3). The relative macronutrient composition of diets between baseline and TRF did not differ. Five participants reported zero alcohol consumption across the entire three-week study period. A summary of total daily EI and macronutrient intake is presented below in Figure 5.4. Correlations between change in macronutrient intake and change in body composition variables across two weeks of TRF are outlined in

Table 5.2. The strongest correlations were between protein intake and fat/lean mass but neither of these reached statistical significance.

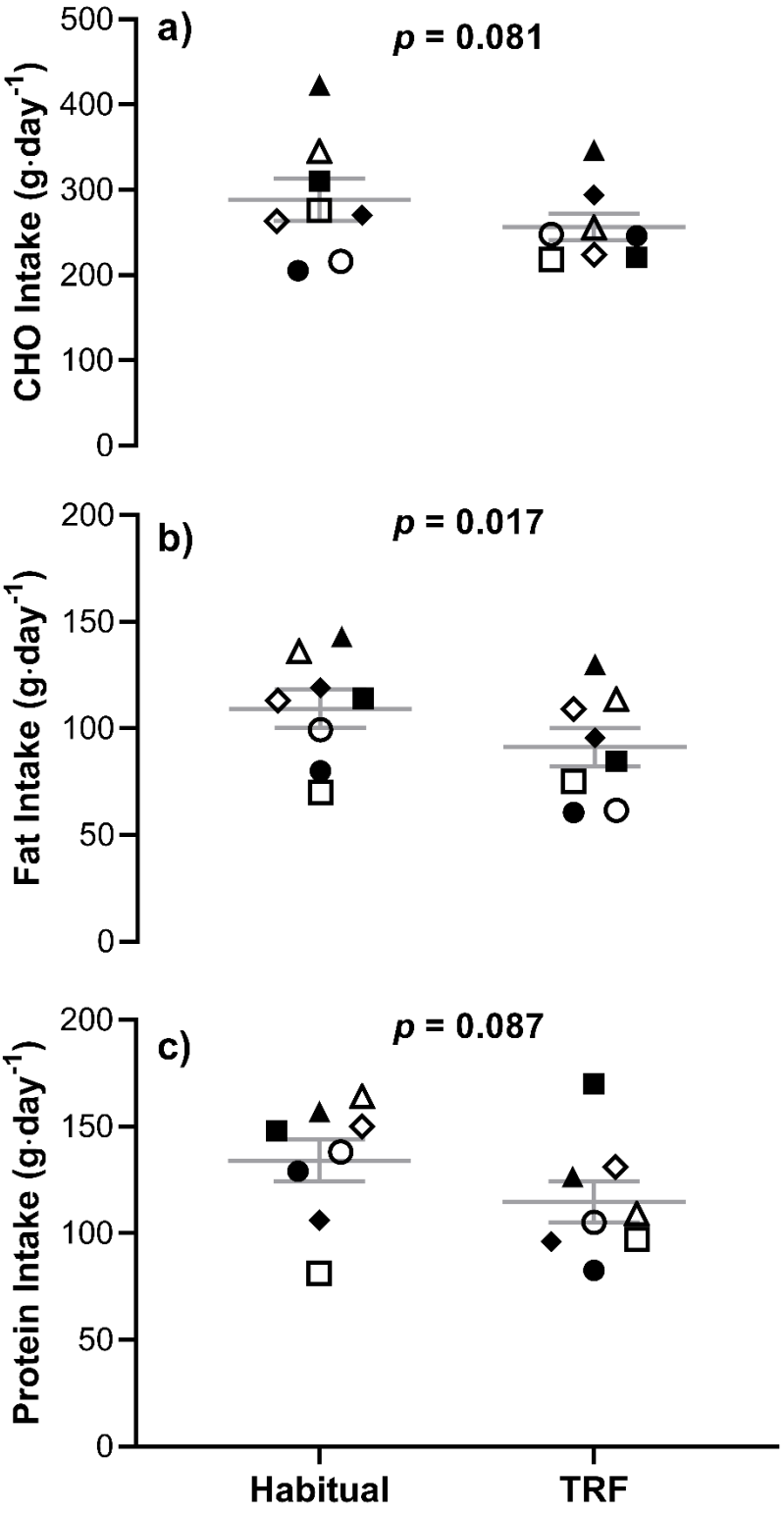


Figure 5.3. Individual change in macronutrient intake.
Self-reported macronutrient intake during one week of habitual diet and two weeks of TRF. The middle horizontal bar represents the mean, the error bars are ± SEM and each shape represent a participant (n=8). *P*-values are from a paired t-test

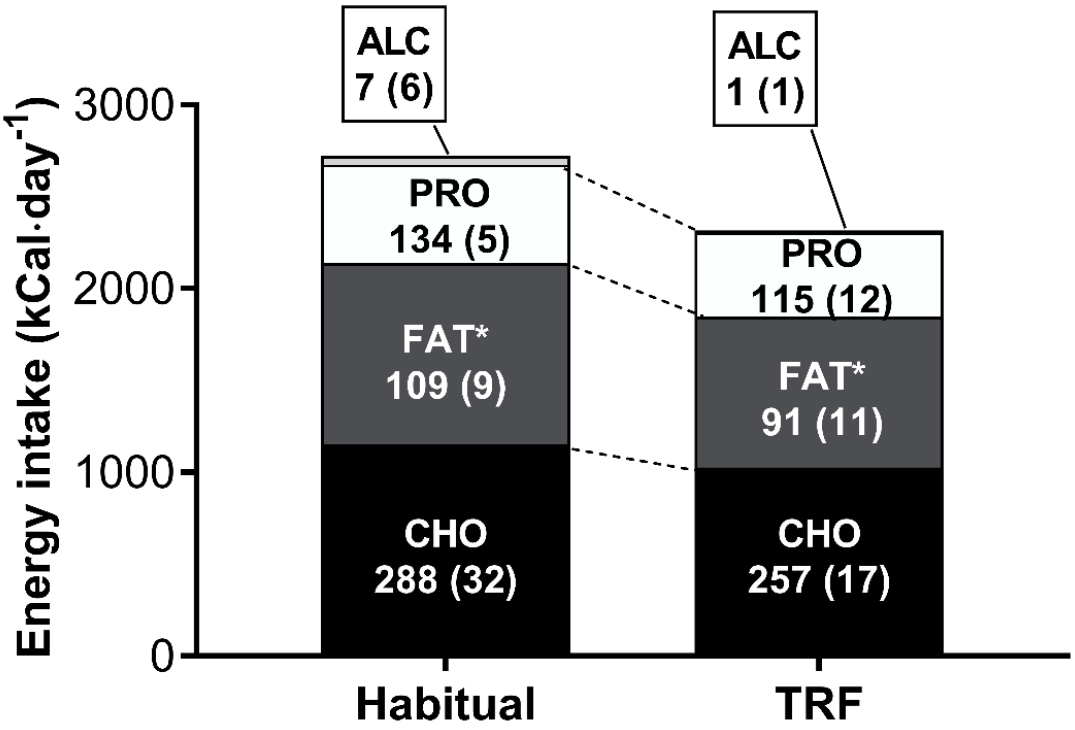


Figure 5.4. Energy and macronutrient intake.
Self-reported daily energy and macronutrient intake during one week of habitual diet and two weeks of TRF. The bars represent the mean energy intake and the text is mean (SEM) of g·day^{-1}, n=8, *$p \leq 0.05$ from habitual. CHO = carbohydrate, PRO = protein, ALC = alcohol.

Table 5.2. Pearson's correlation coefficients
Relationships between change in macronutrient intake and body composition.

	Δ Body mass (kg)	Δ Fat mass (kg)	Δ Lean mass (kg)
Δ CHO (g·day^{-1})	-.218	-.406	.238
Δ Fat (g·day^{-1})	.209	.254	.254
Δ Pro (g·day^{-1})	.323	-.574	.647

Body mass is n=8; fat and lean mass is n=7.

5.3.2 Free-Living Energy Expenditure

Around 20% of study days were excluded from analyses due to an insufficient amount or quality of data (either > 144 min per day 'lost' or > 325 min per day 'recovered'). Total daily PAEE did not differ between the habitual and TRF periods [habitual 1006 (348) versus TRF 1064 (334) $kCal \cdot day^{-1}$] as shown in Figure 5.5. There were no differences in the average daily time spent at light ($1.5 \leq METs < 3$), moderate ($3 \leq METs < 6$) and vigorous (≥ 6 METs) activities, as shown in

Table 5.3. Similarly, the distribution of PA within each day was unchanged.

Intensity of PA	**Habitual**	**TRF**
Light (1.5 ≤ METs < 3)	182 (40)	189 (52)
Moderate (3 ≤ METs < 6)	118 (41)	118 (43)
Vigorous (≥ 6 METs)	13 (11)	20 (13)
08:00 to 16:00	461 (160)	486 (123)
16:00 to 00:00	433 (194)	420 (198)

Data presented as mean (SD); n=8. Daily time (min) spent at different intensities of PA and distribution of PAEE (kCal) within each day during one weeks of habitual diet (baseline) and two weeks of TRF.

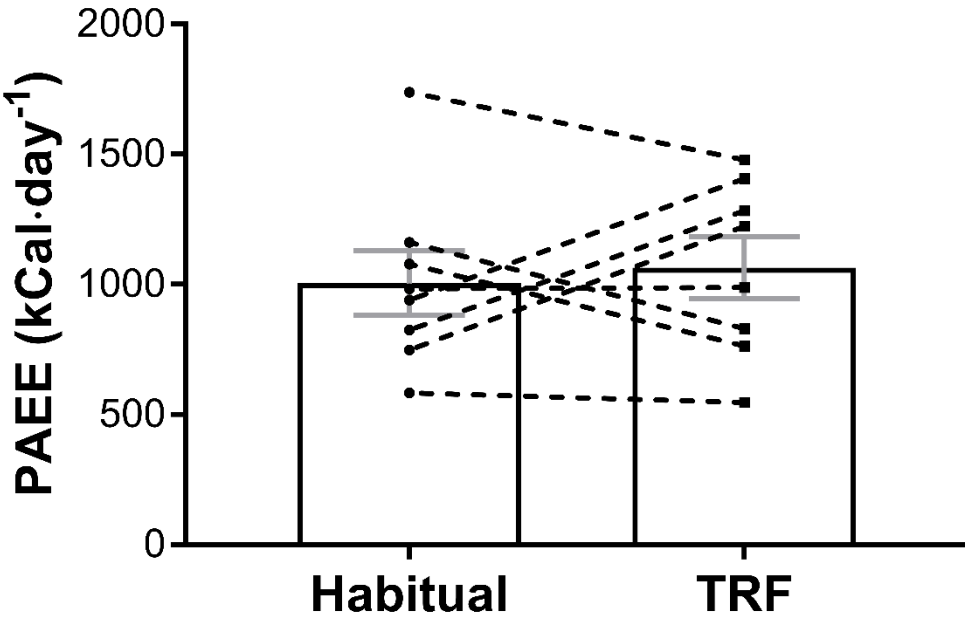


Figure 5.5. Physical activity energy expenditure.
Physical activity energy expenditure (PAEE) during one-week of habitual diet (baseline) and two weeks of TRF. The bars represent the mean ± SEM and dots with connecting lines represent individual participants.

Table 5.3. Intensity and distribution of physical activity.

Intensity of PA	Habitual	TRF
Light (1.5 ≤ METs < 3)	182 (40)	189 (52)
Moderate (3 ≤ METs < 6)	118 (41)	118 (43)
Vigorous (≥ 6 METs)	13 (11)	20 (13)
08:00 to 16:00	461 (160)	486 (123)
16:00 to 00:00	433 (194)	420 (198)

Data presented as mean (SD); n=8. Daily time (min) spent at different intensities of PA and distribution of PAEE (kCal) within each day during one weeks of habitual diet (baseline) and two weeks of TRF.

5.3.3 Body Weight and Composition

Participants' body mass declined during TRF [−1.04 (0.71) kg; $p = 0.004$]. DEXA scans were only available for 7 participants, hence changes in tissue composition (e.g. fat and lean mass) were all n=7 (Figure 5.6). Fat [−0.62 (0.94) kg; $p = 0.132$] and lean

mass [−0.53 (1.34) kg; p = 0.337] remained unchanged after TRF. Reductions in android and gynoid fat mass were significant ($p \leq 0.05$) but relatively low in absolute terms at 0.08 and 0.18 kg, respectively. There were notable interindividual variations in responses to TRF. For instance, one participant gained 1.15 kg of fat and lost 2.92 kg of lean mass. Closer inspection of the DEXA scans reveals the loss of lean mass was almost entirely attributed to the trunk region.

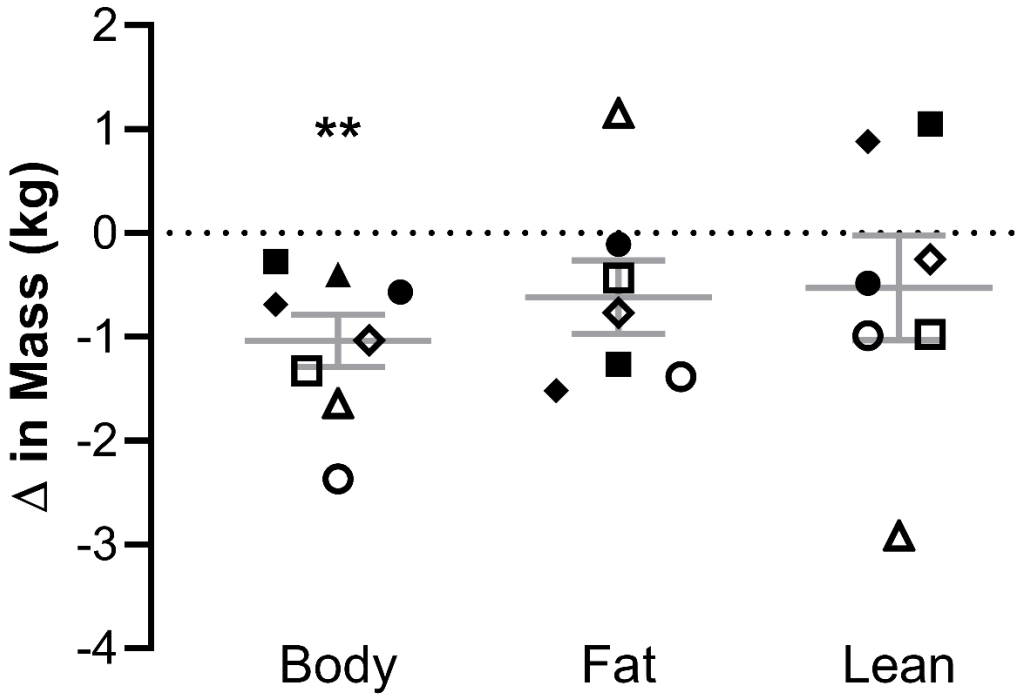


Figure 5.6. Changes in body composition.
Changes in body composition (assessed by DEXA) after two weeks of TRF. The middle horizontal bar is the mean, the error bars are ± SEM and each shape represent an individual participant. Body mass n=8, fat and lean mass n=7, $^{**}p < 0.01$ from habitual.

5.3.4 Fasting Plasma Ghrelin and Testosterone

Plasma concentrations of total ghrelin did not change when assessed in the fasted state [habitual 834 (127) vs TRF 855 (154) ρg·ml^{-1}]. Similarly, fasted testosterone

concentrations also remained similar between trials [habitual 10.5 (4.0) vs TRF 9.6 (5.3) ng·ml^{-1}].

5.3.5 Continuous Glucose Monitoring

Participants were asked to scan their sensor every 8 h to fully capture their diurnal glycaemic profile(s). Overall, adherence was good with < 15% of study days excluded from analyses across the habitual and TRF periods. These were due to the sensor becoming detached or participants forgetting to scan frequently enough. Averages were calculated from the valid days for each participant in the habitual and TRF period. Diurnal interstitial glucose concentrations are shown below in Figure 5.7 for comparison and with 95% confidence intervals (see Appendix) to give an index of variability throughout the 24 h period.

During TRF, there was a sharp increase in interstitial glucose at the start of the eating period, which continued to rise steadily throughout the eating window, reaching a peak of 6.4 (0.6) mmol·L^{-1} shortly after the end of the eating period at 16:30. This steadily declined to 4.6 (0.5) mmol·L^{-1}at 00:00 and continued to fall by a further 0.3 mmol·L^{-1}into the early morning. During participants' habitual diet (baseline), the diurnal glycaemic profiles were less consistent and displayed more inter-individual variation. Two peak interstitial glucose concentrations of around were evident at 14:00 [5.8 (0.5) mmol·L^{-1}] and 21:00 [5.8 (0.4) mmol·L^{-1}], respectively. Notably, glucose concentrations did not decrease consistently until around 23:00. From that point they declined throughout the night but were maintained at higher concentrations than during TRF until around 07:00. When considered across the full 24 h, mean glucose values and indexes of variability were very similar between the two eating patterns

(Table 5.4). However, between 20:00 to 08:00 there were lower mean glucose concentrations (p = 0.046), lower average SD (p = 0.004) and a tendency towards lower coefficient of variations (p = 0.067) during TRF.

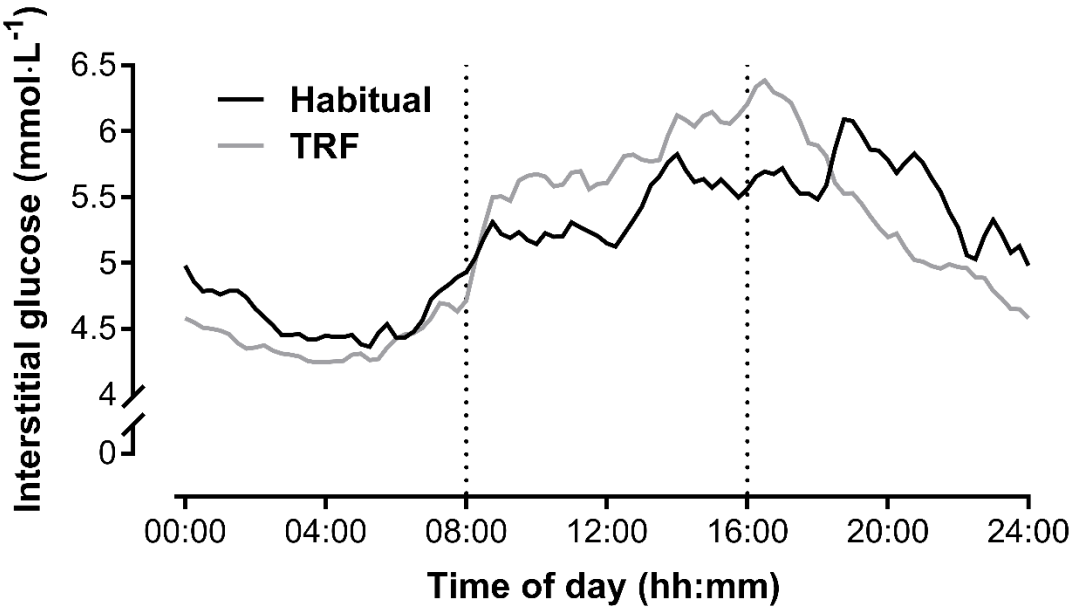


Figure 5.7. Diurnal glycaemic profiles.
Mean interstitial glucose concentrations during one week of habitual diet (baseline) and two weeks of TRF, dotted lines at 08:00 and 16:00 represent the stipulated energy intake window during TRF; n=8.

Table 5.4. Continuous glucose monitoring.
Indexes derived from 24 h continuous glucose monitoring during one week of habitual diet (baseline) and two weeks of caloric restriction.

	Full 24 h		08:00 to 20:00		20:00 to 08:00	
	Habitual	**TRF**	**Habitual**	**TRF**	**Habitual**	**TRF**
No. of valid days (%)	42 (88)	87 (84)	-	-	-	-
Mean glucose ($mmol \cdot L^{-1}$)	5.16 (0.48)	5.17 (0.33)	5.49 (0.52)	5.75 (0.36)	4.93 (0.50)	4.58* (0.33)
Glucose variability (SD)	0.9 (0.1)	1.0 (0.2)	1.0 (0.1)	1.1 (0.2)	0.8 (0.1)	0.6** (0.2)
Glucose variability (CV; %)	18 (3)	20 (3)	18 (2)	19 (3)	17 (4)	14 (4)

Data are displayed as mean (SD); n=8. *$p \leq 0.05$, **$p < 0.01$ for TRF vs habitual.

5.3.6 Glycaemic Response(s)

There were no differences in fasting arterialised or venous glucose concentrations between the habitual and TRF periods. As displayed in Figure 5.8a, arterialised glucose increased at a similar rate after ingestion of the liquid test meal, although a slightly higher peak of 7.76 (0.68) [vs 7.41 (0.95)] $mmol \cdot L^{-1}$ at 40 min was observed after TRF. From that point, the rate of decline was steeper after TRF reaching 3.50 (0.66) [vs 4.04 (0.47)] $mmol \cdot L^{-1}$ at 180 min. The interaction (time x treatment) effect approached statistical significance ($F=1.674$; $p = 0.053$).

Venous blood glucose concentrations peaked at 40 min and were around 1.5 $mmol \cdot L^{-1}$ lower than arterialised blood (Figure 5.8b). There was a significant interaction effect ($F=1.994$; $p = 0.014$) and a tendency towards a treatment effect ($F=3.823$; $p = 0.092$), with a more rapid decline from peak concentrations in the TRF trial. Post-hoc analysis revealed significantly lower venous concentrations between 50 to 80 min after consumption of the liquid test meal. The arteriovenous (A-V) glucose concentrations are displayed in Figure 5.8c. Both treatment ($F=3.662$; $p = 0.097$) and interaction effects ($F=1.646$; $p=0.058$) approached statistical significance. This resulted from a tendency for greater A-V differences in the TRF trial. Subanalysis of the first 90 min of the postprandial period revealed higher A-V differences in the TRF trial ($F=6.887$; $p = 0.034$).

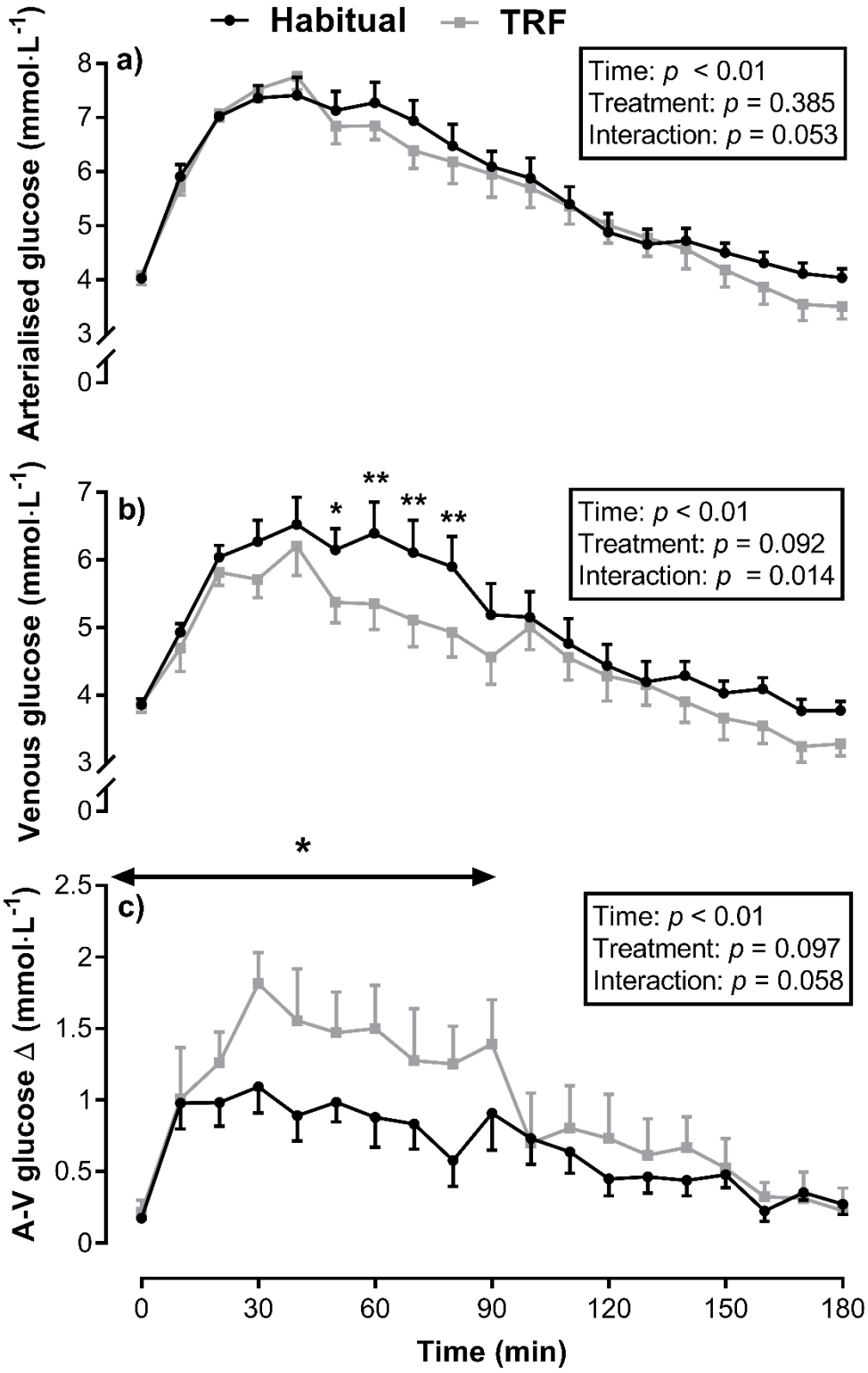


Figure 5.8. Arterialised, venous and A-V differences in glucose.
(a) Arterialised, (b) venous and (c) arteriovenous (A-V) differences in glucose concentrations in response to a liquid test meal. Data are displayed as mean ± SEM; n=8. *$p \leq 0.05$, **$p < 0.01$ habitual vs TRF.

5.3.7 Forearm (Muscle) Blood Flow and Glucose Uptake

Brachial artery blood flow and all forearm substrate uptake values are expressed relative to lean forearm mass. The participant with no DEXA scan had undertaken a study < 6 months prior, which was used to estimate lean forearm mass for both trials. They were weight stable between these periods and only lost 0.2 kg during the two-week TRF period. There were no differences in brachial artery blood flow or glucose uptake between the habitual and TRF periods.

Blood flow (Figure 5.9a) increased after consumption of the liquid test meal ($F=4.711$; $p < 0.001$), this appeared to be numerically greater in the habitual diet trial but there were no statistical differences between trials. Peak values (of ~90 $ml \cdot min^{-1} \cdot kg^{-1}$) were shown at 150 min in the TRF trial compared to 60 min in the habitual diet trial. Forearm glucose uptake (Figure 5.9b) increased to a greater extent in the initial 30 min of the TRF trial and was maintained ~30 $\mu mol \cdot min^{-1} \cdot kg^{-1}$ higher for most of the next 60 min. As a result, there was a significant treatment effect over the initial 90 min ($F=5.608$; $p = 0.050$) but not over the full 180 min ($F=3.115$; $p = 0.121$). Similarly, glucose extraction %, calculated by dividing the A-V differences by the arterialised concentration and multiplying by 100, was increased in the first 90 min of the TRF trial ($F=6.41$; $p = 0.039$).

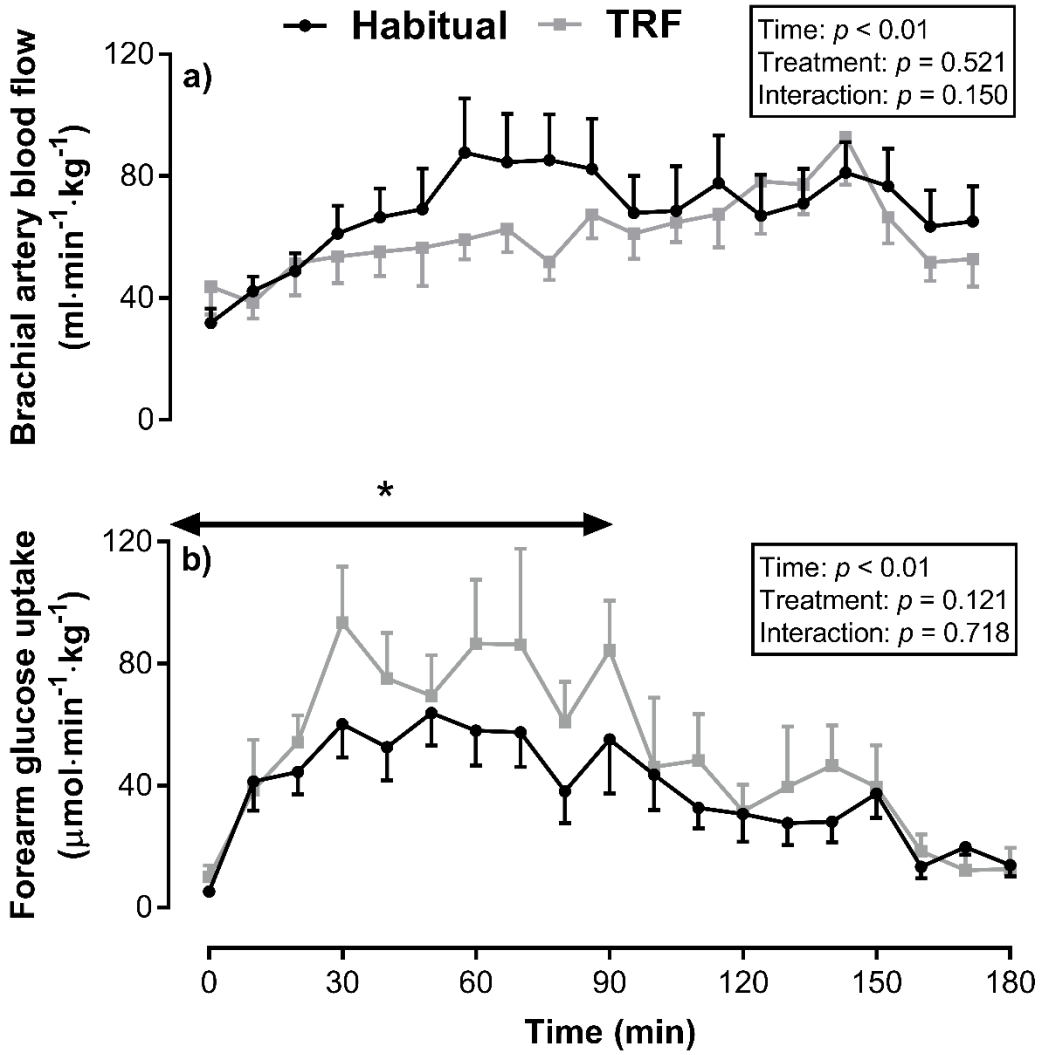


Figure 5.9. Blood flow and glucose uptake.
(a) Brachial artery blood flow and (b) forearm glucose uptake in response to consumption of a liquid test meal. Data displayed is mean ± SEM; n=8. *$p \leq 0.05$ from habitual.

5.3.8 Serum Insulin and Indexes of Whole-Body Insulin Sensitivity

There were no differences in fasting insulin or glucose concentrations and the HOMA-IR score calculated from these variables was also similar (Table 5.5). In both trials, there was a rapid elevation in arterialised serum insulin levels and similar peak values of around 625 ρmol·L^{-1} were obtained at 20 min (Figure 5.10). Across the next 60 min, insulin concentrations decreased by around 80 ρmol·L^{-1} in the habitual trial

compared with over 200 ρmol·L^{-1} in the TRF trial. Slightly lower insulin levels were maintained until the end of the measurement period, where they approached but did not reach fasting concentrations in both trials. Overall, there was a treatment effect for lower postprandial insulin responses in the TRF trial (F=5.61; p = 0.050).

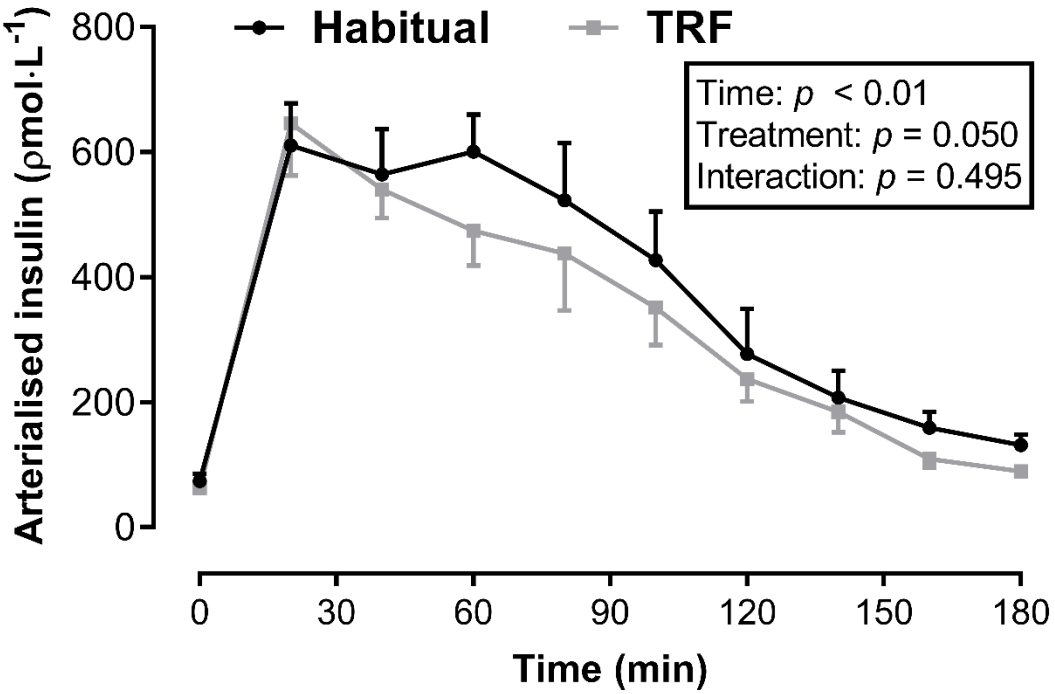


Figure 5.10. Arterialised serum insulin.
Arterialised serum insulin concentrations in response to a liquid test meal. Data is displayed as mean ± SEM; n=8.

Table 5.5. Measures of fasting whole-body insulin sensitivity.

Measure	Habitual	TRF
Fasting glucose (mmol·L^{-1})	4.03 (0.23)	4.08 (0.49)
Fasting insulin (ρmol·L^{-1})	74 (34)	63 (19)
HOMA-IR	1.29 (0.58)	1.10 (0.34)

Data are presented as mean (SD); n=8.

The Matsuda Insulin Sensitivity Index (M-ISI) provides an index of whole-body insulin sensitivity, accounting for both fasting and postprandial responses of circulating insulin and glucose. It is typically calculated across 120 min during a

standard OGTT but the additional protein in the liquid test meal has been shown to delay gastric emptying and prolong the insulinaemic response. This is supported by insulin concentrations remaining around four times higher than basal levels at 120 min (Figure 5.10). When calculated over the full measurement period, the M-ISI was significantly increased in the TRF trial ($p = 0.044$) indicating greater whole-body insulin sensitivity (Figure 5.11). Six out of eight participants had higher M-ISI scores in the TRF trial and of these five had the lowest scores at baseline.

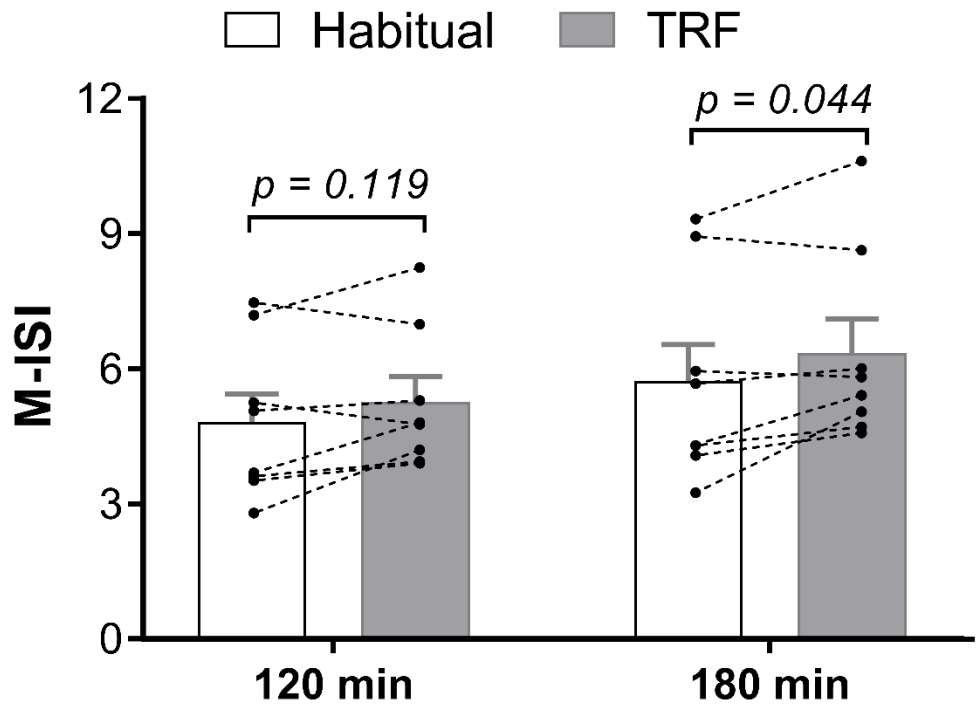


Figure 5.11. Matsuda insulin sensitivity index.
Matsuda insulin sensitivity index (M-ISI) across both 120 and 180 min. The bars represent the mean ± SEM and the dots with connecting lines represent individual changes in participants, n=8.

5.3.9 Plasma Free-Fatty Acids

There were no differences in fasting FFA or treatment/interaction effects in arterialised (Figure 5.12a) or venous (Figure 5.12b) blood. In both blood types,

consumption of the liquid test meal rapidly supressed FFAs which halved from basal levels after 20 min and fell below 0.08 mmol·L^{-1} by 40 min. They were maintained around this concentration for the next 2 h but began to increase again during the final 20 min of the postprandial period. When expressed as A-V differences (Figure 5.12c) there was a trend towards an interaction effect (F=3.639; p = 0.098). Finally, there was a significant treatment effect for net influx of FFAs (Figure 5.12d) into the forearm (F=11.9; p = 0.011), with higher values in the TRF trial. These differences were most pronounced at the fasted (0 min) and final postprandial (180 min) timepoint.

5.3.10 Serum Triglycerides (TAG)

Arterialised TAGs declined after consumption of the liquid test meal in both trials, but no significant treatment effects were found between trials (F=2.736; p = 0.142) (Figure 5.13). Fasting TAGs were numerically, but not statistically, lower in the TRF trial (p = 0.31; n.s) and decreased by 0.16 mmol·L^{-1} at 180 min postprandial, compared to 0.09 mmol·L^{-1} in the habitual trial.

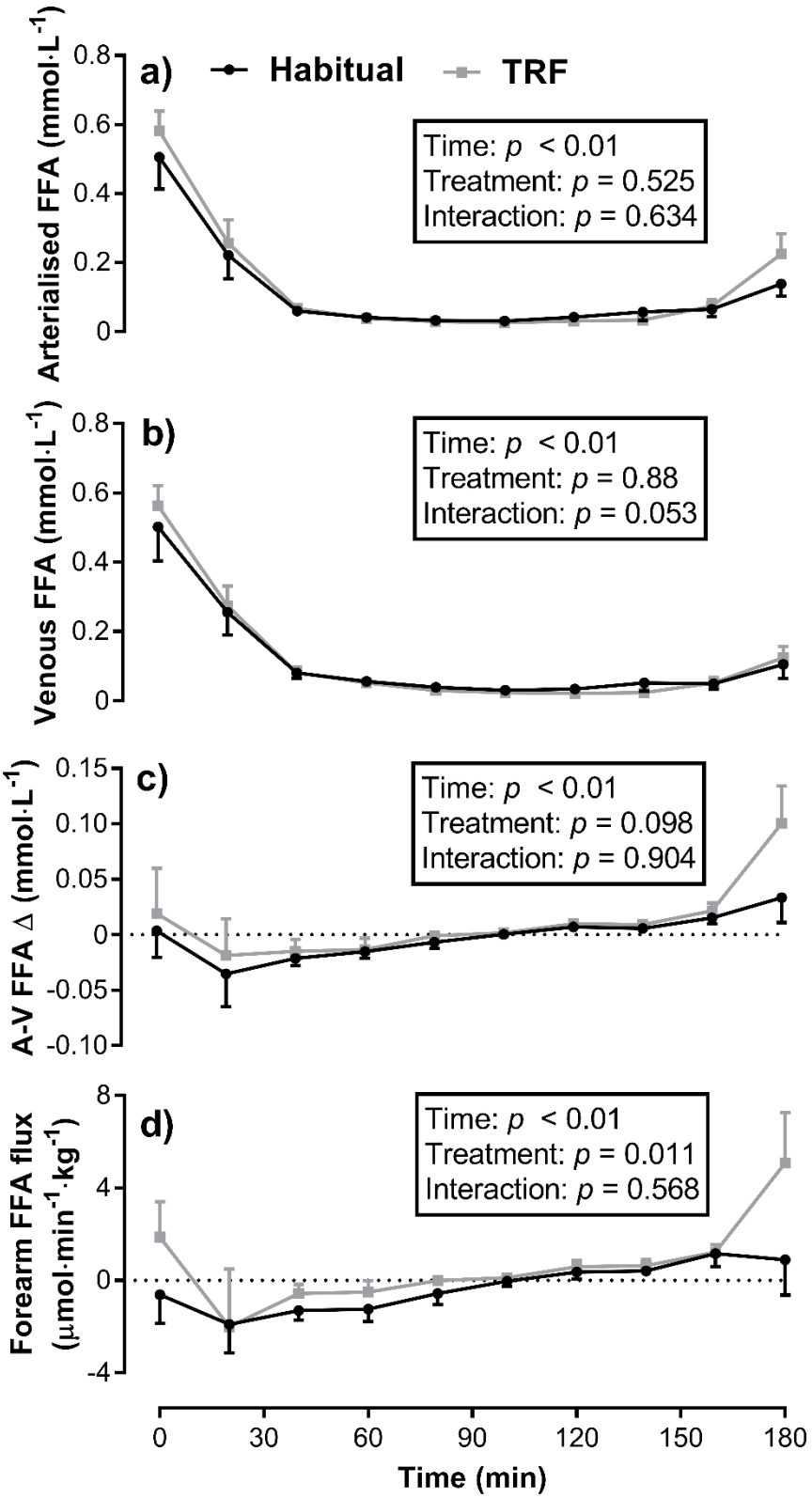


Figure 5.12. Plasma free-fatty acids.

(a) Arterialised, (b) venous, (c) A-V differences and (d) net forearm flux of plasma free-fatty acids (FFA) in response to a liquid test meal. Data are displayed as mean ± SEM; n=8.

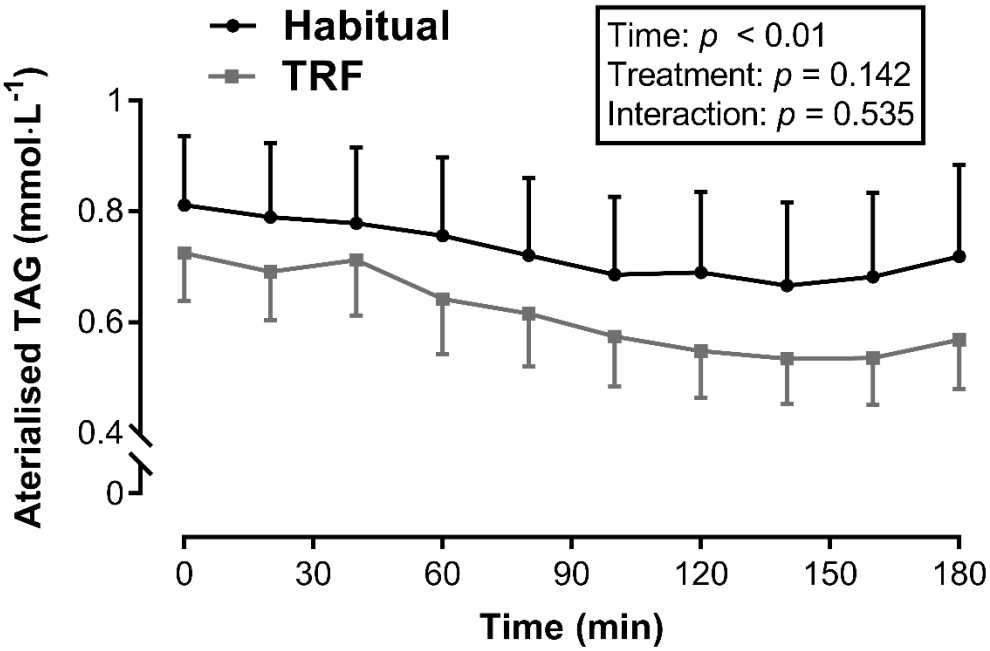


Figure 5.13. Arterialised serum triglycerides.
Arterialised concentrations of triglycerides (TAG) in response to a liquid test meal. Data displayed as mean ± SEM; n=8.

5.3.11 Branched Chain Amino Acids (BCAA)

Fasting arterialised BCAA (Figure 5.14a) were similar, but lower fasting venous BCAAs (Figure 5.14b) were observed in the TRF trial [257 (56) vs 301 (47) μmol·L^{-1}; p = 0.016]. There was a sharp increase in BCAA after 20 min in both blood types and levels remained elevated above fasting concentrations throughout. There were no treatment or interaction effects on postprandial arterialised or venous responses between trials. However, there was a treatment effect for increased A-V differences (F=16.61; p = 0.005) and forearm uptake of BCAA (F=16.55; p = 0.005) in the TRF trial as shown in Figure 5.14c-d.

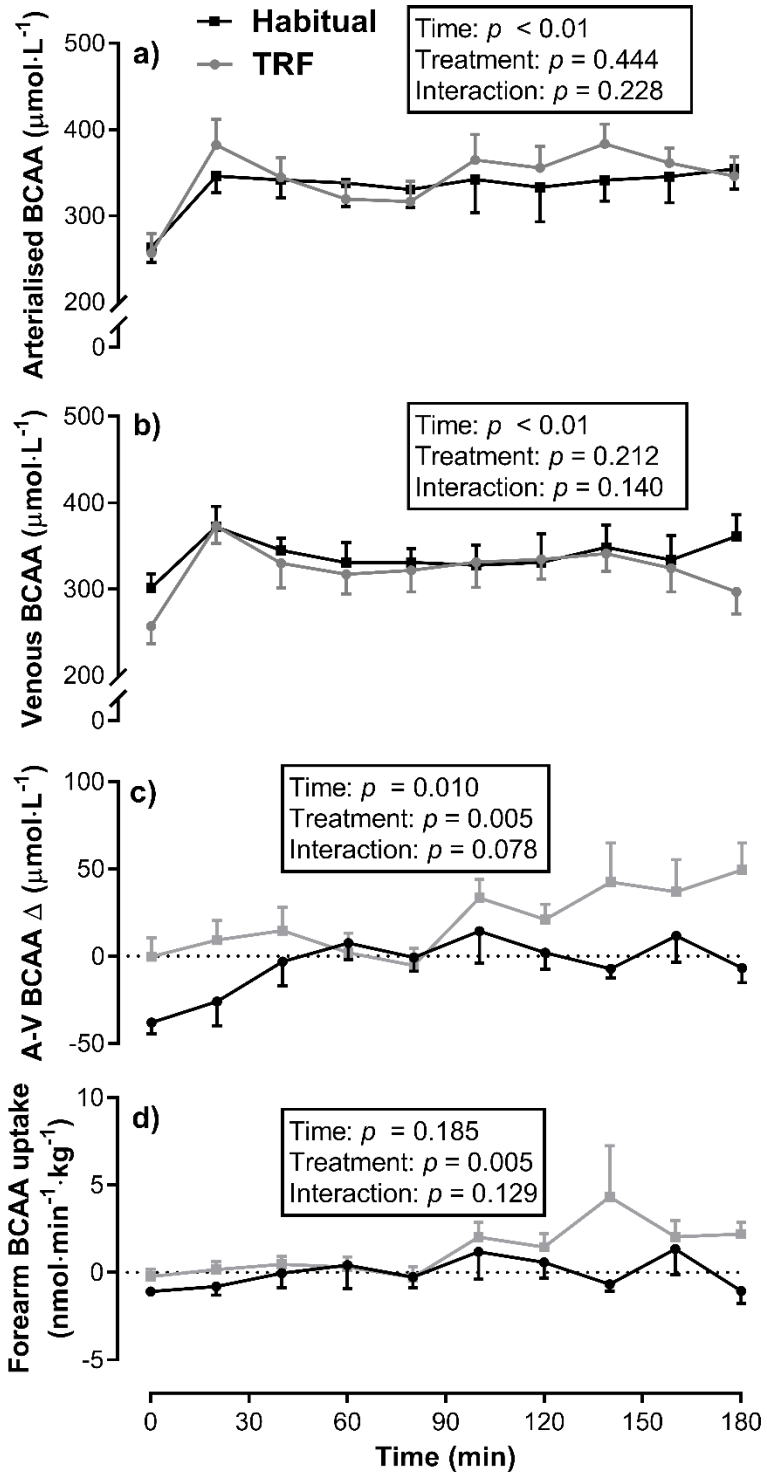


Figure 5.14. Plasma branched chain amino acids.
(a) Arterialised, (b) venous, (c) A-V differences and (d) net flux of plasma BCAAs in response to a liquid test meal. Data are displayed as mean ± SEM; n=8.

5.3.12 Correlation Analysis

Strong negative correlations were found between change in body mass and glucose uptake (Table 5.6). This indicates that greater weight lost during TRF was associated with a larger increase in glucose uptake. There were no other significant correlations found, however the negative correlation between BCAA uptake and dietary protein intake approached significance ($p = 0.056$).

Table 5.6. Correlation analysis of metabolic outcomes.
Correlations between metabolic outcomes and change in body mass / self-reported macronutrient intake during TRF (vs. Habitual).

	Δ Body mass (kg)	**Δ CHO (g·day^{-1})**	**Δ Fat (g·day^{-1})**	**Δ Pro (g·day^{-1})**
Δ **M-ISI$_{120\ min}$**	-.010	.371	.082	.261
Δ **M-ISI$_{180\ min}$**	.012	.290	.203	.355
Δ **Insulin$_{180\ min}$**	.443	-.101	.060	-.375
Δ **Glucose uptake$_{90\ min}$**	-.825*	-.144	-.047	.056
Δ **Glucoseuptake$_{180\ min}$**	-.861**	.139	-.267	.121
Δ **BCAA uptake$_{180\ min}$**	.378	.061	-.039	-.695

Data are n=8 for M-ISI/insulin; n=7 for uptake values; *$p < 0.05$; **$p < 0.01$.

5.3.13 Resting Metabolic Rate and Substrate Oxidation

Resting metabolic rate was unchanged during the intervention [habitual 1828 (247) vs TRF 1812 (460) kCal·day^{-1}] or when expressed relative to total body lean mass [habitual 34.2 (5.3) vs TRF 33.2 (5.6) kCal·day^{-1}·kg^{-1}; n=7]. There was a significant effect of time on the respiratory exchange ratio (RER; corrected for protein oxidation), CHO and fat oxidation within each trial shown in Table 5.7. Rates of CHO oxidation

increased whilst fat oxidation was supressed after consumption of the liquid test meal. In all instances, there were no differences found between trials. Finally, there were no differences between the fasted (uncorrected for protein oxidation as mid-visit was insufficient to assess urea nitrogen excretion rate) measurements obtained pre, mid and post-intervention (data not shown).

Table 5.7. Indirect calorimetry measurements.
Respiratory exchange ratio (RER) and rates of substrate oxidation as assessed by indirect calorimetry (corrected for protein oxidation) in the fasted state and in response to consumption of a liquid test meal.

	Habitual			TRF		
Measure	Fasted	1 h post	2 h 15 min post	Fasted	1 h post	2 h 15 min post
Non-protein RER	0.75 (0.05)	0.84 (0.06)	0.87 (0.05)	0.77 (0.04)	0.83 (0.06)	0.87 (0.04)
CHO oxidation ($g \cdot min^{-1}$)	0.04 (0.06)	0.18 (0.08)	0.19 (0.06)	0.08 (0.06)	0.14 (0.06)	0.18 (0.06)
Fat oxidation ($g \cdot min^{-1}$)	0.11 (0.03)	0.07 (0.04)	0.06 (0.03)	0.09 (0.02)	0.08 (0.04)	0.05 (0.02)

Data are presented as mean (SD); n=8.

5.3.14 Muscle Glycogen Content and Pyruvate Dehydrogenase Complex (PDC) Activity

One participant was excluded from all muscle analyses due to high non-muscle content in one biopsy. Muscle glycogen content was similar in the fasted condition [habitual 359 (66) vs 382 (128) mmol·kg DM^{-1}] and unchanged 3 h after consumption of the liquid test meal [habitual 360 (96) vs TRF 380 (113) mmol·kg DM^{-1}]. Pyruvate dehydrogenase complex (PDC) activity was similar in the fasted condition and significantly increased 3 h after feeding ($F=30.7$; $p = 0.002$) as shown in Figure 5.15. Despite greater changes from the fasted state after feeding in the TRF trial (paired t-

test; p = 0.022), there were no significant differences between TRF and habitual treatments (p = 0.300) or interactions (p = 0.685).

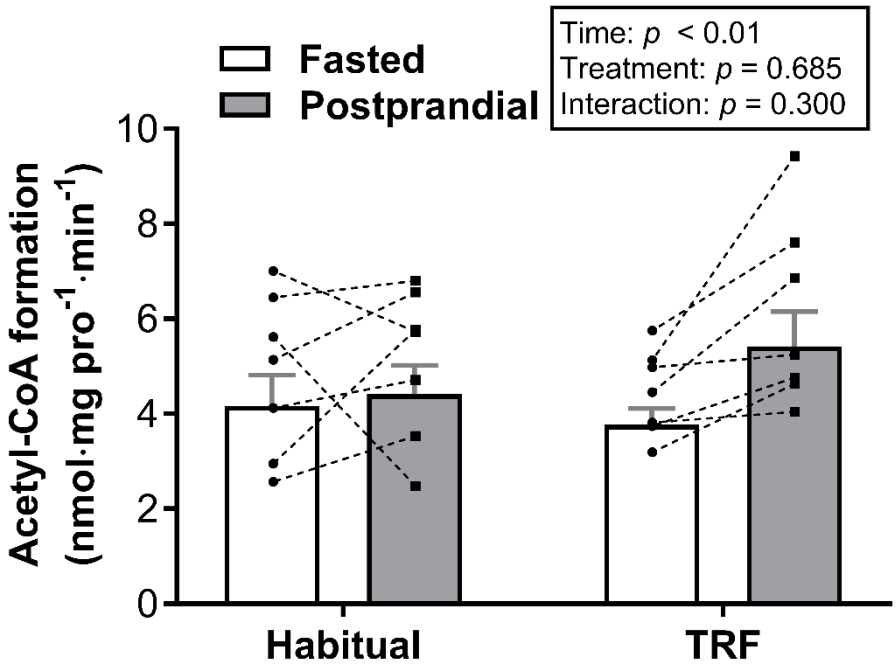


Figure 5.15. Pyruvate dehydrogenase complex activity.
Muscle activity of pyruvate dehydrogenase complex before (fasted) and 3 h after (postprandial) consumption of a liquid test meal. Data is displayed as mean ± SEM and the dots with connecting lines represent individual participants; n=7.

5.3.15 Muscle Protein Content

The content of phospho-Akt^{ser473} and phospho-4E-BP1$^{Thr37/46}$ were both quantified relative to α-actin. The content of p-Akt (Figure 5.16a) in the fasted state was similar between trials and tended to increase after consumption of the liquid test (F=4.466; p = 0.079). The content of p-4E-BP1 was similar in both trials and was unchanged after consumption of the liquid test meal (Figure 5.16b).

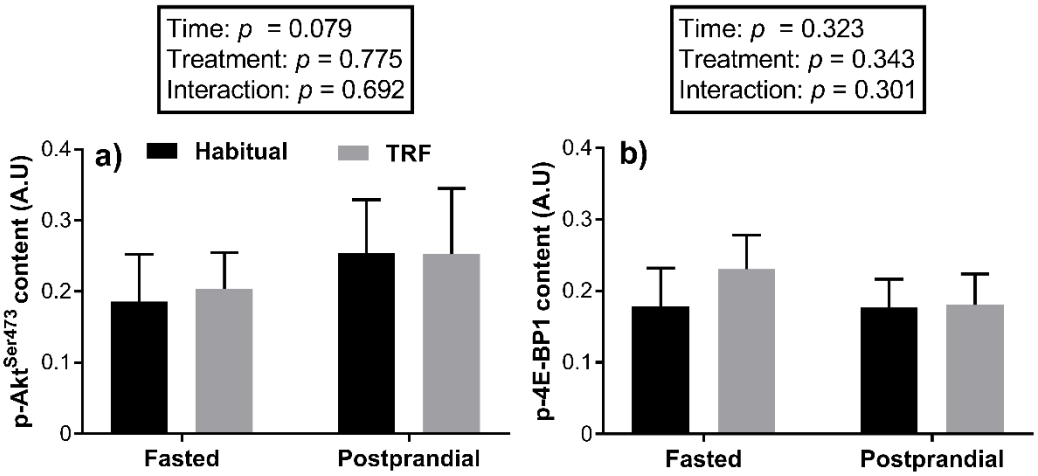


Figure 5.16. Phosphorylation of Akt and 4E-BP1.
Protein content of phospho-Akt^{Ser473} and phospho-4E-BP1$^{Thr37/46}$ in the habitual and TRF trial (fasted) and 3 h after (postprandial) consumption of a liquid test meal. Data are displayed as mean ± SEM; n=7.

5.3.16 Muscle Messenger RNA Expression

ACTA-1 (α-actin) provided the most stable level of mRNA expression between samples (stability level = 0.124) and was used as a housekeeping gene to normalise all others. Five sample/gene combinations were 'undetermined' and a Grubb's outlier test test ($\alpha < 0.01$) identified ten separate sample/gene outliers. These values were replaced with the mean ΔC_T of that gene for the condition to reduce potential biases. Heatmaps using the $\ln(2^{-\Delta\Delta C_T})$ were used to summarise the change in mRNA expression in the fasted state and pattern of response after feeding between trials. A full list of all genes measured is provided in the Appendix.

Effect of TRF vs Habitual Diet on Fasted mRNA Expression

A heatmap summarising the change in fasted skeletal muscle mRNA expression between the habitual and TRF trial is shown in Figure 5.17. The expression of five genes were changed after TRF (all $p \leq 0.05$ from a paired t-test); Acetyl-CoA Carboxylase (ACACB), Beclin-1 (BECN1), Forkhead box protein O1 (FOXO1),

Pyruvate Dehydrogenase Phosphatase Catalytic Subunit 1 (PDP1) and Solute Carrier Family 36 Member 1 (SLC36A1). There was also a tendency ($p = 0.090$) for increased expression of Glycerol-3-Phosphate Acyltransferase, Mitochondrial (GPAM) after TRF. Further details on these genes including the direction of changes and their physiological function is displayed in Table 5.8.

Effect of TRF vs Habitual Diet on mRNA Expression in Response to Feeding

A heatmap summarising the changes in mRNA expression of genes in response to feeding in the TRF and habitual trials is shown in Figure 5.18. A two-way ANOVA was undertaken to assess these responses; a treatment effect indicates a difference in expression between the habitual and TRF trials (considering both fasted and fed expression). An interaction effect suggests a differential pattern of response to feeding. As expected, the mRNA expression of numerous genes changed in response to consumption of the liquid test meal (main effect of feeding) regardless of treatment. Only genes that had a significant ($p \leq 0.05$) or trend ($p \leq 0.10$) towards a treatment or interaction effect are summarised in Table 5.9.

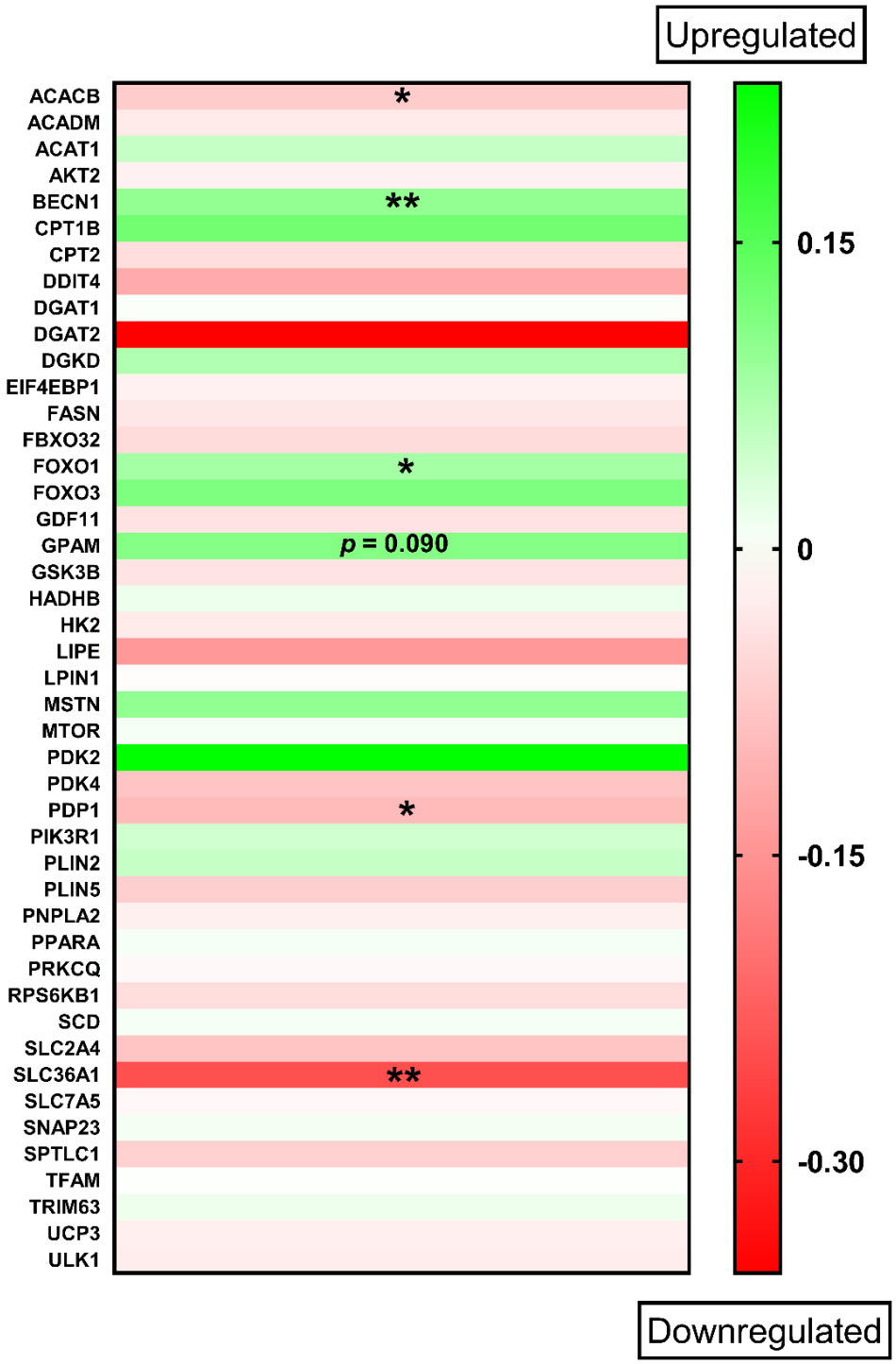


Figure 5.17. Change in mRNA expression in the fasted state.
Change in mRNA expression after two weeks of TRF in the fasted state. The intensity of colour represents the magnitude of change in log ($2^{-\Delta\Delta C_T}$) values. The *p*-values are obtained from a paired t-test on the ΔC_T values; n=7. $^*p \leq 0.05$, $^{**}p < 0.01$.

Table 5.8. Genes that changed in expression between the Habitual and TRF trial in the fasted state.

Acronym	Gene	Δ in expression	Physiological function of protein encoded
ACACB	Acetyl-CoA Carboxylase	↓	Catalyses the synthesis of malonyl-CoA which is substrate for fatty acid synthesis and negative regulator of fatty acid oxidation.
FOXO1	Forkhead box protein O1	↑	Transcription factor that plays a role in the adaptive response to fasting by activating genes involved in lipid oxidation and a negative regulator of PDC activity via activation of PDK4.
PDP1	Pyruvate Dehydrogenase Phosphatase Catalytic Subunit 1	↓	PDP1 activates PDC, which catalyses the irreversible conversion of pyruvate to acetyl-CoA.
SLC36A1	Solute Carrier Family 36 Member 1	↓	This is a system L AA transporter involved in the uptake of small AAs such as glycine and alanine
BECN1	Beclin 1	↑	Plays a role in autophagy.
GPAM	Glyercol-3-Phosphate Acyltransferase, Mitochondrial	↑	Catalyses the first step in TAG synthesis by esterifying a long-chain fatty acyl CoA.

The arrows indicate the direction of change in mRNA expression from the habitual to the TRF trial.

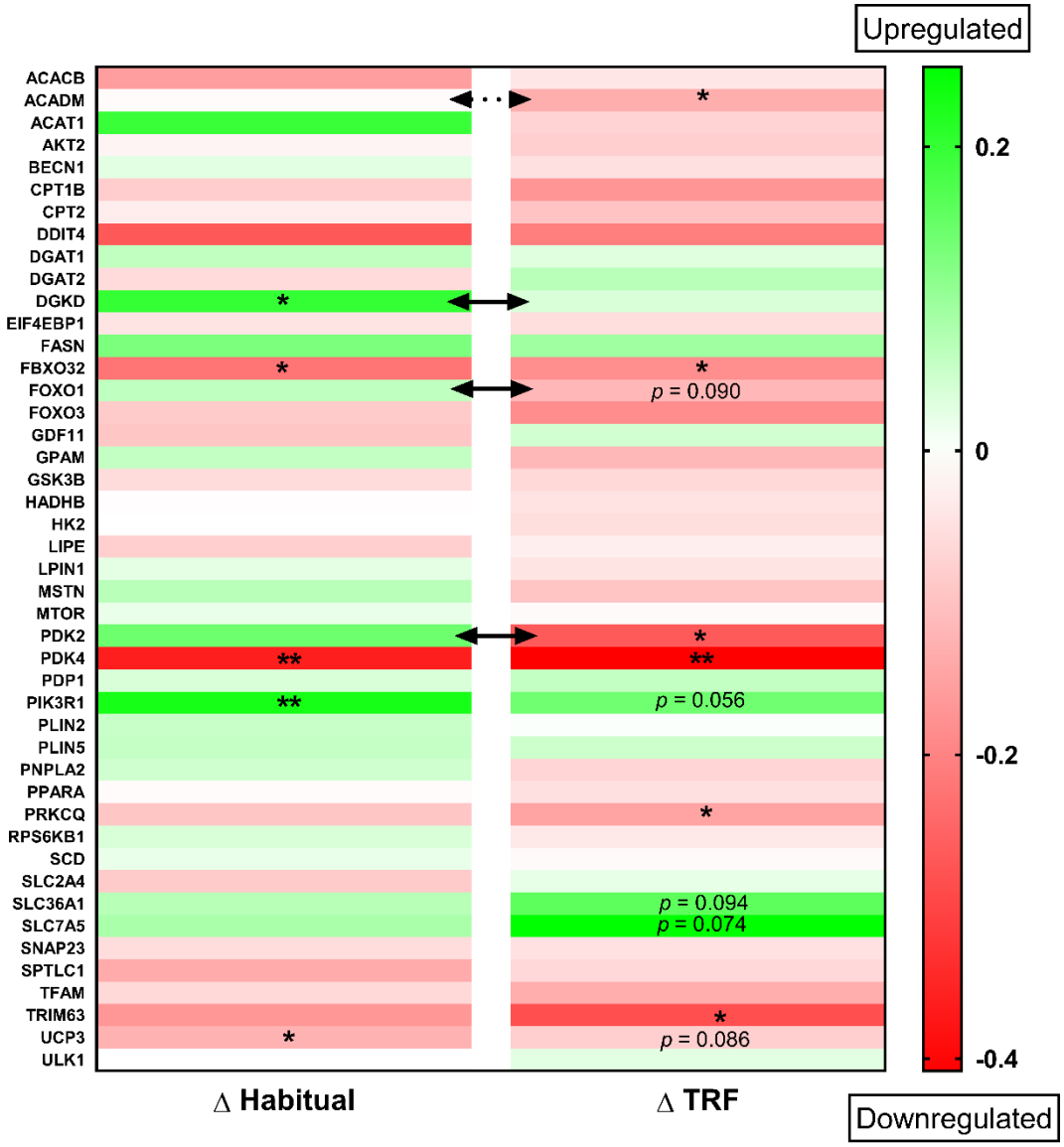


Figure 5.18. Change in mRNA expression after feeding.
Change in mRNA expression after feeding. The intensity of colour represents the magnitude of change in log ($2^{-\Delta\Delta C_T}$)values after feeding. *p*-values are from Bonferroni post-hoc tests after a time (feeding) or interaction effect was obtained. Solid arrows indicate an interaction effect ($p \leq 0.05$), whereas dotted arrows indicate $p \leq 0.10$. *$p \leq 0.05$, **$p < 0.01$; n=7.

Table 5.9. Summary of genes that changed in expression between the Habitual and TRF trial.

Acronym	Gene	Habitual vs TRF (treatment *p*-value)	Response to feeding (interaction *p*-value)	Physiological Function of Protein Encoded
ACADM	Acyl-CoA dehydrogenase medium chain		↓ in TRF ($p = 0.071$)	Catalyses first step in the mitochondrial β-oxidation of medium chain fatty acids.
CPT2	Carnitine palmitoyl transferase II	↓ in TRF ($p = 0.053$)		Key enzyme located on the inner mitochondrial membrane which catalyses the breakdown of acylcarnitines.
DGAT2	Diacylglycerol O-acyltransferase II	↓ in TRF ($p = 0.031$)		Key enzyme in the final stage of TAG synthesis by combining long-chain Acyl CoAs with DAG.
DGKD	Diacylglycerol kinase delta		↑ in habitual ($p = 0.041$)	Phosphorylation of DAG into phosphatidic acid.
FOXO1	Forkhead box protein O1		↓ in TRF ($p = 0.034$)	Transcription factor that plays role in the adaptive response to fasting by activating genes involved in lipid oxidation and a negative regulator of PDC activity via activation of PDK4.
PDK2	Pyruvate dehydrogenase kinase 2		↓ in TRF ($p = 0.009$)	Negative regulator of PDC activity.
SLC36A1	Solute carrier family 36 member 1	↓ in TRF ($p = 0.017$)		System L AA transporter involved in uptake of small AAs including glycine, alanine and proline.

5.4 Discussion

The principal finding of this study was that two weeks of eTRF improved whole-body insulin sensitivity and increased skeletal muscle glucose uptake. The former is supported by the lower insulinaemic response and a higher M-ISI, in response to a CHO and protein drink in the TRF trial. This extends recent findings on overweight men with pre-diabetes (Sutton et al., 2018) to a healthier group. However, unlike the latter study and other research (Moro et al., 2016), no reductions in fasting insulin concentrations were shown. This may reflect the healthier study population, or the shorter length of intervention applied in the present study (2 vs $\geq$ 5 weeks). Moreover, Sutton et al. (2018) undertook metabolic testing after an increased acute fast (18 h) post-TRF, which potentially confounds this finding. In agreement with Sutton et al. (2018) we found improvements in whole-body insulin sensitivity, which emphasises the importance of using dynamic metabolic tests to capture the effects of altering meal pattern distribution. Although different indexes were used to estimate insulin sensitivity (M-ISI vs incremental AUC ratio), these have both been shown to adequately distinguish whole-body insulin sensitivity (Abdul-Ghani et al., 2006).

To our knowledge, this is the first study to estimate the flux of metabolic substrates into skeletal muscle after a TRF intervention. Incorporating protein into the oral glucose challenge permitted simultaneous insight into postprandial glucose and AA metabolism. There was no significant change in delivery (blood flow) to the muscle between trials, although numerically lower values were shown in the TRF trial, which may be related to the lower postprandial insulin concentrations in that trial. Despite this, we found increased forearm (muscle) glucose uptake in the initial 90 min of the postprandial period, which can be attributed to an improved efficiency of glucose

extraction. The increase in glucose uptake is unlikely to be accounted for by an increase in nonoxidative glucose disposal, as muscle glycogen concentrations and the mRNA expression of GSK3β were unaltered between trials and in response to feeding. Previous research has shown increased phosphorylation of GSK3 (Soeters et al., 2009), but no changes in muscle glycogen stores (Halberg et al., 2005) after ADF, although these were assessed using a hyperinsulinaemic clamp.

The mRNA expression of SLC2A4 (encodes GLUT4) and HK2 were unchanged after TRF. Proteins encoded by these genes play key roles in glucose metabolism by facilitating increased uptake and phosphorylation, respectively. However, an absence of change in mRNA expression does not necessarily reflect absence of change in protein content, which can be influenced by post-transcriptional modifications or translocation of the protein to the plasma membrane e.g. GLUT4. Indeed, this study found no changes in mRNA expression of AKT2 but a tendency for increased protein expression of Akt^{Ser473} after feeding. This is likely related to the increased mRNA expression of PIK3R1 (PI3K), which directly phosphorylates Akt and was strongly upregulated in response to feeding in both trials.

Skeletal muscle PDC activation was similar in the basal (fasted) state between trials and comparable to values (~4 nmol·mg pro^{-1}·min^{-1}) previously reported by our group (Stephens et al., 2010). PDC activation increased after consumption of the liquid test meal and although differences were not statistically significant between trials, this was significantly augmented in the TRF trial (Δ+1.65 vs 0.24 nmol·mg pro^{-1}·min^{-1}). When combined with the absence of nonoxidative glucose disposal (based on absence of changes in muscle glycogen content), this could implicate increased oxidative disposal of CHO into the muscle that, at least in part, may explain the increased muscle glucose

uptake observed in the TRF trial. It is possible that we may have seen more pronounced differences in PDC between trials if the postprandial muscle biopsy was obtained earlier than 180 min, for example when glucose uptake and insulin concentrations were both at peak levels during the first 90 min.

The activity of PDC is governed by competing activation from pyruvate dehydrogenase phosphatase (PDP) and inhibition from pyruvate dehydrogenase kinase (PDK). In skeletal muscle, the two predominant isoforms are PDK2 and PDK4 (Spriet et al., 2004). Starvation-induced inhibition of PDC is primarily attributed to upregulated PDK4 (Tsintzas et al., 2006), whereas insulin and feeding activate PDC via suppression of PDK4 (Lee et al., 2004; Pilegaard et al., 2003; Tsintzas et al., 2006) and PDK2 expression (Majer et al., 1998). In the present study, PDK4 was downregulated after feeding to a similar extent in both trials, whereas PDK2 was only downregulated in the TRF trial. The role of PDK2 has attracted considerably less attention than PDK4, likely due to its lower specific activity (Bowker-Kinley et al., 1998). Nevertheless, double knockout rodent models display improved glucose tolerance and insulin sensitivity compared to single knockouts (Jeoung and Harris, 2010). FoxO1 is a key activator of PDK4 and interestingly, we observed a tendency (p = 0.090) for this to be selectively downregulated after feeding in the TRF trial. Along with PDC, FoxO1 is a key regulator of the shift in the response to fasting including stimulation of fatty acid uptake and oxidation (Bastie et al., 2005). The upregulated FoxO1 and downregulated PDP1 expression were detected after a matched duration of acute fast after TRF. Therefore, we speculate this could represent an adaptive response to control fuel oxidation in response to regular periods of fasting.

However, these changes in mRNA expression were not reflected by increased whole-body fat oxidation in the fasted state.

Forearm (skeletal muscle) uptake of BCAA increased to a greater extent after feeding in the TRF trial. In both trials, ingestion of protein resulted in an increase in BCAA uptake and was associated with upregulated mRNA expression of two AA transporters; SLC36A1 and SLC7A5 ($p = 0.063$). The latter is directly involved in the transport of BCAA but is known to work in conjunction with SNAT2/SLC38A2 (see Section 1.5.3), which unfortunately was not measured in this study, to increase intracellular accumulation of AA and stimulate MPS. Although differences did not reach statistical significance, the increase in AA transporter expression after feeding was greater and only approached significance, in the TRF trial (Figure 5.18). Although in the case of SLC36A1, this could be mediated by its lower expression in the fasted state in the TRF trial. Increased BCAA uptake after feeding could represent an adaptive mechanism to potentiate the anabolic response to protein ingestion as the body adjusts to a shorter EI window. This could explain previous observations that TRF promotes improved retention of lean body mass during weight loss (Moro et al., 2016). Maintaining adequate dietary protein intake during TRF is likely to be a key factor involved and this study found a moderate positive correlation between change in protein intake and lean mass after two weeks of TRF ($r = .647$; $p = 0.116$). However, all participants reported exceeding the recommended dietary allowance of 0.8 $g \cdot kgBW^{-1}$ during their habitual diet and TRF. Paradoxically, change in dietary protein intake during TRF was negatively correlated ($r = -.695$; $p = 0.056$) with change in BCAA uptake. The reasons for this are not clear but it must be acknowledged that an increased disposal of BCAA does not necessarily conflate to an increase in MPS, as

their metabolic fate includes oxidation. Whilst we did not detect any changes in urinary nitrogen excretion rates (an estimate of protein oxidation), we cannot exclude this possibility. Future studies should address this by using stable isotopes of non-metabolisable AAs such as phenylalanine, to assess whether increased uptake directly reflects increased incorporation into the muscle protein pool. Were similar results to be shown, TRF could be a nutritional strategy to promote increased maintenance of lean body mass under conditions of weight loss.

This study measured the mRNA expression of several genes involved in anabolic signalling including mTOR and its downstream effectors: RPS6KB1 (S6K1) and EIF4EBP1 (4E-BP1), which all showed no change in response to feeding or between treatments. In line with this, protein content of p4E-BP1$^{Thr37/46}$ was also stable. Other genes involved in the regulation of muscle mass via the ubiquitin-proteasome system include the E3 ubiquitin ligases: FBXO32/atrogin-1 and TRIM63/MuRF1. Both were downregulated after feeding, which may be linked to the upregulated expression of PI3KR1 since its genetic activation abolishes the dexamethasone-induced upregulation of ubiquitin ligases including MuRF1 in C2C12 myotubes (Stitt et al., 2004).

Several genes involved in lipid metabolism were differentially expressed in the TRF trial. In the fasted state ACACB (also known as Acetyl-CoA Carboxylase II; ACC2) was downregulated. This enzyme carboxylates acetyl-CoA to form malonyl-CoA, which inhibits CPT-1 activity, the primary regulator of long-chain acyl CoA entry into the mitochondria and therefore fatty acid oxidation. Although we saw no significant change in CPT-1B expression, a decrease in ACACB could suggest reduced fatty acid synthesis and enhanced fatty acid oxidation in muscle, leading to a

reduction in IMTGs. In support of this, preventing the inhibitory effect of AMPK on ACACB activity leads to increased TAG and ceramide content, along with skeletal muscle IR in rodents (O'Neill et al., 2014).

This study also measured the mRNA expression of three genes involved in DAG metabolism; DGKD and DGAT1 and 2, which are all involved with the synthesis of TAG. The former phosphorylates DAG into phosphatidic acid and was only upregulated after feeding in the habitual trial. There was also a treatment effect for lower expression of DGAT2 in the TRF trial, which catalyses the final stage in TAG synthesis. Overexpression of DGAT2 in type II muscle promotes lipid accumulation and induces IR in rodents (Levin et al., 2007). Taken together, these differences could be indicative of a reduction in intramuscular DAG content after TRF, perhaps due to an increased mobilisation of IMTG during the extended daily fasting periods. A possible reduction in IMTG could also explain the surprising finding of the tendency (p = 0.053) for downregulated expression of CPT2 in the TRF trial. This enzyme is required to generate long-chain acyl CoA from acylcarnitines in the inner mitochondrial matrix.

The enhanced downregulation of ACADM, PDK2 and FOXO1 after feeding in the TRF trial could suggest a greater shift in substrate utilisation from fat to CHO in muscle (metabolic flexibility). However, this was not reflected in measures of whole-body substrate oxidation assessed by indirect calorimetry. As expected, consumption of the liquid test meal caused a rapid reduction in FFA concentrations in both trials, indicating a suppression of lipolysis, accompanied by similar reductions in whole-body fat oxidation. Interestingly, this study found increased muscle FFA net flux in

the TRF trial, this was most prominent at the 0 (fasted) and 180 min timepoint, where higher FFA uptake was observed.

TRF strongly upregulated the fasted mRNA expression of the autophagy related BECN1 (Beclin1). It has been well established that acute fasting activates autophagy, a process that degrades and recycles cellular material, via increased activation of AMPK (Bujak et al., 2015). This inhibits mTOR signalling and upregulates the expression of autophagy-related proteins, including Beclin1 (Kim et al., 2013; Zhang et al., 2016). This may underlie some of the improvements in insulin sensitivity shown after treatment with AMPK agonists (Cokorinos et al., 2017). Interestingly, skeletal muscle from patients with T2D have repressed markers of autophagy (Møller et al., 2017).

There is a paucity of research in humans on the chronic effects of IF on autophagy. A four-day RCT on 11 overweight adults found that eTRF elevated the expression of the autophagy genes: microtubule-associated protein 1 light chain 3 alpha and autophagy-related 12 in the blood (Jamshed et al., 2019). Several studies have measured circulating adiponectin and there is some evidence IF increases this (Halberg et al., 2005; Moro et al., 2016), although this has not been a universal finding (Sutton et al., 2018). Adiponectin has been shown to directly induce autophagic flux in primary skeletal muscle cells in an AMPK-dependent manner and enhance insulin-stimulated glucose uptake (Liu et al., 2015). Moreover, pharmacological administration of adiponectin induces beclin-1 expression in adiponectin knockout mice but does not lead to improvements in insulin sensitivity in autophagy-deficient muscle cells. Circulating adiponectin is positively associated with insulin sensitivity of both glucose and lipid metabolism (Tschritter et al., 2003). Together, these findings

suggest that the insulin sensitising effect of IF may at least be partially attributed to an increase in autophagy, potentially due to a suppression of endoplasmic reticulum stress (Ahlstrom et al., 2017; Yamamoto et al., 2018).

Eight healthy young men completed the study in full and adherence to the TRF eating schedule was high, with only one reported eating event outside of the stipulated EI window. This is further supported by the marked differences in diurnal glycaemic profiles during habitual diets and TRF (Figure 5.7), with emphasis on the lack of glucose excursions after 16:00 during TRF. As expected, glucose concentrations and variability were lower from 20:00 to 08:00 in TRF compared with the habitual period. This window was purposely selected to minimise the contribution of postprandial glucose elevations from the last meal consumed during TRF. However, we found that 24 h glucose concentrations were remarkably similar between the two eating patterns.

The only other study to our knowledge comparing free-living glucose concentrations between a habitual diet and eTRF (09:00 to 17:00) was undertaken on a group of middle-aged overweight men (Hutchison et al., 2019). They found no change in mean 24 h glucose levels but showed reductions in fasting glucose concentrations in eTRF. This was defined as between 4 h after consumption of the last meal of the day until the time of the first meal the next day. This is broadly comparable to the 20:00 to 08:00 window used in the current study, thus is consistent with our findings. Jamshed et al. (2019) assessed the glycaemic responses of overweight males to a controlled eating schedule of three isocaloric meals; eTRF (08:00, 11:00 and 14:00) or control (08:00, 14:00 and 20:00) over a single 24 h period. Participants had followed a control or eTRF eating schedule for 3 days prior to entering a metabolic chamber and eTRF was associated with lower 24 h glucose concentrations. They also

found dampened glycaemic excursions in response to each meal (3 h postprandial period), this was primarily due to the lower inter-meal intervals as participants glucose concentrations were remained elevated between meals. Whether these effects would persist in a more insulin sensitive study population remains to be examined.

The reported habitual daily EI window in this study was approximately 12 h 30 min, which is considerably less than recently reported by Gill and Panda (2015). This study used a student cohort, so these differences may reflect the more heterogenous population examined. In addition, the smartphone app used to track eating behaviour is likely more sensitive to capture this than traditional food diaries. During TRF, the reported daily EI window was just below 7 h with most days between 6 and 8 h, although 13% of days were ≤ 5 h. The reasons for the latter finding are not clear but could relate to days with busier schedules increasing the difficulty of eating at the start/end of the TRF window. Nevertheless, TRF was shown to reduce the average daily EI window by approx. 5 h 30 min, which is comparable to a recent study in a free-living setting (Antoni et al., 2018b).

Accurately quantifying EI in a free-living setting is notoriously difficult as self-report measures are prone to recall and social desirability biases (Ortega et al., 2015; Shim et al., 2014). In line with this, participants reported EI during the baseline week was around 400 kCal·day^{-1} less than their estimated total EE, in the absence of body mass changes. This dropped by a further 400 kCal·day^{-1}during TRF which is broadly consistent with other *ad libitum* studies imposing restrictions on the length of daily EI window (Antoni et al., 2018b; Gabel et al., 2018; LeCheminant et al., 2013; Tinsley et al., 2017). During TRF, participants tended to consume a similar number of meals when compared to their habitual lifestyle but decreased snacking, presumably due to

an absence of hunger. Importantly, there were no changes in the relative macronutrient composition of the diet as has been previously shown in an obese cohort (Gabel et al., 2018). Participants lost an average of 1.04 (0.71) kg across two weeks of TRF, which is primarily attributed to a reduction in EI since no changes in PAEE were evident. This could be interpreted to suggest the extent of underreporting was comparable between the two eating patterns and that unlike in previous findings, the quality of dietary records was maintained over time (Gersovitz et al., 1978).

A major strength of this study was the use of an extensively validated device that was individually calibrated to objectively quantify free-living PA levels. To our knowledge this is the first study to do so during TRF and as previously eluded to; no changes in the total amount, intensity or distribution of PA were shown during TRF. However, this may be partly attributed to instructing participants to maintain their habitual PA patterns throughout the study. Gabel et al. (2018) used pedometers to assess steps/day as an index of PA before and in the final week of a three-month TRF intervention in obese adults and found no changes. Similarly, Hoddy et al. (2016) found no influence of ADF on PA levels of adults with obesity. However, low PA levels were a prerequisite for enrolment and capturing diet-induced changes in PA in an already sedentary population would be difficult. Hutchison et al. (2019) found no statistical differences in PA levels in obese adults between a baseline week and two one-week TRF schedules. Numerically lower indexes of PA (e.g. PAEE was reduced by over 25%) were shown in the eTRF group, thus it is possible that low levels of baseline PA (PAL = 1.4) hampered the ability to detect differences in PA.

The findings of this study are in contrast with the reduction in PA levels/total EE observed during Ramadan (BaHammam et al., 2010; Lessan et al., 2018) and likely

reflects the chronologically opposing eating/fasting windows used. On the other hand, studies extending the overnight fast by skipping breakfast have shown reductions in PA thermogenesis in lean (Betts et al., 2014) but not obese adults (Chowdhury et al., 2016). This was primarily due to reduced PA during the fasting (morning) hours, whereas the present study found no reductions in the fasting (evening) hours. However, the comparisons are somewhat limited as participants in the former two studies were not given explicit instructions to maintain their habitual PA patterns.

The reduction in body mass is unlikely to be caused by changes in total body glycogen stores, as DEXA scans were undertaken after a standardisation protocol that included consumption of a standardised evening meal and a matched duration of overnight fast. Although a change in hepatic glycogen stores cannot be excluded, in line with the findings of an ADF study (Halberg et al., 2005), we showed no changes in muscle glycogen content after TRF. The rate of weight loss (0.52 kg per week) in the present study was higher than previous TRF studies across five weeks in pre-diabetic males (0.28 kg per week; Sutton et al., 2018) and eight weeks in resistance-trained males (0.12 kg per week; Moro et al., 2016), although less than reported in a one week free-living TRF study in obese males (Hutchison et al., 2019). This is perhaps unsurprising given the former was a controlled feeding study that provided all meals in a laboratory setting, whilst dynamically adjusting EI throughout to limit weight loss. Moro et al. (2016) also asked participants to maintain habitual EI during TRF; the increased weight stability could be attributed to the different EI window used (13:00 to 20:00), weekly involvement of a nutritionist, increased nutritional awareness of participants or the resistance training protocol itself. It appears unlikely that the rate of weight loss in the present study would have been sustained over time. Indeed,

previous TRF studies have shown that the initial rate of weight loss tends to plateau after around four weeks in obese adults (Gabel et al., 2018). This is likely due to compensatory mechanisms regulating body weight that include adaptive thermogenesis. However, the translatability of this finding to the current lean study population is unknown.

The present study adds to preliminary evidence that TRF is an efficacious means of inducing a natural caloric deficit on an *ad libitum* diet (Gill and Panda, 2015; Antoni et al., 2018). This has potential applications as a more simplistic, alternative public health message than the traditional approach of calorie counting. However, the sustainability of adopting TRF across the longer-term is relatively unknown, particularly when restricting EI to earlier in the day. Although eTRF may confer additional benefits over other eating patterns, it is likely to be particularly burdensome to social occasions in the evening. Strategies to alleviate this and promote long-term adherence warrant further investigation in human trials. For instance, the metabolic benefits of TRF in rodents persist when unrestricted food access is permitted at the weekend (Chaix et al., 2014; Olsen et al., 2017), which is a promising approach to use in human trials.

Small reductions in android and gynoid fat were the only significant changes in body composition detected after two weeks of TRF. Longer-term interventions of ≥ 8 weeks have found reductions in total (Moro et al., 2016) and proportional levels of body fat (Antoni et al., 2018). Closer inspection revealed that one participant gained 1.15 kg fat and lost 2.92 kg of lean mass, with the latter almost entirely attributed to the trunk region which could be related to differences in intestinal content. Considering that all other participants lost body fat, this likely explains the lack of

significance (p = 0.132). In line with Moro et al. (2016), we detected no changes in lean or appendicular lean mass. However, unlike that study we detected no changes in fasted testosterone levels. Future studies should seek to directly contrast body compositional changes after weight loss from TRF and a prescribed energy deficit.

Two weeks of TRF did not alter RMR despite the accompanying small reduction in body weight. This is consistent with the findings of a previous TRF study (Moro et al. 2016), although there have been conflicting findings when applying an ADF eating pattern (Heilbronn et al., 2005; Soeters et al., 2009). Unlike Moro et al. (2016), who found a reduction in RER (indicating a shift towards increased fat metabolism) in the fasted state, this study uncovered no differences in rates of substrate metabolism between trials. Surprisingly, this persisted even when participants were assessed after a ≥ 16 h fast mid-intervention, which could be due to elevated ketone body metabolism. Early TRF has previously been shown to increase 24 h protein oxidation and lower non-protein RER in overweight adults compared with a control diet of matched food intake consumed in a metabolic chamber (Ravussin et al., 2019). It is also interesting to note that the increase in muscle glucose uptake in the first 90 min of the TRF trial was not reflected by an augmented increase in whole-body CHO oxidation in either postprandial measurement in comparison to the habitual trial.

This study found no changes in total ghrelin levels in the fasted state. Ghrelin is an appetite stimulant that displays diurnal variation and is influenced by feeding frequency (Solomon et al., 2008). It is less understood whether chronically altering temporal distribution of EI will alter the pattern of ghrelin release. No changes in fasting ghrelin levels have been shown after one (Hutchison et al., 2019) or five weeks of eTRF (Sutton et al., 2018). Surprisingly, Ravussin et al. (2019) showed reductions

in morning levels of active ghrelin despite an increased duration of acute fast. It is possible we did not detect changes by measuring total rather than active/acylated ghrelin, although this seems unlikely as total and acylated ghrelin have shown very close agreement (Gibbons et al., 2013). Furthermore, it would have been interesting to assess ghrelin responses in the evening, as well as the postprandial suppression of ghrelin, although no change was shown in the latter by Hutchison et al. (2019). Twelve weeks of obese women following a hypocaloric diet with increased EI at breakfast or dinner led to similar reductions in fasting ghrelin, but a lower postprandial AUC response for the high calorie breakfast group (Jakubowicz et al., 2013).

The major limitation of this study is the small, but significant loss of body mass after two weeks of eTRF. Indeed, there was a strong negative correlation between weight change during TRF and changes in glucose uptake ($p < 0.05$). However, it is important to appreciate that correlation does not imply causation and our analysis was restricted by the small sample size of the study. Nevertheless, this suggests that the metabolic benefits demonstrated cannot be directly attributed to eTRF without including an additional control group with matched weight loss. Despite asking participants to maintain their habitual dietary intake and observing no changes in macronutrient composition between baseline and TRF, it is also possible that some effects were mediated by small differences in diet quality. For instance, we found that participants primarily decreased EI by limiting snack consumption and that prohibiting EI in the evening will almost certainly lead to reductions in alcohol consumption in participants who drink. Furthermore, erratic eating behaviours late in the evening can lead to disruptions in sleep quality (Crispim et al., 2011) which can acutely impair glucose tolerance (Spiegel et al., 1999). Preliminary evidence suggests that shifting a

greater proportion of EI earlier in the day can improve the regularity of sleep/wake cycles (Raynor et al., 2018). Whilst sleep/wake times were not assessed in the present study, this would be an interesting area to explore. Whilst some of the features outlined above may underlie some of the appeals of eTRF to the wider public, they do warrant consideration for researchers seeking to study the effects of eTRF in a free-living setting.

Furthermore, whilst the metabolic improvements detected in this Chapter provide evidence of a change over time, these cannot be directly attribute to eTRF without the inclusion of an additional (randomised) control group (Bland and Altman, 2015). Placebo effects, regression towards the mean and/or changes in lifestyle behaviours (other than the restriction on temporal eating patterns) when participating in a study may all have contributed to these effects. Together these inflate the risk of type I error in our analysis when compared with the gold standard of an RCT; in this instance, including a control group that maintained their habitual diet for two weeks.

This was a short-term study and does not provide any information of the long-term feasibility of this eating pattern. As previously mentioned, eTRF could be disruptive to social occasions particularly during the weekends. Thus, further research is required to examine whether benefits of this approach persist even when it is not applied seven days per week. This would help to facilitate compliance over the long-term, which ultimately determines the efficacy of any nutritional intervention. The study was also only conducted on males and there is preliminary evidence to suggest IF may have different effects in females. For instance, three weeks of ADF adversely affected glucose tolerance in nonobese women but not in men (Heilbronn et al., 2005). This suggests adverse effects of prolonged (≥ 24 h) periods of fasting in females and could

reflect an increased sensitivity of the reproductive system to perturbations in energy balance, which has been shown in rodents (Martin et al., 2009). Thus, TRF and its shorter duration of fasting could be a more appropriate eating pattern to adopt, but further research including females is needed.

Currently it is not well understood whether or how long the metabolic benefits of TRF may persist upon return to a typical eating pattern. A study on Ramadan fasting found that the improvements in blood lipid profile were maintained for at least one month afterwards (Adlouni et al., 1997). Hence future studies could incorporate an additional follow-up visit after returning to habitual eating patterns to assess this, a major factor influencing this is likely to be whether the weight loss induced by TRF is maintained. Finally, larger research studies could seek to stratify individuals based on their circadian chronotype i.e. 'morningness' vs 'eveningness' (Horne and Ostberg, 1976), as this has been shown to influence habitual temporal distribution of EI (Maukonen et al., 2017) and therefore may influence an individual's responsiveness to an eTRF intervention.

In summary, two weeks of eTRF improves whole-body and muscle insulin sensitivity in healthy individuals. In addition, uptake of BCAA (an index of anabolic sensitivity) was increased, although this was not reflected in changes in body composition in this short-term study. Skeletal muscle mRNA expression of several genes involved in lipid, CHO and protein metabolism were also affected by TRF. However, applying TRF in a free-living setting elicits an involuntary reduction in EI and the arising negative energy balance is associated with weight loss. Further research is required to assess the contribution of weight loss to the metabolic effects of TRF.

Chapter 6. Effects of Two Weeks of Daily Caloric Restriction on Basal and Postprandial Metabolism in Healthy Men

6.1 Introduction

Inducing a negative energy balance via caloric restriction (CR) reduces cardiometabolic risk factors in nonobese adults (Kraus et al., 2019; Ravussin et al., 2015) and may delay the onset of age-related diseases through reduction of oxidative stress (Redman et al., 2018). Longitudinal studies in rhesus monkeys, which are used as a model for human ageing, consistently find that CR promotes enhanced insulin sensitivity and glucoregulatory control (Colman et al., 2009; Mattison et al., 2017). On a more extreme level, restricting EI at 600 to 1200 kCal·day^{-1} has even been shown to reverse T2D (Lim et al., 2011) and muscle IR (Petersen et al., 2012).

Many of these benefits are attributed to the associated weight loss (Larson-Meyer et al., 2006) and hence are likely to be augmented in overweight/obese individuals with excessive adipose tissue. Restricting daily EI by 500 kCal·day^{-1} (vs. total EE) is purported to lead to around 1 lb (0.45 kg) of weight loss per week. Whilst this may apply in the short-term, weight loss is a dynamic process and several long-term physiological adaptations occur to limit weight loss, including adaptive thermogenesis (Hall et al., 2011). These compensatory mechanisms likely account for some of the difficulty in weight-loss maintenance across the longer-term.

Interestingly, rodent studies have shown more favourable effects of intermittent vs continuous food access despite similar levels of EI (Sherman et al., 2012; Hatori et al.,

2012; Chaix et al., 2014; Mitchell et al., 2019). This suggests some of the metabolic improvements associated with intermittent fasting (IF) may be independent of energy balance. More studies are emerging in humans, preliminary findings suggest comparable effects of CR and intermittent energy restriction on weight loss and cardiovascular risk factors (Sundfør et al., 2018), including enhanced insulin sensitivity (Harvie et al., 2011). A promising novel approach includes a subtype of intermittent energy restriction: eTRF, which may confer additional benefits over traditional IF protocols. This involves restricting EI to earlier in the day, in line with diurnal variations in energy metabolism (see Section 1.7.6 and 1.7.7).

In Chapter 5, we extended recent findings of Sutton et al. (2018) to show that two weeks of eTRF improved skeletal muscle and whole-body insulin sensitivity in healthy lean individuals. This eating pattern did not restrict EI, indeed participants were encouraged to maintain their habitual dietary intake. Despite this, and in agreement with previous research in a free-living setting (Tinsley et al., 2017; Antoni et al., 2018), eTRF led to a 15% (~400 kCal·day^{-1}) reduction in self-reported EI. This resulted in an average weight loss of 1.04 (0.71) kg across two weeks, which although small, precludes the assertion that the metabolic effects of eTRF are due to the change in eating pattern alone. Indeed, there was a strong negative correlation between change in body weight after eTRF and change in glucose uptake ($p < 0.05$). Therefore, this study was undertaken to replicate the weight loss observed with TRF using CR, without altering participants habitual temporal distribution of EI. Since dietary composition can influence the metabolic effects of weight loss (Golay et al., 1996; Kirk et al., 2009), macronutrient composition was matched to what participants reported during TRF.

6.2 Methods

6.2.1 Participants

This study was an extension of the TRF study detailed in Chapter 5. Therefore, the inclusion and exclusion criteria(s) stated in Section 2.1.3 and 5.2.1 were applied here. Descriptive characteristics of participants at the time of the first main visit are presented below in Table 6.1.

Table 6.1. Descriptive characteristics of study participants.

Age (years)	Body Mass (kg)	BMI ($kg \cdot m^{-2}$)	Body Fat† (%)	Lean Mass† (%)
24 (5)	77.7 (12.9)	23.8 (1.5)	22.0 (8.3)	74.8 (7.6)

Data is mean (SD); n=8, †n=7.

6.2.2 Experimental Design

This study consisted of a one-week baseline (habitual period) period, followed by a two-week dietary intervention (CR) and is summarised in Figure 6.1. Each participant visited the laboratory at the start of the baseline period to undergo an incremental treadmill protocol, in order to obtain an individual HR-EE relationship (Brage et al., 2007). They wore an Actiheart, CGM and recorded all food intake during the baseline week in order to establish habitual dietary and PA patterns. After an overnight fast, they visited the laboratory to assess their metabolic response to a CHO and protein liquid test meal (as outlined in Chapter 5; see Figure 5.2). From the next day, they were asked to follow a food and drink plan prescribed by the experimenters. Halfway through the two-week intervention, participants visited the laboratory after an overnight fast to assess changes in body mass and undergo a resting indirect calorimetry measurement. Occasionally, the dietary plan for the second week was adjusted according to changes in body mass at this stage. Following another week of

the prescribed diet, they returned to the laboratory to undergo identical follow up metabolic testing.

6.2.3 Dietary Prescription

Total EI during CR was calculated by subtracting 400 $kCal \cdot day^{-1}$ from the average total EE estimated from the Actiheart during one week of habitual lifestyle. The average caloric deficit prescribed was −13 (1) %. The macronutrient composition of food and drink provided was matched to that reported in Chapter 5; 45% CHO, 35% fat and 20% protein (as a % of total EI). Each participant was provided with an individualised nutrition plan detailing caloric and macronutrient composition of item(s) provided. If in exceptional circumstances, participants were unable to consume the prescribed meal, they were asked to consume a balanced meal comparable in total energy content. Participants were asked to restrict alcohol consumption to ≤ 1 unit per day but were permitted unlimited consumption of unsweetened soft-drinks or black coffee/tea. They were required to log all food and drink consumption in food diaries. Finally, they were asked to not consciously alter their typical temporal distribution of EI or PA levels for the duration of the study.

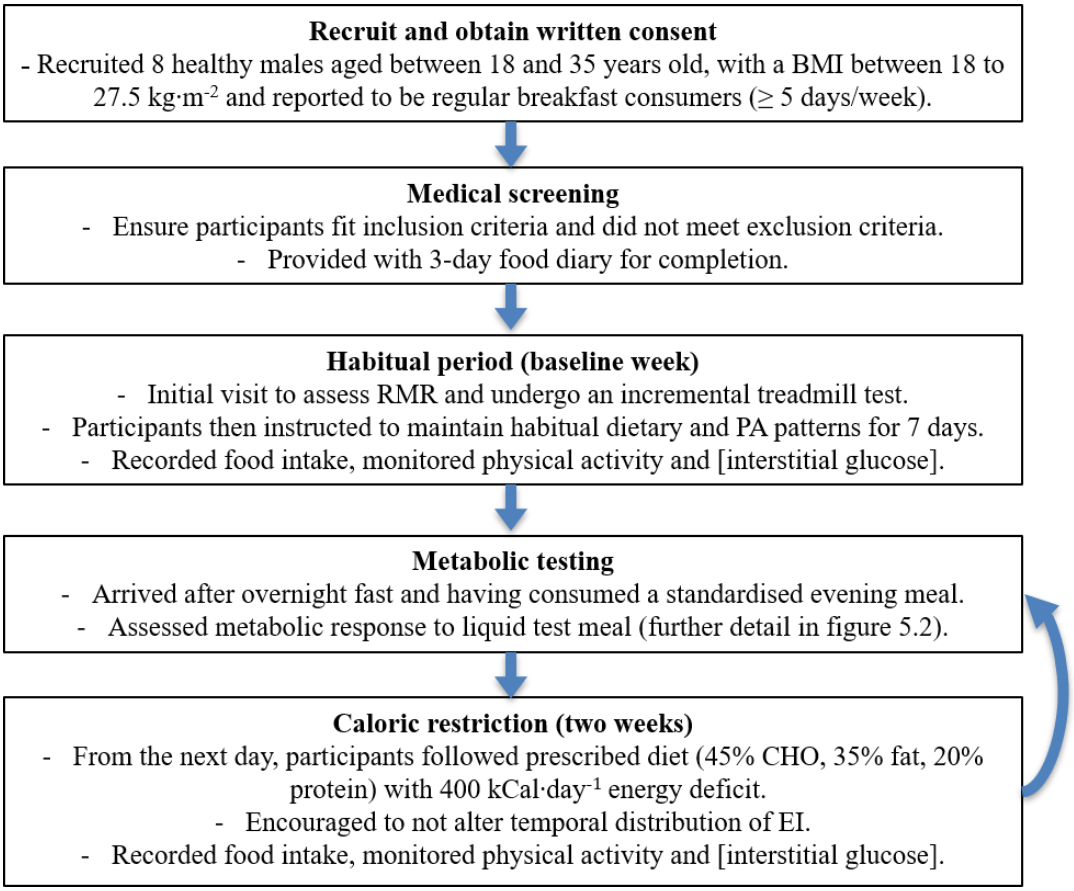


Figure 6.1. Schematic of experimental design.

6.2.4 Statistical Analysis

All statistical analysis was undertaken using GraphPad Prism 7.0 (GraphPad Software Inc., San Diego, CA, USA). Significance was accepted at $p \leq 0.05$. Data in text and tables are presented as mean ± SD and error bars in figures represent SEM unless otherwise stated. A student's paired t-test (two-tailed) was used to compare two means (e.g. PAEE). A one-way ANOVA was used to compare pre, mid and post-intervention data obtained from indirect calorimetry. For all other variables, a two-way repeated measures ANOVA (time x habitual/CR trial) was employed (e.g. insulinaemic response). When significant treatment or interaction effects were

identified, post-hoc multiple comparisons were undertaken using Bonferroni corrections to reduce the chance of type I error.

6.3 Results

6.3.1 Free-Living Energy Expenditure

In total, just under 25% of study days were excluded from analyses due to obtaining an insufficient amount or quality of data (either > 144 min per day 'lost' or > 325 min per day 'recovered'). Importantly, only five out of 48 (~10%) of these days were during the habitual period that was used to prescribe EI during CR. Overall, total daily PAEE was similar between the habitual and CR periods [habitual 1044 (173) vs CR 1055 (327) $kCal \cdot day^{-1}$], as shown below in Figure 6.2. In line with this, there were no differences in the average daily time spent at light ($1.5 \leq METs < 3$), moderate ($3 \leq METs < 6$) and vigorous (≥ 6 METs) intensity PA, as shown in Table 6.2.

Intensity of PA	Habitual	Caloric Restriction
Light (1.5 ≤ METs < 3)	187 (58)	180 (70)
Moderate (3 ≤ METs < 6)	113 (52)	133 (70)
Vigorous (≥ 6 METs)	14 (8)	13 (5)

Data presented as mean (SD); n=8.

Table 6.2. Intensity of physical activity.
Daily time (min) spent in light, moderate and vigorous physical activity.

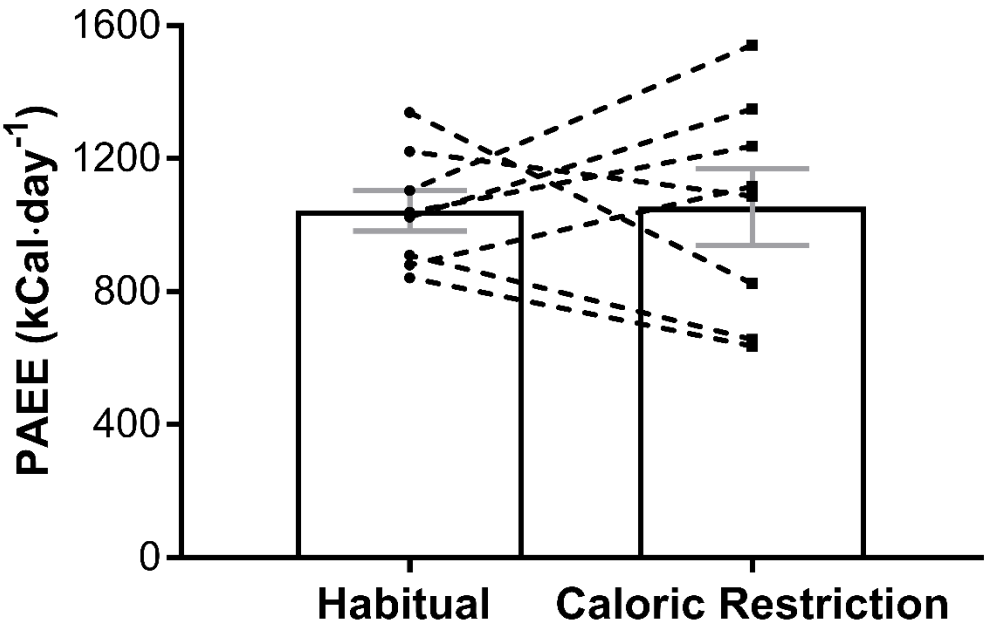


Figure 6.2. Physical activity energy expenditure.
Physical activity energy expenditure (PAEE) during one-week of habitual diet (baseline) and two weeks of caloric restriction. The bars represent the mean ± SEM and dots with connecting lines represent individual participants.

6.3.2 Body Composition

As expected, participants lost body mass during two weeks of CR [−1.24 (1.00) kg; p = 0.001] which was similar to the 1.04 (0.71) kg body mass loss after TRF in Chapter 5. The changes in key anthropometric characteristics after CR are presented in Table 6.3. This study found no significant changes in fat or lean body mass loss and the decline in these were similar in magnitude to those observed during TRF. In line with the previous study, there was a reduction in android fat but unlike after TRF, there was no significant change found in gynoid fat (p = 0.255).

Table 6.3. Body composition.
Body composition (assessed by DEXA) after one week of habitual diet and two weeks of caloric restriction.

Anthropometric Δ (kg)	Habitual	Caloric Restriction
Body mass	77.68 (12.93)	76.43 (12.59)**
Lean mass	57.42 (6.74)	56.95 (6.78)
Fat mass	17.17 (8.93)	16.43 (8.94)
Appendicular lean mass	27.56 (3.62)	27.22 (3.33)
Android fat	1.58 (0.89)	1.46 (0.87)**
Gynoid fat	3.56 (1.71)	3.45 (1.70)

Data presented as mean (SD); n=8 for body mass and n=7 for all other measures.
**$p < 0.01$ change from baseline.

6.3.3 Continuous Glucose Monitoring

There were no differences in mean 24 h interstitial glucose concentrations or any reported indexes of glucose variability, shown in Table 6.4. In addition, the patterns of diurnal glycaemic profiles were similar between the habitual and CR period (Figure 6.3). In both periods, there was a steady rise in interstitial glucose concentrations from just below 5 mmol·L^{-1}at 07:00 to around 6 mmol·L^{-1} at 15:00. It was maintained around 6 mmol·L^{-1} until 22:00, where it tended to steadily decline throughout the night. Overall, the CGM data is consistent with the similarity in self-reported daily EI window between the two periods [baseline 11 h 20 min (1 h 16 min) vs CR 11 h 41 min (1 h 2 min)].

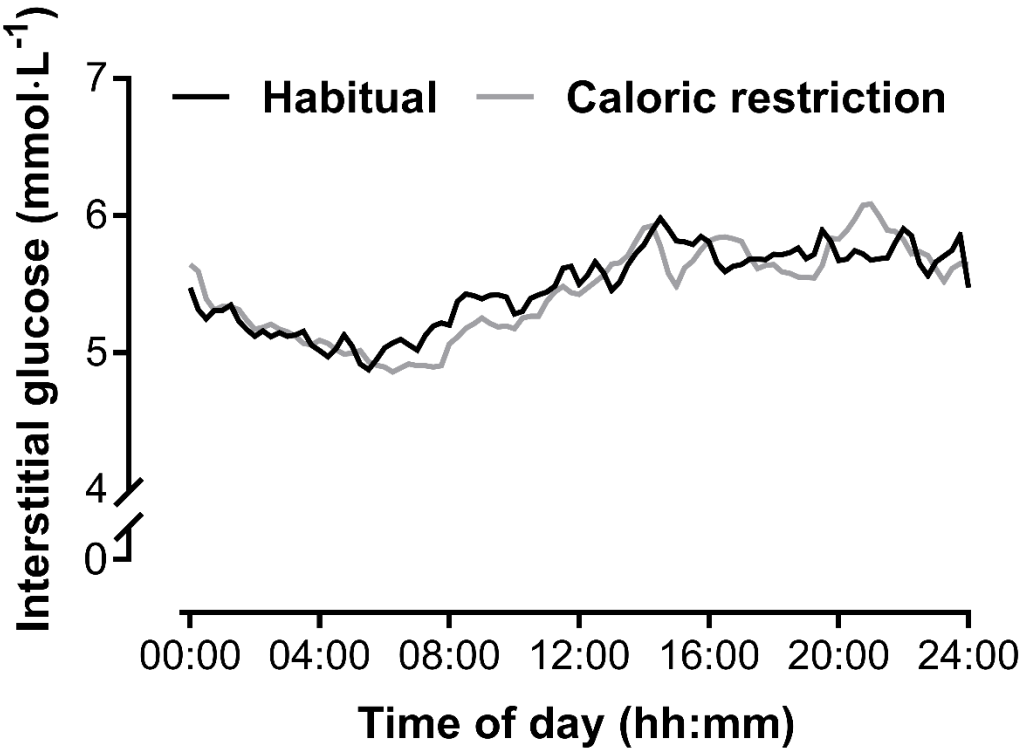


Figure 6.3. Diurnal glycaemic profiles.
Mean interstitial glucose concentrations during one week of habitual diet (baseline) and two weeks of caloric restriction; n=8.

Table 6.4. Continuous glucose monitoring.
Indexes derived from 24h continuous glucose monitoring during one week of habitual diet (baseline) and two weeks of caloric restriction.

	Habitual	Caloric Restriction
No. of valid days (% of total)	42 (88%)	77 (74%)
Mean glucose (mmol·L^{-1})	5.5 (0.4)	5.4 (0.2)
Glucose variability (SD)	0.8 (0.2)	0.7 (0.3)
Glucose variability (CV; %)	14 (3)	13 (2)

Data presented as mean (SD); n=8.

6.3.4 Glycaemic, Haemodynamic and Muscle Insulin Sensitivity Response(s)

There were no differences in fasting blood glucose (arterialised or venous), brachial artery blood flow or glucose uptake between the trials. The arterialised glucose response was more pronounced in the CR trial, reaching a peak of 7.4 mmol·L^{-1} vs 6.8

mmol·L^{-1} (Figure 6.4a). There was a significant interaction (time x treatment) effect (F=1.923; p = 0.019), with higher glucose concentrations most evident between 30 to 80 min in the CR trial. The pattern of response and statistical significance remained when the two participants with no deep vein cannulation were excluded. The differing pattern of response between trials was replicated in venous blood (Figure 6.4b), with elevated glucose concentrations between 20 to 80 min in the CR trial. However, neither the treatment (F=4.876; p = 0.078) or interaction (F=1.701; p = 0.054) effects reached statistical significance.

There were no treatment or interaction effects for A-V differences (Figure 6.5a), brachial artery blood flow (Figure 6.5b) or forearm glucose uptake (Figure 6.5c), an index of muscle insulin sensitivity. Blood flow and all substrate uptake values were standardised relative to forearm lean mass. The participant with a missing DEXA scan was also one of the two participants with no deep vein cannulation. Blood flow increased to a similar extent after consumption of the drink in both trials (F=5.26; p < 0.001). Peak A-V differences of ~1.8 mmol·L^{-1} were observed between 40 and 50 min, whereas peak glucose uptake values of ~95 μmol·min^{-1}·kg^{-1} were shown between 70 to 80 min.

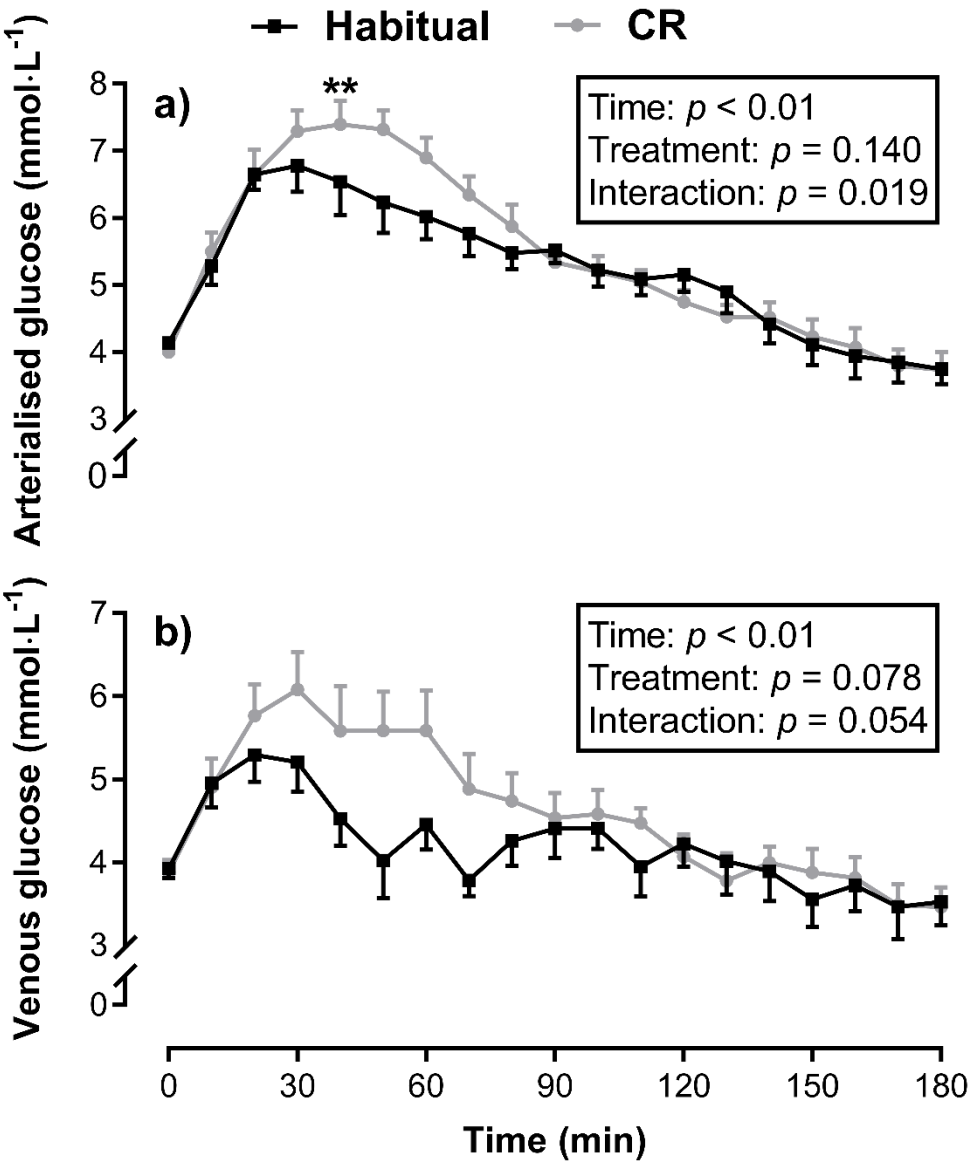


Figure 6.4. Arterialised and venous glucose.
(a) Arterialised and (b) venous glucose concentrations in response to a liquid test meal in the habitual and caloric restriction trial. Data are displayed as mean ± SEM; n=8 for arterialised and n=6 for deep venous blood. $^{**}p < 0.01$.

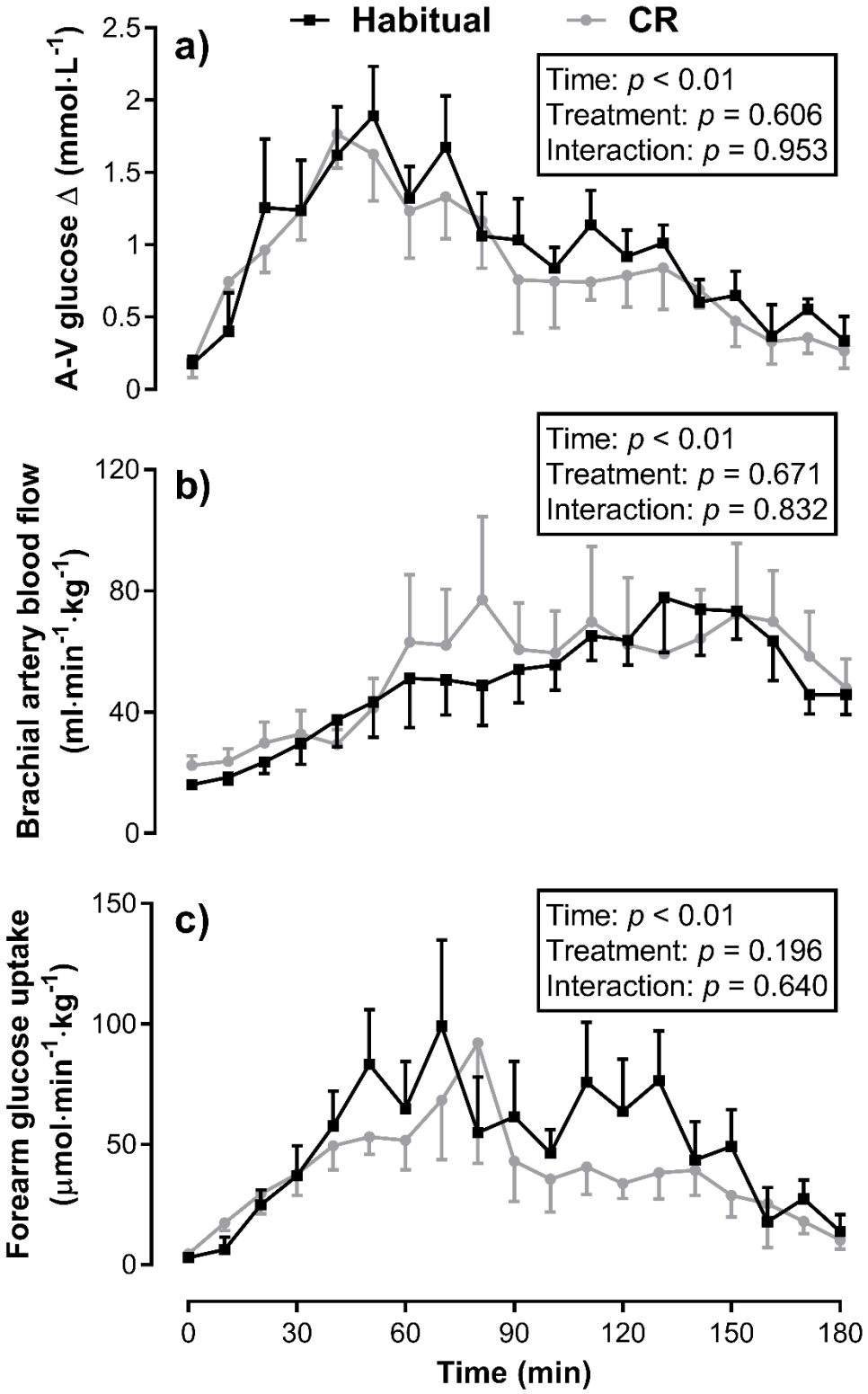


Figure 6.5. Glucose uptake and influencing factors.
(a) Arteriovenous differences in glucose, (b) brachial artery blood flow and (c) forearm glucose uptake in response to a liquid test meal in the habitual and caloric restriction trial. Data are displayed as mean ± SEM; n=6.

6.3.5 Serum Insulin and Indexes of Whole-Body Insulin Sensitivity

Fasting concentrations of arterialised insulin and glucose in the habitual and CR trial are displayed below in Table 6.5. There were no changes in either variable, or the HOMA-IR derived from these. The M-ISI considers postprandial glycaemic (Figure 6.4) and insulinaemic responses (Figure 6.6). There were no differences in the M-ISI calculated over 120 (p = 0.166) or 180 min (p = 0.138). Furthermore, there were no treatment or interaction effects for the insulinaemic response. In both trials, serum insulin concentrations were rapidly elevated 20 min after consumption of the drink and peak values of ~600 ρmol·L^{-1} were shown after 40 min. From that point, they steadily declined throughout each trial approaching, but not reaching, fasting concentrations after 180 min postprandially.

Table 6.5. Measures of fasting and postprandial whole-body insulin sensitivity.

Measure	Habitual	Caloric Restriction
Fasting glucose (mmol·L^{-1})	4.13 (0.22)	4.00 (0.37)
Fasting insulin (ρmol·L^{-1})	37 (12)	43 (14)
HOMA-IR	0.98 (0.36)	1.08 (0.32)
M-ISI$_{120\ min}$	7.7 (2.3)	6.6 (1.1)
M-ISI$_{180\ min}$	9.0 (2.4)	7.7 (1.3)

Data are presented as mean (SD); n=8.

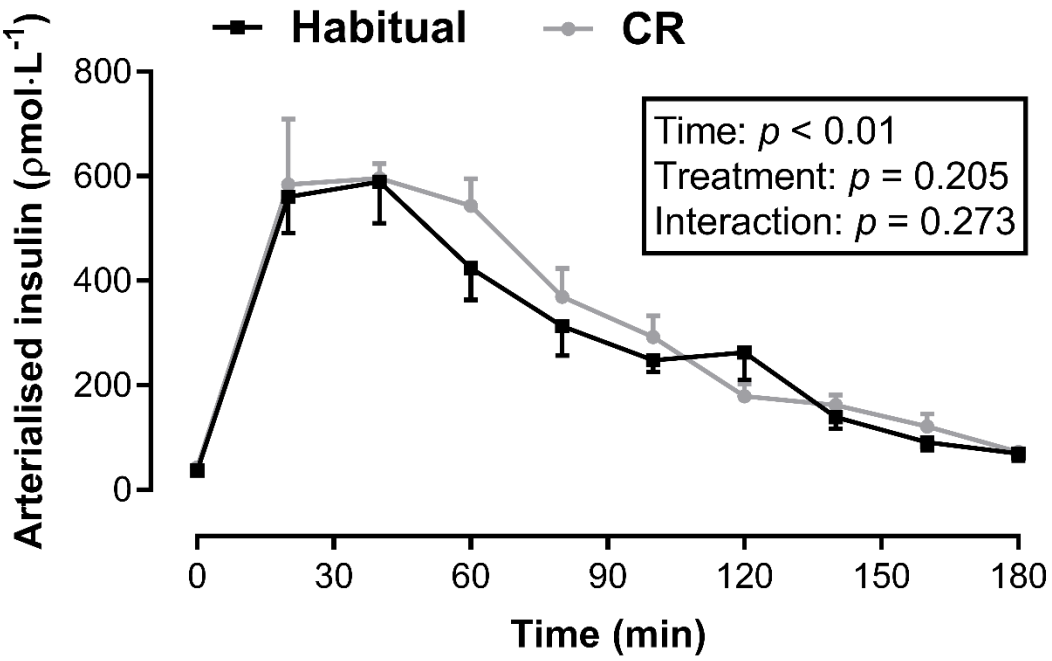


Figure 6.6. Arterialised serum insulin.
Arterialised serum insulin concentrations in response to a liquid test meal in the habitual and caloric restriction trial. Data is displayed as mean ± SEM; n=8.

6.3.6 Plasma Free-Fatty Acids

Both arterialised and venous FFA concentrations were rapidly supressed in both trials, from around 0.55 mmol·L^{-1} to below 0.1 mmol·L^{-1}, within 60 min post-drink consumption. Arterialised FFA (Figure 6.7a) were maintained below this level throughout the CR trial, whereas there was an elevation after 140 min in the habitual trial and a significant interaction (treatment x time) effect (F=1.431; p = 0.015). A significant interaction effect (F=3.584, p = 0.002) also emerged in venous FFA (Figure 6.7b), with an attenuated reduction in the CR trial during the initial 20 min, whereas lower levels were found in the last 20 min. There were no significant effects on the A-V differences in FFA concentrations (Figure 6.7c). However, overall there was a decreased net FFA flux into the forearm (Figure 6.7d) during the CR trial (F=10.63; p = 0.021).

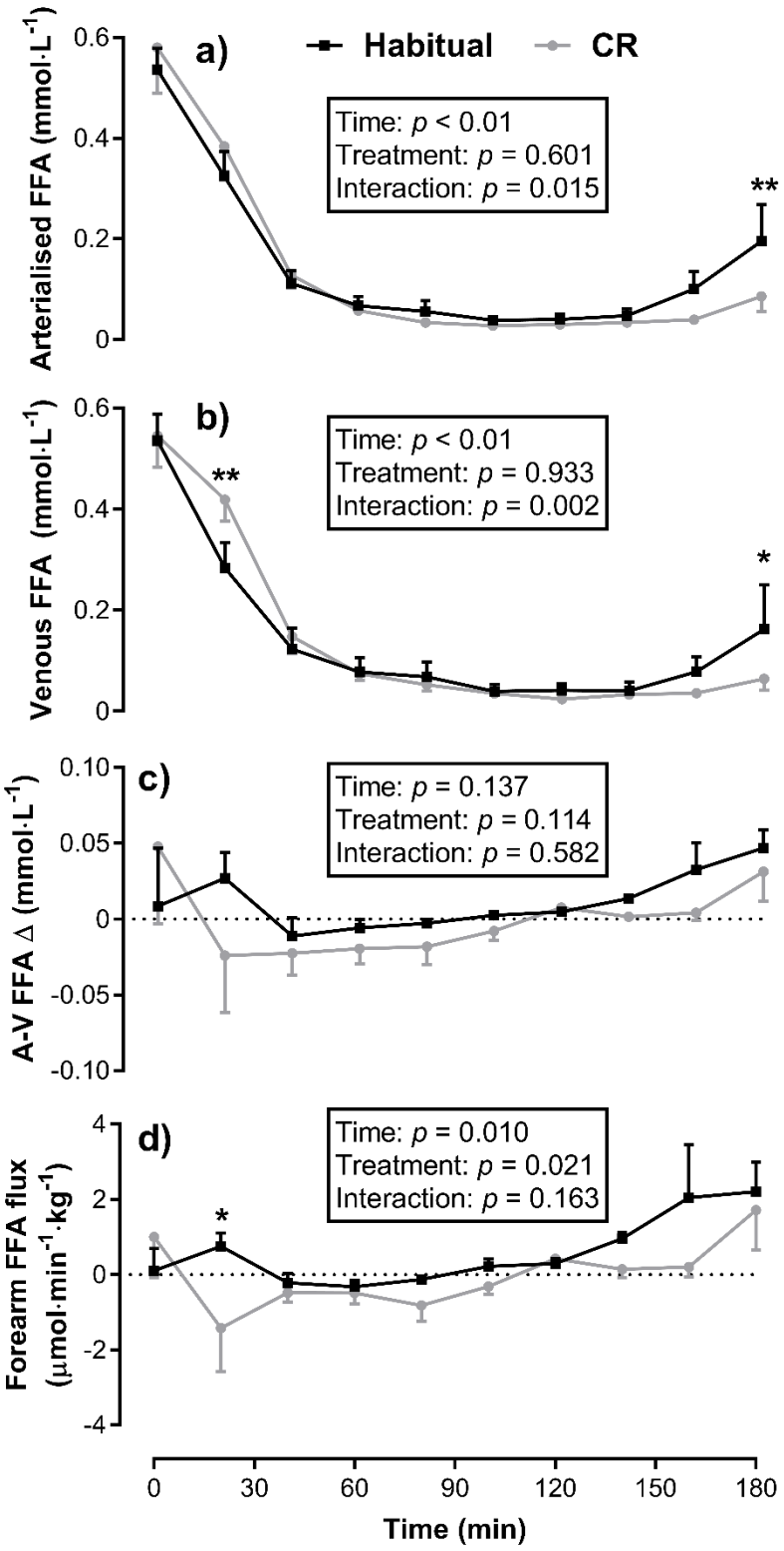


Figure 6.7. Plasma free-fatty acids.

(a) Arterialised, (b) venous, (c) A-V differences in FFA and (d) forearm FFA uptake in response to a liquid test meal in the habitual and caloric restriction trial. Data are displayed as mean ± SEM; n=8 for arterialised FFA and n=6 for all other graphs. *$p \leq 0.05$, **$p < 0.01$.

6.3.7 Serum Triglycerides (TAG)

Fasting arterialised serum TAG concentrations were around 0.7 mmol·L^{-1} in both trials and the pattern of postprandial responses were very similar between trials (Figure 6.8). Overall, TAG concentrations steadily declined from 40 min onwards and reached around 0.55 mmol·L^{-1} by the end of each trial.

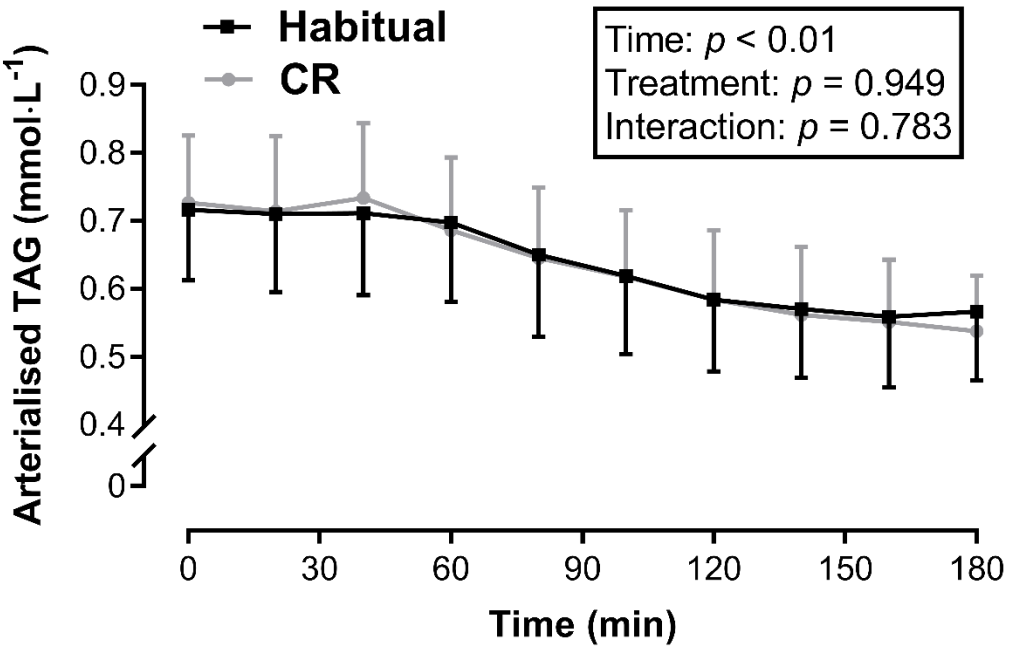


Figure 6.8. Arterialised serum triglycerides.
Arterialised triglyceride (TAG) concentrations in response to a liquid test meal in the habitual and caloric restriction trial. Data is displayed as mean ± SEM; n=8.

6.3.8 Plasma Branched Chain Amino Acids

Arterialised plasma concentrations of BCAA increased by around 50% from fasted values in the initial 20 min after drink consumption (Figure 6.9a) and remained elevated throughout both trials. There was a tendency for lower fasted venous BCAA concentrations in the habitual trial (p = 0.052), whilst a similar postprandial pattern of response to arterialised blood emerged (Figure 6.9b). There was a treatment effect for A-V differences (F=8.169; p = 0.036), in all but one timepoint (60 min) there were

greater A-V differences in the habitual trial (Figure 6.9c). There was a tendency (time effect $p = 0.077$) for the net flux of BCAA across the forearm to move from negative to positive throughout the postprandial period (Figure 6.9d). There was also a tendency for increased uptake of BCAA into the forearm in the habitual trial when compared to CR ($F=6.527$; $p = 0.051$).

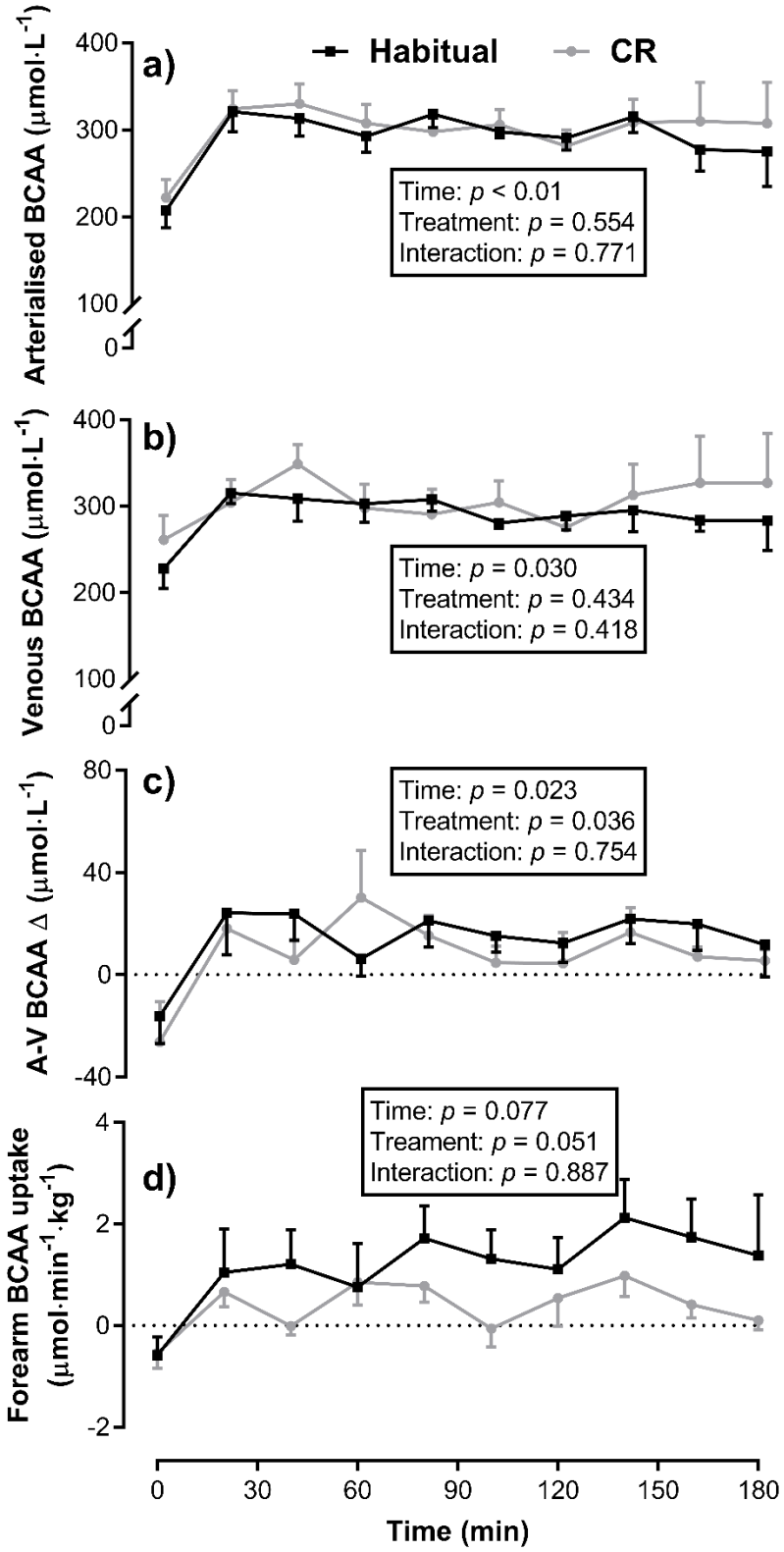


Figure 6.9. Plasma branched chain amino acids.

(a) Arterialised, (b) venous, (c) A-V differences and (d) net forearm uptake of branched chain amino acids (BCAA) in response to the liquid test meal. Data are displayed as mean ± SEM; n=8 for arterialised BCAA and n=6 for all others.

6.3.9 Resting Metabolic Rate and Substrate Oxidation

Resting metabolic rate did not change between the habitual and CR trial [habitual 1937 (259) vs CR 1857 (198) kCal·day^{-1}] or when expressed relative to total lean body mass [habitual 33.3 (3.3) vs CR 33.0 (5.3) kCal·day^{-1}·kg^{-1}; n=7]. Similarly, there were no differences in RER or rates of substrate oxidation when assessed at the same timepoint in each trial, as shown below in Table 6.6. The RER (F=10.12; p = 0.002) and rates of CHO oxidation (F=11.41; p = 0.001) increased to a similar extent throughout the postprandial period in both trials. On the other hand, rates of fat oxidation were supressed after consumption of the liquid test meal (F=6.27; p = 0.011). There were no treatment or interaction effects in any of these measures.

Table 6.6. Indirect calorimetry measurements.
Respiratory exchange ratio (RER) and rates of substrate oxidation as assessed by indirect calorimetry in response to consumption of a liquid test meal in the habitual and caloric restriction (CR) trial.

	Habitual			**CR**		
Measure	Fasted	1 h post	2 h 15 min post	Fasted	1 h post	2 h 15 min post
RER	0.75 (0.07)	0.83 (0.09)	0.88 (0.07)	0.76 (0.04)	0.86 (0.08)	0.88 (0.03)
CHO oxidation (g·min^{-1})	0.11 (0.09)	0.19 (0.11)	0.23 (0.08)	0.06 (0.04)	0.17 (0.10)	0.22 (0.04)
Fat oxidation (g·min^{-1})	0.12 (0.04)	0.09 (0.06)	0.06 (0.04)	0.10 (0.02)	0.06 (0.04)	0.06 (0.02)

Data are presented as mean (SD); n=8.

6.4 Discussion

The principle findings from this study were that two weeks of CR, without altering temporal distribution of EI, did not lead to any improvements in whole-body insulin sensitivity or skeletal muscle glucose uptake. Similarly, there were no increases in net forearm BCAA uptake after CR.

As expected, there was a significant reduction in body mass after two weeks of CR. Considering there were no detectable changes in PA, this can be attributed to the energy deficit induced by CR. The extent of weight loss was comparable to that observed during TRF [1.24 (1.00) vs 1.04 (0.71) kg]. In the current study, participants maintained their habitual temporal distribution of daily EI at ~11 h 30 min across the habitual and CR period, which is supported by the similarity in diurnal glycaemic profiles (Figure 6.3). The daily EI window reported during CR was around 5 h longer than reported during TRF in Chapter 5. Therefore, it appears reasonable to assert that the metabolic effects elicited by each study will predominantly reflect the differences in the temporal distribution of EI. Although only within-group comparisons were made and the two studies were not directly compared.

The composition of weight loss was indistinguishable between the two eating patterns. Previous research has associated TRF with increased fat loss (Antoni et al., 2018; Gabel et al., 2018). However, these studies were longer-term (≥ 10 weeks) and undertaken on overweight/obese adults. In lean adults, eight weeks of combined resistance training and TRF elicited more fat loss than a matched control diet (Moro et al., 2016). Overall, it appears likely that two weeks of TRF is insufficient to discern any diet-mediated changes in body composition. Therefore, whether the increase in

BCAA uptake post-TRF would manifest in improved retention of lean body mass during weight loss remains an interesting area for further exploration.

In accordance with TRF, this study found no changes in fasting insulin, glucose or HOMA-IR. However, higher arterialised and venous glucose concentrations were evident between 30 to 80 min postprandial in the CR trial. The reasons for this are unclear, since circulating insulin levels were similar between trials. Ultimately, these differences resulted in similar A-V glucose differences. Unlike TRF, CR was not associated with any improvements in insulin sensitivity derived from; skeletal muscle glucose uptake, M-ISI or the insulinaemic response to the liquid test meal. This was not an unexpected finding since the extent of weight loss was moderate and participants were not IR. Indeed, comparisons with the literature is problematic as most weight loss studies impose a more severe CR, over a longer duration (Ravussin et al., 2015; Kraus et al., 2019) and/or apply them on individuals who were overweight/obese (Heymsfield et al., 2000; Larson-Meyer et al., 2006).

In this study, there was a decreased net uptake of FFAs and a tendency ($p = 0.051$) for reduced BCAA uptake into the forearm in the CR trial. Whereas opposing directions of responses were shown in the TRF trial. These relatively lower fluxes (vs. glucose uptake) may be more sensitive to smaller changes in metabolism. For instance, in comparison to the habitual trial, insulin concentrations were numerically higher in the CR trial and statistically lower in the TRF trial, which could have influenced the net flux of BCAA/FFAs into the forearm.

Consumption of the liquid test meal rapidly supressed lipolysis, as indicated by marked reductions in arterialised and venous FFA concentrations in both trials. As a result, no tangible net FFA uptake was demonstrated until ≥ 120 min, which the

differences between the two trials are primarily attributed to. Forearm BCAA flux tended to shift from net release to uptake after consumption of the CHO and protein drink in both trials. However, the net change in BCAA uptake after CR was significantly lower than after TRF, again implicating the change in temporal distribution of EI as responsible. Future research should be undertaken to replicate these findings and assess the physiological relevance if so, for instance by using stable isotope tracers to assess MPS response.

This study found no changes in RMR or rates of substrate oxidation at the same timepoint between each trial. Indeed, absolute values were very similar to those reported in the TRF trial. In which, consumption of the CHO and protein drink increased the RER and rates of CHO oxidation, whilst supressing fat oxidation rates from fasting values. This indicates that neither two weeks of CR or TRF alter the pattern of whole-body fuel oxidation at rest or postprandially.

Direct statistical comparisons between were not made between CR and eTRF as participants were not randomised and moreover, one individual participated in both arms of the study. Randomisation was not undertaken as we sought to establish and closely match the weight loss that occurred across two weeks of eTRF under free-living conditions in a subsequent group.

This study did not address the feasibility of CR or directly compare this with eTRF, although this would be more appropriate in an RCT. Reported adherence to both eating patterns was high, which may simply reflect the short-term nature of each intervention. Future studies could seek to analyse more subjective feelings of appetite/hunger experienced by participants during each eating pattern. Although precise eating times would likely have to be prescribed or supervised for any meaningful comparison(s) to

be made. In addition, it would be interesting to combine this approach with measurements of appetite hormones to see if the metabolic adaptations differ in response to each eating pattern. Anecdotally, most participants in the TRF study reported the first 2 to 3 days as most challenging, which could relate to the hormonal entrainment of appetite hormones to feeding patterns (Solomon et al., 2008).

In summary, daily CR elicited a very similar weight loss to TRF and in both instances, PA was unchanged. The primary difference between these trials was the temporal distribution of EI, which was unchanged in this study but reduced by ~5.5 h during the TRF study. Unlike TRF, daily CR was not associated with any improvements in skeletal muscle and whole-body insulin sensitivity or forearm BCAA uptake. This suggests that the metabolic benefits of eTRF, described in Chapter 5, are independent of its effects on energy balance and weight loss.

Chapter 7. General Discussion

7.1 Overview of Findings

The general aim of this thesis was to explore interactions between insulin and anabolic resistance in human skeletal muscle using nutritional approaches that alter substrate availability. The effect of exogenous provision of SFA were examined *in vivo* (Chapter 3) and in a physiologically relevant model of skeletal muscle (Chapter 4). Contrary to our hypotheses, prior ingestion of an oral lipid load (~65% SFA) did not impair any index of insulin sensitivity and enhanced the subsequent incorporation of dietary [1-^{13}C] phenylalanine into the myofibrillar pool. On the other hand, pre-treatment of myotubes with 0.25 mM palmitate attenuated insulin-stimulated glucose uptake, inhibited system A transport of AA and tended to downregulate MPS. This suggests that, in the absence of IR, elevated lipid availability does not impair the anabolic response to AA.

The metabolic effects of eTRF, a novel approach combining extended daily fasting periods with shifting EI to earlier within the day, were examined in Chapter 5. Two weeks of eTRF improved skeletal muscle and whole-body insulin sensitivity in healthy males. This enhancement in insulin sensitivity was associated with a positive protein balance across skeletal muscle (as indicated by increased net uptake of BCAA) in response to oral protein ingestion. However, eTRF was associated with an involuntary reduction in free-living EI, which in the absence of compensatory changes in PA, induced a negative energy balance and was associated with a modest (~1 kg) but significant weight loss. To address this, the response of a control group (matched for age, BMI and PA) to a prescribed CR diet was examined. Despite losing a

comparable amount of weight, the metabolic effects of eTRF were not replicated by CR, suggesting that the benefits of eTRF are, at least in part, independent of its effect on energy balance and weight loss.

7.2 Interactions between Insulin and Anabolic Resistance

Lipotoxicity is implicated in the pathophysiology of IR, with lipid overflow leading to an accumulation of lipid-derived intermediates into ectopic tissue(s), including skeletal muscle (Section 1.4.3/1.4.4). Elevated adiposity and/or circulating FFA in overweight/obese individuals is likely involved in their increased susceptibility to IR and may underlie their blunted MPS response to protein ingestion (Beals et al., 2016). Elevating fatty acid availability experimentally via an intravenous lipid and heparin infusion consistently induces IR of CHO metabolism (Boden et al., 1994; Tsintzas et al., 2007) and has been shown to attenuate the subsequent incorporation of dietary AA into the muscle (Stephens et al., 2015).

Exogenous provision of SFA enhanced the subsequent incorporation of dietary [1- ^{13}C] phenylalanine into the myofibrillar pool in overweight/obese males but was associated with downregulated AA transport and MPS in primary human myotubes. The discrepancies between the *in vivo* (Chapter 3) and *in vitro* (Chapter 4) findings and those observed in previous research, likely reflect the different experimental models and study designs used. Oral ingestion of a lipid-rich drink induces IR in young and healthy participants (Nowotny et al., 2013) but did not in Chapter 3. Pilot data from our laboratory has shown the same experimental protocol used in Chapter 3 induces whole-body IR in healthy, young participants. Taken together, this supports

previous work suggesting obese individuals may be less susceptible to lipid-induced IR (Manco et al., 2004). Possibly due to this population already showing a degree of resistance to the effects of insulin, supported by the elevated HOMA-IR in Chapter 3.

Lipid-induced anabolic resistance has been associated with supressed 4E-BP1 signalling (Stephens et al., 2015; Smiles et al., 2019). Since insulin is a key mediator of mTORC1 signalling, one possibility is that a loss of insulin sensitivity may be necessary to observe anabolic resistance. Our findings in Chapter 4 suggest an inhibitory role of fatty acids on AA transporter function, independent of 4E-BP1, in our cell model. In Chapter 3, participants ingested the SFA drink 4 h prior to the CHO and protein drink. As a result, it is possible that lipid availability was not raised up to (Smiles et al., 2019) or maintained at (Stephens et al., 2015) high enough levels (vs. lipid infusions) to disrupt postprandial AA handling and/or impair anabolic signalling.

In Chapter 4, pre-treatment of myotubes with palmitate was used as an acute model of IR and shown to directly impair AA transport function. Although this has not been measured under similar conditions *in vivo*, this may have played a role in the attenuated MPS response after a lipid infusion (Stephens et al., 2015). One potential unifying mechanism is the accumulation of lipid-derived intermediates. Ceramide (formed from palmitate) has been shown to impair system A transport of AA *in vitro* (Hyde et al., 2005), although this study failed to replicate inhibitory effects on mTORC1 signalling. It has been suggested that transport between the blood and interstitial fluid is the rate-limiting step in the accumulation of intracellular AA (Miller et al., 2004). However, it is unclear whether this would persist under conditions of lipid-induced IR *in vivo*, where AA transporter function may be directly inhibited by fatty acids and less sensitive to insulin/AA-stimulated translocation.

Overall, our results suggest that dietary lipid overload, in the absence of IR, is not detrimental to the anabolic effects of AA ingestion. This could explain why, providing that protein consumption is adequate, individuals typically gain both body fat and lean mass during chronic overfeeding studies (Bray et al., 2015).

7.3 Applications of Time-Restricted Feeding

Consistent with previous research imposing restrictions on the length of the daily EI window in a free-living setting (LeCheminant et al., 2013; Tinsley et al., 2017; Gabel et al., 2018; Antoni et al., 2018), eTRF elicited an involuntary reduction in EI. Thus, in order to explore the metabolic effects of changing the temporal distribution of EI, a control (CR) group appears to be a prerequisite.

Remarkably, despite lower postprandial insulin levels in the eTRF trial, forearm (skeletal muscle) glucose and BCAA uptake were increased. Skeletal muscle plays an important role in the disposal of an oral glucose load (Kelley et al., 1988). Our results show for the first time that skeletal muscle contributes to improvements in whole-body insulin sensitivity after eTRF. As brachial artery blood flow (delivery) was numerically lower in the eTRF trial, these effects were entirely attributable to increased extraction, which implicates enhanced activation of respective glucose (i.e. GLUT4) and BCAA (i.e. SLC3) transporters.

Chapter 5 combined functional metabolic measurements i.e. PDC activity and glycogen content, with more exploratory outcomes i.e. mRNA expression, to investigate potential mechanisms behind the increase in glucose uptake and its metabolic fate. Taken together, our analysis is more suggestive of an increase in oxidative glucose disposal. This was supported by the absence of any changes in

muscle glycogen and numerically greater feeding-induced activation of PDC in the eTRF trial. As well as the reduced expression of FOXO1 and PDK2 genes after feeding, which are both negative regulators of PDC. However, it must be acknowledged that this was not reflected in augmented rates of whole-body postprandial CHO oxidation.

Irrespective of the underlying mechanism, an enhancement in insulin sensitivity is beneficial, since it provides a good index of metabolic health and is an independent predictor of future cardiovascular disease even in healthy individuals (Yip et al., 1998; Facchini et al., 2010). It was notable that within this healthy cohort, participants with lower M-ISI (whole-body insulin sensitivity) at baseline were more likely to improve this after TRF, than those with higher M-ISI. However, this could also reflect regression to the mean; the tendency for baseline measurements of a given variable at extreme ends of a distribution to be closer to the mean in a follow-up measurement (Thomas et al., 2019). Nevertheless, it appears reasonable to hypothesise that individuals at an increased susceptibility to developing metabolic disease(s) may benefit most and recent work has shown a beneficial effect of adopting TRF in adults with obesity (Hutchison et al., 2019). Our results suggest that eTRF would lead to a natural reduction in EI and moreover, augment the insulin sensitising effect of the weight loss accompanying this.

eTRF has been shown to enhance insulin sensitivity in individuals with pre-diabetes (Sutton et al., 2018) but the effects on individuals with T2D have not yet been examined. A more cautious approach to IF is recommended in this population due to concerns over hypoglycaemia. Nevertheless, TRF may be a more suitable approach than more restrictive forms of IF, such as alternate day fasting. It also has potential

applications as an alternative to CR. For instance, as a dietary strategy to promote a more sustainable maintenance of weight loss during the stepped return to normal eating of T2D patients in remission following substantial weight loss (Taylor et al., 2008; Steven et al., 2016). Clearly, TRF and other forms of IF should not be recommended to specific populations including; young children, those with eating disorders, pregnant women or the frail elderly.

7.4 Strengths and Limitations

The strengths of Chapter 3 are the use of a more 'real-life' model of oral fat ingestion, as opposed to intravenous infusion. Which, along with the use of intrinsically labelled [1-^{13}C] phenylalanine milk protein (vs free AA), better account for potential effects on digestion and absorption kinetics. The main limitation is the lack of an isocaloric control for the SFA drink; hence the effect on dietary [1-^{13}C] phenylalanine incorporation are potentially confounded by differences in acute energy balance between trials.

Human primary cultures used in Chapter 4 better represent *in vivo* biological variability (vs cell lines) and retention of the donor phenotype was maximised. However, this restricted sample size and the number of replicates for some experiments. Furthermore, any *in vitro* model will not fully represent the complex processes and metabolic milieu of skeletal muscle *in vivo*. Fatty acid treatment(s) were also undertaken at more physiological concentrations than typically reported. Although it was demonstrated that the effects of fatty acids on system A transport of AA were not specific to palmitate, only palmitate was used to examine the effects on MPS and signalling pathways. This is not representative of the mixture of fatty acids and other circulating metabolites encountered *in vivo*.

The primary strength of Chapters 5 and 6 was the similarity of weight-loss elicited by each pattern of eating in a free-living setting in two closely matched groups, using a diet matched for macronutrient composition. This was imperative in order to make valid comparisons between the metabolic effects of each dietary approach. By utilising the A-V forearm balance model, we highlight skeletal muscle as an important tissue modulating the metabolic effects of eTRF. Other strengths of these Chapters include the use of an individually calibrated, combined HR and accelerometer to objectively quantify free-living PA. Furthermore, CGM provided an insight into the effects of changing temporal eating patterns on glycaemic control, as well as providing a key verification of adherence throughout eTRF.

The main limitation of Chapters 5 and 6 was the lack of direct comparisons made between the two interventions. We did not deem it appropriate to directly compare these as the CR study was undertaken after the eTRF study and hence participants were not randomised to either intervention. Whilst this approach allowed us to quantify the weight loss of eTRF under free-living conditions and match this in the subsequent CR group, it also inflated the risk of a type I error in our analyses.

Both interventions were relatively short-term (two weeks), hence we have little information on the long-term feasibility of TRF (vs CR). Moreover, these Chapters only examined the response of a healthy group of young males, thus findings to other populations cannot be extrapolated. Finally, as in all free-living studies imposing restrictions on the length of daily eating windows, it is possible some effects were mediated by subtle changes in lifestyle behaviours. We did not detect any changes in PA but this may have been influenced by instructing participants to maintain habitual

PA levels throughout the study. Other factors such as changes in quality of dietary intake and/or regularity of sleep-wake cycles may have been susceptible to change.

7.5 Future Research Directions

There are several promising avenues to explore the interactions between insulin and anabolic resistance. Firstly, Chapter 3 could be repeated using an isocaloric Control (vs Lipid) drink, to assess if the effects are independent of changes in acute energy balance. Next, it would be interesting to study the effects of a younger, healthier and more insulin-sensitive population. Pilot data from our laboratory and other data (Nowotny et al., 2013) suggest they may be more prone to IR after ingestion of a lipid drink, which could affect the subsequent incorporation of AA into the muscle. Finally, there is some evidence suggesting that females are less susceptible to lipid-induced IR (Frias et al., 2001; Høeg et al., 2011), although this has been contested (Cusi, 2011). Considering this, it would be interesting to clarify these gender differences and examine their potential influence on anabolic resistance.

The associations between lipid-induced IR and the accumulation of lipid intermediates have been consistently demonstrated using *in vitro* cell models. Emerging lipidomic research has shown that the physiological role of these intermediates are likely specific to the isoform, chain-length and/or degree of saturation. Thus, the natural progression for cell culture experiments would be to explore the effects of blocking the synthesis of specific intermediates. A problem to resolve in this area is the compensatory mechanisms that may affect other enzyme pathways. For instance, chronic inhibition of serine palmitoyl transferase reduces ceramide content in rat skeletal muscle cells but increases the proportion of palmitate channelled into DAG (Watson et al., 2009).

TRF has potential applications as a simplistic dietary strategy to promote/maintain weight loss and enhance insulin sensitivity. However, larger scale research projects are necessary to examine its sustainability (vs CR) across longer periods of time. Whilst preliminary research suggests that eTRF may confer additional benefits, direct comparisons between different eating windows would be useful. This will help to inform practical strategies for the growing number of individuals choosing to self-experiment with IF/TRF.

There is a paucity of TRF studies including females. Given that the responses and sensitivity to fasting may differ between sexes, this is an area that requires further exploration. Incorporating more sensitive measurements of insulin sensitivity i.e. hyperinsulinaemic euglycaemic clamp, together with muscle/adipose tissue biopsies will hopefully begin to elucidate more of the mechanisms underlying the metabolic benefits of TRF. Finally, altering feeding patterns has been shown to affect intestinal microbiota composition in rodents independently of dietary composition (Zarrinpar et al., 2014). Emerging data suggest temporal distribution of EI and the length of the overnight fast exerts influences on the gut microbiome in humans (Kaczmarek et al., 2017). Therefore, the effects of TRF on the gut microbiome should be investigated.

7.6 Conclusion

Despite concerted efforts, global rates of obesity and its associated metabolic disorders continue to rise. This thesis provides an insight into the effects of acutely manipulating lipid availability on skeletal muscle metabolism. It reinforces the complexity of this relationship, which is highly affected by the choice of experimental model and study design. We demonstrate that two weeks of eTRF promotes enhanced insulin sensitivity, and glucose and BCAA uptake into skeletal muscle, independent

of weight loss. This may be partly attributed to the effects of prolonged daily fasting on lipid metabolism dynamics, but also contributes to increasing evidence supporting the concept of chrononutrition. eTRF appears to be a viable, alternative dietary strategy to calorie counting and exerts beneficial metabolic effects independently of weight loss. Such an accessible approach warrants further exploration in larger-scale research projects for its potential application to combat some of the deleterious health effects of the modern Western lifestyle.

References

Abdul-Ghani, M. A., Tripathy, D., & DeFronzo, R. A. (2006). Contributions of beta-cell dysfunction and insulin resistance to the pathogenesis of impaired glucose tolerance and impaired fasting glucose. *Diabetes Care, 29*(5), 1130-1139.

Abumrad, N. N., Rabin, D., Diamond, M. P., & Lacy, W. W. (1981). Use of a heated superficial hand vein as an alternative site for the measurement of amino acid concentrations and for the study of glucose and alanine kinetics in man. *Metabolism, 30*(9), 936-940.

Acheson, K. J., B. Zahorska-Markiewicz, P. Pittet, K. Anantharaman, and E. Jéquier, 1980, Caffeine and coffee: their influence on metabolic rate and substrate utilization in normal weight and obese individuals: Am J Clin Nutr, v. 33, p. 989-97.

Acheson, K. J., Schutz, Y., Bessard, T., Anantharaman, K., Flatt, J. P., & Jéquier, E. (1988). Glycogen storage capacity and de novo lipogenesis during massive carbohydrate overfeeding in man. *Am J Clin Nutr, 48*(2), 240-247.

Adams, C. M. (2007). Role of the transcription factor ATF4 in the anabolic actions of insulin and the anti-anabolic actions of glucocorticoids. *J Biol Chem, 282*(23), 16744-16753.

Adams, J. M., Pratipanawatr, T., Berria, R., Wang, E., DeFronzo, R. A., Sullards, M. C., et al. (2004). Ceramide content is increased in skeletal muscle from obese insulin-resistant humans. *Diabetes, 53*(1), 25-31.

Adlouni, A., Ghalim, N., Benslimane, A., Lecerf, J. M., & Saile, R. (1997). Fasting during Ramadan induces a marked increase in high-density lipoprotein cholesterol and decrease in low-density lipoprotein cholesterol. *Ann Nutr Metab, 41*(4), 242-249.

Ahlstrom, P., Rai, E., Chakma, S., Cho, H. H., Rengasamy, P., & Sweeney, G. (2017). Adiponectin improves insulin sensitivity via activation of autophagic flux. *J Mol Endocrinol, 59*(4), 339-350.

Al-Khalili, L., Chibalin, A. V., Kannisto, K., Zhang, B. B., Permert, J., Holman, G. D., et al. (2003). Insulin action in cultured human skeletal muscle cells during differentiation: assessment of cell surface GLUT4 and GLUT1 content. *Cell Mol Life Sci, 60*(5), 991-998.

Amati, F., Dubé, J. J., Alvarez-Carnero, E., Edreira, M. M., Chomentowski, P., Coen, P. M., et al. (2011). Skeletal muscle triglycerides, diacylglycerols, and ceramides in insulin resistance: another paradox in endurance-trained athletes? *Diabetes, 60*(10), 2588-2597.

Andersson, A., Nälsén, C., Tengblad, S., & Vessby, B. (2002). Fatty acid composition of skeletal muscle reflects dietary fat composition in humans. *Am J Clin Nutr, 76*(6), 1222-1229.

Anthony, J. C., Anthony, T. G., Kimball, S. R., & Jefferson, L. S. (2001). Signaling pathways involved in translational control of protein synthesis in skeletal muscle by leucine. *J Nutr, 131*(3), 856S-860S.

Anton, S. D., Moehl, K., Donahoo, W. T., Marosi, K., Lee, S. A., Mainous, A. G., et al. (2018). Flipping the Metabolic Switch: Understanding and Applying the Health Benefits of Fasting. *Obesity (Silver Spring), 26*(2), 254-268.

Antoni, R., Johnston, K. L., Collins, A. L., & Robertson, M. D. (2018). Intermittent v. continuous energy restriction: differential effects on postprandial glucose and lipid metabolism following matched weight loss in overweight/obese participants. *Br J Nutr, 119*(5), 507-516.

Antoni, R., Robertson, T. M., Robertson, M. D., & Johnston, J. D. (2018). A pilot feasibility study exploring the effects of a moderate time-restricted feeding intervention on energy intake, adiposity and metabolic physiology in free-living human subjects. *Journal of Nutritional Science, 7*, e22.

Aparicio, N. J., Puchulu, F. E., Gagliardino, J. J., Ruiz, M., Llorens, J. M., Ruiz, J., et al. (1974). Circadian variation of the blood glucose, plasma insulin and human growth hormone levels in response to an oral glucose load in normal subjects. *Diabetes, 23*(2), 132-137.

Arble, D. M., Bass, J., Laposky, A. D., Vitaterna, M. H., & Turek, F. W. (2009). Circadian timing of food intake contributes to weight gain. *Obesity (Silver Spring), 17*(11), 2100-2102.

Arciero, P. J., Ormsbee, M. J., Gentile, C. L., Nindl, B. C., Brestoff, J. R., & Ruby, M. (2013). Increased protein intake and meal frequency reduces abdominal fat during energy balance and energy deficit. *Obesity (Silver Spring), 21*(7), 1357-1366.

Arner, P., & Rydén, M. (2015). Fatty Acids, Obesity and Insulin Resistance. *Obes Facts, 8*(2), 147-155.

Assah, F. K., Ekelund, U., Brage, S., Wright, A., Mbanya, J. C., & Wareham, N. J. (2011). Accuracy and validity of a combined heart rate and motion sensor for the measurement of free-living physical activity energy expenditure in adults in Cameroon. *Int J Epidemiol, 40*(1), 112-120.

Ausk, K. J., Boyko, E. J., & Ioannou, G. N. (2010). Insulin resistance predicts mortality in nondiabetic individuals in the U.S. *Diabetes Care, 33*(6), 1179-1185.

Baba, H., Zhang, X. J., & Wolfe, R. R. (1995). Glycerol gluconeogenesis in fasting humans. *Nutrition, 11*(2), 149-153.

Bachmann, O. P., Dahl, D. B., Brechtel, K., Machann, J., Haap, M., Maier, T., et al. (2001). Effects of intravenous and dietary lipid challenge on intramyocellular lipid content and the relation with insulin sensitivity in humans. *Diabetes, 50*(11), 2579-2584.

BaHammam, A., Alrajeh, M., Albabtain, M., Bahammam, S., & Sharif, M. (2010). Circadian pattern of sleep, energy expenditure, and body temperature of young healthy men during the intermittent fasting of Ramadan. *Appetite, 54*(2), 426-429.

Bahammam, A. S., Alaseem, A. M., Alzakri, A. A., & Sharif, M. M. (2013). The effects of Ramadan fasting on sleep patterns and daytime sleepiness: An objective assessment. *J Res Med Sci, 18*(2), 127-131.

Baharians, Z., & Schönthal, A. H. (1998). Autoregulation of protein phosphatase type 2A expression. *J Biol Chem, 273*(30), 19019-19024.

Bahijri, S., Borai, A., Ajabnoor, G., Abdul Khaliq, A., AlQassas, I., Al-Shehri, D., et al. (2013). Relative metabolic stability, but disrupted circadian cortisol secretion during the fasting month of Ramadan. *PLoS One, 8*(4), e60917.

Bailey, T., Bode, B. W., Christiansen, M. P., Klaff, L. J., & Alva, S. (2015). The Performance and Usability of a Factory-Calibrated Flash Glucose Monitoring System. *Diabetes Technol Ther, 17*(11), 787-794.

Baird, F. E., Bett, K. J., MacLean, C., Tee, A. R., Hundal, H. S., & Taylor, P. M. (2009). Tertiary active transport of amino acids reconstituted by coexpression of System A and L transporters in Xenopus oocytes. *Am J Physiol Endocrinol Metab, 297*(3), E822-829.

Bajaj, M., Suraamornkul, S., Romanelli, A., Cline, G. W., Mandarino, L. J., Shulman, G. I., et al. (2005). Effect of a sustained reduction in plasma free fatty acid concentration on intramuscular long-chain fatty Acyl-CoAs and insulin action in type 2 diabetic patients. *Diabetes, 54*(11), 3148-3153.

Bandín, C., Scheer, F. A., Luque, A. J., Ávila-Gandía, V., Zamora, S., Madrid, J. A., et al. (2015). Meal timing affects glucose tolerance, substrate oxidation and circadian-related variables: A randomized, crossover trial. *Int J Obes (Lond), 39*(5), 828-833.

Bandyopadhyay, G. K., Yu, J. G., Ofrecio, J., & Olefsky, J. M. (2006). Increased malonyl-CoA levels in muscle from obese and type 2 diabetic subjects lead to decreased fatty acid oxidation and increased lipogenesis; thiazolidinedione treatment reverses these defects. *Diabetes, 55*(8), 2277-2285.

Bassett, D. R. (2012). Device-based monitoring in physical activity and public health research. *Physiol Meas, 33*(11), 1769-1783.

Bastie, C. C., Nahlé, Z., McLoughlin, T., Esser, K., Zhang, W., Unterman, T., et al. (2005). FoxO1 stimulates fatty acid uptake and oxidation in muscle cells through CD36-dependent and -independent mechanisms. *J Biol Chem, 280*(14), 14222-14229.

Beals, J. W., Sukiennik, R. A., Nallabelli, J., Emmons, R. S., van Vliet, S., Young, J. R., et al. (2016). Anabolic sensitivity of postprandial muscle protein synthesis to the ingestion of a protein-dense food is reduced in overweight and obese young adults. *Am J Clin Nutr, 104*(4), 1014-1022.

Beckett, P. R., Hardin, D. S., Davis, T. A., Nguyen, H. V., Wray-Cahen, D., & Copeland, K. C. (1996). Spectrophometric assay for measuring branched-chain amino acid concentrations: application for measuring the sensitivity of protein metabolism to insulin. *Anal Biochem, 240*(1), 48-53.

Bentzinger, C. F., Romanino, K., Cloëtta, D., Lin, S., Mascarenhas, J. B., Oliveri, F., et al. (2008). Skeletal muscle-specific ablation of raptor, but not of rictor, causes metabolic changes and results in muscle dystrophy. *Cell Metab, 8*(5), 411-424.

Bergström, J., and E. Hultman, 1966, Muscle glycogen synthesis after exercise: an enhancing factor localized to the muscle cells in man: Nature, v. 210, p. 309-10.

Bergstrom, J. (1975). Percutaneous needle biopsy of skeletal muscle in physiological and clinical research. *Scand J Clin Lab Invest, 35*(7), 609-616.

Berntsen, S., Hageberg, R., Aandstad, A., Mowinckel, P., Anderssen, S. A., Carlsen, K. H., et al. (2010). Validity of physical activity monitors in adults participating in free-living activities. *Br J Sports Med, 44*(9), 657-664.

Besson, H., Brage, S., Jakes, R. W., Ekelund, U., & Wareham, N. J. (2010). Estimating physical activity energy expenditure, sedentary time, and physical activity intensity by self-report in adults. *Am J Clin Nutr, 91*(1), 106-114.

Betts, J. A., Richardson, J. D., Chowdhury, E. A., Holman, G. D., Tsintzas, K., & Thompson, D. (2014). The causal role of breakfast in energy balance and health: a randomized controlled trial in lean adults. *Am J Clin Nutr, 100*(2), 539-547.

Blaak, E. E. (2004). Basic disturbances in skeletal muscle fatty acid metabolism in obesity and type 2 diabetes mellitus. *Proc Nutr Soc, 63*(2), 323-330.

Blachnio-Zabielska, A., Baranowski, M., Zabielski, P., & Gorski, J. (2010). Effect of high fat diet enriched with unsaturated and diet rich in saturated fatty acids on

sphingolipid metabolism in rat skeletal muscle. *J Cell Physiol, 225*(3), 786-791.

Black, A. E., Goldberg, G. R., Jebb, S. A., Livingstone, M. B., Cole, T. J., & Prentice, A. M. (1991). Critical evaluation of energy intake data using fundamental principles of energy physiology: 2. Evaluating the results of published surveys. *Eur J Clin Nutr, 45*(12), 583-599.

Bland, J. M., and D. G. Altman, 2015, Best (but oft forgotten) practices: testing for treatment effects in randomized trials by separate analyses of changes from baseline in each group is a misleading approach: Am J Clin Nutr, v. 102, p. 991-4.

Blundell, J. E., Burley, V. J., Cotton, J. R., & Lawton, C. L. (1993). Dietary fat and the control of energy intake: evaluating the effects of fat on meal size and postmeal satiety. *Am J Clin Nutr, 57*(5 Suppl), 772S-777S; discussion 777S-778S.

Bo, S., Fadda, M., Castiglione, A., Ciccone, G., De Francesco, A., Fedele, D., et al. (2015). Is the timing of caloric intake associated with variation in diet-induced thermogenesis and in the metabolic pattern? A randomized cross-over study. *Int J Obes (Lond), 39*(12), 1689-1695.

Boden, G. (2001). Pathogenesis of type 2 diabetes. Insulin resistance. *Endocrinol Metab Clin North Am, 30*(4), 801-815, v.

Boden, G., Chen, X., Ruiz, J., White, J. V., & Rossetti, L. (1994). Mechanisms of fatty acid-induced inhibition of glucose uptake. *J Clin Invest, 93*(6), 2438-2446.

Boden, G., Homko, C., Mozzoli, M., Showe, L. C., Nichols, C., & Cheung, P. (2005). Thiazolidinediones upregulate fatty acid uptake and oxidation in adipose tissue of diabetic patients. *Diabetes, 54*(3), 880-885.

Bolster, D. R., Crozier, S. J., Kimball, S. R., & Jefferson, L. S. (2002). AMP-activated protein kinase suppresses protein synthesis in rat skeletal muscle through down-regulated mammalian target of rapamycin (mTOR) signaling. *J Biol Chem, 277*(27), 23977-23980.

Bonadonna, R. C., Saccomani, M. P., Cobelli, C., & DeFronzo, R. A. (1993). Effect of insulin on system A amino acid transport in human skeletal muscle. *J Clin Invest, 91*(2), 514-521.

Bond, P. (2016). Regulation of mTORC1 by growth factors, energy status, amino acids and mechanical stimuli at a glance. *J Int Soc Sports Nutr, 13*, 8.

Bonen, A., Campbell, S. E., Benton, C. R., Chabowski, A., Coort, S. L., Han, X. X., et al. (2004). Regulation of fatty acid transport by fatty acid translocase/CD36. *Proc Nutr Soc, 63*(2), 245-249.

Bonen, A., Luiken, J. J., Arumugam, Y., Glatz, J. F., & Tandon, N. N. (2000). Acute regulation of fatty acid uptake involves the cellular redistribution of fatty acid translocase. *J Biol Chem, 275*(19), 14501-14508.

Bonen, A., Han, X. X., Habets, D. D., Febbraio, M., Glatz, J. F., & Luiken, J. J. (2007). A null mutation in skeletal muscle FAT/CD36 reveals its essential role in insulin- and AICAR-stimulated fatty acid metabolism. *Am J Physiol Endocrinol Metab, 292*(6), E1740-1749.

Borkman, M., Storlien, L. H., Pan, D. A., Jenkins, A. B., Chisholm, D. J., & Campbell, L. V. (1993). The relation between insulin sensitivity and the fatty-acid composition of skeletal-muscle phospholipids. *N Engl J Med, 328*(4), 238-244.

Boushel, R., Gnaiger, E., Schjerling, P., Skovbro, M., Kraunsøe, R., & Dela, F. (2007). Patients with type 2 diabetes have normal mitochondrial function in skeletal muscle. *Diabetologia, 50*(4), 790-796.

Bowen, A. J., & Reeves, R. L. (1967). Diurnal variation in glucose tolerance. *Arch Intern Med, 119*(3), 261-264.

Bowker-Kinley, M. M., Davis, W. I., Wu, P., Harris, R. A., & Popov, K. M. (1998). Evidence for existence of tissue-specific regulation of the mammalian pyruvate dehydrogenase complex. *Biochem J, 329 (Pt 1)*, 191-196.

Bradley, U., Spence, M., Courtney, C. H., McKinley, M. C., Ennis, C. N., McCance, D. R., et al. (2009). Low-fat versus low-carbohydrate weight reduction diets: effects on weight loss, insulin resistance, and cardiovascular risk: a randomized control trial. *Diabetes, 58*(12), 2741-2748.

Brage, S., Brage, N., Franks, P. W., Ekelund, U., & Wareham, N. J. (2005). Reliability and validity of the combined heart rate and movement sensor Actiheart. *Eur J Clin Nutr, 59*(4), 561-570.

Brage, S., Ekelund, U., Brage, N., Hennings, M. A., Froberg, K., Franks, P. W., et al. (2007). Hierarchy of individual calibration levels for heart rate and accelerometry to measure physical activity. *J Appl Physiol (1985), 103*(2), 682-692.

Bray, G. A., & Popkin, B. M. (1998). Dietary fat intake does affect obesity! *Am J Clin Nutr, 68*(6), 1157-1173.

Bray, G. A., Redman, L. M., de Jonge, L., Covington, J., Rood, J., Brock, C., et al. (2015). Effect of protein overfeeding on energy expenditure measured in a metabolic chamber. *Am J Clin Nutr, 101*(3), 496-505.

Brechtel, K., Dahl, D. B., Machann, J., Bachmann, O. P., Wenzel, I., Maier, T., et al. (2001). Fast elevation of the intramyocellular lipid content in the presence of

circulating free fatty acids and hyperinsulinemia: a dynamic 1H-MRS study. *Magn Reson Med, 45*(2), 179-183.

Breen, L., Stokes, K. A., Churchward-Venne, T. A., Moore, D. R., Baker, S. K., Smith, K., et al. (2013). Two weeks of reduced activity decreases leg lean mass and induces "anabolic resistance" of myofibrillar protein synthesis in healthy elderly. *J Clin Endocrinol Metab, 98*(6), 2604-2612.

Brouns, F., Bjorck, I., Frayn, K. N., Gibbs, A. L., Lang, V., Slama, G., et al. (2005). Glycaemic index methodology. *Nutr Res Rev, 18*(1), 145-171.

Brownson, R. C., Boehmer, T. K., & Luke, D. A. (2005). Declining rates of physical activity in the United States: what are the contributors? *Annu Rev Public Health, 26*, 421-443.

Bryner, R. W., Woodworth-Hobbs, M. E., Williamson, D. L., & Alway, S. E. (2012). Docosahexaenoic Acid protects muscle cells from palmitate-induced atrophy. *ISRN Obes, 2012*, 647348.

Buettner, R., Parhofer, K. G., Woenckhaus, M., Wrede, C. E., Kunz-Schughart, L. A., Schölmerich, J., et al. (2006). Defining high-fat-diet rat models: metabolic and molecular effects of different fat types. *J Mol Endocrinol, 36*(3), 485-501.

Bujak, A. L., Crane, J. D., Lally, J. S., Ford, R. J., Kang, S. J., Rebalka, I. A., et al. (2015). AMPK activation of muscle autophagy prevents fasting-induced hypoglycemia and myopathy during aging. *Cell Metab, 21*(6), 883-890.

Burke, T. M., Markwald, R. R., McHill, A. W., Chinoy, E. D., Snider, J. A., Bessman, S. C., et al. (2015). Effects of caffeine on the human circadian clock in vivo and in vitro. *Sci Transl Med, 7*(305), 305ra146.

Byrne, M. M., Sturis, J., & Polonsky, K. S. (1995). Insulin secretion and clearance during low-dose graded glucose infusion. *Am J Physiol, 268*(1 Pt 1), E21-27.

Cahill, G. F. (2006). Fuel metabolism in starvation. *Annu Rev Nutr, 26*, 1-22.

Calbet, J. A., & MacLean, D. A. (1997). Role of caloric content on gastric emptying in humans. *J Physiol, 498 (Pt 2)*, 553-559.

Calle, E. E., Thun, M. J., Petrelli, J. M., Rodriguez, C., & Heath, C. W. (1999). Body-mass index and mortality in a prospective cohort of U.S. adults. *N Engl J Med, 341*(15), 1097-1105.

Canuto, R., da Silva Garcez, A., Kac, G., de Lira, P. I. C., & Olinto, M. T. A. (2017). Eating frequency and weight and body composition: a systematic review of observational studies. *Public Health Nutr, 20*(12), 2079-2095.

Carlson, O., Martin, B., Stote, K. S., Golden, E., Maudsley, S., Najjar, S. S., et al. (2007). Impact of reduced meal frequency without caloric restriction on glucose regulation in healthy, normal-weight middle-aged men and women. *Metabolism, 56*(12), 1729-1734.

Carter, S., Clifton, P. M., & Keogh, J. B. (2016). The effects of intermittent compared to continuous energy restriction on glycaemic control in type 2 diabetes; a pragmatic pilot trial. *Diabetes Res Clin Pract, 122*, 106-112.

Cazzolli, R., Carpenter, L., Biden, T. J., & Schmitz-Peiffer, C. (2001). A role for protein phosphatase 2A-like activity, but not atypical protein kinase Czeta, in the inhibition of protein kinase B/Akt and glycogen synthesis by palmitate. *Diabetes, 50*(10), 2210-2218.

Cha, B. S., Ciaraldi, T. P., Park, K. S., Carter, L., Mudaliar, S. R., & Henry, R. R. (2005). Impaired fatty acid metabolism in type 2 diabetic skeletal muscle cells is reversed by PPARgamma agonists. *Am J Physiol Endocrinol Metab, 289*(1), E151-159.

Chaix, A., Zarrinpar, A., Miu, P., & Panda, S. (2014). Time-restricted feeding is a preventative and therapeutic intervention against diverse nutritional challenges. *Cell Metab, 20*(6), 991-1005.

Chakravarthy, M. V., & Booth, F. W. (2004). Eating, exercise, and "thrifty" genotypes: connecting the dots toward an evolutionary understanding of modern chronic diseases. *J Appl Physiol (1985), 96*(1), 3-10.

Chan, J. M., Rimm, E. B., Colditz, G. A., Stampfer, M. J., & Willett, W. C. (1994). Obesity, fat distribution, and weight gain as risk factors for clinical diabetes in men. *Diabetes Care, 17*(9), 961-969.

Chavez, J. A., Knotts, T. A., Wang, L. P., Li, G., Dobrowsky, R. T., Florant, G. L., et al. (2003). A role for ceramide, but not diacylglycerol, in the antagonism of insulin signal transduction by saturated fatty acids. *J Biol Chem, 278*(12), 10297-10303.

Chen, C., Williams, P. F., Cooney, G. J., Caterson, I. D., & Turtle, J. R. (1992). The effects of fasting and refeeding on liver glycogen synthase and phosphorylase in obese and lean mice. *Horm Metab Res, 24*(4), 161-166.

Cherrington, A. D. (1999). Banting Lecture 1997. Control of glucose uptake and release by the liver in vivo. *Diabetes, 48*(5), 1198-1214.

Ching, J. K., Rajguru, P., Marupudi, N., Banerjee, S., & Fisher, J. S. (2010). A role for AMPK in increased insulin action after serum starvation. *Am J Physiol Cell Physiol, 299*(5), C1171-1179.

Chowdhury, E. A., Richardson, J. D., Holman, G. D., Tsintzas, K., Thompson, D., & Betts, J. A. (2016). The causal role of breakfast in energy balance and health: a randomized controlled trial in obese adults. *Am J Clin Nutr, 103*(3), 747-756.

Church, T. S., Thomas, D. M., Tudor-Locke, C., Katzmarzyk, P. T., Earnest, C. P., Rodarte, R. Q., et al. (2011). Trends over 5 decades in U.S. occupation-related physical activity and their associations with obesity. *PLoS One, 6*(5), e19657.

Clarke, S. D. (2000). Polyunsaturated fatty acid regulation of gene transcription: a mechanism to improve energy balance and insulin resistance. *Br J Nutr, 83 Suppl 1*, S59-66.

Coen, P. M., Dubé, J. J., Amati, F., Stefanovic-Racic, M., Ferrell, R. E., Toledo, F. G., et al. (2010). Insulin resistance is associated with higher intramyocellular triglycerides in type I but not type II myocytes concomitant with higher ceramide content. *Diabetes, 59*(1), 80-88.

Cokorinos, E. C., Delmore, J., Reyes, A. R., Albuquerque, B., Kjøbsted, R., Jørgensen, N. O., et al. (2017). Activation of Skeletal Muscle AMPK Promotes Glucose Disposal and Glucose Lowering in Non-human Primates and Mice. *Cell Metab, 25*(5), 1147-1159.e1110.

Coles, D. R., Cooper, K. E., Mottram, R. F., & Occleshaw, J. V. (1958). The source of blood samples withdrawn from deep forearm veins via catheters passed upstream from the median cubital vein. *J Physiol, 142*(2), 323-328.

Coll, T., Eyre, E., Rodríguez-Calvo, R., Palomer, X., Sánchez, R. M., Merlos, M., et al. (2008). Oleate reverses palmitate-induced insulin resistance and inflammation in skeletal muscle cells. *J Biol Chem, 283*(17), 11107-11116.

Colman, R. J., Anderson, R. M., Johnson, S. C., Kastman, E. K., Kosmatka, K. J., Beasley, T. M., et al. (2009). Caloric restriction delays disease onset and mortality in rhesus monkeys. *Science, 325*(5937), 201-204.

Cong, L. N., Chen, H., Li, Y., Zhou, L., McGibbon, M. A., Taylor, S. I., et al. (1997). Physiological role of Akt in insulin-stimulated translocation of GLUT4 in transfected rat adipose cells. *Mol Endocrinol, 11*(13), 1881-1890.

Constantin-Teodosiu, D., Cederblad, G., & Hultman, E. (1991). A sensitive radioisotopic assay of pyruvate dehydrogenase complex in human muscle tissue. *Anal Biochem, 198*(2), 347-351.

Cooper, K. E., Edholm, O. G., & Mottram, R. F. (1955). The blood flow in skin and muscle of the human forearm. *J Physiol, 128*(2), 258-267.

Cooperberg, B. A., & Cryer, P. E. (2010). Insulin reciprocally regulates glucagon secretion in humans. *Diabetes, 59*(11), 2936-2940.

Covington, J. D., Myland, C. K., Rustan, A. C., Ravussin, E., Smith, S. R., & Bajpeyi, S. (2015). Effect of serial cell passaging in the retention of fiber type and mitochondrial content in primary human myotubes. *Obesity (Silver Spring), 23*(12), 2414-2420.

Crispim, C. A., Zimberg, I. Z., dos Reis, B. G., Diniz, R. M., Tufik, S., & de Mello, M. T. (2011). Relationship between food intake and sleep pattern in healthy individuals. *J Clin Sleep Med, 7*(6), 659-664.

Cross, D. A., Alessi, D. R., Cohen, P., Andjelkovich, M., & Hemmings, B. A. (1995). Inhibition of glycogen synthase kinase-3 by insulin mediated by protein kinase B. *Nature, 378*(6559), 785-789.

Crouter, S. E., Churilla, J. R., & Bassett, D. R. (2008). Accuracy of the Actiheart for the assessment of energy expenditure in adults. *Eur J Clin Nutr, 62*(6), 704-711.

Cunningham, J. J. (1991). Body composition as a determinant of energy expenditure: a synthetic review and a proposed general prediction equation. *Am J Clin Nutr, 54*(6), 963-969.

Cusi, K. (2011). Comment on: Hoeg et al. Lipid-induced insulin resistance affects women less than men and is not accompanied by inflammation or impaired proximal insulin signaling. Diabetes 2011;60:64-73. *Diabetes, 60*(9), e23; author reply e24.

Daousi, C., Casson, I. F., Gill, G. V., MacFarlane, I. A., Wilding, J. P., & Pinkney, J. H. (2006). Prevalence of obesity in type 2 diabetes in secondary care: association with cardiovascular risk factors. *Postgrad Med J, 82*(966), 280-284.

De Larichaudy, J., Zufferli, A., Serra, F., Isidori, A. M., Naro, F., Dessalle, K., et al. (2012). TNF-α- and tumor-induced skeletal muscle atrophy involves sphingolipid metabolism. *Skelet Muscle, 2*(1), 2.

DeFronzo, R. A., Gunnarsson, R., Björkman, O., Olsson, M., & Wahren, J. (1985). Effects of insulin on peripheral and splanchnic glucose metabolism in noninsulin-dependent (type II) diabetes mellitus. *J Clin Invest, 76*(1), 149-155.

DeFronzo, R. A., & Matsuda, M. (2010). Reduced time points to calculate the composite index. *Diabetes Care, 33*(7), e93.

DeFronzo, R. A., Tobin, J. D., & Andres, R. (1979). Glucose clamp technique: a method for quantifying insulin secretion and resistance. *Am J Physiol, 237*(3), E214-223.

DeFronzo, R. A., & Tripathy, D. (2009). Skeletal muscle insulin resistance is the primary defect in type 2 diabetes. *Diabetes Care, 32 Suppl 2*, S157-163.

Delahaye, L. B., Bloomer, R. J., Butawan, M. B., Wyman, J. M., Hill, J. L., Lee, H. W., et al. (2018). Time-restricted feeding of a high-fat diet in male C57BL/6 mice reduces adiposity but does not protect against increased systemic inflammation. *Appl Physiol Nutr Metab, 43*(10), 1033-1042.

Demetrius, L. (2005). Of mice and men. When it comes to studying ageing and the means to slow it down, mice are not just small humans. *EMBO Rep, 6 Spec No*, S39-44.

Dickinson, J. M., Drummond, M. J., Coben, J. R., Volpi, E., & Rasmussen, B. B. (2013). Aging differentially affects human skeletal muscle amino acid transporter expression when essential amino acids are ingested after exercise. *Clin Nutr, 32*(2), 273-280.

Dickinson, J. M., Fry, C. S., Drummond, M. J., Gundermann, D. M., Walker, D. K., Glynn, E. L., et al. (2011). Mammalian target of rapamycin complex 1 activation is required for the stimulation of human skeletal muscle protein synthesis by essential amino acids. *J Nutr, 141*(5), 856-862.

Dimopoulos, N., Watson, M., Sakamoto, K., & Hundal, H. S. (2006). Differential effects of palmitate and palmitoleate on insulin action and glucose utilization in rat L6 skeletal muscle cells. *Biochem J, 399*(3), 473-481.

Dobrowsky, R. T., Kamibayashi, C., Mumby, M. C., & Hannun, Y. A. (1993). Ceramide activates heterotrimeric protein phosphatase 2A. *J Biol Chem, 268*(21), 15523-15530.

Dresner, A., Laurent, D., Marcucci, M., Griffin, M. E., Dufour, S., Cline, G. W., et al. (1999). Effects of free fatty acids on glucose transport and IRS-1-associated phosphatidylinositol 3-kinase activity. *J Clin Invest, 103*(2), 253-259.

Dreyer, H. C., Fujita, S., Cadenas, J. G., Chinkes, D. L., Volpi, E., & Rasmussen, B. B. (2006). Resistance exercise increases AMPK activity and reduces 4E-BP1 phosphorylation and protein synthesis in human skeletal muscle. *J Physiol, 576*(Pt 2), 613-624.

Drummond, M. J., Dickinson, J. M., Fry, C. S., Walker, D. K., Gundermann, D. M., Reidy, P. T., et al. (2012). Bed rest impairs skeletal muscle amino acid transporter expression, mTORC1 signaling, and protein synthesis in response to essential amino acids in older adults. *Am J Physiol Endocrinol Metab, 302*(9), E1113-1122.

Drummond, M. J., Fry, C. S., Glynn, E. L., Dreyer, H. C., Dhanani, S., Timmerman, K. L., et al. (2009). Rapamycin administration in humans blocks the contraction-induced increase in skeletal muscle protein synthesis. *J Physiol, 587*(Pt 7), 1535-1546.

Drummond, M. J., Glynn, E. L., Fry, C. S., Timmerman, K. L., Volpi, E., & Rasmussen, B. B. (2010). An increase in essential amino acid availability upregulates amino acid transporter expression in human skeletal muscle. *Am J Physiol Endocrinol Metab, 298*(5), E1011-1018.

Dubé, J. J., Amati, F., Stefanovic-Racic, M., Toledo, F. G., Sauers, S. E., & Goodpaster, B. H. (2008). Exercise-induced alterations in intramyocellular lipids and insulin resistance: the athlete's paradox revisited. *Am J Physiol Endocrinol Metab, 294*(5), E882-888.

Duncan, R. E., Ahmadian, M., Jaworski, K., Sarkadi-Nagy, E., & Sul, H. S. (2007). Regulation of lipolysis in adipocytes. *Annu Rev Nutr, 27*, 79-101.

Dyar, K. A., Hubert, M. J., Mir, A. A., Ciciliot, S., Lutter, D., Greulich, F., et al. (2018). Transcriptional programming of lipid and amino acid metabolism by the skeletal muscle circadian clock. *PLoS Biol, 16*(8), e2005886.

Dyck, D. J., Peters, S. J., Glatz, J., Gorski, J., Keizer, H., Kiens, B., et al. (1997). Functional differences in lipid metabolism in resting skeletal muscle of various fiber types. *Am J Physiol, 272*(3 Pt 1), E340-351.

Ellis, B. A., Poynten, A., Lowy, A. J., Furler, S. M., Chisholm, D. J., Kraegen, E. W., et al. (2000). Long-chain acyl-CoA esters as indicators of lipid metabolism and insulin sensitivity in rat and human muscle. *Am J Physiol Endocrinol Metab, 279*(3), E554-560.

Erion, D. M., & Shulman, G. I. (2010). Diacylglycerol-mediated insulin resistance. *Nat Med, 16*(4), 400-402.

Esparza, J., Fox, C., Harper, I. T., Bennett, P. H., Schulz, L. O., Valencia, M. E., et al. (2000). Daily energy expenditure in Mexican and USA Pima indians: low physical activity as a possible cause of obesity. *Int J Obes Relat Metab Disord, 24*(1), 55-59.

Evans, K., Nasim, Z., Brown, J., Butler, H., Kauser, S., Varoqui, H., et al. (2007). Acidosis-sensing glutamine pump SNAT2 determines amino acid levels and mammalian target of rapamycin signalling to protein synthesis in L6 muscle cells. *J Am Soc Nephrol, 18*(5), 1426-1436.

Facchini, F. S., Hua, N., Abbasi, F., & Reaven, G. M. (2001). Insulin resistance as a predictor of age-related diseases. *J Clin Endocrinol Metab, 86*(8), 3574-3578.

Farshchi, H. R., Taylor, M. A., & Macdonald, I. A. (2005). Deleterious effects of omitting breakfast on insulin sensitivity and fasting lipid profiles in healthy lean women. *Am J Clin Nutr, 81*(2), 388-396.

Felig, P., Owen, O. E., Wahren, J., & Cahill, G. F. (1969). Amino acid metabolism during prolonged starvation. *J Clin Invest, 48*(3), 584-594.

Feng, X. T., Wang, T. Z., Leng, J., Chen, Y., Liu, J. B., Liu, Y., et al. (2012). Palmitate contributes to insulin resistance through downregulation of the Src-mediated phosphorylation of Akt in C2C12 myotubes. *Biosci Biotechnol Biochem, 76*(7), 1356-1361.

Ferrannini, E. (1998). Insulin resistance versus insulin deficiency in non-insulin-dependent diabetes mellitus: problems and prospects. *Endocr Rev, 19*(4), 477-490.

Figueiredo, V. C., Markworth, J. F., & Cameron-Smith, D. (2017). Considerations on mTOR regulation at serine 2448: implications for muscle metabolism studies. *Cell Mol Life Sci, 74*(14), 2537-2545.

Foster, D. W. (2012). Malonyl-CoA: the regulator of fatty acid synthesis and oxidation. *J Clin Invest, 122*(6), 1958-1959.

Fox, T. E., Houck, K. L., O'Neill, S. M., Nagarajan, M., Stover, T. C., Pomianowski, P. T., et al. (2007). Ceramide recruits and activates protein kinase C zeta (PKC zeta) within structured membrane microdomains. *J Biol Chem, 282*(17), 12450-12457.

Frayn, K. N. (1983). Calculation of substrate oxidation rates in vivo from gaseous exchange. *J Appl Physiol Respir Environ Exerc Physiol, 55*(2), 628-634.

Frias, J. P., Macaraeg, G. B., Ofrecio, J., Yu, J. G., Olefsky, J. M., & Kruszynska, Y. T. (2001). Decreased susceptibility to fatty acid-induced peripheral tissue insulin resistance in women. *Diabetes, 50*(6), 1344-1350.

Fryburg, D. A., Barrett, E. J., Louard, R. J., & Gelfand, R. A. (1990). Effect of starvation on human muscle protein metabolism and its response to insulin. *Am J Physiol, 259*(4 Pt 1), E477-482.

Fujita, S., Glynn, E. L., Timmerman, K. L., Rasmussen, B. B., & Volpi, E. (2009). Supraphysiological hyperinsulinaemia is necessary to stimulate skeletal muscle protein anabolism in older adults: evidence of a true age-related insulin resistance of muscle protein metabolism. *Diabetologia, 52*(9), 1889-1898.

Fujita, S., Rasmussen, B. B., Cadenas, J. G., Grady, J. J., & Volpi, E. (2006). Effect of insulin on human skeletal muscle protein synthesis is modulated by insulin-induced changes in muscle blood flow and amino acid availability. *Am J Physiol Endocrinol Metab, 291*(4), E745-754.

Gabel, K., Hoddy, K. K., Haggerty, N., Song, J., Kroeger, C. M., Trepanowski, J. F., et al. (2018). Effects of 8-hour time restricted feeding on body weight and metabolic disease risk factors in obese adults: A pilot study. *Nutr Healthy Aging, 4*(4), 345-353.

Gallen, I. W., & Macdonald, I. A. (1990). Effect of two methods of hand heating on body temperature, forearm blood flow, and deep venous oxygen saturation. *Am J Physiol, 259*(5 Pt 1), E639-643.

Garaulet, M., Gómez-Abellán, P., Alburquerque-Béjar, J. J., Lee, Y. C., Ordovás, J. M., & Scheer, F. A. (2013). Timing of food intake predicts weight loss effectiveness. *Int J Obes (Lond), 37*(4), 604-611.

Garber, A. J., Menzel, P. H., Boden, G., & Owen, O. E. (1974). Hepatic ketogenesis and gluconeogenesis in humans. *J Clin Invest, 54*(4), 981-989.

Gaster, M. (2010). Substrate overload: Glucose oxidation in human myotubes conquers palmitate oxidation through anaplerosis. *Biochem Biophys Res Commun, 391*(3), 1369-1373.

Gaster, M., Petersen, I., Højlund, K., Poulsen, P., & Beck-Nielsen, H. (2002). The diabetic phenotype is conserved in myotubes established from diabetic subjects: evidence for primary defects in glucose transport and glycogen synthase activity. *Diabetes, 51*(4), 921-927.

Gersovitz, M., Madden, J. P., & Smiciklas-Wright, H. (1978). Validity of the 24-hr. dietary recall and seven-day record for group comparisons. *J Am Diet Assoc, 73*(1), 48-55.

Gibbons, C., Caudwell, P., Finlayson, G., Webb, D. L., Hellström, P. M., Näslund, E., et al. (2013). Comparison of postprandial profiles of ghrelin, active GLP-1, and total PYY to meals varying in fat and carbohydrate and their association with hunger and the phases of satiety. *J Clin Endocrinol Metab, 98*(5), E847-855.

Gill, S., & Panda, S. (2015). A Smartphone App Reveals Erratic Diurnal Eating Patterns in Humans that Can Be Modulated for Health Benefits. *Cell Metab, 22*(5), 789-798.

Gingras, A. C., Gygi, S. P., Raught, B., Polakiewicz, R. D., Abraham, R. T., Hoekstra, M. F., et al. (1999). Regulation of 4E-BP1 phosphorylation: a novel two-step mechanism. *Genes Dev, 13*(11), 1422-1437.

Glynn, E. L., Fry, C. S., Drummond, M. J., Timmerman, K. L., Dhanani, S., Volpi, E., et al. (2010). Excess leucine intake enhances muscle anabolic signaling but not net protein anabolism in young men and women. *J Nutr, 140*(11), 1970-1976.

Golay, A., Allaz, A. F., Morel, Y., de Tonnac, N., Tankova, S., & Reaven, G. (1996). Similar weight loss with low- or high-carbohydrate diets. *Am J Clin Nutr, 63*(2), 174-178.

Gonzalez, E., & McGraw, T. E. (2006). Insulin signaling diverges into Akt-dependent and -independent signals to regulate the recruitment/docking and the fusion of GLUT4 vesicles to the plasma membrane. *Mol Biol Cell, 17*(10), 4484-4493.

Goodman, C. A., & Hornberger, T. A. (2013). Measuring protein synthesis with SUnSET: a valid alternative to traditional techniques? *Exerc Sport Sci Rev, 41*(2), 107-115.

Goodman, C. A., Mabrey, D. M., Frey, J. W., Miu, M. H., Schmidt, E. K., Pierre, P., et al. (2011). Novel insights into the regulation of skeletal muscle protein synthesis as revealed by a new nonradioactive in vivo technique. *FASEB J, 25*(3), 1028-1039.

Goodpaster, B. H., He, J., Watkins, S., & Kelley, D. E. (2001). Skeletal muscle lipid content and insulin resistance: evidence for a paradox in endurance-trained athletes. *J Clin Endocrinol Metab, 86*(12), 5755-5761.

Goodyear, L. J., Hirshman, M. F., Napoli, R., Calles, J., Markuns, J. F., Ljungqvist, O., et al. (1996). Glucose ingestion causes GLUT4 translocation in human skeletal muscle. *Diabetes, 45*(8), 1051-1056.

Gorissen, S. H., Burd, N. A., Hamer, H. M., Gijsen, A. P., Groen, B. B., & van Loon, L. J. (2014). Carbohydrate coingestion delays dietary protein digestion and absorption but does not modulate postprandial muscle protein accretion. *J Clin Endocrinol Metab, 99*(6), 2250-2258.

Gorissen, S. H. M., Burd, N. A., Kramer, I. F., van Kranenburg, J., Gijsen, A. P., Rooyackers, O., et al. (2017). Co-ingesting milk fat with micellar casein does not affect postprandial protein handling in healthy older men. *Clin Nutr, 36*(2), 429-437.

Greenhaff, P. L., Karagounis, L. G., Peirce, N., Simpson, E. J., Hazell, M., Layfield, R., et al. (2008). Disassociation between the effects of amino acids and insulin on signaling, ubiquitin ligases, and protein turnover in human muscle. *Am J Physiol Endocrinol Metab, 295*(3), E595-604.

Griffiths, A. J., Humphreys, S. M., Clark, M. L., Fielding, B. A., & Frayn, K. N. (1994). Immediate metabolic availability of dietary fat in combination with carbohydrate. *Am J Clin Nutr, 59*(1), 53-59.

Groop, L. C., Bonadonna, R. C., DelPrato, S., Ratheiser, K., Zyck, K., Ferrannini, E., et al. (1989). Glucose and free fatty acid metabolism in non-insulin-dependent diabetes mellitus. Evidence for multiple sites of insulin resistance. *J Clin Invest, 84*(1), 205-213.

Gudbjörnsdóttir, S., Sjöstrand, M., Strindberg, L., Wahren, J., & Lönnroth, P. (2003). Direct measurements of the permeability surface area for insulin and glucose in human skeletal muscle. *J Clin Endocrinol Metab, 88*(10), 4559-4564.

Gupta, N. J., Kumar, V., & Panda, S. (2017). A camera-phone based study reveals erratic eating pattern and disrupted daily eating-fasting cycle among adults in India. *PLoS One, 12*(3), e0172852.

Hajduch, E., Litherland, G. J., & Hundal, H. S. (2001). Protein kinase B (PKB/Akt)--a key regulator of glucose transport? *FEBS Lett, 492*(3), 199-203.

Halberg, N., Henriksen, M., Söderhamn, N., Stallknecht, B., Ploug, T., Schjerling, P., et al. (2005). Effect of intermittent fasting and refeeding on insulin action in healthy men. *J Appl Physiol (1985), 99*(6), 2128-2136.

Hall, K. D., Ayuketah, A., Brychta, R., Cai, H., Cassimatis, T., Chen, K. Y., et al. (2019). Ultra-Processed Diets Cause Excess Calorie Intake and Weight Gain: An Inpatient Randomized Controlled Trial of Ad Libitum Food Intake. *Cell Metab*.

Hall, K. D., Sacks, G., Chandramohan, D., Chow, C. C., Wang, Y. C., Gortmaker, S. L., et al. (2011). Quantification of the effect of energy imbalance on bodyweight. *Lancet, 378*(9793), 826-837.

Hamman, R. F., Wing, R. R., Edelstein, S. L., Lachin, J. M., Bray, G. A., Delahanty, L., et al. (2006). Effect of weight loss with lifestyle intervention on risk of diabetes. *Diabetes Care, 29*(9), 2102-2107.

Hancock, C. R., Han, D. H., Chen, M., Terada, S., Yasuda, T., Wright, D. C., et al. (2008). High-fat diets cause insulin resistance despite an increase in muscle mitochondria. *Proc Natl Acad Sci U S A, 105*(22), 7815-7820.

Harris, R. C., Hultman, E., & Nordesjö, L. O. (1974). Glycogen, glycolytic intermediates and high-energy phosphates determined in biopsy samples of musculus quadriceps femoris of man at rest. Methods and variance of values. *Scand J Clin Lab Invest, 33*(2), 109-120.

Harvie, M. N., Pegington, M., Mattson, M. P., Frystyk, J., Dillon, B., Evans, G., et al. (2011). The effects of intermittent or continuous energy restriction on weight loss and metabolic disease risk markers: a randomized trial in young overweight women. *Int J Obes (Lond), 35*(5), 714-727.

Hatori, M., Vollmers, C., Zarrinpar, A., DiTacchio, L., Bushong, E. A., Gill, S., et al. (2012). Time-restricted feeding without reducing caloric intake prevents metabolic diseases in mice fed a high-fat diet. *Cell Metab, 15*(6), 848-860.

He, W., Barak, Y., Hevener, A., Olson, P., Liao, D., Le, J., et al. (2003). Adipose-specific peroxisome proliferator-activated receptor gamma knockout causes insulin resistance in fat and liver but not in muscle. *Proc Natl Acad Sci U S A, 100*(26), 15712-15717.

Health and Social Care Information Centre. (2009). Health Survey for England - 2008: Physical activity and fitness. Retrieved 13/09/2019, from https://digital.nhs.uk/data-and-information/publications/statistical/health-survey-for-england/health-survey-for-england-2008-physical-activity-and-fitness#key-facts

Heijboer, A. C., Donga, E., Voshol, P. J., Dang, Z. C., Havekes, L. M., Romijn, J. A., et al. (2005). Sixteen hours of fasting differentially affects hepatic and muscle insulin sensitivity in mice. *J Lipid Res, 46*(3), 582-588.

Heilbronn, L. K., Gan, S. K., Turner, N., Campbell, L. V., & Chisholm, D. J. (2007). Markers of mitochondrial biogenesis and metabolism are lower in overweight and obese insulin-resistant subjects. *J Clin Endocrinol Metab, 92*(4), 1467-1473.

Heilbronn, L. K., Smith, S. R., Martin, C. K., Anton, S. D., & Ravussin, E. (2005). Alternate-day fasting in nonobese subjects: effects on body weight, body composition, and energy metabolism. *Am J Clin Nutr, 81*(1), 69-73.

Helmrich, S. P., Ragland, D. R., Leung, R. W., & Paffenbarger, R. S. (1991). Physical activity and reduced occurrence of non-insulin-dependent diabetes mellitus. *N Engl J Med, 325*(3), 147-152.

Henique, C., Mansouri, A., Fumey, G., Lenoir, V., Girard, J., Bouillaud, F., et al. (2010). Increased mitochondrial fatty acid oxidation is sufficient to protect skeletal muscle cells from palmitate-induced apoptosis. *J Biol Chem, 285*(47), 36818-36827.

Hennessey, J. V., Chromiak, J. A., Della Ventura, S., Guertin, J., & MacLean, D. B. (1997). Increase in percutaneous muscle biopsy yield with a suction-enhancement technique. *J Appl Physiol (1985), 82*(6), 1739-1742.

Hennig, B., & Watkins, B. A. (1989). Linoleic acid and linolenic acid: effect on permeability properties of cultured endothelial cell monolayers. *Am J Clin Nutr, 49*(2), 301-305.

Herder, C., & Roden, M. (2011). Genetics of type 2 diabetes: pathophysiologic and clinical relevance. *Eur J Clin Invest, 41*(6), 679-692.

Heymsfield, S. B., Segal, K. R., Hauptman, J., Lucas, C. P., Boldrin, M. N., Rissanen, A., et al. (2000). Effects of weight loss with orlistat on glucose tolerance and progression to type 2 diabetes in obese adults. *Arch Intern Med, 160*(9), 1321-1326.

Hill, A. M., LaForgia, J., Coates, A. M., Buckley, J. D., & Howe, P. R. (2007). Estimating abdominal adipose tissue with DXA and anthropometry. *Obesity (Silver Spring), 15*(2), 504-510.

Hoddy, K. K., Gibbons, C., Kroeger, C. M., Trepanowski, J. F., Barnosky, A., Bhutani, S., et al. (2016). Changes in hunger and fullness in relation to gut peptides before and after 8 weeks of alternate day fasting. *Clin Nutr, 35*(6), 1380-1385.

Hodge, B. A., Wen, Y., Riley, L. A., Zhang, X., England, J. H., Harfmann, B. D., et al. (2015). The endogenous molecular clock orchestrates the temporal separation of substrate metabolism in skeletal muscle. *Skelet Muscle, 5*, 17.

Høeg, L. D., Sjøberg, K. A., Jeppesen, J., Jensen, T. E., Frøsig, C., Birk, J. B., et al. (2011). Lipid-induced insulin resistance affects women less than men and is not accompanied by inflammation or impaired proximal insulin signaling. *Diabetes, 60*(1), 64-73.

Hoeks, J., van Herpen, N. A., Mensink, M., Moonen-Kornips, E., van Beurden, D., Hesselink, M. K., et al. (2010). Prolonged fasting identifies skeletal muscle mitochondrial dysfunction as consequence rather than cause of human insulin resistance. *Diabetes, 59*(9), 2117-2125.

Holland, W. L., Bikman, B. T., Wang, L. P., Yuguang, G., Sargent, K. M., Bulchand, S., et al. (2011). Lipid-induced insulin resistance mediated by the proinflammatory receptor TLR4 requires saturated fatty acid-induced ceramide biosynthesis in mice. *J Clin Invest, 121*(5), 1858-1870.

Holland, W. L., Brozinick, J. T., Wang, L. P., Hawkins, E. D., Sargent, K. M., Liu, Y., et al. (2007). Inhibition of ceramide synthesis ameliorates glucocorticoid-, saturated-fat-, and obesity-induced insulin resistance. *Cell Metab, 5*(3), 167-179.

Horne, J. A., & Ostberg, O. (1976). A self-assessment questionnaire to determine morningness-eveningness in human circadian rhythms. *Int J Chronobiol, 4*(2), 97-110.

Hu, F. B. (2011). Globalization of diabetes: the role of diet, lifestyle, and genes. *Diabetes Care, 34*(6), 1249-1257.

Hu, S., Wang, L., Yang, D., Li, L., Togo, J., Wu, Y., et al. (2018). Dietary Fat, but Not Protein or Carbohydrate, Regulates Energy Intake and Causes Adiposity in Mice. *Cell Metab, 28*(3), 415-431.e414.

Huang, C., Thirone, A. C., Huang, X., & Klip, A. (2005). Differential contribution of insulin receptor substrates 1 versus 2 to insulin signaling and glucose uptake in l6 myotubes. *J Biol Chem, 280*(19), 19426-19435.

Hundal, H. S., & Taylor, P. M. (2009). Amino acid transceptors: gate keepers of nutrient exchange and regulators of nutrient signaling. *Am J Physiol Endocrinol Metab, 296*(4), E603-613.

Hutchison, A. T., Regmi, P., Manoogian, E. N. C., Fleischer, J. G., Wittert, G. A., Panda, S., et al. (2019). Time-Restricted Feeding Improves Glucose Tolerance in Men at Risk for Type 2 Diabetes: A Randomized Crossover Trial. *Obesity (Silver Spring), 27*(5), 724-732.

Hyde, R., Cwiklinski, E. L., MacAulay, K., Taylor, P. M., & Hundal, H. S. (2007). Distinct sensor pathways in the hierarchical control of SNAT2, a putative amino acid transceptor, by amino acid availability. *J Biol Chem, 282*(27), 19788-19798.

Hyde, R., Hajduch, E., Powell, D. J., Taylor, P. M., & Hundal, H. S. (2005). Ceramide down-regulates System A amino acid transport and protein synthesis in rat skeletal muscle cells. *FASEB J, 19*(3), 461-463.

Hyde, R., Taylor, P. M., & Hundal, H. S. (2003). Amino acid transporters: roles in amino acid sensing and signalling in animal cells. *Biochem J, 373*(Pt 1), 1-18.

Høeg, L. D., Sjøberg, K. A., Jeppesen, J., Jensen, T. E., Frøsig, C., Birk, J. B., et al. (2011). Lipid-induced insulin resistance affects women less than men and is not accompanied by inflammation or impaired proximal insulin signaling. *Diabetes, 60*(1), 64-73.

Højlund, K., Poulsen, M., Staehr, P., Brusgaard, K., & Beck-Nielsen, H. (2002). Effect of insulin on protein phosphatase 2A expression in muscle in type 2 diabetes. *Eur J Clin Invest, 32*(12), 918-923.

Itani, S. I., Ruderman, N. B., Schmieder, F., & Boden, G. (2002). Lipid-induced insulin resistance in human muscle is associated with changes in diacylglycerol, protein kinase C, and IkappaB-alpha. *Diabetes, 51*(7), 2005-2011.

Izumida, Y., Yahagi, N., Takeuchi, Y., Nishi, M., Shikama, A., Takarada, A., et al. (2013). Glycogen shortage during fasting triggers liver-brain-adipose neurocircuitry to facilitate fat utilization. *Nat Commun, 4*, 2316.

Jakubowicz, D., Barnea, M., Wainstein, J., & Froy, O. (2013). High caloric intake at breakfast vs. dinner differentially influences weight loss of overweight and obese women. *Obesity (Silver Spring), 21*(12), 2504-2512.

Jamshed, H., Beyl, R. A., Della Manna, D. L., Yang, E. S., Ravussin, E., & Peterson, C. M. (2019). Early Time-Restricted Feeding Improves 24-Hour Glucose Levels and Affects Markers of the Circadian Clock, Aging, and Autophagy in Humans. *Nutrients, 11*(6).

Jain, S. S., Chabowski, A., Snook, L. A., Schwenk, R. W., Glatz, J. F., Luiken, J. J., et al. (2009). Additive effects of insulin and muscle contraction on fatty acid

transport and fatty acid transporters, FAT/CD36, FABPpm, FATP1, 4 and 6. *FEBS Lett, 583*(13), 2294-2300.

Jans, A., van Hees, A. M., Gjelstad, I. M., Sparks, L. M., Tierney, A. C., Risérus, U., et al. (2012). Impact of dietary fat quantity and quality on skeletal muscle fatty acid metabolism in subjects with the metabolic syndrome. *Metabolism, 61*(11), 1554-1565.

Janssen, I., Heymsfield, S. B., Wang, Z. M., & Ross, R. (2000). Skeletal muscle mass and distribution in 468 men and women aged 18-88 yr. *J Appl Physiol (1985), 89*(1), 81-88.

Jensen, M. D., Caruso, M., Heiling, V., & Miles, J. M. (1989). Insulin regulation of lipolysis in nondiabetic and IDDM subjects. *Diabetes, 38*(12), 1595-1601.

Jensen, M. D., & Heiling, V. J. (1991). Heated hand vein blood is satisfactory for measurements during free fatty acid kinetic studies. *Metabolism, 40*(4), 406-409.

Jensen, M. D., Kanaley, J. A., Reed, J. E., & Sheedy, P. F. (1995). Measurement of abdominal and visceral fat with computed tomography and dual-energy x-ray absorptiometry. *Am J Clin Nutr, 61*(2), 274-278.

Jeoung, N. H., & Harris, R. A. (2010). Role of pyruvate dehydrogenase kinase 4 in regulation of blood glucose levels. *Korean Diabetes J, 34*(5), 274-283.

Ji, L., Guo, X., Guo, L., Ren, Q., Yu, N., & Zhang, J. (2017). A Multicenter Evaluation of the Performance and Usability of a Novel Glucose Monitoring System in Chinese Adults With Diabetes. *J Diabetes Sci Technol, 11*(2), 290-295.

Jucker, B. M., Rennings, A. J., Cline, G. W., Petersen, K. F., & Shulman, G. I. (1997). In vivo NMR investigation of intramuscular glucose metabolism in conscious rats. *Am J Physiol, 273*(1 Pt 1), E139-148.

Kaczmarek, J. L., Musaad, S. M., & Holscher, H. D. (2017). Time of day and eating behaviors are associated with the composition and function of the human gastrointestinal microbiota. *Am J Clin Nutr, 106*(5), 1220-1231.

Kahleova, H., Lloren, J. I., Mashchak, A., Hill, M., & Fraser, G. E. (2017). Meal Frequency and Timing Are Associated with Changes in Body Mass Index in Adventist Health Study 2. *J Nutr, 147*(9), 1722-1728.

Kahn, B. B., Alquier, T., Carling, D., & Hardie, D. G. (2005). AMP-activated protein kinase: ancient energy gauge provides clues to modern understanding of metabolism. *Cell Metab, 1*(1), 15-25.

Kant, A. K., & Graubard, B. I. (2015). 40-year trends in meal and snack eating behaviors of American adults. *J Acad Nutr Diet, 115*(1), 50-63.

Karamanlis, A., Chaikomin, R., Doran, S., Bellon, M., Bartholomeusz, F. D., Wishart, J. M., et al. (2007). Effects of protein on glycemic and incretin responses and gastric emptying after oral glucose in healthy subjects. *Am J Clin Nutr, 86*(5), 1364-1368.

Katsanos, C. S., Aarsland, A., Cree, M. G., & Wolfe, R. R. (2009). Muscle protein synthesis and balance responsiveness to essential amino acids ingestion in the presence of elevated plasma free fatty acid concentrations. *J Clin Endocrinol Metab, 94*(8), 2984-2990.

Katsanos, C. S., Kobayashi, H., Sheffield-Moore, M., Aarsland, A., & Wolfe, R. R. (2005). Aging is associated with diminished accretion of muscle proteins after the ingestion of a small bolus of essential amino acids. *Am J Clin Nutr, 82*(5), 1065-1073.

Kelley, D., Mitrakou, A., Marsh, H., Schwenk, F., Benn, J., Sonnenberg, G., et al. (1988). Skeletal muscle glycolysis, oxidation, and storage of an oral glucose load. *J Clin Invest, 81*(5), 1563-1571.

Kelley, D. E., He, J., Menshikova, E. V., & Ritov, V. B. (2002). Dysfunction of mitochondria in human skeletal muscle in type 2 diabetes. *Diabetes, 51*(10), 2944-2950.

Kelley, D. E., & Mandarino, L. J. (2000). Fuel selection in human skeletal muscle in insulin resistance: a reexamination. *Diabetes, 49*(5), 677-683.

Kelley, D. E., Mokan, M., Simoneau, J. A., & Mandarino, L. J. (1993). Interaction between glucose and free fatty acid metabolism in human skeletal muscle. *J Clin Invest, 92*(1), 91-98.

Kershaw, E. E., Hamm, J. K., Verhagen, L. A., Peroni, O., Katic, M., & Flier, J. S. (2006). Adipose triglyceride lipase: function, regulation by insulin, and comparison with adiponutrin. *Diabetes, 55*(1), 148-157.

Kersten, S., Seydoux, J., Peters, J. M., Gonzalez, F. J., Desvergne, B., & Wahli, W. (1999). Peroxisome proliferator-activated receptor alpha mediates the adaptive response to fasting. *J Clin Invest, 103*(11), 1489-1498.

Kiens, B., Lithell, H., Mikines, K. J., & Richter, E. A. (1989). Effects of insulin and exercise on muscle lipoprotein lipase activity in man and its relation to insulin action. *J Clin Invest, 84*(4), 1124-1129.

Kim, J., Kim, Y. C., Fang, C., Russell, R. C., Kim, J. H., Fan, W., et al. (2013). Differential regulation of distinct Vps34 complexes by AMPK in nutrient stress and autophagy. *Cell, 152*(1-2), 290-303.

Kim, J. K., Fillmore, J. J., Sunshine, M. J., Albrecht, B., Higashimori, T., Kim, D. W., et al. (2004). PKC-theta knockout mice are protected from fat-induced insulin resistance. *J Clin Invest, 114*(6), 823-827.

Kim, Y. B., Nikoulina, S. E., Ciaraldi, T. P., Henry, R. R., & Kahn, B. B. (1999). Normal insulin-dependent activation of Akt/protein kinase B, with diminished activation of phosphoinositide 3-kinase, in muscle in type 2 diabetes. *J Clin Invest, 104*(6), 733-741.

Kirk, E., Reeds, D. N., Finck, B. N., Mayurranjan, S. M., Mayurranjan, M. S., Patterson, B. W., et al. (2009). Dietary fat and carbohydrates differentially alter insulin sensitivity during caloric restriction. *Gastroenterology, 136*(5), 1552-1560.

Klein, S., Sakurai, Y., Romijn, J. A., & Carroll, R. M. (1993). Progressive alterations in lipid and glucose metabolism during short-term fasting in young adult men. *Am J Physiol, 265*(5 Pt 1), E801-806.

Klip, A., Li, G., & Logan, W. J. (1984). Induction of sugar uptake response to insulin by serum depletion in fusing L6 myoblasts. *Am J Physiol, 247*(3 Pt 1), E291-296.

Koopman, K. E., Caan, M. W., Nederveen, A. J., Pels, A., Ackermans, M. T., Fliers, E., et al. (2014). Hypercaloric diets with increased meal frequency, but not meal size, increase intrahepatic triglycerides: a randomized controlled trial. *Hepatology, 60*(2), 545-553.

Koutsari, C., Ali, A. H., Mundi, M. S., & Jensen, M. D. (2011). Storage of circulating free fatty acid in adipose tissue of postabsorptive humans: quantitative measures and implications for body fat distribution. *Diabetes, 60*(8), 2032-2040.

Kouw, I. W. K., van Dijk, J. W., Horstman, A. M. H., Kramer, I. F., Goessens, J. P. B., van Dielen, F. M. H., et al. (2019). Basal and Postprandial Myofibrillar Protein Synthesis Rates Do Not Differ between Lean and Obese Middle-Aged Men. *J Nutr*.

Kraegen, E. W., Cooney, G. J., & Turner, N. (2008). Muscle insulin resistance: a case of fat overconsumption, not mitochondrial dysfunction. *Proc Natl Acad Sci U S A, 105*(22), 7627-7628.

Kraus, W. E., Bhapkar, M., Huffman, K. M., Pieper, C. F., Krupa Das, S., Redman, L. M., et al. (2019). 2 years of calorie restriction and cardiometabolic risk (CALERIE): exploratory outcomes of a multicentre, phase 2, randomised controlled trial. *Lancet Diabetes Endocrinol, 7*(9), 673-683.

Kruszynska, Y. T., Mukherjee, R., Jow, L., Dana, S., Paterniti, J. R., & Olefsky, J. M. (1998). Skeletal muscle peroxisome proliferator- activated receptor-gamma

expression in obesity and non- insulin-dependent diabetes mellitus. *J Clin Invest, 101*(3), 543-548.

Kruszynska, Y. T., Worrall, D. S., Ofrecio, J., Frias, J. P., Macaraeg, G., & Olefsky, J. M. (2002). Fatty acid-induced insulin resistance: decreased muscle PI3K activation but unchanged Akt phosphorylation. *J Clin Endocrinol Metab, 87*(1), 226-234.

Krützfeldt, J., Kausch, C., Volk, A., Klein, H. H., Rett, K., Häring, H. U., et al. (2000). Insulin signaling and action in cultured skeletal muscle cells from lean healthy humans with high and low insulin sensitivity. *Diabetes, 49*(6), 992-998.

Kurpad, A. V., Khan, K., & Elia, M. (1994). The effect of arterialization of blood by hand warming on the interpretation of forearm metabolic studies. *Physiol Meas, 15*(2), 139-145.

Kwon, B., & Querfurth, H. W. (2015). Palmitate activates mTOR/p70S6K through AMPK inhibition and hypophosphorylation of raptor in skeletal muscle cells: Reversal by oleate is similar to metformin. *Biochimie, 118*, 141-150.

Laakso, M., Edelman, S. V., Brechtel, G., & Baron, A. D. (1990). Decreased effect of insulin to stimulate skeletal muscle blood flow in obese man. A novel mechanism for insulin resistance. *J Clin Invest, 85*(6), 1844-1852.

Lager, S., Jansson, T., & Powell, T. L. (2014). Differential regulation of placental amino acid transport by saturated and unsaturated fatty acids. *Am J Physiol Cell Physiol, 307*(8), C738-744.

Lai, M., Chandrasekera, P. C., & Barnard, N. D. (2014). You are what you eat, or are you? The challenges of translating high-fat-fed rodents to human obesity and diabetes. *Nutr Diabetes, 4*, e135.

Larson-Meyer, D. E., Heilbronn, L. K., Redman, L. M., Newcomer, B. R., Frisard, M. I., Anton, S., et al. (2006). Effect of calorie restriction with or without exercise on insulin sensitivity, beta-cell function, fat cell size, and ectopic lipid in overweight subjects. *Diabetes Care, 29*(6), 1337-1344.

Le Bacquer, O., Combe, K., Patrac, V., Ingram, B., Combaret, L., Dardevet, D., et al. (2019). 4E-BP1 and 4E-BP2 double knockout mice are protected from aging-associated sarcopenia. *J Cachexia Sarcopenia Muscle, 10*(3), 696-709.

Lean, M. E., Leslie, W. S., Barnes, A. C., Brosnahan, N., Thom, G., McCombie, L., et al. (2018). Primary care-led weight management for remission of type 2 diabetes (DiRECT): an open-label, cluster-randomised trial. *Lancet, 391*(10120), 541-551.

LeCheminant, J. D., Christenson, E., Bailey, B. W., & Tucker, L. A. (2013). Restricting night-time eating reduces daily energy intake in healthy young men: a short-term cross-over study. *Br J Nutr, 110*(11), 2108-2113.

Lee, F. N., Zhang, L., Zheng, D., Choi, W. S., & Youn, J. H. (2004). Insulin suppresses PDK-4 expression in skeletal muscle independently of plasma FFA. *Am J Physiol Endocrinol Metab, 287*(1), E69-74.

Lehrke, M., & Lazar, M. A. (2005). The many faces of PPARgamma. *Cell, 123*(6), 993-999.

Leone, T. C., Weinheimer, C. J., & Kelly, D. P. (1999). A critical role for the peroxisome proliferator-activated receptor alpha (PPARalpha) in the cellular fasting response: the PPARalpha-null mouse as a model of fatty acid oxidation disorders. *Proc Natl Acad Sci U S A, 96*(13), 7473-7478.

Lessan, N., Saadane, I., Alkaf, B., Hambly, C., Buckley, A. J., Finer, N., et al. (2018). The effects of Ramadan fasting on activity and energy expenditure. *Am J Clin Nutr, 107*(1), 54-61.

Levin, M. C., Monetti, M., Watt, M. J., Sajan, M. P., Stevens, R. D., Bain, J. R., et al. (2007). Increased lipid accumulation and insulin resistance in transgenic mice expressing DGAT2 in glycolytic (type II) muscle. *Am J Physiol Endocrinol Metab, 293*(6), E1772-1781.

Li, F., Duan, Y., Li, Y., Tang, Y., Geng, M., Oladele, O. A., et al. (2015). Effects of dietary n-6:n-3 PUFA ratio on fatty acid composition, free amino acid profile and gene expression of transporters in finishing pigs. *Br J Nutr, 113*(5), 739-748.

Lim, E. L., Hollingsworth, K. G., Aribisala, B. S., Chen, M. J., Mathers, J. C., & Taylor, R. (2011). Reversal of type 2 diabetes: normalisation of beta cell function in association with decreased pancreas and liver triacylglycerol. *Diabetologia, 54*(10), 2506-2514.

Lipina, C., Macrae, K., Suhm, T., Weigert, C., Blachnio-Zabielska, A., Baranowski, M., et al. (2013). Mitochondrial substrate availability and its role in lipid-induced insulin resistance and proinflammatory signaling in skeletal muscle. *Diabetes, 62*(10), 3426-3436.

Liu, D., Moberg, E., Kollind, M., Lins, P. E., Adamson, U., & Macdonald, I. A. (1992). Arterial, arterialized venous, venous and capillary blood glucose measurements in normal man during hyperinsulinaemic euglycaemia and hypoglycaemia. *Diabetologia, 35*(3), 287-290.

Liu, L., Chen, L., Luo, Y., Chen, W., Zhou, H., Xu, B., et al. (2010). Rapamycin inhibits IGF-1 stimulated cell motility through PP2A pathway. *PLoS One, 5*(5), e10578.

Liu, L., Zhang, Y., Chen, N., Shi, X., Tsang, B., & Yu, Y. H. (2007). Upregulation of myocellular DGAT1 augments triglyceride synthesis in skeletal muscle and protects against fat-induced insulin resistance. *J Clin Invest, 117*(6), 1679-1689.

Liu, Y., Palanivel, R., Rai, E., Park, M., Gabor, T. V., Scheid, M. P., et al. (2015). Adiponectin stimulates autophagy and reduces oxidative stress to enhance insulin sensitivity during high-fat diet feeding in mice. *Diabetes, 64*(1), 36-48.

Luiken, J. J., Koonen, D. P., Willems, J., Zorzano, A., Becker, C., Fischer, Y., et al. (2002). Insulin stimulates long-chain fatty acid utilization by rat cardiac myocytes through cellular redistribution of FAT/CD36. *Diabetes, 51*(10), 3113-3119.

Lundsgaard, A. M., Sjøberg, K. A., Høeg, L. D., Jeppesen, J., Jordy, A. B., Serup, A. K., et al. (2017). Opposite Regulation of Insulin Sensitivity by Dietary Lipid Versus Carbohydrate Excess. *Diabetes, 66*(10), 2583-2595.

Luo, J. Q., Chen, D. W., & Yu, B. (2013). Upregulation of amino acid transporter expression induced by L-leucine availability in L6 myotubes is associated with ATF4 signaling through mTORC1-dependent mechanism. *Nutrition, 29*(1), 284-290.

Macrae, K., Stretton, C., Lipina, C., Blachnio-Zabielska, A., Baranowski, M., Gorski, J., et al. (2013). Defining the role of DAG, mitochondrial function, and lipid deposition in palmitate-induced proinflammatory signaling and its counter-modulation by palmitoleate. *J Lipid Res, 54*(9), 2366-2378.

Mahajan, A., Taliun, D., Thurner, M., Robertson, N. R., Torres, J. M., Rayner, N. W., et al. (2018). Fine-mapping type 2 diabetes loci to single-variant resolution using high-density imputation and islet-specific epigenome maps. *Nat Genet, 50*(11), 1505-1513.

Maeda, N., Takahashi, M., Funahashi, T., Kihara, S., Nishizawa, H., Kishida, K., et al. (2001). PPARgamma ligands increase expression and plasma concentrations of adiponectin, an adipose-derived protein. *Diabetes, 50*(9), 2094-2099.

Majer, M., Popov, K. M., Harris, R. A., Bogardus, C., & Prochazka, M. (1998). Insulin downregulates pyruvate dehydrogenase kinase (PDK) mRNA: potential mechanism contributing to increased lipid oxidation in insulin-resistant subjects. *Mol Genet Metab, 65*(2), 181-186.

Manco, M., Bertuzzi, A., Salinari, S., Scarfone, A., Calvani, M., Greco, A. V., et al. (2004). The ingestion of saturated fatty acid triacylglycerols acutely affects insulin secretion and insulin sensitivity in human subjects. *Br J Nutr, 92*(6), 895-903.

Mansell, P. I., & Macdonald, I. A. (1990). The effect of starvation on insulin-induced glucose disposal and thermogenesis in humans. *Metabolism, 39*(5), 502-510.

Martin, B., Pearson, M., Brenneman, R., Golden, E., Wood, W., Prabhu, V., et al. (2009). Gonadal transcriptome alterations in response to dietary energy intake: sensing the reproductive environment. *PLoS One, 4*(1), e4146.

Masgrau, A., Mishellany-Dutour, A., Murakami, H., Beaufrère, A. M., Walrand, S., Giraudet, C., et al. (2012). Time-course changes of muscle protein synthesis associated with obesity-induced lipotoxicity. *J Physiol, 590*(20), 5199-5210.

Matsuda, M., & DeFronzo, R. A. (1999). Insulin sensitivity indices obtained from oral glucose tolerance testing: comparison with the euglycemic insulin clamp. *Diabetes Care, 22*(9), 1462-1470.

Matthews, D. R., Hosker, J. P., Rudenski, A. S., Naylor, B. A., Treacher, D. F., & Turner, R. C. (1985). Homeostasis model assessment: insulin resistance and beta-cell function from fasting plasma glucose and insulin concentrations in man. *Diabetologia, 28*(7), 412-419.

Mattison, J. A., Colman, R. J., Beasley, T. M., Allison, D. B., Kemnitz, J. W., Roth, G. S., et al. (2017). Caloric restriction improves health and survival of rhesus monkeys. *Nat Commun, 8*, 14063.

Maughan, R. J., Watson, J. S., & Weir, J. (1984). The relative proportions of fat, muscle and bone in the normal human forearm as determined by computed tomography. *Clin Sci (Lond), 66*(6), 683-689.

Maukonen, M., Kanerva, N., Partonen, T., Kronholm, E., Tapanainen, H., Kontto, J., et al. (2017). Chronotype differences in timing of energy and macronutrient intakes: A population-based study in adults. *Obesity (Silver Spring), 25*(3), 608-615.

McDowell, H. E., Christie, G. R., Stenhouse, G., & Hundal, H. S. (1995). Leucine activates system A amino acid transport in L6 rat skeletal muscle cells. *Am J Physiol, 269*(5 Pt 1), C1287-1294.

McDowell, H. E., Eyers, P. A., & Hundal, H. S. (1998). Regulation of System A amino acid transport in L6 rat skeletal muscle cells by insulin, chemical and hyperthermic stress. *FEBS Lett, 441*(1), 15-19.

McGuire, E. A., Helderman, J. H., Tobin, J. D., Andres, R., & Berman, M. (1976). Effects of arterial versus venous sampling on analysis of glucose kinetics in man. *J Appl Physiol, 41*(4), 565-573.

McKinsey Global Institute. (2014). Overcoming obesity: An initial economic analysis. Retrieved 13/09/2019, from

https://www.mckinsey.com/~/media/McKinsey/Business%20Functions/Economic%20Studies%20TEMP/Our%20Insights/How%20the%20world%20could%20better%20fight%20obesity/MGI_Overcoming_obesity_Full_report.ashx

McQuaid, S. E., Hodson, L., Neville, M. J., Dennis, A. L., Cheeseman, J., Humphreys, S. M., et al. (2011). Downregulation of adipose tissue fatty acid trafficking in obesity: a driver for ectopic fat deposition? *Diabetes, 60*(1), 47-55.

Meigs, J. B., Mittleman, M. A., Nathan, D. M., Tofler, G. H., Singer, D. E., Murphy-Sheehy, P. M., et al. (2000). Hyperinsulinemia, hyperglycemia, and impaired hemostasis: the Framingham Offspring Study. *JAMA, 283*(2), 221-228.

Meng, H., Janssen, P. M., Grange, R. W., Yang, L., Beggs, A. H., Swanson, L. C., et al. (2014). Tissue triage and freezing for models of skeletal muscle disease. *J Vis Exp*(89).

Mihalik, S. J., Goodpaster, B. H., Kelley, D. E., Chace, D. H., Vockley, J., Toledo, F. G., et al. (2010). Increased levels of plasma acylcarnitines in obesity and type 2 diabetes and identification of a marker of glucolipotoxicity. *Obesity (Silver Spring), 18*(9), 1695-1700.

Miller, S., Chinkes, D., MacLean, D. A., Gore, D., & Wolfe, R. R. (2004). In vivo muscle amino acid transport involves two distinct processes. *Am J Physiol Endocrinol Metab, 287*(1), E136-141.

Mitchell, C. J., McGregor, R. A., D'Souza, R. F., Thorstensen, E. B., Markworth, J. F., Fanning, A. C., et al. (2015). Consumption of Milk Protein or Whey Protein Results in a Similar Increase in Muscle Protein Synthesis in Middle Aged Men. *Nutrients, 7*(10), 8685-8699.

Mitchell, S. J., Bernier, M., Mattison, J. A., Aon, M. A., Kaiser, T. A., Anson, R. M., et al. (2019). Daily Fasting Improves Health and Survival in Male Mice Independent of Diet Composition and Calories. *Cell Metab, 29*(1), 221-228.e223.

Mittendorfer, B., Liem, O., Patterson, B. W., Miles, J. M., & Klein, S. (2003). What does the measurement of whole-body fatty acid rate of appearance in plasma by using a fatty acid tracer really mean? *Diabetes, 52*(7), 1641-1648.

Mittendorfer, B., Volpi, E., & Wolfe, R. R. (2001). Whole body and skeletal muscle glutamine metabolism in healthy subjects. *Am J Physiol Endocrinol Metab, 280*(2), E323-333.

Montagnani, M., Chen, H., Barr, V. A., & Quon, M. J. (2001). Insulin-stimulated activation of eNOS is independent of Ca2+ but requires phosphorylation by Akt at Ser(1179). *J Biol Chem, 276*(32), 30392-30398.

Moro, C., Galgani, J. E., Luu, L., Pasarica, M., Mairal, A., Bajpeyi, S., et al. (2009). Influence of gender, obesity, and muscle lipase activity on intramyocellular lipids in sedentary individuals. *J Clin Endocrinol Metab, 94*(9), 3440-3447.

Moro, T., Tinsley, G., Bianco, A., Marcolin, G., Pacelli, Q. F., Battaglia, G., et al. (2016). Effects of eight weeks of time-restricted feeding (16/8) on basal metabolism, maximal strength, body composition, inflammation, and cardiovascular risk factors in resistance-trained males. *J Transl Med, 14*(1), 290.

Mott, D. M., Stone, K., Gessel, M. C., Bunt, J. C., & Bogardus, C. (2008). Palmitate action to inhibit glycogen synthase and stimulate protein phosphatase 2A increases with risk factors for type 2 diabetes. *Am J Physiol Endocrinol Metab, 294*(2), E444-450.

Murton, A. J., Marimuthu, K., Mallinson, J. E., Selby, A. L., Smith, K., Rennie, M. J., et al. (2015). Obesity Appears to Be Associated With Altered Muscle Protein Synthetic and Breakdown Responses to Increased Nutrient Delivery in Older Men, but Not Reduced Muscle Mass or Contractile Function. *Diabetes, 64*(9), 3160-3171.

Mîinea, C. P., Sano, H., Kane, S., Sano, E., Fukuda, M., Peränen, J., et al. (2005). AS160, the Akt substrate regulating GLUT4 translocation, has a functional Rab GTPase-activating protein domain. *Biochem J, 391*(Pt 1), 87-93.

Möller-Loswick, A. C., Bennegård, K., & Lundholm, K. (1991). The forearm and leg perfusion techniques in man do not give the same metabolic information. *Clinical Physiology and Functional Imaging, 11*(4).

Møller, A. B., Kampmann, U., Hedegaard, J., Thorsen, K., Nordentoft, I., Vendelbo, M. H., et al. (2017). Altered gene expression and repressed markers of autophagy in skeletal muscle of insulin resistant patients with type 2 diabetes. *Sci Rep, 7*, 43775.

Moore, M. C., K. C. Coate, J. J. Winnick, Z. An, and A. D. Cherrington, 2012, Regulation of hepatic glucose uptake and storage in vivo: Adv Nutr, v. 3, p. 286-94.

Nardi, F., Hoffmann, T. M., Stretton, C., Cwiklinski, E., Taylor, P. M., & Hundal, H. S. (2015). Proteasomal modulation of cellular SNAT2 (SLC38A2) abundance and function by unsaturated fatty acid availability. *J Biol Chem, 290*(13), 8173-8184.

Nardi, F., Lipina, C., Magill, D., Hage Hassan, R., Hajduch, E., Gray, A., et al. (2014). Enhanced insulin sensitivity associated with provision of mono and polyunsaturated fatty acids in skeletal muscle cells involves counter modulation of PP2A. *PLoS One, 9*(3), e92255.

National Health Service. (2018). Health Survey for England 2017: Adult and child overweight and obesity. Retrieved 13/09/2019, from http://healthsurvey.hscic.gov.uk/media/78619/HSE17-Adult-Child-BMI-rep.pdf

Nauck, M., Stöckmann, F., Ebert, R., & Creutzfeldt, W. (1986). Reduced incretin effect in type 2 (non-insulin-dependent) diabetes. *Diabetologia, 29*(1), 46-52.

Nehlin, J. O., Just, M., Rustan, A. C., & Gaster, M. (2011). Human myotubes from myoblast cultures undergoing senescence exhibit defects in glucose and lipid metabolism. *Biogerontology, 12*(4), 349-365.

Neilson, H. K., Robson, P. J., Friedenreich, C. M., & Csizmadi, I. (2008). Estimating activity energy expenditure: how valid are physical activity questionnaires? *Am J Clin Nutr, 87*(2), 279-291.

Nicklin, P., Bergman, P., Zhang, B., Triantafellow, E., Wang, H., Nyfeler, B., et al. (2009). Bidirectional transport of amino acids regulates mTOR and autophagy. *Cell, 136*(3), 521-534.

Nielsen, J., Mogensen, M., Vind, B. F., Sahlin, K., Højlund, K., Schrøder, H. D., et al. (2010). Increased subsarcolemmal lipids in type 2 diabetes: effect of training on localization of lipids, mitochondria, and glycogen in sedentary human skeletal muscle. *Am J Physiol Endocrinol Metab, 298*(3), E706-713.

Nilsson, L. H., & Hultman, E. (1973). Liver glycogen in man--the effect of total starvation or a carbohydrate-poor diet followed by carbohydrate refeeding. *Scand J Clin Lab Invest, 32*(4), 325-330.

Nowotny, B., Zahiragic, L., Krog, D., Nowotny, P. J., Herder, C., Carstensen, M., et al. (2013). Mechanisms underlying the onset of oral lipid-induced skeletal muscle insulin resistance in humans. *Diabetes, 62*(7), 2240-2248.

O'Dea, K. (1991). Westernisation, insulin resistance and diabetes in Australian aborigines. *Med J Aust, 155*(4), 258-264.

O'Leary, M. F., Wallace, G. R., Bennett, A. J., Tsintzas, K., & Jones, S. W. (2017). IL-15 promotes human myogenesis and mitigates the detrimental effects of TNFα on myotube development. *Sci Rep, 7*(1), 12997.

O'Neill, H. M., Lally, J. S., Galic, S., Thomas, M., Azizi, P. D., Fullerton, M. D., et al. (2014). AMPK phosphorylation of ACC2 is required for skeletal muscle fatty acid oxidation and insulin sensitivity in mice. *Diabetologia, 57*(8), 1693-1702.

Olefsky, J. M., & Nolan, J. J. (1995). Insulin resistance and non-insulin-dependent diabetes mellitus: cellular and molecular mechanisms. *Am J Clin Nutr, 61*(4 Suppl), 980S-986S.

Olsen, M. K., Choi, M. H., Kulseng, B., Zhao, C. M., & Chen, D. (2017). Time-restricted feeding on weekdays restricts weight gain: A study using rat models of high-fat diet-induced obesity. *Physiol Behav, 173*, 298-304.

Ortega, R. M., Pérez-Rodrigo, C., & López-Sobaler, A. M. (2015). Dietary assessment methods: dietary records. *Nutr Hosp, 31 Suppl 3*, 38-45.

Paffenbarger, R. S., Hyde, R. T., Wing, A. L., Lee, I. M., Jung, D. L., & Kampert, J. B. (1993). The association of changes in physical-activity level and other lifestyle characteristics with mortality among men. *N Engl J Med, 328*(8), 538-545.

Palii, S. S., Thiaville, M. M., Pan, Y. X., Zhong, C., & Kilberg, M. S. (2006). Characterization of the amino acid response element within the human sodium-coupled neutral amino acid transporter 2 (SNAT2) System A transporter gene. *Biochem J, 395*(3), 517-527.

Pan, D. A., Lillioja, S., Kriketos, A. D., Milner, M. R., Baur, L. A., Bogardus, C., et al. (1997). Skeletal muscle triglyceride levels are inversely related to insulin action. *Diabetes, 46*(6), 983-988.

Pan, D. A., & Storlien, L. H. (1993). Dietary lipid profile is a determinant of tissue phospholipid fatty acid composition and rate of weight gain in rats. *J Nutr, 123*(3), 512-519.

Pennings, B., Boirie, Y., Senden, J. M., Gijsen, A. P., Kuipers, H., & van Loon, L. J. (2011). Whey protein stimulates postprandial muscle protein accretion more effectively than do casein and casein hydrolysate in older men. *Am J Clin Nutr, 93*(5), 997-1005.

Perdomo, G., Commerford, S. R., Richard, A. M., Adams, S. H., Corkey, B. E., O'Doherty, R. M., et al. (2004). Increased beta-oxidation in muscle cells enhances insulin-stimulated glucose metabolism and protects against fatty acid-induced insulin resistance despite intramyocellular lipid accumulation. *J Biol Chem, 279*(26), 27177-27186.

Pereira, S., Marliss, E. B., Morais, J. A., Chevalier, S., & Gougeon, R. (2008). Insulin resistance of protein metabolism in type 2 diabetes. *Diabetes, 57*(1), 56-63.

Perseghin, G., Ghosh, S., Gerow, K., & Shulman, G. I. (1997). Metabolic defects in lean nondiabetic offspring of NIDDM parents: a cross-sectional study. *Diabetes, 46*(6), 1001-1009.

Petersen, K. F., Dufour, S., Morino, K., Yoo, P. S., Cline, G. W., & Shulman, G. I. (2012). Reversal of muscle insulin resistance by weight reduction in young, lean, insulin-resistant offspring of parents with type 2 diabetes. *Proc Natl Acad Sci U S A, 109*(21), 8236-8240.

Petersen, K. F., Hendler, R., Price, T., Perseghin, G., Rothman, D. L., Held, N., et al. (1998). 13C/31P NMR studies on the mechanism of insulin resistance in obesity. *Diabetes, 47*(3), 381-386.

Petersen, K. F., & Shulman, G. I. (2006). Etiology of insulin resistance. *Am J Med, 119*(5 Suppl 1), S10-16.

Peterson, R. T., Desai, B. N., Hardwick, J. S., & Schreiber, S. L. (1999). Protein phosphatase 2A interacts with the 70-kDa S6 kinase and is activated by inhibition of FKBP12-rapamycinassociated protein. *Proc Natl Acad Sci U S A, 96*(8), 4438-4442.

Petro, A. E., Cotter, J., Cooper, D. A., Peters, J. C., Surwit, S. J., & Surwit, R. S. (2004). Fat, carbohydrate, and calories in the development of diabetes and obesity in the C57BL/6J mouse. *Metabolism, 53*(4), 454-457.

Pettee Gabriel, K. K., Morrow, J. R., & Woolsey, A. L. (2012). Framework for physical activity as a complex and multidimensional behavior. *J Phys Act Health, 9 Suppl 1*, S11-18.

Pettit, F. H., Pelley, J. W., & Reed, L. J. (1975). Regulation of pyruvate dehydrogenase kinase and phosphatase by acetyl-CoA/CoA and NADH/NAD ratios. *Biochem Biophys Res Commun, 65*(2), 575-582.

Peyrollier, K., Hajduch, E., Blair, A. S., Hyde, R., & Hundal, H. S. (2000). L-leucine availability regulates phosphatidylinositol 3-kinase, p70 S6 kinase and glycogen synthase kinase-3 activity in L6 muscle cells: evidence for the involvement of the mammalian target of rapamycin (mTOR) pathway in the L-leucine-induced up-regulation of system A amino acid transport. *Biochem J, 350 Pt 2*, 361-368.

Phillips, S. M., Tipton, K. D., Aarsland, A., Wolf, S. E., & Wolfe, R. R. (1997). Mixed muscle protein synthesis and breakdown after resistance exercise in humans. *Am J Physiol, 273*(1 Pt 1), E99-107.

Pickersgill, L., Litherland, G. J., Greenberg, A. S., Walker, M., & Yeaman, S. J. (2007). Key role for ceramides in mediating insulin resistance in human muscle cells. *J Biol Chem, 282*(17), 12583-12589.

Pickup, J. C., Freeman, S. C., & Sutton, A. J. (2011). Glycaemic control in type 1 diabetes during real time continuous glucose monitoring compared with self monitoring of blood glucose: meta-analysis of randomised controlled trials using individual patient data. *BMJ, 343*, d3805.

Pietrobelli, A., Formica, C., Wang, Z., & Heymsfield, S. B. (1996). Dual-energy X-ray absorptiometry body composition model: review of physical concepts. *Am J Physiol, 271*(6 Pt 1), E941-951.

Pilegaard, H., Saltin, B., & Neufer, P. D. (2003). Effect of short-term fasting and refeeding on transcriptional regulation of metabolic genes in human skeletal muscle. *Diabetes, 52*(3), 657-662.

Pinilla, J., Aledo, J. C., Cwiklinski, E., Hyde, R., Taylor, P. M., & Hundal, H. S. (2011). SNAT2 transceptor signalling via mTOR: a role in cell growth and proliferation? *Front Biosci (Elite Ed), 3*, 1289-1299.

Potts, J. L., Coppack, S. W., Fisher, R. M., Humphreys, S. M., Gibbons, G. F., & Frayn, K. N. (1995). Impaired postprandial clearance of triacylglycerol-rich lipoproteins in adipose tissue in obese subjects. *Am J Physiol, 268*(4 Pt 1), E588-594.

Powell, D. J., Turban, S., Gray, A., Hajduch, E., & Hundal, H. S. (2004). Intracellular ceramide synthesis and protein kinase Czeta activation play an essential role in palmitate-induced insulin resistance in rat L6 skeletal muscle cells. *Biochem J, 382*(Pt 2), 619-629.

Raben, A., Agerholm-Larsen, L., Flint, A., Holst, J. J., & Astrup, A. (2003). Meals with similar energy densities but rich in protein, fat, carbohydrate, or alcohol have different effects on energy expenditure and substrate metabolism but not on appetite and energy intake. *Am J Clin Nutr, 77*(1), 91-100.

Ramachandran, A., Snehalatha, C., Shetty, A. S., & Nanditha, A. (2012). Trends in prevalence of diabetes in Asian countries. *World J Diabetes, 3*(6), 110-117.

Randle, P. J., Garland, P. B., Hales, C. N., & Newsholme, E. A. (1963). The glucose fatty-acid cycle. Its role in insulin sensitivity and the metabolic disturbances of diabetes mellitus. *Lancet, 1*(7285), 785-789.

Ravussin, E., Beyl, R. A., Poggiogalle, E., Hsia, D. S., & Peterson, C. M. (2019). Early Time-Restricted Feeding Reduces Appetite and Increases Fat Oxidation But Does Not Affect Energy Expenditure in Humans. *Obesity (Silver Spring), 27*(8), 1244-1254.

Ravussin, E., Redman, L. M., Rochon, J., Das, S. K., Fontana, L., Kraus, W. E., et al. (2015). A 2-Year Randomized Controlled Trial of Human Caloric Restriction: Feasibility and Effects on Predictors of Health Span and Longevity. *J Gerontol A Biol Sci Med Sci, 70*(9), 1097-1104.

Raynor, H. A., Li, F., & Cardoso, C. (2018). Daily pattern of energy distribution and weight loss. *Physiol Behav, 192*, 167-172.

Redman, L. M., Smith, S. R., Burton, J. H., Martin, C. K., Il'yasova, D., & Ravussin, E. (2018). Metabolic Slowing and Reduced Oxidative Damage with Sustained Caloric Restriction Support the Rate of Living and Oxidative Damage Theories of Aging. *Cell Metab, 27*(4), 805-815.e804.

Rivas, D. A., Yaspelkis, B. B., Hawley, J. A., & Lessard, S. J. (2009). Lipid-induced mTOR activation in rat skeletal muscle reversed by exercise and 5'-aminoimidazole-4-carboxamide-1-beta-D-ribofuranoside. *J Endocrinol, 202*(3), 441-451.

Robertson, M. D., Henderson, R. A., Vist, G. E., & Rumsey, R. D. (2002). Extended effects of evening meal carbohydrate-to-fat ratio on fasting and postprandial substrate metabolism. *Am J Clin Nutr, 75*(3), 505-510.

Roden, M., & Shulman, G. I. (1999). Applications of NMR spectroscopy to study muscle glycogen metabolism in man. *Annu Rev Med, 50*, 277-290.

Roden, M., Stingl, H., Chandramouli, V., Schumann, W. C., Hofer, A., Landau, B. R., et al. (2000). Effects of free fatty acid elevation on postabsorptive endogenous glucose production and gluconeogenesis in humans. *Diabetes, 49*(5), 701-707.

Rommel, C., Bodine, S. C., Clarke, B. A., Rossman, R., Nunez, L., Stitt, T. N., et al. (2001). Mediation of IGF-1-induced skeletal myotube hypertrophy by PI(3)K/Akt/mTOR and PI(3)K/Akt/GSK3 pathways. *Nat Cell Biol, 3*(11), 1009-1013.

Rothman, D. L., Magnusson, I., Katz, L. D., Shulman, R. G., & Shulman, G. I. (1991). Quantitation of hepatic glycogenolysis and gluconeogenesis in fasting humans with 13C NMR. *Science, 254*(5031), 573-576.

Rothman, D. L., Shulman, R. G., & Shulman, G. I. (1992). 31P nuclear magnetic resonance measurements of muscle glucose-6-phosphate. Evidence for reduced insulin-dependent muscle glucose transport or phosphorylation activity in non-insulin-dependent diabetes mellitus. *J Clin Invest, 89*(4), 1069-1075.

Ruderman, N. B., Saha, A. K., Vavvas, D., & Witters, L. A. (1999). Malonyl-CoA, fuel sensing, and insulin resistance. *Am J Physiol, 276*(1), E1-E18.

Ruge, T., Hodson, L., Cheeseman, J., Dennis, A. L., Fielding, B. A., Humphreys, S. M., et al. (2009). Fasted to fed trafficking of Fatty acids in human adipose tissue reveals a novel regulatory step for enhanced fat storage. *J Clin Endocrinol Metab, 94*(5), 1781-1788.

Sadur, C. N., & Eckel, R. H. (1982). Insulin stimulation of adipose tissue lipoprotein lipase. Use of the euglycemic clamp technique. *J Clin Invest, 69*(5), 1119-1125.

Sancak, Y., Peterson, T. R., Shaul, Y. D., Lindquist, R. A., Thoreen, C. C., Bar-Peled, L., et al. (2008). The Rag GTPases bind raptor and mediate amino acid signaling to mTORC1. *Science, 320*(5882), 1496-1501.

Sarabia, V., Lam, L., Burdett, E., Leiter, L. A., & Klip, A. (1992). Glucose transport in human skeletal muscle cells in culture. Stimulation by insulin and metformin. *J Clin Invest, 90*(4), 1386-1395.

Saxton, R. A., & Sabatini, D. M. (2017). mTOR Signaling in Growth, Metabolism, and Disease. *Cell, 169*(2), 361-371.

Scherrer, U., Randin, D., Vollenweider, P., Vollenweider, L., & Nicod, P. (1994). Nitric oxide release accounts for insulin's vascular effects in humans. *J Clin Invest, 94*(6), 2511-2515.

Schmidt, E. K., Clavarino, G., Ceppi, M., & Pierre, P. (2009). SUnSET, a nonradioactive method to monitor protein synthesis. *Nat Methods, 6*(4), 275-277.

Schmittgen, T. D., & Livak, K. J. (2008). Analyzing real-time PCR data by the comparative C(T) method. *Nat Protoc, 3*(6), 1101-1108.

Schoenfeld, B. J., Aragon, A. A., & Krieger, J. W. (2015). Effects of meal frequency on weight loss and body composition: a meta-analysis. *Nutr Rev, 73*(2), 69-82.

Schofield, W. N. (1985). Predicting basal metabolic rate, new standards and review of previous work. *Hum Nutr Clin Nutr, 39 Suppl 1*, 5-41.

Schulz, L. O., Bennett, P. H., Ravussin, E., Kidd, J. R., Kidd, K. K., Esparza, J., et al. (2006). Effects of traditional and western environments on prevalence of type 2 diabetes in Pima Indians in Mexico and the U.S. *Diabetes Care, 29*(8), 1866-1871.

Shepherd, P. R., & Kahn, B. B. (1999). Glucose transporters and insulin action--implications for insulin resistance and diabetes mellitus. *N Engl J Med, 341*(4), 248-257.

Sherman, H., Genzer, Y., Cohen, R., Chapnik, N., Madar, Z., & Froy, O. (2012). Timed high-fat diet resets circadian metabolism and prevents obesity. *FASEB J, 26*(8), 3493-3502.

Shim, J. S., Oh, K., & Kim, H. C. (2014). Dietary assessment methods in epidemiologic studies. *Epidemiol Health, 36*, e2014009.

Shulman, G. I. (2000). Cellular mechanisms of insulin resistance. *J Clin Invest, 106*(2), 171-176.

Sidossis, L. S., Mittendorfer, B., Walser, E., Chinkes, D., & Wolfe, R. R. (1998). Hyperglycemia-induced inhibition of splanchnic fatty acid oxidation increases hepatic triacylglycerol secretion. *Am J Physiol, 275*(5), E798-805.

Simopoulos, A. P. (2016). An Increase in the Omega-6/Omega-3 Fatty Acid Ratio Increases the Risk for Obesity. *Nutrients, 8*(3), 128.

Smeuninx, B., Mckendry, J., Wilson, D., Martin, U., & Breen, L. (2017). Age-Related Anabolic Resistance of Myofibrillar Protein Synthesis Is Exacerbated in Obese Inactive Individuals. *J Clin Endocrinol Metab, 102*(9), 3535-3545.

Smiles, W. J., Churchward-Venne, T. A., van Loon, L. J. C., Hawley, J. A., & Camera, D. M. (2019). A single bout of strenuous exercise overcomes lipid-induced anabolic resistance to protein ingestion in overweight, middle-aged men. *FASEB J, 33*(6), 7009-7017.

Smith, G. I., Atherton, P., Reeds, D. N., Mohammed, B. S., Rankin, D., Rennie, M. J., et al. (2011a). Dietary omega-3 fatty acid supplementation increases the rate of muscle protein synthesis in older adults: a randomized controlled trial. *Am J Clin Nutr, 93*(2), 402-412.

Smith, G. I., Atherton, P., Reeds, D. N., Mohammed, B. S., Rankin, D., Rennie, M. J., et al. (2011b). Omega-3 polyunsaturated fatty acids augment the muscle protein anabolic response to hyperinsulinaemia-hyperaminoacidaemia in healthy young and middle-aged men and women. *Clin Sci (Lond), 121*(6), 267-278.

Smith, K. J., Gall, S. L., McNaughton, S. A., Blizzard, L., Dwyer, T., & Venn, A. J. (2010). Skipping breakfast: longitudinal associations with cardiometabolic risk factors in the Childhood Determinants of Adult Health Study. *Am J Clin Nutr, 92*(6), 1316-1325.

Soeters, M. R., Lammers, N. M., Dubbelhuis, P. F., Ackermans, M., Jonkers-Schuitema, C. F., Fliers, E., et al. (2009). Intermittent fasting does not affect whole-body glucose, lipid, or protein metabolism. *Am J Clin Nutr, 90*(5), 1244-1251.

Solomon, T. P., Chambers, E. S., Jeukendrup, A. E., Toogood, A. A., & Blannin, A. K. (2008). The effect of feeding frequency on insulin and ghrelin responses in human subjects. *Br J Nutr, 100*(4), 810-819.

Spiegel, K., Leproult, R., & Van Cauter, E. (1999). Impact of sleep debt on metabolic and endocrine function. *Lancet, 354*(9188), 1435-1439.

Spriet, L. L., Tunstall, R. J., Watt, M. J., Mehan, K. A., Hargreaves, M., & Cameron-Smith, D. (2004). Pyruvate dehydrogenase activation and kinase expression in human skeletal muscle during fasting. *J Appl Physiol (1985), 96*(6), 2082-2087.

St-Jean-Pelletier, F., Pion, C. H., Leduc-Gaudet, J. P., Sgarioto, N., Zovilé, I., Barbat-Artigas, S., et al. (2017). The impact of ageing, physical activity, and pre-

frailty on skeletal muscle phenotype, mitochondrial content, and intramyocellular lipids in men. *J Cachexia Sarcopenia Muscle, 8*(2), 213-228.

Stephens, F. B., Chee, C., Wall, B. T., Murton, A. J., Shannon, C. E., van Loon, L. J., et al. (2015). Lipid-induced insulin resistance is associated with an impaired skeletal muscle protein synthetic response to amino acid ingestion in healthy young men. *Diabetes, 64*(5), 1615-1620.

Stephens, F. B., Mendis, B., Shannon, C. E., Cooper, S., Ortori, C. A., Barrett, D. A., et al. (2014). Fish oil omega-3 fatty acids partially prevent lipid-induced insulin resistance in human skeletal muscle without limiting acylcarnitine accumulation. *Clin Sci (Lond), 127*(5), 315-322.

Stephens, F. B., Norton, L., Jewell, K., Chokkalingam, K., Parr, T., & Tsintzas, K. (2010). Basal and insulin-stimulated pyruvate dehydrogenase complex activation, glycogen synthesis and metabolic gene expression in human skeletal muscle the day after a single bout of exercise. *Exp Physiol, 95*(7), 808-818.

Steven, S., Hollingsworth, K. G., Al-Mrabeh, A., Avery, L., Aribisala, B., Caslake, M., et al. (2016). Very Low-Calorie Diet and 6 Months of Weight Stability in Type 2 Diabetes: Pathophysiological Changes in Responders and Nonresponders. *Diabetes Care, 39*(5), 808-815.

Stewart, W. K., & Fleming, L. W. (1973). Features of a successful therapeutic fast of 382 days' duration. *Postgrad Med J, 49*(569), 203-209.

Stitt, T. N., Drujan, D., Clarke, B. A., Panaro, F., Timofeyva, Y., Kline, W. O., et al. (2004). The IGF-1/PI3K/Akt pathway prevents expression of muscle atrophy-induced ubiquitin ligases by inhibiting FOXO transcription factors. *Mol Cell, 14*(3), 395-403.

Storlien, L. H., Jenkins, A. B., Chisholm, D. J., Pascoe, W. S., Khouri, S., & Kraegen, E. W. (1991). Influence of dietary fat composition on development of insulin resistance in rats. Relationship to muscle triglyceride and omega-3 fatty acids in muscle phospholipid. *Diabetes, 40*(2), 280-289.

Stote, K. S., Baer, D. J., Spears, K., Paul, D. R., Harris, G. K., Rumpler, W. V., et al. (2007). A controlled trial of reduced meal frequency without caloric restriction in healthy, normal-weight, middle-aged adults. *Am J Clin Nutr, 85*(4), 981-988.

Straczkowski, M., Kowalska, I., Nikolajuk, A., Dzienis-Straczkowska, S., Kinalska, I., Baranowski, M., et al. (2004). Relationship between insulin sensitivity and sphingomyelin signaling pathway in human skeletal muscle. *Diabetes, 53*(5), 1215-1221.

Strath, S. J., Brage, S., & Ekelund, U. (2005). Integration of physiological and accelerometer data to improve physical activity assessment. *Med Sci Sports Exerc, 37*(11 Suppl), S563-571.

Sui, X., LaMonte, M. J., Laditka, J. N., Hardin, J. W., Chase, N., Hooker, S. P., et al. (2007). Cardiorespiratory fitness and adiposity as mortality predictors in older adults. *JAMA, 298*(21), 2507-2516.

Sundfør, T. M., Svendsen, M., & Tonstad, S. (2018). Effect of intermittent versus continuous energy restriction on weight loss, maintenance and cardiometabolic risk: A randomized 1-year trial. *Nutr Metab Cardiovasc Dis, 28*(7), 698-706.

Sutton, E. F., Beyl, R., Early, K. S., Cefalu, W. T., Ravussin, E., & Peterson, C. M. (2018). Early Time-Restricted Feeding Improves Insulin Sensitivity, Blood Pressure, and Oxidative Stress Even without Weight Loss in Men with Prediabetes. *Cell Metab, 27*(6), 1212-1221.e1213.

Szendroedi, J., Yoshimura, T., Phielix, E., Koliaki, C., Marcucci, M., Zhang, D., et al. (2014). Role of diacylglycerol activation of PKCθ in lipid-induced muscle insulin resistance in humans. *Proc Natl Acad Sci U S A, 111*(26), 9597-9602.

Tardif, N., Salles, J., Guillet, C., Tordjman, J., Reggio, S., Landrier, J. F., et al. (2014). Muscle ectopic fat deposition contributes to anabolic resistance in obese sarcopenic old rats through eIF2α activation. *Aging Cell, 13*(6), 1001-1011.

Tardif, N., Salles, J., Landrier, J. F., Mothe-Satney, I., Guillet, C., Boue-Vaysse, C., et al. (2011). Oleate-enriched diet improves insulin sensitivity and restores muscle protein synthesis in old rats. *Clin Nutr, 30*(6), 799-806.

Tarnopolsky, M. A., Rennie, C. D., Robertshaw, H. A., Fedak-Tarnopolsky, S. N., Devries, M. C., & Hamadeh, M. J. (2007). Influence of endurance exercise training and sex on intramyocellular lipid and mitochondrial ultrastructure, substrate use, and mitochondrial enzyme activity. *Am J Physiol Regul Integr Comp Physiol, 292*(3), R1271-1278.

Taylor, R. (2008). Pathogenesis of type 2 diabetes: tracing the reverse route from cure to cause. *Diabetologia, 51*(10), 1781-1789.

Taylor, R., Magnusson, I., Rothman, D. L., Cline, G. W., Caumo, A., Cobelli, C., et al. (1996). Direct assessment of liver glycogen storage by 13C nuclear magnetic resonance spectroscopy and regulation of glucose homeostasis after a mixed meal in normal subjects. *J Clin Invest, 97*(1), 126-132.

Taylor, R., Price, T. B., Katz, L. D., Shulman, R. G., & Shulman, G. I. (1993). Direct measurement of change in muscle glycogen concentration after a mixed meal in normal subjects. *Am J Physiol, 265*(2 Pt 1), E224-229.

Templeman, I., Gonzalez, J. T., Thompson, D., & Betts, J. A. (2019). The role of intermittent fasting and meal timing in weight management and metabolic health. *Proc Nutr Soc*, 1-12.

The Emerging Risk Factors Collaboration. (2010). Diabetes mellitus, fasting blood glucose concentration, and risk of vascular disease: a collaborative meta-analysis of 102 prospective studies. *The Lancet, 375*(9733), 2215-2222.

Thiebaud, D., Jacot, E., DeFronzo, R. A., Maeder, E., Jequier, E., & Felber, J. P. (1982). The effect of graded doses of insulin on total glucose uptake, glucose oxidation, and glucose storage in man. *Diabetes, 31*(11), 957-963.

Thiébaud, D., DeFronzo, R. A., Jacot, E., Golay, A., Acheson, K., Maeder, E., et al. (1982). Effect of long chain triglyceride infusion on glucose metabolism in man. *Metabolism, 31*(11), 1128-1136.

Thompson, D., Batterham, A. M., Bock, S., Robson, C., & Stokes, K. (2006). Assessment of low-to-moderate intensity physical activity thermogenesis in young adults using synchronized heart rate and accelerometry with branched-equation modeling. *J Nutr, 136*(4), 1037-1042.

Thoreen, C. C., Kang, S. A., Chang, J. W., Liu, Q., Zhang, J., Gao, Y., et al. (2009). An ATP-competitive mammalian target of rapamycin inhibitor reveals rapamycin-resistant functions of mTORC1. *J Biol Chem, 284*(12), 8023-8032.

Timmers, S., de Vogel-van den Bosch, J., Hesselink, M. K., van Beurden, D., Schaart, G., Ferraz, M. J., et al. (2011). Paradoxical increase in TAG and DAG content parallel the insulin sensitizing effect of unilateral DGAT1 overexpression in rat skeletal muscle. *PLoS One, 6*(1), e14503.

Tinsley, G. M., Forsse, J. S., Butler, N. K., Paoli, A., Bane, A. A., La Bounty, P. M., et al. (2017). Time-restricted feeding in young men performing resistance training: A randomized controlled trial. *Eur J Sport Sci, 17*(2), 200-207.

Torgerson, J. S., Hauptman, J., Boldrin, M. N., & Sjöström, L. (2004). XENical in the prevention of diabetes in obese subjects (XENDOS) study: a randomized study of orlistat as an adjunct to lifestyle changes for the prevention of type 2 diabetes in obese patients. *Diabetes Care, 27*(1), 155-161.

Trepanowski, J. F., and R. J. Bloomer, 2010, The impact of religious fasting on human health: Nutr J, v. 9, p. 57.

Troiano, R. P. (2005). A timely meeting: objective measurement of physical activity. *Med Sci Sports Exerc, 37*(11 Suppl), S487-489.

Tschakovsky, M. E., Shoemaker, J. K., & Hughson, R. L. (1995). Beat-by-beat forearm blood flow with Doppler ultrasound and strain-gauge plethysmography. *J Appl Physiol (1985), 79*(3), 713-719.

Tschritter, O., Fritsche, A., Thamer, C., Haap, M., Shirkavand, F., Rahe, S., et al. (2003). Plasma adiponectin concentrations predict insulin sensitivity of both glucose and lipid metabolism. *Diabetes, 52*(2), 239-243.

Tsintzas, K., Chokkalingam, K., Jewell, K., Norton, L., Macdonald, I. A., & Constantin-Teodosiu, D. (2007). Elevated free fatty acids attenuate the insulin-induced suppression of PDK4 gene expression in human skeletal muscle: potential role of intramuscular long-chain acyl-coenzyme A. *J Clin Endocrinol Metab, 92*(10), 3967-3972.

Tsintzas, K., Jewell, K., Kamran, M., Laithwaite, D., Boonsong, T., Littlewood, J., et al. (2006). Differential regulation of metabolic genes in skeletal muscle during starvation and refeeding in humans. *J Physiol, 575*(Pt 1), 291-303.

Tsintzas, K., Stephens, F. B., Snijders, T., Wall, B. T., Cooper, S., Mallinson, J., et al. (2017). Intramyocellular lipid content and lipogenic gene expression responses following a single bout of resistance type exercise differ between young and older men. *Exp Gerontol, 93*, 36-45.

Turpin-Nolan, S. M., Hammerschmidt, P., Chen, W., Jais, A., Timper, K., Awazawa, M., et al. (2019). CerS1-Derived C. *Cell Rep, 26*(1), 1-10.e17.

Van Cauter, E., Désir, D., Decoster, C., Féry, F., & Balasse, E. O. (1989). Nocturnal decrease in glucose tolerance during constant glucose infusion. *J Clin Endocrinol Metab, 69*(3), 604-611.

van Loon, L. J., Koopman, R., Stegen, J. H., Wagenmakers, A. J., Keizer, H. A., & Saris, W. H. (2003). Intramyocellular lipids form an important substrate source during moderate intensity exercise in endurance-trained males in a fasted state. *J Physiol, 553*(Pt 2), 611-625.

van Moorsel, D., Hansen, J., Havekes, B., Scheer, F. A. J. L., Jörgensen, J. A., Hoeks, J., et al. (2016). Demonstration of a day-night rhythm in human skeletal muscle oxidative capacity. *Mol Metab, 5*(8), 635-645.

Vander Haar, E., Lee, S. I., Bandhakavi, S., Griffin, T. J., & Kim, D. H. (2007). Insulin signalling to mTOR mediated by the Akt/PKB substrate PRAS40. *Nat Cell Biol, 9*(3), 316-323.

Verrillo, A., De Teresa, A., Martino, C., Di Chiara, G., Pinto, M., Verrillo, L., et al. (1989). Differential roles of splanchnic and peripheral tissues in determining diurnal fluctuation of glucose tolerance. *Am J Physiol, 257*(4 Pt 1), E459-465.

Vessby, B., Uusitupa, M., Hermansen, K., Riccardi, G., Rivellese, A. A., Tapsell, L. C., et al. (2001). Substituting dietary saturated for monounsaturated fat impairs insulin sensitivity in healthy men and women: The KANWU Study. *Diabetologia, 44*(3), 312-319.

Villars, C., Bergouignan, A., Dugas, J., Antoun, E., Schoeller, D. A., Roth, H., et al. (2012). Validity of combining heart rate and uniaxial acceleration to measure free-living physical activity energy expenditure in young men. *J Appl Physiol (1985), 113*(11), 1763-1771.

Vincent, M. A., Barrett, E. J., Lindner, J. R., Clark, M. G., & Rattigan, S. (2003). Inhibiting NOS blocks microvascular recruitment and blunts muscle glucose uptake in response to insulin. *Am J Physiol Endocrinol Metab, 285*(1), E123-129.

Volpi, E., Sheffield-Moore, M., Rasmussen, B. B., & Wolfe, R. R. (2001). Basal muscle amino acid kinetics and protein synthesis in healthy young and older men. *JAMA, 286*(10), 1206-1212.

Wakelam, M. J. (1998). Diacylglycerol--when is it an intracellular messenger? *Biochim Biophys Acta, 1436*(1-2), 117-126.

Walker, D. K., Drummond, M. J., Dickinson, J. M., Borack, M. S., Jennings, K., Volpi, E., et al. (2014). Insulin increases mRNA abundance of the amino acid transporter SLC7A5/LAT1 via an mTORC1-dependent mechanism in skeletal muscle cells. *Physiol Rep, 2*(3), e00238.

Warram, J. H., Martin, B. C., Krolewski, A. S., Soeldner, J. S., & Kahn, C. R. (1990). Slow glucose removal rate and hyperinsulinemia precede the development of type II diabetes in the offspring of diabetic parents. *Ann Intern Med, 113*(12), 909-915.

Watson, M. L., Coghlan, M., & Hundal, H. S. (2009). Modulating serine palmitoyl transferase (SPT) expression and activity unveils a crucial role in lipid-induced insulin resistance in rat skeletal muscle cells. *Biochem J, 417*(3), 791-801.

Weir, J. B. (1949). New methods for calculating metabolic rate with special reference to protein metabolism. *J Physiol, 109*(1-2), 1-9.

Wellek, S., and M. Blettner, 2012, On the proper use of the crossover design in clinical trials: part 18 of a series on evaluation of scientific publications: Dtsch Arztebl Int, v. 109, p. 276-81.

Westerterp, K. R. (2004). Diet induced thermogenesis. *Nutr Metab (Lond), 1*(1), 5.

Wilkes, E. A., Selby, A. L., Atherton, P. J., Patel, R., Rankin, D., Smith, K., et al. (2009). Blunting of insulin inhibition of proteolysis in legs of older subjects may contribute to age-related sarcopenia. *Am J Clin Nutr, 90*(5), 1343-1350.

Winzell, M. S., & Ahrén, B. (2004). The high-fat diet-fed mouse: a model for studying mechanisms and treatment of impaired glucose tolerance and type 2 diabetes. *Diabetes, 53 Suppl 3*, S215-219.

Wolfe, R. R. (2002). Regulation of muscle protein by amino acids. *J Nutr, 132*(10), 3219S-3224S.

Wolfe, R. R., Peters, E. J., Klein, S., Holland, O. B., Rosenblatt, J., & Gary, H. (1987). Effect of short-term fasting on lipolytic responsiveness in normal and obese human subjects. *Am J Physiol, 252*(2 Pt 1), E189-196.

Woodworth-Hobbs, M. E., Hudson, M. B., Rahnert, J. A., Zheng, B., Franch, H. A., & Price, S. R. (2014). Docosahexaenoic acid prevents palmitate-induced activation of proteolytic systems in C2C12 myotubes. *J Nutr Biochem, 25*(8), 868-874.

Wu, P., Inskeep, K., Bowker-Kinley, M. M., Popov, K. M., & Harris, R. A. (1999). Mechanism responsible for inactivation of skeletal muscle pyruvate dehydrogenase complex in starvation and diabetes. *Diabetes, 48*(8), 1593-1599.

Yamamoto, S., Kuramoto, K., Wang, N., Situ, X., Priyadarshini, M., Zhang, W., et al. (2018). Autophagy Differentially Regulates Insulin Production and Insulin Sensitivity. *Cell Rep, 23*(11), 3286-3299.

Yang, M., Wei, D., Mo, C., Zhang, J., Wang, X., Han, X., et al. (2013). Saturated fatty acid palmitate-induced insulin resistance is accompanied with myotube loss and the impaired expression of health benefit myokine genes in C2C12 myotubes. *Lipids Health Dis, 12*, 104.

Yeh, J. I., Gulve, E. A., Rameh, L., & Birnbaum, M. J. (1995). The effects of wortmannin on rat skeletal muscle. Dissociation of signaling pathways for insulin- and contraction-activated hexose transport. *J Biol Chem, 270*(5), 2107-2111.

Yip, J., Facchini, F. S., & Reaven, G. M. (1998). Resistance to insulin-mediated glucose disposal as a predictor of cardiovascular disease. *J Clin Endocrinol Metab, 83*(8), 2773-2776.

Yoshino, J., Almeda-Valdes, P., Patterson, B. W., Okunade, A. L., Imai, S., Mittendorfer, B., et al. (2014). Diurnal variation in insulin sensitivity of glucose metabolism is associated with diurnal variations in whole-body and cellular fatty acid metabolism in metabolically normal women. *J Clin Endocrinol Metab, 99*(9), E1666-1670.

Yu, Y., & Chai, J. (2015). The function of miRNAs and their potential as therapeutic targets in burn-induced insulin resistance (review). *Int J Mol Med, 35*(2), 305-310.

Yuan, J. S., Reed, A., Chen, F., & Stewart, C. N. (2006). Statistical analysis of real-time PCR data. *BMC Bioinformatics, 7*, 85.

Yuzefovych, L., Wilson, G., & Rachek, L. (2010). Different effects of oleate vs. palmitate on mitochondrial function, apoptosis, and insulin signaling in L6 skeletal muscle cells: role of oxidative stress. *Am J Physiol Endocrinol Metab, 299*(6), E1096-1105.

Zarrinpar, A., Chaix, A., Yooseph, S., & Panda, S. (2014). Diet and feeding pattern affect the diurnal dynamics of the gut microbiome. *Cell Metab, 20*(6), 1006-1017.

Zhang, D., Wang, W., Sun, X., Xu, D., Wang, C., Zhang, Q., et al. (2016). AMPK regulates autophagy by phosphorylating BECN1 at threonine 388. *Autophagy, 12*(9), 1447-1459.

Zurlo, F., Larson, K., Bogardus, C., & Ravussin, E. (1990). Skeletal muscle metabolism is a major determinant of resting energy expenditure. *J Clin Invest, 86*(5), 1423-1427.

Appendix

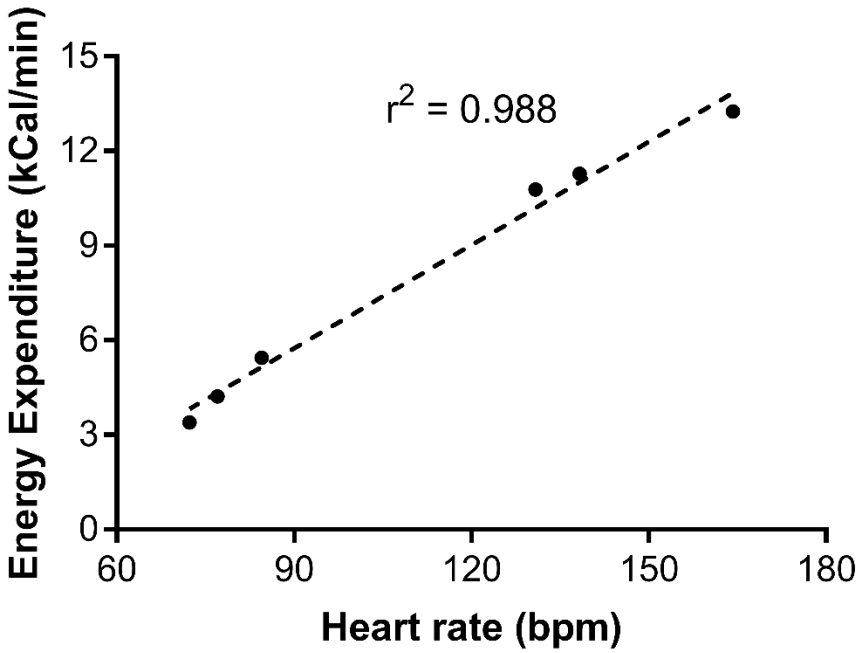
Appendix A. [^{14}C] Oxaloacetate Preparation

[^{14}C] oxaloacetate is unstable and was synthesised fresh on the day of each experiment. It was formed from [^{14}C]-aspartic acid using α-ketoglutarate and glutamate-oxaloacetate (GOT) in a 0.5 M HEPES buffer (pH 7.4) with 11 mM EDTA:

$$[^{14}\mathrm{C}]\ \text{aspartic acid} + \alpha\text{-ketoglutarate} \xrightarrow{GOT} [^{14}\mathrm{C}]\ \text{oxaloacetate} + \text{glutamate}$$

The transamination reaction was terminated using 1 M perchloric acid for 5 min, then ice-cold 0.6 M KOH and further diluted with 11 mM EDTA.

Appendix B. Actiheart Calibration



Linear regression of heart rate vs energy expenditure.
A representative example of one participants heart rate and energy expenditure responses to an incremental treadmill test protocol. Data was from the final min (steady state) of each stage and was used to individually calibrate the Actiheart.

Appendix C. Full List of Genes Measured

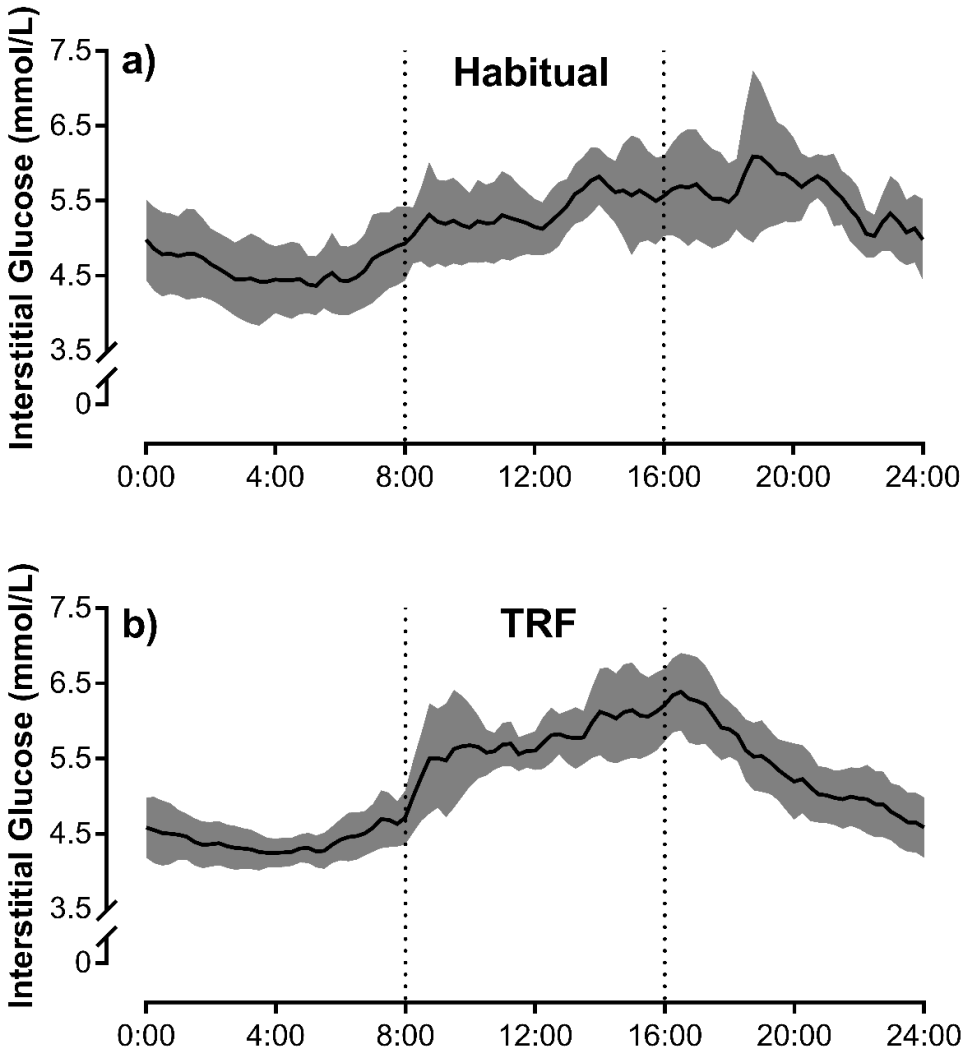
Appendix C. Full list of genes measured for skeletal muscle mRNA expression in Chapter 5.

Acronym	Gene name
ACACB	acetyl-CoA carboxylase beta
ACADM	acyl-CoA dehydrogenase, C-4 to C-12 straight chain
ACAT1	acetyl-CoA acetyltransferase 1
ACTA1*	actin, alpha 1, skeletal muscle
AKT2	v-akt murine thymoma viral oncogene homolog 2
BECN1	beclin 1, autophagy related
CPT1B	carnitine palmitoyltransferase 1B (muscle)
CPT2	carnitine palmitoyltransferase 2
DDIT4	DNA-damage-inducible transcript 4
DGAT1	diacylglycerol O-acyltransferase 1
DGAT2	diacylglycerol O-acyltransferase 2
DGKD	diacylglycerol kinase, delta 130kDa
EIF4EBP1	eukaryotic translation initiation factor 4E binding protein 1
FASN	fatty acid synthase
FBXO32	F-box protein 32
FOXO1	forkhead box O1
FOXO3	forkhead box O3
GAPDH*	glyceraldehyde-3-phosphate dehydrogenase
GDF11	growth differentiation factor 11
GPAM	glycerol-3-phosphate acyltransferase, mitochondrial
GSK3B	glycogen synthase kinase 3 beta
HADHB	hydroxyacyl-CoA dehydrogenase/3-ketoacyl-CoA thiolase/enoyl-CoA hydratase (trifunctional protein), beta subunit
HK2	hexokinase 2
HMBS*	hydroxymethylbilane synthase
LIPE	lipase, hormone-sensitive
LPIN1	lipin 1
MSTN	myostatin
MTOR	mechanistic target of rapamycin (serine/threonine kinase)
PDK2	pyruvate dehydrogenase kinase, isozyme 2
PDK4	pyruvate dehydrogenase kinase, isozyme 4
PDP1	pyruvate dehyrogenase phosphatase catalytic subunit 1
PIK3R1	phosphoinositide-3-kinase, regulatory subunit 1 (alpha)
PLIN2	perilipin 2
PLIN5	perilipin 5
PNPLA2	patatin-like phospholipase domain containing 2
PPARA	peroxisome proliferator-activated receptor alpha
PRKCQ	protein kinase C, theta
RPS6KB1	ribosomal protein S6 kinase, 70kDa, polypeptide 1
SCD	stearoyl-CoA desaturase (delta-9-desaturase)

SLC2A4	solute carrier family 2 (facilitated glucose transporter), member 4
SLC36A1	solute carrier family 36 (proton/amino acid symporter), member 1
SLC7A5	solute carrier family 7 (amino acid transporter light chain, L system), member 5
SNAP23	synaptosomal-associated protein, 23kDa
SPTLC1	serine palmitoyltransferase, long chain base subunit 1
TFAM	transcription factor A, mitochondrial
TRIM63	tripartite motif containing 63, E3 ubiquitin protein ligase
UCP3	uncoupling protein 3 (mitochondrial, proton carrier)
ULK1	unc-51 like autophagy activating kinase 1

*Housekeeping gene(s) not included in analysis.

Appendix D. Glycaemic Profiles



Appendix D. Diurnal glycaemic profiles with 95% CI shade.
Diurnal glycaemic profiles during one week of habitual diet (baseline) and two weeks of TRF. Data are display as mean with shaded areas representing the 95% confidence interval (CI).

Appendix E. PIPS Reflective Statement

Note to examiners:

This statement is included as an appendix to the thesis in order that the thesis accurately captures the PhD training experienced by the candidate as a BBSRC Doctoral Training Partnership student.

The Professional Internship for PhD Students is a compulsory 3-month placement which must be undertaken by DTP students. It is usually centred on a specific project and must not be related to the PhD project. This reflective statement is designed to capture the skills development which has taken place during the student's placement and the impact on their career plans it has had.

I completed my internship at the Centre for Longitudinal Studies, University College London. This has a renowned reputation for undertaking some of the largest birth cohort studies in the world. I chose to do my internship here to gain an insight into longitudinal studies, which are powerful evidence sources that have helped to establish many of the risk factors for the development of chronic disease(s).

During my time at UCL, I primarily worked on data analysis from the Millennium Cohort Study (MCS) and was supervised by Professor Emla Fitzsimmons. The MCS is a birth cohort study following around 19,000 children across the UK born in 2000/2001. My project was primarily focused on the physical activity data, which had been objectively assessed using accelerometers. I had access to data collected at ages 11 and 14.

Initially, we were interested in using simple linear regression models to examine the association(s) between socio-demographic characteristics and physical activity.

From here, we explored the association of cross-sectional and longitudinal physical activity levels on adiposity / BMI. Finally, I explored the associations between objectively measured physical activity levels with entries (10 min blocks) within self-reported time-use/activity diaries.

Overall, it was interesting to gain exposure to a different research area. The challenges in this field were very different to what I was accustomed to. When working with such large datasets it is not possible to manually check all datapoints, thus it is integral to develop and apply automated data quality checks to maximise data integrity. This was one of my main achievements during the PIPS and helped to improve the reliability of all subsequent analyses. At the end of the three months I submitted a draft paper to my PIPS supervisor. We have recently been in touch and I am hoping that they will publish an edited version of the manuscript.

During this placement I also gained an appreciation of the sheer scale of work involved in planning and managing data collection from large longitudinal studies. It emphasised the importance of using clear and translatable data outcomes that can be used in statistical models. I believe this project helped to improve my data analytical skills. On a separate note, it was nice to have a short break from my PhD project to put my work back into perspective and come back refocused for the final year of the project.